The development of efficient two-photon singlet oxygen sensitizers

Nielsen, Christian Benedikt

Publication date:
2005

Document Version
Publisher's PDF, also known as Version of record

Risø-PhD-10(EN)

The development of efficient two-photon singlet oxygen sensitizers

Christian Benedikt Nielsen

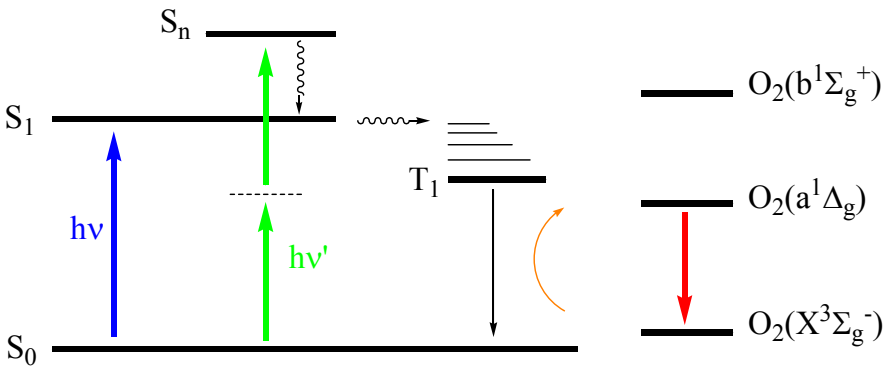

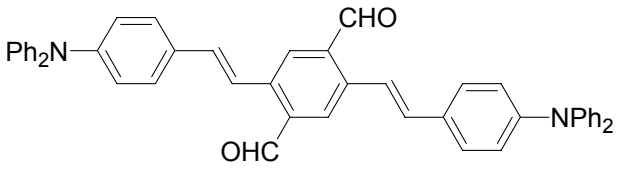

Risø National Laboratory
Roskilde
Department of Chemistry, University of Aarhus
Aarhus
Denmark
April 2005

Author: Christian Benedikt Nielsen
Title: The development of efficient two-photon singlet oxygen sensitizers.
Department: Danish Polymer Centre, Risø National Laboratory, and Department of Chemistry, University of Aarhus.

This thesis is submitted in partial fulfilment of the requirements for the Ph.D. degree at The University of Aarhus.

Abstract:

The development of efficient two-photon singlet oxygen sensitizers is addressed focusing on organic synthesis. Photophysical measurements were carried out on new lipophilic molecules, where two-photon absorption cross sections and singlet oxygen quantum yields were measured. Design principles for making efficient two-photon singlet oxygen sensitizers were then constructed from these results. Charge-transfer in the excited state of the prepared molecules was shown to play a pivotal role in the generation of singlet oxygen. This was established through studies of substituent effects on both the singlet oxygen yield and the two-photon absorption cross section, where it was revealed that a careful balancing of the amount of charge transfer present in the excited state of the sensitizer is necessary to obtain both a high singlet oxygen quantum yield and a high two-photon cross section. An increasing amount of charge-transfer is beneficial for high two-photon absorption cross sections but is counter-productive for singlet oxygen generation. The design principles obtained from the studies in lipophilic solvents were applied to synthesize water-soluble two-photon singlet oxygen sensitizers with the potential applicability for biological studies. Stability issues of these sensitizers were also addressed. Gas-phase measurements of the triplet quantum yield carried out on some of the sensitizers provided complementary information to the solution phase date and revealed that unsuccessful singlet oxygen sensitizers had low triplet quantum yields. The synthesis of porphyrins with donor-acceptor architecture was investigated and it was shown that these biologically friendly molecules could not be brought to generate singlet oxygen in a two-photon irradiation scheme. Finally, the theoretical methods available for calculating two-photon absorption cross sections were applied to small molecules and provided insight on errors inherent in calculated cross sections.

Risø-PhD-10(EN)
April 2005

ISBN 87-550-3426-8

Group's own reg. no.:
1820500-16

Sponsorship: Danish Polymer Centre, Risø National Laboratory, and The University of Aarhus.

Cover : Jablonsky diagram illustrating the photosensitized generation of singlet oxygen and an example of a sensitizer.

Risø National Laboratory
Information Service Department
P.O.Box 49
DK-4000 Roskilde
Denmark
Telephone +45 46774004
bibl@risoe.dk
Fax +45 46774013
www.risoe.dk

Contents

PREFACE
GOALS AND OBJECTIVES

The goal of the present project was to design and prepare organic molecules that function as singlet oxygen sensitizers and that can generate singlet oxygen in a two-photon irradiation scheme. The two most important physical properties such sensitizers must posses are a large two-photon absorption (TPA) cross section and a large singlet oxygen quantum yield. A further goal was to make the sensitizers soluble in appropriate solvents, particularly in the biologically relevant solvent water. For many applications, a successful sensitizer is also stable to prolonged irradiation, whereas other applications warrant degradation over a finite period of time. An obvious goal was then to understand the factors that influence stability. One use for two-photon singlet oxygen sensitizers is to apply them in photodynamic cancer therapy (PDT), which is a technique used to destroy cancer-infected tissue using photo-induced singlet oxygen. The intention was also to use the sensitizers in the new field of oxygen imaging, where singlet oxygen is detected through its phosphorescence from a spatially resolved region in space.

Biological samples are transparent above approximately 800 nm, which dictated one of the goals of the present project; The singlet oxygen sensitizers must have TPA maximum above 800 nm. Organic chromophores typically absorb in the wavelength region 300-600 nm, which means that exciting the chromophore in a two-photon irradiation scheme requires light in the wavelength region 600-1200 nm.

The tools used in this project were organic synthesis, photophysical measurements and computational studies. Access to a wide variety of molecules is necessary for looking at trends of the properties mentioned above and, to this end, synthetic work was undertaken to prepare molecules with different donor-acceptor architectures and functionalities that impart solubility in specific solvents. The photophysical characterizations consisted of measuring TPA action spectra, singlet oxygen quantum yields, fluorescence lifetimes and quantum yields, and triplet-triplet absorption spectra. Electrochemical studies and X-ray structures provided additional information

about the synthesized molecules. Computational studies were undertaken to clarify trends observed in the relative TPA cross sections.

A general overview of the individual chapters is summarized in the following.

Chapter 1: Photophysical processes pertinent to process of singlet oxygen production in either a one- or a two-photon process are discussed in this chapter including the discussion of the molecular properties that facilitate large two-photon absorption cross sections and large singlet oxygen quantum yields.

Chapter 2: The synthesis of a series of lipophilic oligo phenylene-vinylenes is described.

Chapter 3: Detailed photophysical studies were carried out on the molecules described in chapter 2 including the measurements of singlet oxygen quantum yields and relative two-photon absorption cross sections. Triplet-triplet absorption spectra were recorded for two molecules and crystallographic information for one of the prepared oligo phenylene-vinylenes also provide information on the studied molecules.

Chapter 4: Water-soluble singlet oxygen sensitizers were prepared using the design principles for making two-photon singlet oxygen sensitizers discussed in Chapter 2. Photostability is an important issue, and degradation studies for some of the sensitizers are described. Production of singlet oxygen in water using a two-photon irradiation scheme is also illustrated for one of the sensitizers.

Chapter 5: Singlet oxygen production was investigated as a function of protonating basic sites on the sensitizer molecule.

Chapter 6: Problems in the synthesis of porphyrins with varying substituents are briefly discussed. Symmetrical porphyrins were investigated with respect to their use as singlet oxygen sensitizers, and attempts were also made to generate singlet oxygen in a two-photon irradiation scheme using these molecules.

Chapter 7: Triplet quantum yields and lifetimes were measured in the gas-phase for a series of the sensitizers described in Chapter 4. These properties are discussed in this chapter.

Chapter 8: Theoretical two-photon absorption cross sections for water and a series of organic molecules were obtained through sophisticated *ab initio* calculations. The results from these calculations are discussed and compared to experimental values.

CHAPTER 1
INTRODUCTION TO PHOTOPHYSICS, STRUCTURE–PROPERTY RELATIONS AND SYNTHETIC STRATEGIES

Abstract: *Singlet oxygen can be generated using a sensitizer. In this case the triplet state of the sensitizer is populated in a photo-induced process. Quenching of the triplet sensitizer with ground state oxygen can generate singlet oxygen very efficiently. In designing efficient two-photon singlet oxygen sensitizers, detailed knowledge of the photophysics of the sensitizer excited state is a necessity. Ways of promoting intersystem crossing in molecules with large TPA cross sections and singlet oxygen quantum yields are proposed.*

1.1 The interest in singlet oxygen

Singlet molecular oxygen is an important species in many chemical reactions. As an example, singlet oxygen readily reacts with unsaturated organic molecules as shown in Figure 1-1.

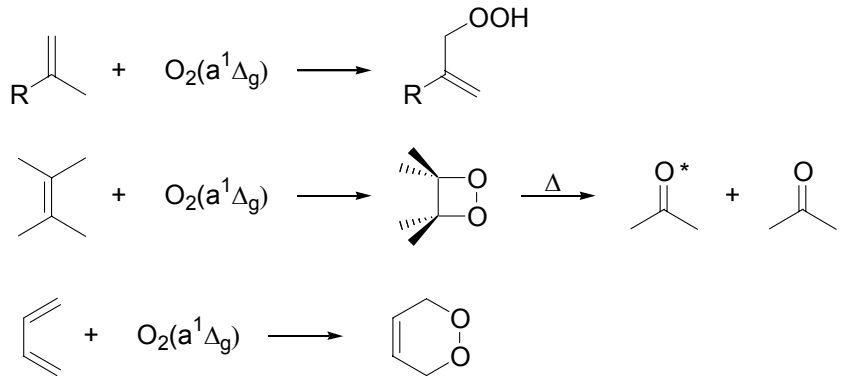

Figure 1-1: The ene reaction of singlet oxygen with double bonds (top), the 2+2 cycloaddition of singlet oxygen with double bonds and subsequent heating leading to an excited state ketone and a ground state ketone (middle) and the 4+2 cycloaddition with a diene.

Due to the high reactivity of singlet oxygen it is responsible for many degradation processes of *e.g.* polymers[1-3] and the photosensitized production of singlet oxygen also has important ramifications in photomedicine.[4-8]

1.2 Generating singlet oxygen

A simplistic orbital diagram of the lowest electronic states of oxygen is depicted in Figure 1-2. The transition from ground state oxygen to the lowest excited state is a spin forbidden (triplet-singlet), parity forbidden (gerade-gerade) and angular momentum forbidden (Σ-Δ) process and thus direct irradiation of ground state oxygen does not produce excited state oxygen molecules in appreciable amount.[9,10]

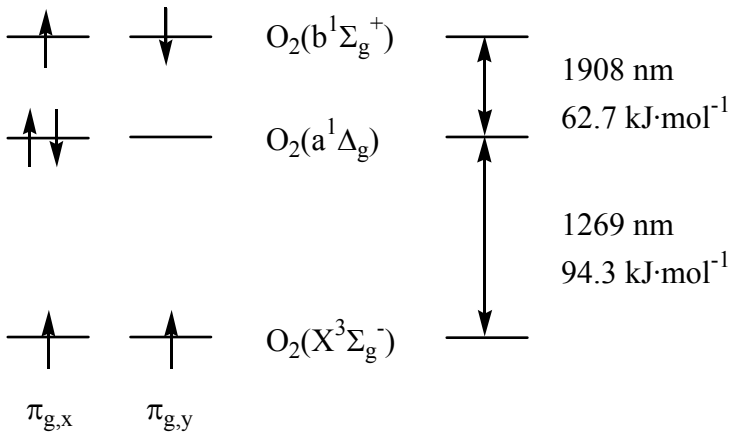

Figure 1-2: Orbital diagram of the lowest electronic states of oxygen showing the distribution of the two highest energy electrons in the degenerate highest occupied molecular orbitals of O_2. The energy differences between the states are given in nm and in kJ·mol^{-1} (gas phase values).

Once formed, the $^1\Sigma_g^+$ state of oxygen rapidly decays into the lower lying $^1\Delta_g$ state and, from here on, the term "singlet oxygen" is used to refer to the $^1\Delta_g$ state.

A photosensitizer is typically used to generate singlet oxygen (see Figure 1-3). Photosensitized production of singlet oxygen[9] occurs by populating an excited singlet state of the sensitizer, using either a two-photon or a one-photon irradiation scheme. For centrosymmetric sensitizer molecules, the state populated upon one-photon irradiation is different from that initially populated upon two-photon irradiation. However, it is usually assumed that, independent of the excitation method, Kasha's rule will hold and that all subsequent photophysics and photochemistry originate from one common state; the vibrationally-relaxed, lowest-energy excited singlet state S_1. Intersystem crossing from this state followed by internal conversion leads to population of the first excited triplet state, which is quenched by ground state oxygen yielding singlet oxygen and the sensitizer in its ground state. This whole process is

more efficient than the direct irradiation scheme for singlet oxygen production as no symmetry rules are broken.

Quenching an excited singlet state of the sensitizer by $O_2(X^3\Sigma_g^-)$ can also lead to the formation of singlet oxygen.[9] Thus it is possible for $O_2(X^3\Sigma_g^-)$ to quench both singlet and triplet states of the sensitizer giving an upper limit of 2 and not 1 for the quantum yield of singlet oxygen production. The mechanism presented above for singlet oxygen production is somewhat simplified as many other photochemical processes can occur.[9]

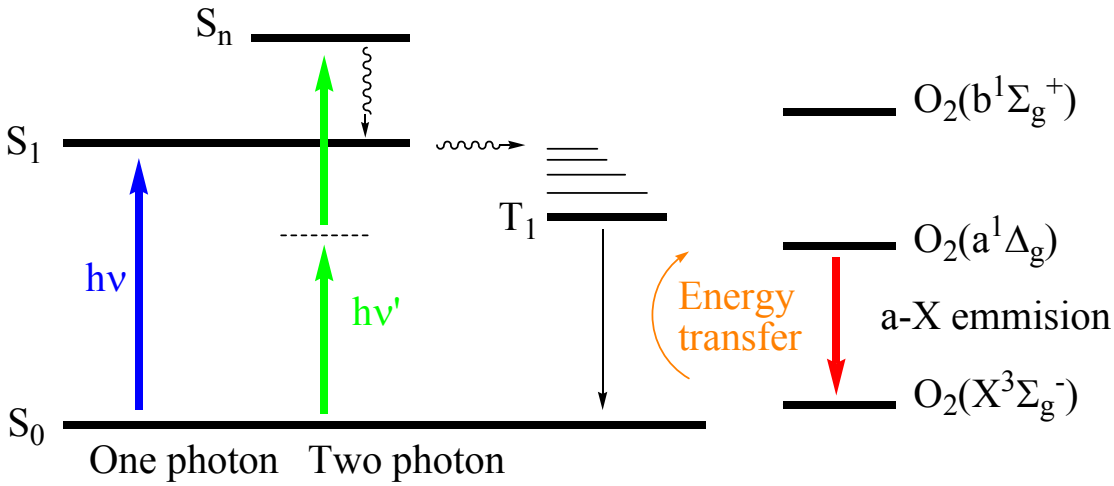

Figure 1-3: Jablonsky diagram illustrating the production of singlet oxygen by irradiating a sensitizer using either a one- or two-photon absorption scheme. The sensitizer is excited to a higher electronic state that relaxes to the first excited singlet state, S_1. The triplet state is populated by intersystem crossing, which further relaxes to the ground state while exciting molecular oxygen. Singlet oxygen can then be monitored from its phosphorescence at 1270 nm.

One advantage of using a two-photon irradiation scheme for generating singlet oxygen is that two-photon experiments are performed by irradiating the sample at wavelengths, where dominant one-photon transitions generally are absent. This means that better depth penetration can be obtained in a sample. Moreover, because the probability of absorbing two photons increases quadratically with the photon flux, excited state production can be limited to a small volume defined by a focussed laser where a sufficiently high fluence is obtained.

Singlet oxygen production using a sensitizer can be quantified according to,[9]

$$\Phi_\Delta = p_S^{O_2} f_S^\Delta + \Phi_T p_T^{O_2} S_\Delta , \quad (1.1)$$

where $p_S^{O_2}$ and $p_T^{O_2}$ are the fractions of S_1 and T_1 states quenched by oxygen, f_S^Δ, is the efficiency of singlet oxygen production during O_2 quenching of S_1, and Φ_T is the triplet quantum yield. The parameter S_Δ is the efficiency of singlet oxygen production during O_2 quenching of T_1. Because of long triplet lifetimes, the main pathway for singlet oxygen generation is $O_2(X^3\Sigma_g^-)$-quenching of the T_1 state of the sensitizer and this process occurs almost with complete quenching ($p_T^{O_2} \approx 1$). Incomplete quenching is observed when the triplet state has a short lifetime, due, for example to fast intersystem crossing or in the presence of other quenchers. Even though $p_T^{O_2} \approx 1$, most sensitizers have S_Δ values smaller than unity.[9]

The electronic configuration of the photosensitizer triplet state is of importance for the S_Δ value. Sensitizers with a ketone functionality and a $n\pi^*$-T_1 state, have S_Δ values in the range 0.3-0.5. However, sensitizers containing multiple ketone functionalities have S_Δ values near unity. The efficiencies of singlet oxygen generation from $\pi\pi^*$-excited states of aromatic hydrocarbons are near unity when the $S_0 \rightarrow T_1$ transition energy is very high or the oxidation potential is very low. Similar observations have been made for $\pi\pi^*$-excited aromatic ketones. The presence of heavy atoms in the sensitizer also promotes singlet oxygen generation if the triplet state originates from an $n\pi^*$-state. Studies of $n\pi^*$-excited halogenated acetone derivatives showed a correlation between the S_Δ values and the square of the spin-orbit coupling term of the halogen atom. No effect of a heavy atom on the S_Δ value was found for the similar $\pi\pi^*$-excited acetone derivatives. Apart from carbonyl groups and heavy atoms, the oxidation potential of the sensitizer also influences the singlet oxygen generation but different dependencies of S_Δ on E_{ox} with different classes of sensitizers are found in the literature.[9]

The discussion above serves to illustrate that the factors determining whether or not a sensitizer has a high Φ_Δ value are complex issues. Nevertheless, some guidelines exist. Since singlet oxygen typically is generated by quenching the sensitizer triplet state, a high triplet quantum yield often characterizes a molecule with a high Φ_Δ value.[9] Functional groups that promote intersystem crossing are carbonyl groups, heavy atoms and heterocycles with non-bonding π-electrons in orbitals perpendicular to the rest of the aromatic π-electron system (*i.e.* pyridine). These findings can be explained by the expression for spin-orbit coupling matrix elements and conservation of the total angular momentum. The latter is formulated in more general terms in the El-Sayed selection rules, which states that changes in orbital occupancy and hence, orbital angular momentum, facilitate changes in spin angular momentum. Thus, transitions such as $^1(\pi\pi^*)\rightarrow{}^3(n\pi^*)$ or $^1(n\pi^*)\rightarrow{}^3(\pi\pi^*)$ are allowed.[11,12] There exist some empirical relations correlating the rate constant for singlet oxygen production with certain molecular properties of the sensitizer.[13] Recently it has been established that the rate constant for singlet oxygen production from the ππ*-excited state of the sensitizer can be expressed as,[9,13]

$$k_T = k_{\Delta E} + k_{CT}\,, \tag{1.2}$$

where k_T is the total rate constant for singlet oxygen production, $k_{\Delta E}$ is the contribution to the total rate constant due to a non-charge transfer encounter complex between the sensitizer and oxygen, and k_{CT} is the contribution due to a charge transfer encounter complex between the sensitizer and oxygen. An empirical relation between $\log(k_{\Delta E})$ and the excess energy ΔE (the T_1-S_0 energy difference of the sensitizer minus the $O_2(b^1\Sigma_g^+)$-$O_2(X^3\Sigma_g^-)$ or the $O_2(a^1\Delta_g)$-$O_2(X^3\Sigma_g^-)$ energy difference) was found to be a fourth order polynomial.[13] An empirical relation for $\log(k_{CT})$ was also found to be,

$$\log(k_{CT}) = c_0 + c_1 - c_2\Delta G_{CET}\,, \tag{1.3}$$

where c_1 and c_2 are positive empirical constants and ΔG_{CET} is the free energy for complete energy transfer from the T_1-excited sensitizer to O_2 and is given by the Rehm-Weller equation,

$$\Delta G_{CET} = F(E_{ox} - E_{red}) - E_T + C, \tag{1.4}$$

where F is the Faraday constant, E_{ox} is the oxidation potential of the sensitizer, E_{red} is the reduction potential of molecular oxygen, E_T is the triplet energy of the sensitizer and C is the electrostatic interaction energy. Thus, the rate constant for singlet production from a ππ*-excited sensitizer seems to be dependent on two major properties of the sensitizer, the oxidation potential and the triplet energy. Nevertheless, as pointed out above, other dependencies may be observed for nπ*-excited sensitizers.[13]

1.3 Singlet and triplet excited states

A great deal of work has been done on the photophysical characterization of oligo- and polyphenylene vinylenes, oligo- and polythiophenes, and oligo- and polyenes particularly in the context of two-photon absorption.[14-23] Oligo phenylene-vinylenes have also been shown to be efficient two-photon singlet oxygen sensitizers.[24,25] It is obvious then to use the oligo phenylene-vinylene skeleton as a template for deducing molecular design principles in making efficient two-photon singlet oxygen sensitizers.

As discussed above, oxygen quenching of sensitizer triplet states is efficient. Thus, a large triplet quantum yield is a desirable property of a potential singlet oxygen sensitizer. It is therefore important to have some insight in to the relation between molecular structure and the photophysical properties. Radiative decay (fluorescence) is unwanted in designing a molecule with a high triplet quantum yield as this process depopulates the first singlet excited state resulting in a low triplet quantum yield. The parity of the S_1 state is important for determining whether or not the molecule fluoresces as typical polyenes can only fluoresce if the S_1 state is ungerade (see Figure 1-4).[11]

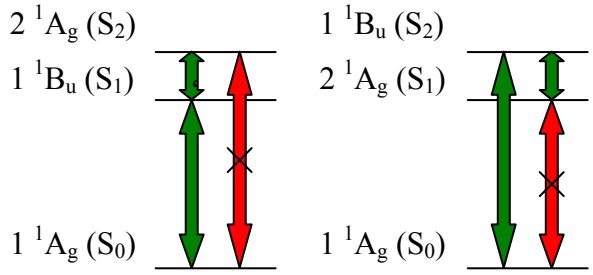

Figure 1-4: Ground state (1 ^1A_g or S_0), lowest one-photon allowed singlet excited state (1 ^1B_u) and lowest two-photon allowed singlet-excited state (2 ^1A_g) for oligothiophenes and oligophynelene vinylenes (2 ^1A_g > 1 ^1B_u) (left) and linear polyenes (2 ^1A_g < 1 ^1B_u) (right). Allowed transitions are indicated with double-headed arrows (representing absorption and emision), forbidden transitions with crossed arrows.

In general, a decrease of the separation of ground and excited state is observed with increasing oligomer size as a result of the extension of the π-delocalized system.[26,27] However, the S_0-S_1 excitation energy changes more with the chain length than that of S_0-T_1.[28-30] Enhancement in rate constants for intersystem crossing for longer chains is also observed and attributed to a lowering of the S_1-T_1 energy gap for longer chains:[29,31] Apparently, molecules with longer conjugation lengths seems to have higher triplet quantum yield which then translates into a design principle for making singlet oxygen sensitizers.

In general, intersystem crossing occurs when the molecule adopts a critical geometry such that the singlet and triplet potential energy surfaces are almost equal in energy. For example, molecular vibrations that lead to electric dipoles in the same region of space, such as the transition dipoles for the singlet and triplet state, are favourable for achieving high intersystem crossing rate constants. Intersystem crossing typically occurs between (nπ*) and (ππ*) states meaning that vibrations that cause displacement of atoms possessing substantial n- or π-electron density are favourable. Such vibrations can be envisaged in displacement of *i.e.* oxygen or nitrogen atoms.[12] Other methods to increase the rate constant for intersystem crossing is to introduce heavy atoms in the molecule, which has sound theoretical basis in Fermi's golden rule: The rate constant for intersystem crossing in many molecules is proportional to the squared atom number of the heavy atom.[11,12] The design principle deduced from these observations, is that functional groups containing oxygen, nitrogen or halogen

atoms pendant on a π-conjugated system should be optimal for obtaining a high singlet oxygen quantum yield.

As will be pointed out below, the sensitizers designed and prepared in the present work typically have electron acceptor-donor architectures due to the desire to have large transition dipole moments between the ground and excited singlet state. Acceptor-donor molecules often have excited states with charge-transfer character. It is then expected that the encounter complex between an excited state sensitizer molecule and oxygen also will posses some CT character.

Intersystem crossing for certain exciplexes has been investigated by Gould and co-workers,[32-34] where particular acceptor/donor/solvent combinations were used to control the extent of charge-transfer character in the exciplexes ranging from essentially zero to complete charge-transfer (radical anion-radical cation pairs). In a more recent work, Gould and co-workers investigated the dependence of the intersystem crossing rate constant as a function of the S_1-T_1 energy gap for the same system.[32] They found an exponential relation between the intersystem crossing rate constant and the S_1-T_1 energy gap and furthermore discussed the mechanism responsible for intersystem crossing in molecules with charge-transfer excited states; In a mainly localized excited singlet state of a donor-acceptor exciplex ($^1A^*D$), intersystem crossing leads directly to the locally excited triplet state ($^3A^*D$) and the rate constant increases with decreasing S_1-T_1 energy gap. The mechanism for intersystem crossing is, in this case, supposed to be spin-orbit coupling. If the excited state of the exciplex is pure ion-like ($^1A^{\cdot-}D^{\cdot+}$), intersystem crossing can occur directly to the locally excited triplet state ($^3A^*D$) or through an intermediate triplet charge-transfer state ($^3A^{\cdot-}D^{\cdot+}$) followed by electron transfer to the locally excited triplet state and the rate constant for intersystem crossing is not dependent on the S_1-T_1 energy gap.[32] Lim has shown[35] that, in the one-electron approximation, the spin-orbit coupling matrix elements between the ($^1A^{\cdot-}D^{\cdot+}$) and ($^3A^{\cdot-}D^{\cdot+}$) states are zero as the orbital occupation is the same for each state making the hyperfine interactions responsible for intersystem crossing between these two states. Direct evidence for this mechanism has been obtained in covalently linked donor/acceptor systems.[36-42] Hyperfine interactions can only expected to be of importance for promoting intersystem crossing when the energy difference between the singlet and triplet CT

states (the ($^1A^{\cdot-}D^{\cdot+}$) and ($^3A^{\cdot-}D^{\cdot+}$) states) is small, *i.e.* when electronic coupling is weak between the donor and acceptor parts.[32] Indeed, hyperfine interactions have been shown to govern singlet oxygen production[43] but it is not possible to deduce structure-property relations for the sensitizers, where hyperfine interactions are responsible for the generation of singlet oxygen. This serves to illustrate that it is indeed difficult *a priori* to determine whether a given molecule is a good singlet oxygen sensitizer. By moderating the extent of CT character in the sensitizer, the CT character in the sensitizer-oxygen encounter complex should also be moderated thus avoiding a pure ion-like complex. It has been ascertained that, in a given sensitizer and/or sensitizer-oxygen complex, significant CT character can adversely affect singlet oxygen yields by providing an independent pathway for the deactivation of sensitizer excited stated states that competes with energy transfer to $O_2(X^3\Sigma_g^-)$.[44,45] In the present context, it is expected that the extent of intermolecular CT character in the sensitizer complex will reflect the extent to which intramolecular charge seperation occurs in the sensitzer. Control of the CT character can be controlled by careful selection of the donor and acceptor groups in the sensitizer molecule.

1.4 Two-photon absorption

A second dimension to the problem of generating singlet oxygen is now considered: The singlet oxygen sensitizer needs to be a good two-photon absorber as well as generate singlet oxygen in high yield. Thus, in the following the design principles for making molecules with a large two-photon absorption cross section are discussed.

The simultaneous absorption of two photons by a molecule or an atom leading to an electronic transition with an energy corresponding to the combined energy of the photons involved was first proposed by Maria Göppert-Mayer[46] in 1931. She suggested the possibility of this event on the basis of Dirac's second order pertubation theory. However, the process is improbable and in order to observe the process a very high irradiating intensity is needed for two photons to combine at the same point in space and at the same point in time. The development of high-energy pulsed lasers facilitated the experimental confirmation of this process in an experiment in 1961, where Eu^{3+} was excited in a two-photon absorption process.[47] In the recent years, aided by the development of femtosecond lasers, the community has seen great

success in the development of materials with large two-photon absorption cross sections. Such materials have given new impetus for the design of imaging applications,[48-52] optical limiters, 3D microfabrication,[53-55] lasing materials[56-58] and also two-photon sensitized production of singlet oxygen.[24,25,59,60]

In a two-photon excitation event, the molecule is excited through a virtual state as illustrated in Figure 1-5.

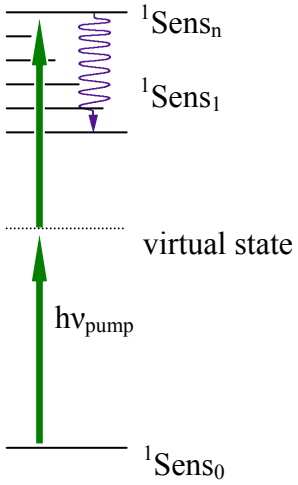

Figure 1-5: Two-photon excitation through a virtual state.

The virtual state can be considered as a linear combination of the real states of the molecule. The two-photon absorption cross section, δ, is a parameter that describes how well a molecule absorbs two photons and, as such, is the analogue of the one-photon cross section which is directly related to the molar absorption coefficient. The two-photon cross section can be defined as,[50]

$$\delta = \Delta t \cdot \Delta A \cdot \sigma , \tag{1.5}$$

where Δt is the time-interval in which the two photons are combined, ΔA is the spatial area in which they combine, and σ is the one-photon absorption cross section. A typical cross section for a one-photon excitation is 10^{-17} cm^2. Even though the one-photon absorption cross section has the unit of an area, it should not be mistaken for the actual area of interaction. The two-photon absorption cross section is seen to have the unit $cm^4 \cdot s$ and this combination of SI units has been given the name a Göppert-

Mayer (GM) unit (10^{-50} $cm^4 \cdot s$ = 1 GM). It is often seen in the literature that per photon and per molecule is "attached" to the SI-unit ($cm^4 \cdot s \cdot molecule^{-1}$ and $cm^4 \cdot s \cdot molecule^{-1} \cdot photon^{-1}$) but this is unnecessary and misleading because *per molecule* and *per photon* is already specified in that we are looking at a cross section of interaction (an intrinsic property). It is also improper use of SI units. Most molecules have two-photon cross sections between 0.1 GM-10 GM, however designing molecules properly can lead to cross sections (claimed) as large as 4000 GM.[61]

Within the electric dipole approximation the two-photon absorption cross sections of a molecule can be calculated using Eq. (1.6),[46,60,62]

$$\delta = \frac{\pi^2 e^4}{c^2 \varepsilon_0^2 h^2} \omega^2 \left| \sum_i \frac{\left\langle \Psi_f \left| \vec{\mu} \right| \Psi_i \right\rangle \left\langle \Psi_i \left| \vec{\mu} \right| \Psi_g \right\rangle}{\omega_i - \omega} \right|^2 g(2\omega), \tag{1.6}$$

where e is the charge of the electron, c is the speed of light, ε_0 is the vacuum permittivity, h is Planck's constant, ω is the laser frequency, $g(2\omega)$ is the line width function (Gaussian) of the final state, $\vec{\mu}$ is the dipole operator, Ψ_f is the final state, Ψ_i is an intermediate virtual state, g is the ground state, and ω_i is the energy between the ground state and the intermediate state expressed as a frequency. An inspection of Eq. (1.6) reveals three ways of increasing the two-photon absorption cross section. These are discussed below.

Narrowing the excitation bandwidth of the line width function, $g(2\omega)$, will result in an increase of the line width function at its maximum value since it is a normalized function. Decreasing the width of the line width function is done by narrowing the density of states function for the final electronic state, which means fewer vibrational states in the vicinity of the excited state. By increasing the conjugation length of a π-conjugated system an increase of the density of states for all the electronic states is obtained. Thus, attempting to decrease the line width function is not a viable strategy as large π-conjugated molecules are one of the requirements for the molecules pertinent to the present work.

An obvious possibility is to have a one-photon transition close to the two-photon laser frequency. This will create a singularity in Eq. (1.6) as a ω_i-ω difference of zero would be obtained. In practice, this would require a one-photon allowed transition in the area of 800 to 1200 nm, and not many molecules have one-photon absorption maxima in that area. A possible strategy to achieve transition energies in that wavelength region is to have a large conjugation length but this would then impose solubility problems. Some examples exist of molecules that absorb in the near infrared. Cho and co-workers[63], for example, have reported the one-photon maxima of a series of long oligoporphyrins.

The most common approach in the molecular design of molecules with large TPA cross sections is to introduce functional groups in the molecules that give rise to large transition dipole moments.[61,64-66] A variety of molecular templates have been used in this approach including distyrylbenzenes and naphthalene derivatives.[24,25,61,64-68] Most of these compounds are centrosymmetric and are designed for use as fluorescence probes. High transition dipole moments, however, are not always necessary to obtain molecules with large TPA cross sections. Polyfluorenes, for example, exhibit a large cross section of approximately 70,000 GM. This large value has been suggested to be the result of the high molecular weight and therefore larger conjugation compared to low molecular weight molecules.[69] Similar findings have been obtained for certain dendrimers.[70]

In the following, a "molecular gallery" will be presented of some of the more recent developed molecules with high TPA cross sections. This gallery also demonstrates some of the molecular design principles discussed above.

1.4.1 Naphthalene derivatives

The first work on two-photon photosensitised production of singlet oxygen was carried out using sensitizers based on a naphthalene template (see Figure 1-6).[24,25]

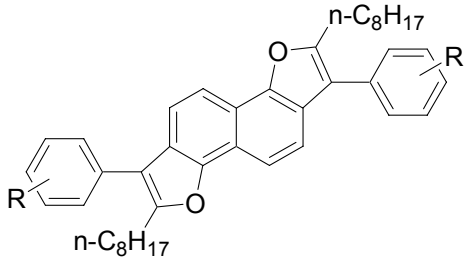

Functional group		TPA cross section (GM) in toluene
R =	H	8
	4-CN	139
	4-CHO	205
	4-Br	7
	4-COPh	70

Figure 1-6: Naphthalene-based sensitzers used for two-photon photosensitised production of singlet oxygen. The TPA cross sections were determined by measuring relative cross sections using *E,E*-2,5-dicyano-1,4-bis-[2-(4'-diphenylamino-phenyl)-vinyl]-benzene as the standard.[24,25]

The sensitizers in Figure 1-6 can be characterized as acceptor-donor-acceptor molecules with benzene rings as π-linkers. Octyl groups have been introduced to facilitate solubility in toluene. The TPA cross sections given in Figure 1-6 were measured using the phosphorescence intensity from singlet oxygen: The photosensitized production of singlet oxygen was used to probe the efficiency of light absorption by the sensitizer in a two-photon process. In these experiments, a laser is focused into a solution of the sensitizer in toluene. The time-resolved 1270 nm phosphorescence of singlet oxygen [$O_2(a^1\Delta_g) \rightarrow O_2(X^3\Sigma_g^-)$] is then monitored from the laser beam focal point. The intensity of the singlet oxygen signal thus detected, normalized by the singlet oxygen quantum efficiency of that particular molecule, yields a parameter that is proportional to the two-photon absorption cross section. Absolute values for the cross section can be obtained by comparing these relative data to data similarly recorded from *E,E*-2,5-dicyano-1,4-bis-[2-(4'-diphenylamino-phenyl)-vinyl]-benzene as the TPA cross section for this compound has been reported in the literature.[61]

1.4.2 Distyryl benzene derivatives

The standard used for measuring the TPA cross sections in the present work is *E, E*-2,5-dicyano-1,4-bis-[2-(4'-diphenylamino-phenyl)-vinyl]-benzene shown in Figure 1-7.

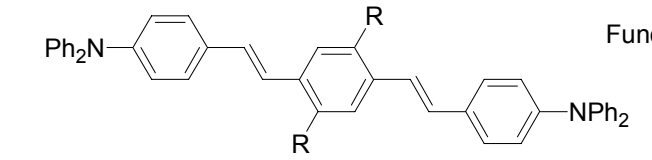

Functional group		TPA cross section (GM) in toluene	
R =	Br	450	
	CN	**1890**	**standard**

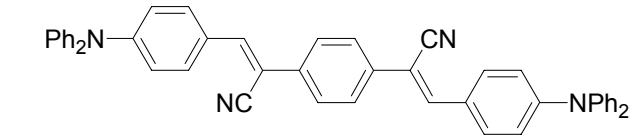

690

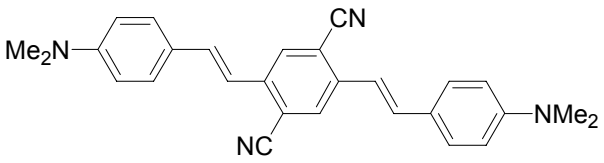

1750

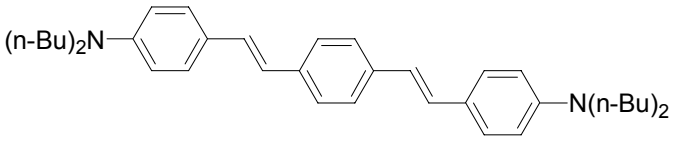

995

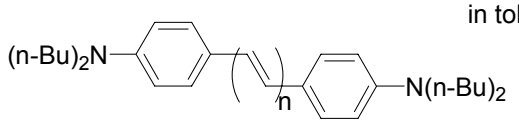

	Fluorescense quantum yield in toluene	TPA cross section (GM) in toluene
n = 1	0.90	200
2	0.80	260
3	0.76	320
4	0.42	425
5	0.023	1300

Figure 1-7: Molecules investigated by Marder and coworkers.[61,64-66,68] The TPA cross sections were measured by monitoring the fluorescence intensity subsequent to two-photon initiation. The standard used for the measurements was flourescein and the experiments were done on a nanosecond laser system with toluene as the solvent.

Marder and co-workers[55,61,65,66,68] have prepared and investigated a series of compounds similar to those in Figure 1-7, in which both the number of double bonds separating the benzene rings and also the end-group functionalization were varied. However, from a chemical perspective, the variations observed in the cross sections as a function of these changes are not very systematic.[55,61,65,66,68] Nevertheless, the authors of these studies have deduced some structure-property relations for the TPA cross section stating that an increase in conjugation length and increasing donor and acceptor strengths of the substituents leads to larger TPA cross sections. Similar observations were reported by Strehmel and co-workers[67] who investigated compounds resembling the distyryl benzenes in Figure 1-7.

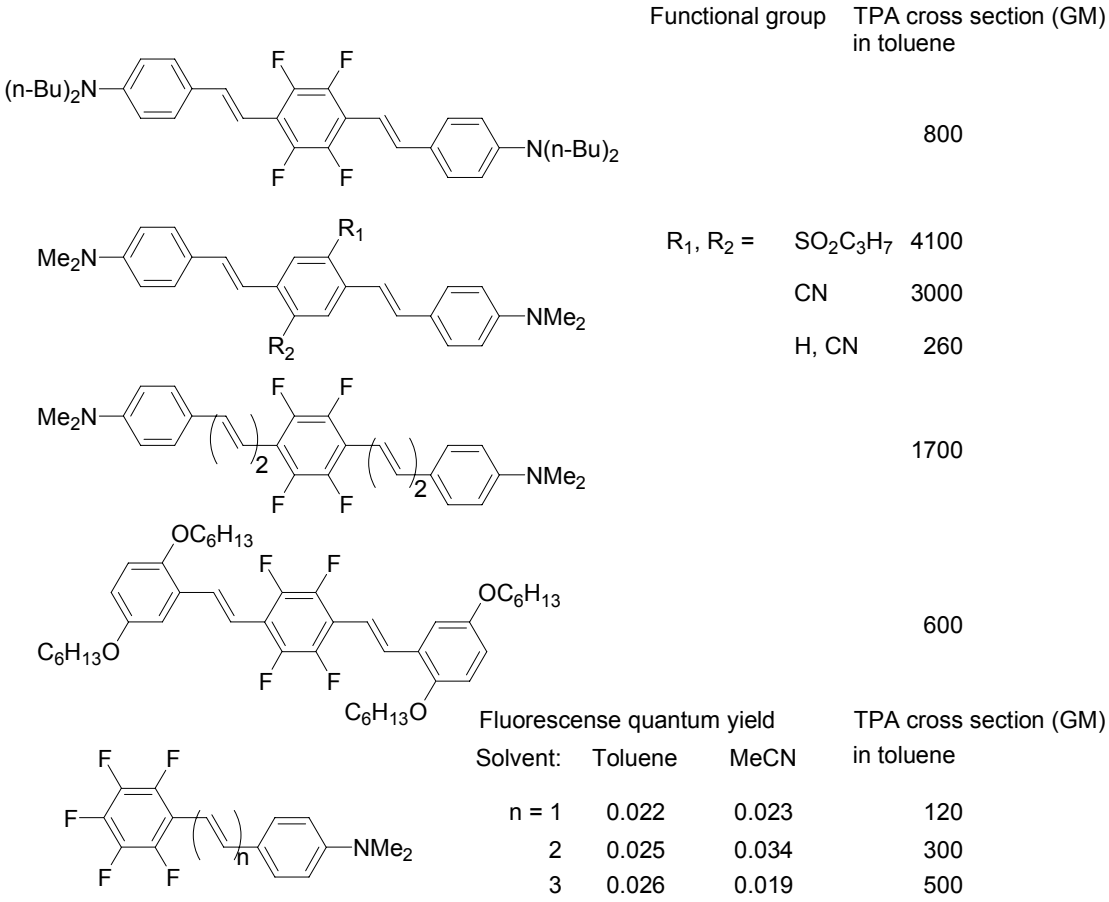

Figure 1-8: TPA cross sections and fluorescence quantum yields for the compounds prepared and investigated by Strehmel and co-workers.[67] The cross sections were determined by monitoring fluorescence, using fluorescein fluorescence as the standard. The experiments were done with a femtosecond laser system using toluene as the solvent.

It is particularly noteworthy that Strehmel[67] and Marder[55,61,65,66,68] both have measured a TPA cross section for *E, E*-2,5-dicyano-1,4-bis-[2-(4'-dimethylamino-phenyl)-vinyl]-benzene. Strehmel reports a value of 3000 GM (using femtosecond laser pulses) and Marder reports 1750 GM (using nanosecond laser pulses and 1710 GM using femtosecond laser pulses), and both groups have used the same fluorescence standards (fluorescein in water at pH 11). Strehmel uses another standard as well, *E, E*-2,5-dicyano-1,4-bis-[2-(4'-dibutylamino-phenyl)-vinyl]-benzene (see Figure 1-7) in toluene, where the TPA cross section is reported by Marder to be 995 GM. Thus, the relative numbers of the TPA cross sections reported by Strehmel are not the same as those reported by Marder even though they use the same standards. In fairness, it

should be noted that large errors accompany reported values of TPA cross sections as there are many variables in the measurements of an absolute TPA cross section.[59]

Tykwinski *et al.* have stated[71] that molecules with no inversion symmetry elements appear to the most promising candidates to have a large nonlinear optical properties, and thereby a large TPA cross section. These findings are based on the measured hyperpolarizabilities, γ, for the molecules in Figure 1-9 using the third harmonic generation technique: The imaginary part of the second hyperpolarizability is proportional to the TPA cross section.[72]

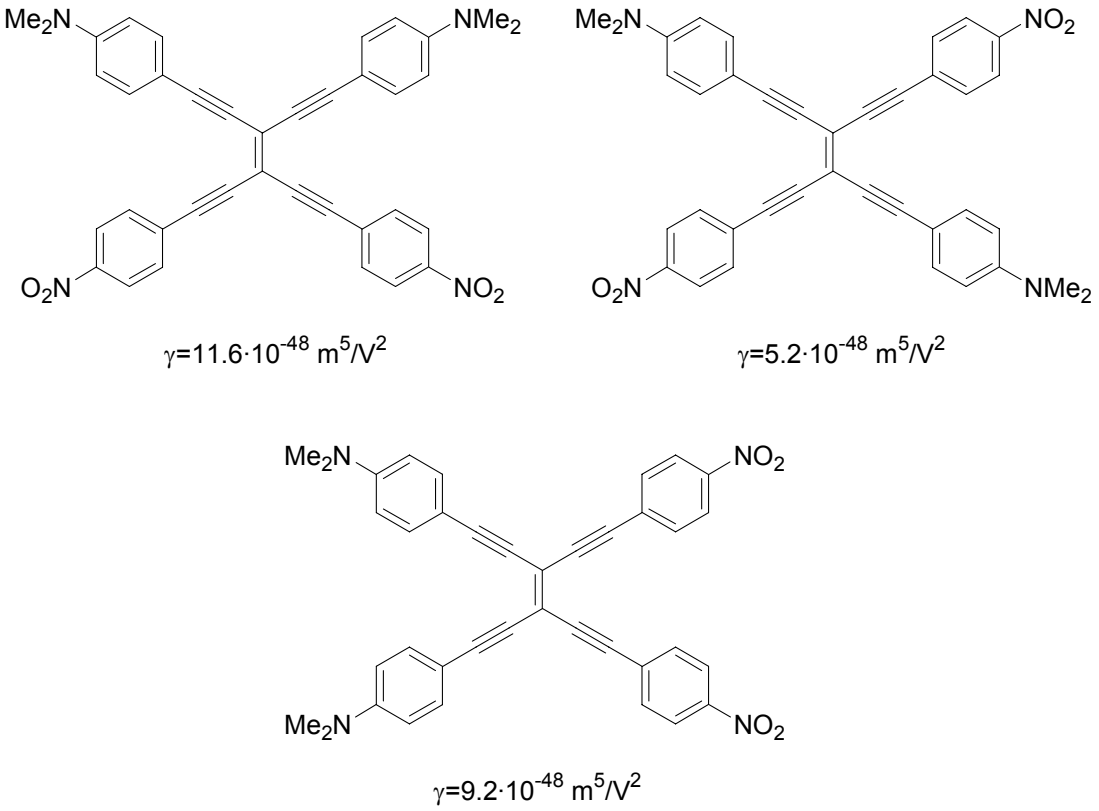

Figure 1-9: Second hyperpolarizability as a ”function” of symmetry.

From these data, they noted a clear increase in γ when changing from centrosymmetric molecules to acentric compounds. A similar trend is then expected for the TPA cross section as well. All the distyryl benzenes studied by Marder, Strehmel and other groups have an inversion center but nevertheless have large cross sections. For a centrosymmetric molecule, the TPA maximum does not occur at twice the wavelength of the one-photon absorption maximum.

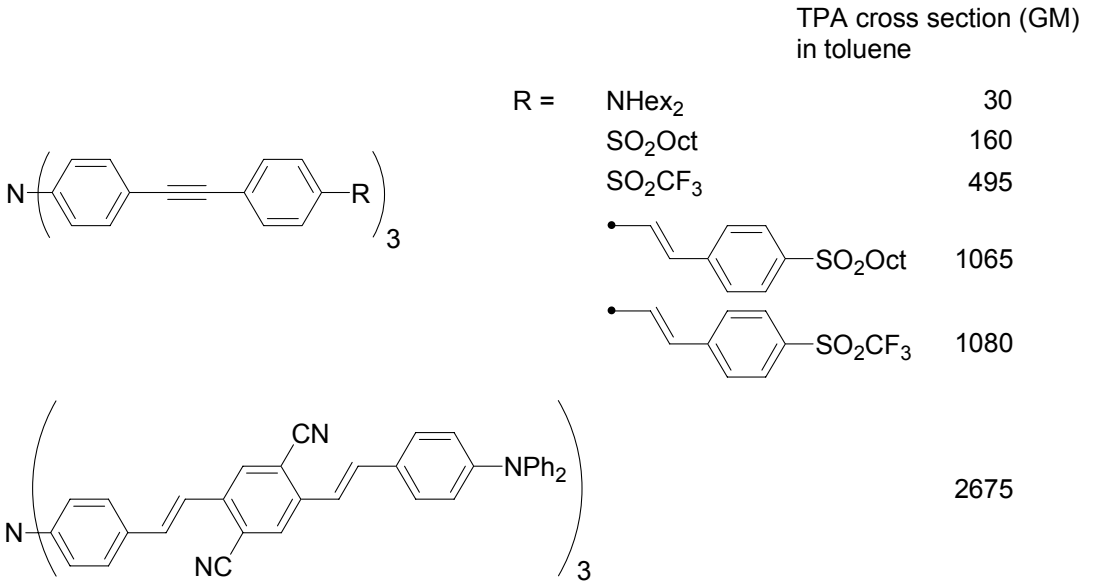

Figure 1-10: Examples of other molecules that have been shown to posses large TPA cross sections.[73,74]

Common to most of the newly synthesized molecules that posses large TPA cross sections is that amino groups (mostly diphenylamine) are used as electron donors.[73,74]

Marder[55,61,65,66,68] and Strehmel[67] have both measured fluorescence quantum yields for a series of oligoenes. The compounds investigated by Marder (see Figure 1-7) have electron donating groups (dibutylamino) at each end of the oligoene chain and the compounds investigated by Strehmel have an acceptor in one end and a donor in the other end of the oligoene chain. The fluorescence quantum yields of the donor-donor oligoenes show the same dependence on the number of double bonds: The fluorescence quantum yields decreases with increasing number of double bonds. The quantum yields of the donor-acceptor oligoenes are small (<0.05) and seem unaffected by the number of double bonds. However, the donor-acceptor molecules do not have an inversion center so it is not possible to assign parity to the excited states.

Common to all of the examples illustrated above is that strong electron donor and acceptor groups and an increase in conjugation length seem to give a high TPA cross section.

1.5 Synthetic strategies

The main conclusions drawn from the survey presented above regarding the molecular design of two-photon absorbers and singlet oxygen sensitizers can be summarized in the following points:

1. It is difficult to predict, based solely on the structure, whether a molecule will be a good two-photon singlet oxygen sensitizer or not. However, because it is easier to predict if a molecule will have a large triplet quantum yield, the singlet oxygen sensitizer is designed to have such and then tested experimentally to see if it makes singlet oxygen in high yield.
2. Large conjugation lengths and polarizable groups can give large TPA cross sections and large triplet quantum yields.
3. Strong electron donating and withdrawing groups in a donor-acceptor type molecule can give large TPA cross sections (due to charge-transfer) but this might be counter productive as charge transfer can shut down singlet oxygen production.
4. Heavy atoms such as bromine promotes intersystem crossing due to an increasing spin-orbit coupling in the molecule. Also, carbonyl groups and in general functional groups with non-bonding (occupied) π-orbitals perpendicular to the rest of the molecular π-electron system promotes intersystem crossing according to El-Sayed's selection rules. However, if one functional group promoting intersystem crossing is already present in the molecule, introducing further groups with the intent to increase the intersystem crossing rate constant may have a minimal effect.

These points have been used as guidelines for preparing the singlet oxygen sensitizers in the present work. The syntheses carried out centers around assembling a specific molecular framework substituted with a variety of functional groups. Typically the sensitizer consists of aryl groups connected by polarizable π-linkers such as double and triple bonds (see Figure 1-11).

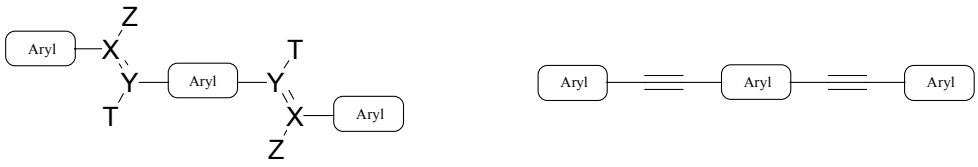

Figure 1-11: A schematic representation of molecules typically used for non-linear optical applications.

The strategy applied in the present work is to first synthesize the aryl building blocks and then couple them into the target molecule late in the synthetic scheme. This means that the functional groups needed for the coupling must be compatible with the chemistry needed for assembling the aryl groups, and also the other way around. The functional groups introduced are typical donor and acceptor groups such as amino and nitro groups. In the present work, strategies have also been devised to introduce functional groups that impart water solubility. Water solubility can be achieved either by having the sensitizer as a salt and/or by having enough non-ionic hydrophilic functionalizations present in the sensitizer. An example of a non-ionic functional group that imparts water solubility is polyethylene glycol.

The reactions that have been successfully applied in the present work to assemble aryl building blocks are the Horner-Wadsworth-Emmons (HWE), Heck-coupling, and the Knoevenagel reactions. A wide variety of reactions have been used to prepare the aryl building blocks and the details of these synthetic steps will be presented in following chapters.

1.6 Measurements of TPA cross-sections

The TPA cross sections reported in the present work were determined by monitoring the singlet oxygen phosphorescence signal from the sensitizer upon irradiation with a laser beam, and comparing the signal observed with that observed from a standard as described earlier (see above and Ref. 59) The experimental setup is shown in Figure 1-12 and is described in Ref. 75, 60 and 59.

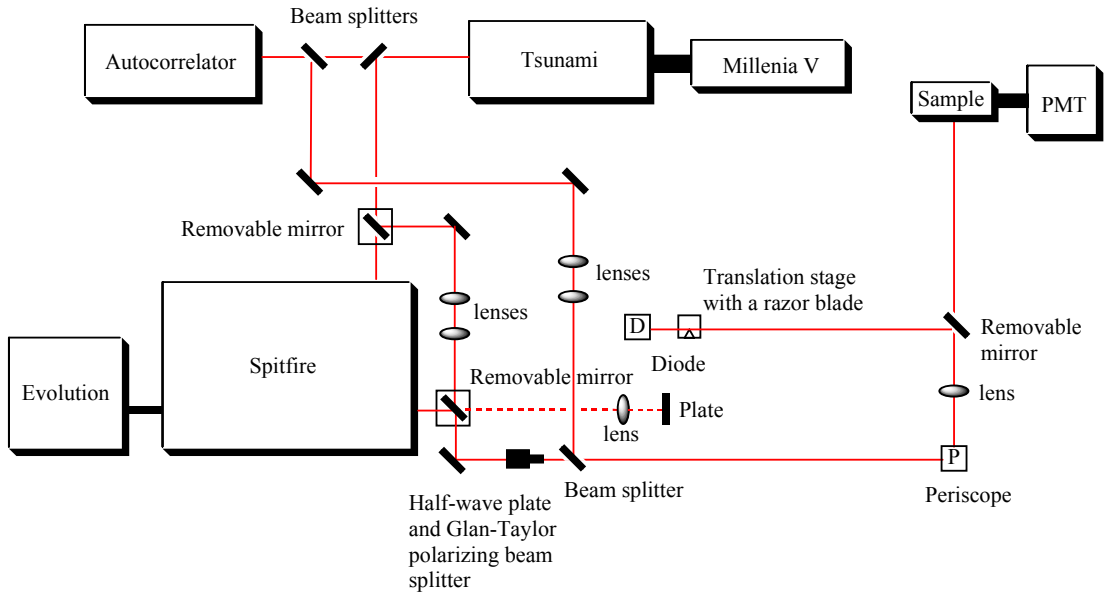

Figure 1-12: Experimental setup used for measuring the TPA cross section using the singlet oxygen phosphorescence technique.

In short, the heart of the system is the femtosecond laser (the Millenia V and Tsunami in Figure 1-12) that is operated at 80 MHz. This laser is set to pump an amplifier (Spitfire) whose primary purpose is to reduce the repetition rate to 1 kHz, which is suitable for singlet oxygen experiments [$O_2(a^1\Delta_g)$ has a comperatively long lifetime]. The singlet oxygen phosphorescence intensity is measured by placing a 1270 nm filter in front of a photomultiplier tube (PMT), which is used in a single photon counting mode. The action spectra were recorded varying the wavelength of the laser beam from 765 nm to 845 nm. At each wavelength, measurements with different powers of the beam were carried out. Singlet oxygen is generated from the irradiated sample (as discussed previously) by quenching the formed sensitizer triplet state with ground state oxygen. By monitoring the intensity of light at 1270 nm as a function of time after excitation with the laser beam, a decay spectrum as the one depicted in Figure 1-13, is observed.

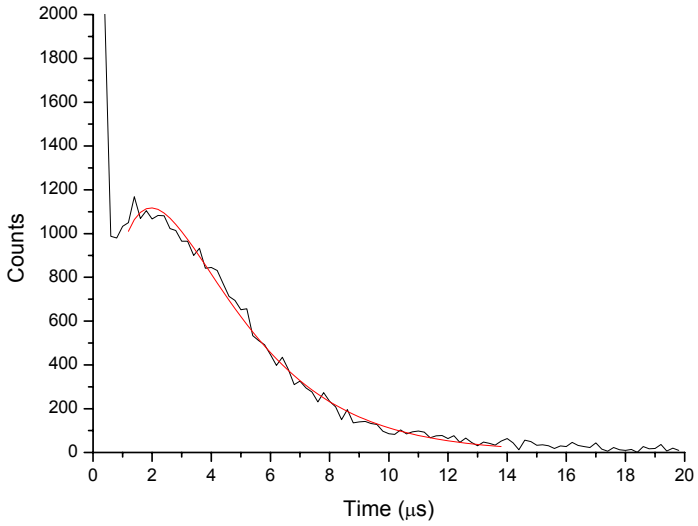

Figure 1-13: Typical decay spectrum obtained by single photon counting the singlet oxygen phosphorescence intensity as a function of time after irradiation with the laser beam. The intense "spike" preceding the singlet oxygen signal is due to a combination of sensitizer fluorescence, scattered laser light, and luminescence from the optics used. The data were recorded from an H_2O solution.

The spike occurring right after excitation is due to scattered laser light, residual fluorescence from the sample and luminescence from the optics. The rising and falling components (consisting of two exponential functions) are due to the formation and decay of singlet oxygen. In order not to detect the residual fluorescence in the experiment, the PMT only detects the intensity of the 1270 nm light some time after the sample is irradiated by the laser beam. This signal is corrected for background light by subtracting the intensity measured after the singlet oxygen phosphorescence decay has died off. Such data are recorded for both the molecule under study as well as the standard sensitizer. The TPA cross section is then calculated according to,

$$\delta_{sample} = \frac{I_{\Delta}^{sample}\Phi_{\Delta}^{standard}C_{standard}}{I_{\Delta}^{standard}\Phi_{\Delta}^{standard}C_{sample}} \cdot \delta_{standard} \cdot N_{\lambda}, \tag{1.7}$$

where I_{Δ}^{sample} and $I_{\Delta}^{standard}$ are the singlet oxygen phosphorescence signals, Φ_{Δ}^{sample} and $\Phi_{\Delta}^{standard}$ are the singlet oxygen quantum yields, C_{sample} and $C_{standard}$ are the concentrations, and δ_{sample} and $\delta_{standard}$ are the two-photon absorption cross sections

for the sample and standard, respectively. N_λ is a wavelength dependent normalization constant determined from the action spectra of the standard. As the standard *E,E*-2,5-dicyano-1,4-bis-[2-(4'-diphenylamino-phenyl)-vinyl]-benzene was chosen (shown in Figure 1-7 and Figure 1-14). The measurement of the action spectrum of this compound was described in Ref. 60 and 59. The spectrum is shown in Figure 1-14.

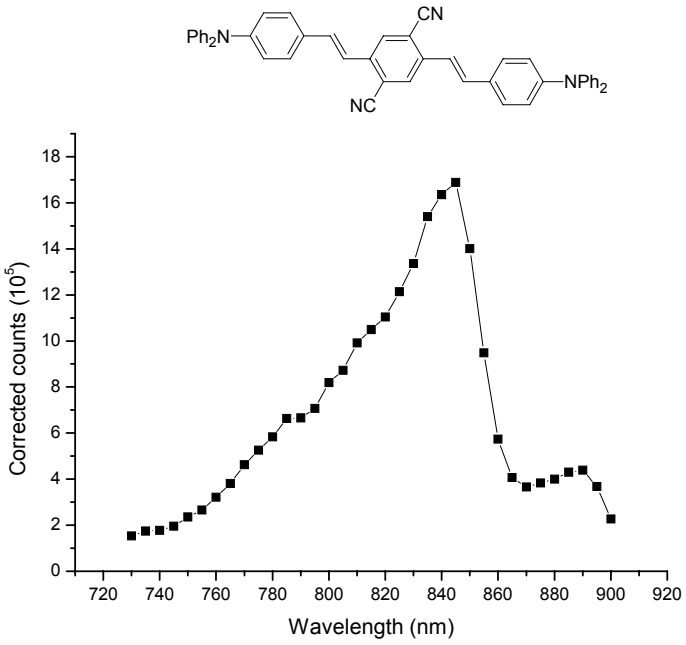

Figure 1-14: TPA action spectrum of the standard used in the present work.

The TPA maxima is observed at 845 nm in agreement with Ref. 61 and 65. However, the absolute TPA cross section was determined to be 210±34 GM in Ref. 60, whereas a number of different values ranging from 15.4 GM at 808 nm[76] to the remarkably large values of 1890 GM, 1940 GM and 3670 GM has been reported.[61,65] In the following, the cross sections measured for a given molecule at a given wavelength will simply be reported relative to the standard. Assignment of the absolute cross section can then occur once an acceptable value for the standard has been obtained.

Reference List

1. Sheats, J. R.; Roitman, D. B. *Synth. Met.* **1998**, *95*, 79-85.
2. Scurlock, R. D.; Wang, B. J.; Ogilby, P. R.; Sheats, J. R.; Clough, R. L. *J. Am. Chem. Soc.* **1995**, *117*, 10194-10202.
3. Cumpston, B. H.; Jensen, K. F. *Trends in Polymer Science* **1996**, *4*, 151-157.
4. Foote, C. S., Valentine, J. S., Greenberg, A., and Liebman, J. F. Ed. *Active Oxygen in Chemistry*; Chapman and Hall: London, 1995.
5. Frimer, A. A. Ed. *Singlet Oxygen*; CRC Press: Boca Raton, 1985; Vol. I-IV.
6. Wilkinson, F.; Helman, W. P.; Ross, A. B. *J. Phys. Chem. Ref. Data* **1995**, *24*, 663-1021.
7. Wilkinson, F.; Helman, W. P.; Ross, A. B. *J. Phys. Chem. Ref. Data* **1993**, *22*, 113-262.
8. Ogilby, P. R.; Kristiansen, M.; Martire, D. O.; Scurlock, R. D.; Taylor, V. L.; Clough, R. L. *Adv. Chem. Ser.* **1996**, *249*, 113-126.
9. Schweitzer, C.; Schmidt, R. *Chem. Rev.* **2003**, *103*, 1685-1757.
10. Herzberg, G. *Molecular Spectra and Molecular Structure. I. Diatomic Molecules*; Prentice-Hall: New York, 1939.
11. Klessinger, M.; Michl, J. *Excited States and Photochemistry of Organic Molecules*; VCH Publishers, Inc.: New York, 1995.
12. Turro, N. J. *Modern Molecular Photochemistry*; University Science Books: Sausalito, 1991.
13. Schweitzer, C.; Mehrdad, Z.; Noll, A.; Grabner, E. W.; Schmidt, R. *J. Phys. Chem. A* **2003**, *107*, 2192-2198.
14. Greenham, N. C.; Moratti, S. C.; Bradley, D. D. C.; Friend, R. H.; Holmes, A. B. *Nature* **1993**, *365*, 628-630.
15. Katz, H. E.; Bent, S. F.; Wilson, W. L.; Schilling, M. L.; Ungashe, S. B. *J. Am. Chem. Soc.* **1994**, *116*, 6631-6635.
16. Segura, J. L.; Martin, N. *J. Mater. Chem.* **2000**, *10*, 2403-2435.
17. Martin, R. E.; Diederich, F. *Angew. Chem. Int. Ed. Engl.* **1999**, *38*, 1350-1377.
18. Scherf, U. *Carbon Rich Compounds Ii* **1999**, *201*, 163-222.
19. Kraft, A.; Grimsdale, A. C.; Holmes, A. B. *Angew. Chem. Int. Ed. Engl.* **1998**, *37*, 402-428.
20. Tour, J. M. *Chem. Rev.* **1996**, *96*, 537-553.

21. Salaneck, W. R.; Lundström, I.; Ranby, B. *Conjugated Polymers and Related Materials*; Oxford University Press: Oxford, 1993.

22. Müllen, K. *Pure Appl. Chem.* **1993**, *65*, 89-96.

23. Müllen, K.; Wegner, G. *Electronic Materials: The Oligomer Approach*; Wiley-VCH: Weinheim, 1998.

24. Poulsen, T. D.; Frederiksen, P. K.; Jørgensen, M.; Mikkelsen, K. V.; Ogilby, P. R. *J. Phys. Chem. A* **2001**, *105*, 11488-11495.

25. Frederiksen, P. K.; Jørgensen, M.; Ogilby, P. R. *J. Am. Chem. Soc.* **2001**, *123*, 1215-1221.

26. Samuel, I. D. W.; Crystall, B.; Rumbles, G.; Burn, P. L.; Holmes, A. B.; Friend, R. H. *Chem. Phys. Lett.* **1993**, *213*, 472-478.

27. Beljonne, D.; Shuai, Z.; Friend, R. H.; Brédas, J. L. *J. Chem. Phys.* **1995**, *102*, 2042-2049.

28. Bennati, M.; Nemeth, K.; Surjan, P. R.; Mehring, M. *J. Chem. Phys.* **1996**, *105*, 4441-4447.

29. Beljonne, D.; Cornil, J.; Friend, R. H.; Janssen, R. A. J.; Brédas, J. L. *J. Am. Chem. Soc.* **1996**, *118*, 6453-6461.

30. Bennati, M.; Grupp, A.; Bauerle, P.; Mehring, M. *Molecular Crystals and Liquid Crystals Science and Technology Section A-Molecular Crystals and Liquid Crystals* **1994**, *256*, 751-756.

31. Peeters, E.; Ramos, A. M.; Meskers, S. C. J.; Janssen, R. A. J. *J. Chem. Phys.* **2000**, *112*, 9445-9454.

32. Gould, I. R.; Boiani, J. A.; Gaillard, E. B.; Goodman, J. L.; Farid, S. *J. Phys. Chem. A* **2003**, *107*, 3515-3524.

33. Gould, I. R.; Young, R. H.; Mueller, L. J.; Albrecht, A. C.; Farid, S. *J. Am. Chem. Soc.* **1994**, *116*, 8188-8199.

34. Gould, I. R.; Young, R. H.; Mueller, L. J.; Albrecht, A. C.; Farid, S. *J. Am. Chem. Soc.* **1994**, *116*, 3147-3148.

35. Lim, B. T.; Okajima, S.; Chandra, A. K.; Lim, E. C. *Chem. Phys. Lett.* **1981**, *79*, 22-27.

36. Wiederrecht, G. P.; Svec, W. A.; Wasielewski, M. R.; Galili, T.; Levanon, H. *J. Am. Chem. Soc.* **2000**, *122*, 9715-9722.

37. Wasielewski, M. R.; Johnson, D. G.; Svec, W. A.; Kersey, K. M.; Minsek, D. W. *J. Am. Chem. Soc.* **1988**, *110*, 7219-7221.

38. Carbonera, D.; Di Valentin, M.; Corvaja, C.; Agostini, G.; Giacometti, G.; Liddell, P. A.; Kuciauskas, D.; Moore, A. L.; Moore, T. A.; Gust, D. *J. Am. Chem. Soc.* **1998**, *120*, 4398-4405.

39. van Willigen, H.; Jones, G.; Farahat, M. S. *J. Phys. Chem.* **1996**, *100*, 3312-3316.

40. Carbonera, D.; Di Valentin, M.; Corvaja, C.; Giacometti, G.; Agostini, G.; Liddell, P. A.; Moore, A. L.; Moore, T. A.; Gust, D. *J. Photochem. Photobiol. A* **1997**, *105*, 329-335.

41. Carbonera, D.; Di Valentin, M.; Agostini, G.; Giacometti, G.; Liddell, P. A.; Gust, D.; Moore, A. L.; Moore, T. A. *Appl. Magn. Res.* **1997**, *13*, 487-504.

42. Wiederrecht, G. P.; Svec, W. A.; Wasielewski, M. R. *J. Am. Chem. Soc.* **1999**, *121*, 7726-7727.

43. Ogilby, P. R.; Sanetra, J. *J. Phys. Chem.* **1993**, *97*, 4689-4694.

44. Kristiansen, M.; Scurlock, R. D.; Iu, K. K.; Ogilby, P. R. *J. Phys. Chem.* **1991**, *95*, 5190-5197.

45. McGarvey, D. J.; Szekeres, P. G.; Wilkinson, F. *Chem. Phys. Lett.* **1992**, *199*, 314-319.

46. Göppert-Mayer, M. *Ann. Phys.* **1931**, *9*, 273-294.

47. Kaiser, W.; Garrett, C. G. B. *Phys. Rev. Lett.* **1961**, *7*, 229-331.

48. Belfield, K. D.; Liu, Y.; Negres, R. A.; Fan, M.; Pan, G.; Hagan, D. J.; Hernandez, F. E. *Chem. Mater.* **2002**, *14*, 3663-3667.

49. Denk, W.; Strickler, J. H.; Webb, W. W. *Science* **1990**, *248*, 73-76.

50. Williams, R. M.; Piston, D. W.; Webb, W. W. *FASEB J.* **1994**, *8*, 804-813.

51. He, G. S.; Markowicz, P. P.; Lin, T. C.; Prasad, P. N. *Nature* **2002**, *415*, 767-770.

52. Reinhardt, B. A.; Brott, L. L.; Clarson, S. J.; Dillard, A. G.; Bhatt, J. C.; Kannan, R.; Yuan, L. X.; He, G. S.; Prasad, P. N. *Chem. Mater.* **1998**, *10*, 1863-1874.

53. Watanabe, T.; Akiyama, M.; Totani, K.; Kuebler, S. M.; Stellacci, F.; Wenseleers, W.; Braun, K.; Marder, S. R.; Perry, J. W. *Adv. Funct. Mater.* **2002**, *12*, 611-614.

54. Belfield, K. D.; Ren, X.; Hagan, D. J.; Van Stryland, E. W.; Dubikovsky, V.; Miesak, E. J. *Abstr. Pap. -Am. Chem. Soc.* **1999**, *218*, U629-U630.

55. Cumpston, B. H.; Ananthavel, S. P.; Barlow, S.; Dyer, D. L.; Ehrlich, J. E.; Erskine, L. L.; Heikal, A. A.; Kuebler, S. M.; Lee, I. Y. S.; McCord-Maughon,

D.; Qin, J. Q.; Rockel, H.; Rumi, M.; Wu, X. L.; Marder, S. R.; Perry, J. W. *Nature* **1999**, *398*, 51-54.

56. He, G. S.; Prasad, P. N. *J. Opt. Soc. Am. B* **1998**, *15*, 1078-1085.

57. He, G. S.; Cheng, N.; Prasad, P. N.; Liu, D.; Liu, S. H. *J. Opt. Soc. Am. B* **1998**, *15*, 1086-1095.

58. Narang, U.; Zhao, C. F.; Bhawalkar, J. D.; Bright, F. V.; Prasad, P. N. *J. Phys. Chem.* **1996**, *100*, 4521-4525.

59. Frederiksen, P. K.; McIlroy, S. P.; Nielsen, C. B.; Nikolajsen, L.; Skovsen, E.; Jørgensen, M.; Mikkelsen, K. V.; Ogilby, P. R. *J. Am. Chem. Soc.* **2005**, *127*, 255-269.

60. Frederiksen, P. K. "The Two-Photon Photosensitized Production of Singlet Oxygen," 2003, Ph. D. dissertation, University of Aarhus

61. Albota, M.; Beljonne, D.; Brédas, J. L.; Ehrlich, J. E.; Fu, J. Y.; Heikal, A. A.; Hess, S. E.; Kogej, T.; Levin, M. D.; Marder, S. R.; McCord-Maughon, D.; Perry, J. W.; Rockel, H.; Rumi, M.; Subramaniam, C.; Webb, W. W.; Wu, X. L.; Xu, C. *Science* **1998**, *281*, 1653-1656.

62. McClain, W. M. *Acc. Chem. Res.* **1974**, *7*, 129-135.

63. Cho, H. S.; Jeong, D. H.; Cho, S.; Kim, D.; Matsuzaki, Y.; Tanaka, K.; Tsuda, A.; Osuka, A. *J. Am. Chem. Soc.* **2002**, *124*, 14642-14654.

64. Marder, S.; Perry, J. Two Photon or Higher-Order Absorbing Optical Materials and Methods of Use. [US 6,267,913]. 2001.

65. Pond, S. J. K.; Rumi, M.; Levin, M. D.; Parker, T. C.; Beljonne, D.; Day, M. W.; Brédas, J. L.; Marder, S. R.; Perry, J. W. *J. Phys. Chem. A* **2002**, *106*, 11470-11480.

66. Rumi, M.; Ehrlich, J. E.; Heikal, A. A.; Perry, J. W.; Barlow, S.; Hu, Z. Y.; McCord-Maughon, D.; Parker, T. C.; Rockel, H.; Thayumanavan, S.; Marder, S. R.; Beljonne, D.; Brédas, J. L. *J. Am. Chem. Soc.* **2000**, *122*, 9500-9510.

67. Strehmel, B.; Sarker, A. M.; Detert, H. *ChemPhysChem* **2003**, *4*, 249-259.

68. Zojer, E.; Beljonne, D.; Kogej, T.; Vogel, H.; Marder, S. R.; Perry, J. W.; Brédas, J. L. *J. Chem. Phys.* **2002**, *116*, 3646-3658.

69. Najechalski, P.; Morel, Y.; Stephan, O.; Baldeck, P. L. *Chem. Phys. Lett.* **2001**, *343*, 44-48.

70. Drobizhev, M.; Karotki, A.; Rebane, A.; Spangler, C. W. *Opt. Lett.* **2001**, *26*, 1081-1083.

71. Tykwinski, R. R.; Gubler, U.; Martin, R. E.; Diederich, F.; Bosshard, C.; Günter, P. *J. Phys. Chem. B* **1998**, *102*, 4451-4465.

72. Cronstrand, P.; Norman, P.; Luo, Y.; Ågren, H. *J. Chem. Phys.* **2004**, *121*, 2020-2029.

73. Porrés, L.; Mongin, O.; Katan, C.; Charlot, M.; Pons, T.; Mertz, J.; Blanchard-Desce, M. *Org. Lett.* **2004**, *6*, 47-50.

74. Mongin, O.; Porrés, L.; Moreaux, L.; Mertz, J.; Blanchard-Desce, M. *Org. Lett.* **2002**, *4*, 719-722.

75. Skovsen, E. "Non-linear Two-Photon Singlet Oxygen Emmision Microscopy," 2005, Ph. D. dissertation, University of Aarhus

76. Zhang, B. J.; Jeon, S. J. *Chem. Phys. Lett.* **2003**, *377*, 210-216.

CHAPTER 2

SYNTHESIS OF OLIGO PHENYLENE–VINYLENES

Abstract: *The general structure of the majority of molecules studied is a centrosymmetric distyrylbenzene substituted with various electron donor and acceptor groups. These molecules are synthesized from either Horner-Wadsworth-Emmons reactions or Heck-couplings using aldehydes, phosphonate esters, dibromo-benzenes and vinylenes as building blocks*

2.1 Introduction

The oligo phenylene-vinylene (OPV) class of compounds is well characterized, and many synthetic reports regarding the preparation of these compounds have been made. Thus, the OPV structure makes a good template for designing singlet oxygen sensitizers and for deducing molecular design principles pertinent for singlet oxygen sensitizers. A general structure of the compounds prepared in the present work is depicted in Figure 2-1.

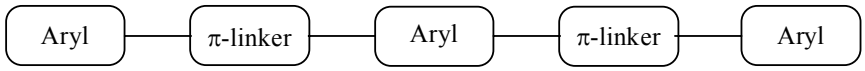

Figure 2-1: General structure of the singlet oxygen sensitizers prepared in the present work.

The prepared compounds are symmetric around the middle aryl ring (thus possessing an inversion center) in order to make the syntheses easier. Various electron donating and accepting groups have been placed on the end- and middle-aryl rings to investigate the impact CT and conjugation length will have on the singlet oxygen quantum yield. Compounds were also prepared where the π-linker was varied, *e.g.* a triple bond instead of a double bond.

2.2 Synthesis of the OPV sensitizers

The OPV's were mainly synthesized from initially prepared building blocks in either a Horner-Wadsworth-Emmons (HWE) or a Heck reaction. Thus the building blocks needed were phosphonate esters, vinylenes, aldehydes and bromine functionalized aromatic compounds. In the section that follows, the syntheses of these building blocks are presented first.

Not all of the molecules synthesized were examined in photophysical experiments. The most important molecules described in the present chapter, which were subjected to detailed photophysical studies are shown in Chart 2-1.

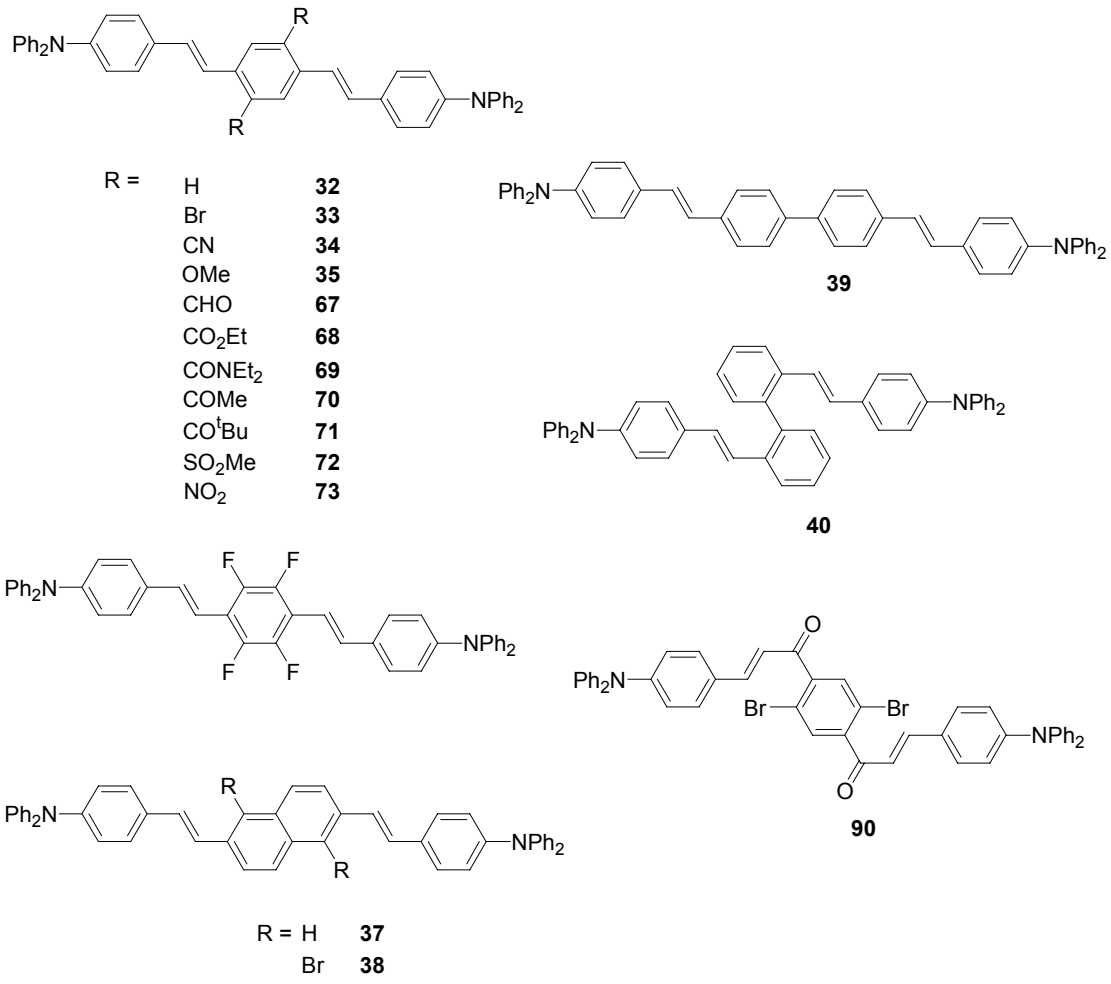

Chart 2-1: Most important molecules studied in the present chapter.

2.2.1 Aldehydes and related building blocks

A series of aldehydes were prepared for the synthesis and two important building blocks used in the present work are 4-diphenylamino-benzaldehyde (**1**) and diphenyl-(4-vinyl-phenyl)-amine (**2**), which were chosen due to the electron donating properties of the amino group. A reason for choosing the diphenylamino end-group for the OPV compounds is that this group has been shown to induce better photostability in comparison with dialkylamino groups.[1] Likewise, in comparison to a dialkylamino group a triarylamino group is a less efficient quencher of singlet oxygen.[2] The syntheses of these compounds, which are based on literature procedures,[3-5] are shown in Scheme 2-1.

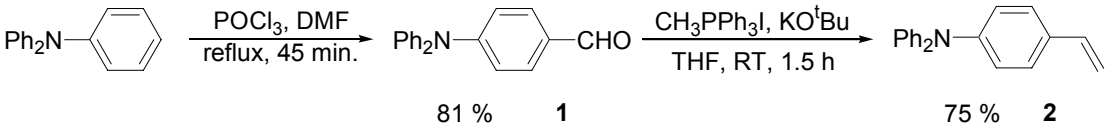

Scheme 2-1: Preperation of 4-diphenylamino-benzaldehyde and diphenyl-(4-vinyl-phenyl)-amine.

The imidazole of 9,10-phenanthrequinone has previously been shown to induce interesting optical properties, when incorporated in an extended aromatic system.[6] For this reason, and because it is a large aromatic system which could potentially contribute to a large TPA cross section, the aldehyde **5** was made (Scheme 2-2), with the intent to react it with phosphonate esters and make OPV's of this building block. The synthesis of a similar compound (with a *meta* substitution pattern on the benzene ring) has previously been described.[7] This synthesis was adapted in the preparation of the aldehyde **5**, where 9,10-phenanthrequinone was initially reacted with 4-bromo-benzaldehyde and ammonium hydrogen carbonate in refluxing acetic acid to form the imidazole in 93 % yield. This imidazole was then *N*-methylated with methyl iodide (in 74 % yield) in a Menschutkin reaction. Finally, a bromine-to-lithium exchange followed by reaction with DMF afforded the aldehyde in 76 % yield. It was possible to grow crystals of **4** suitable for determining the X-ray structure.

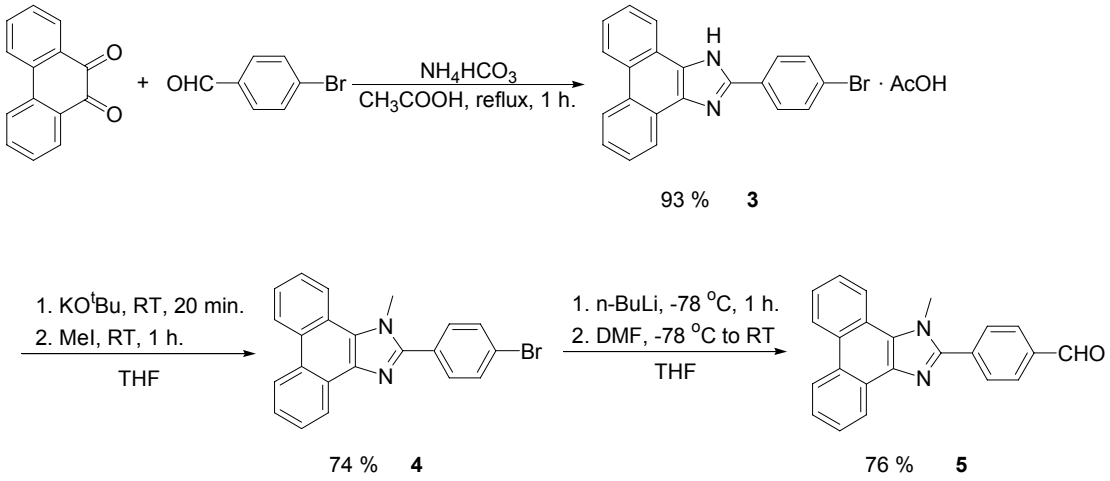

Scheme 2-2: Preparation of an imidazole.

Attempts to make other imidazoles using the method described above were made. It has been reported that by using mono acetal protected terephthalaldehyde instead of bromo-benzaldehyde in the formation of the imidazole ring shown in Scheme 2-2, the imidazole substituted benzaldehyde was then isolated after workup.[8] Attempts were made to react monoacetal protected terephthalaldehyde with other 1,2-diones such as 4,4'-dibromo-benzil in refluxing acetic acid and with both ammonium hydrogen carbonate and ammonium acetate. The goal was to isolate an imidazole substituted benzaldehyde (after removal of the acetal group during workup), but only starting materials were isolated. Recently, this type of reaction for making imidazoles has been reported to proceed in high yield and with short reaction times using microwave irradiation.[9,10] The procedure given in these reports was tried, but a product was isolated, which ^{1}H-NMR data and MALDI-TOF spectrum were consistent with the product shown in Scheme 2-3.

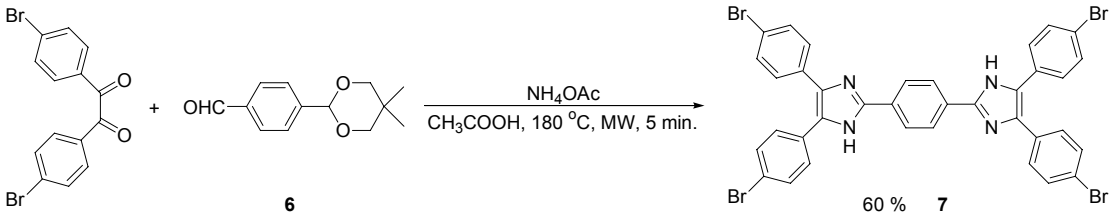

Scheme 2-3: Attempt to make an acetal protected imidazole substituted benzaldehyde under microwave conditions.

Apparently, the acetal protecting group was not stable to the reaction conditions (probably due to the high pressure of ~14 bar in the reaction container), and the liberated aldehyde could then react with the benzil forming another imidazole ring.

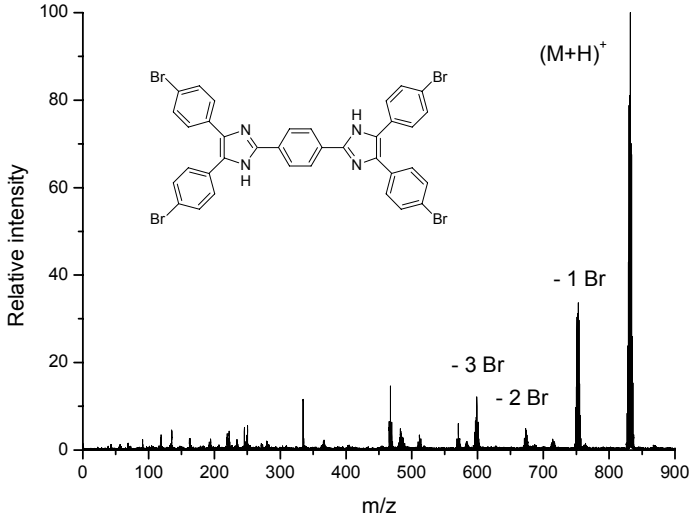

Figure 2-2: MALDI-TOF spectrum of the product isolated from the reaction in Scheme 2-3. No matrix was used.

The MALDI-TOF spectrum shows the loss of up to three bromine atoms and the isotopic distribution pattern of the molecular ion is consistent with a molecule containing four bromine atoms.

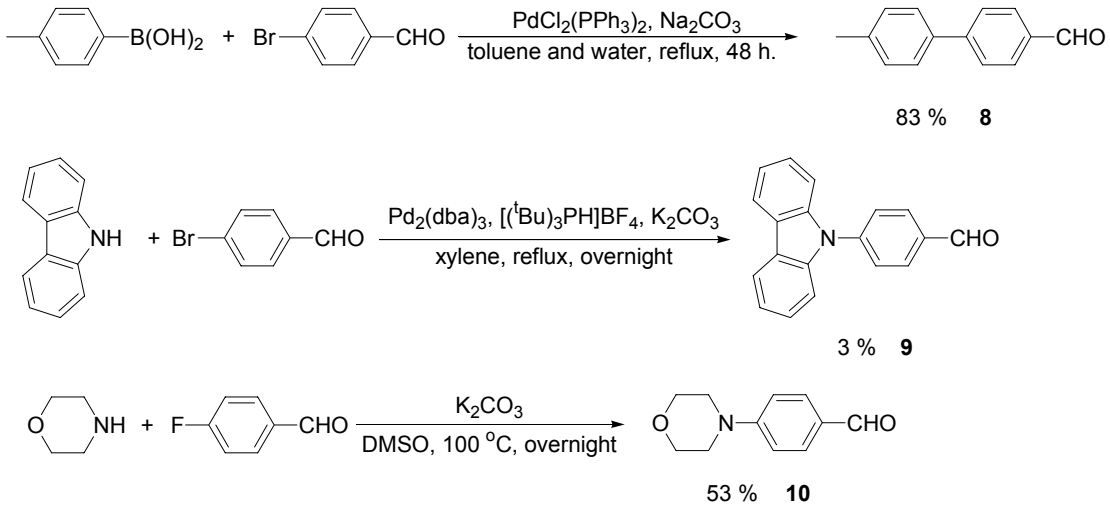

Scheme 2-4: The preperation of aldehydes.

Persuing the idea of OPV's end-capped with groups promoting long conjugation lengths (mesomeric substitution), aldehyde **8** was prepared in a Suzuki reaction with 4-tolyl-boronic acid and 4-bromo-benzaldehyde in 83 % yield as described in Ref. 11. The carbazole aldehyde **9** was prepared in a Pd catalyzed amination reaction with carbazole and 4-bromo-benzaldehyde. The yield was surprisingly low and is explained by a slow conversion of the reactants due to a poor choice of Pd catalyst and ligand. Watanabe and co-workers[12] prepared the same molecule by using 4-chloro-benzaldehyde and $Pd(OAc)_2$ as the catalyst with the highly reactive ligand $P(^tBu)_3$, and obtained the carbazole aldehyde in 71 % yield. It has also been reported that the carbazole aldehyde can made in an Ar-nucleophilic substitution with 4-flouro-benzaldehyde and carbazole.[3] The carbazole aldehyde **9** is the "locked" analog to the diphenylamino aldehyde **1** as the two phenyl rings are connected by a C-C-bond forcing a planar structure and should, as such, posses a longer conjugation length. Instead of having functionalities with long conjugation lengths at the termini of the OPV's, variation of the donor-strength of the end-group was considered. To this end, **10** was prepared in an Ar-nucleophilic substitution with morpholine and 4-flouro-benzaldehyde as described in Ref. 13.

2.2.2 Bromo-methyl compounds as precursors for phosphonate esters

A class of compounds that served as key building blocks in the present work is phosphonate esters, which were prepared from bromo-methyl derivatives. Most of the bromo-methyl derivatives were prepared by NBS bromination from methyl-substituted aromatic compounds as shown in Scheme 2-5.

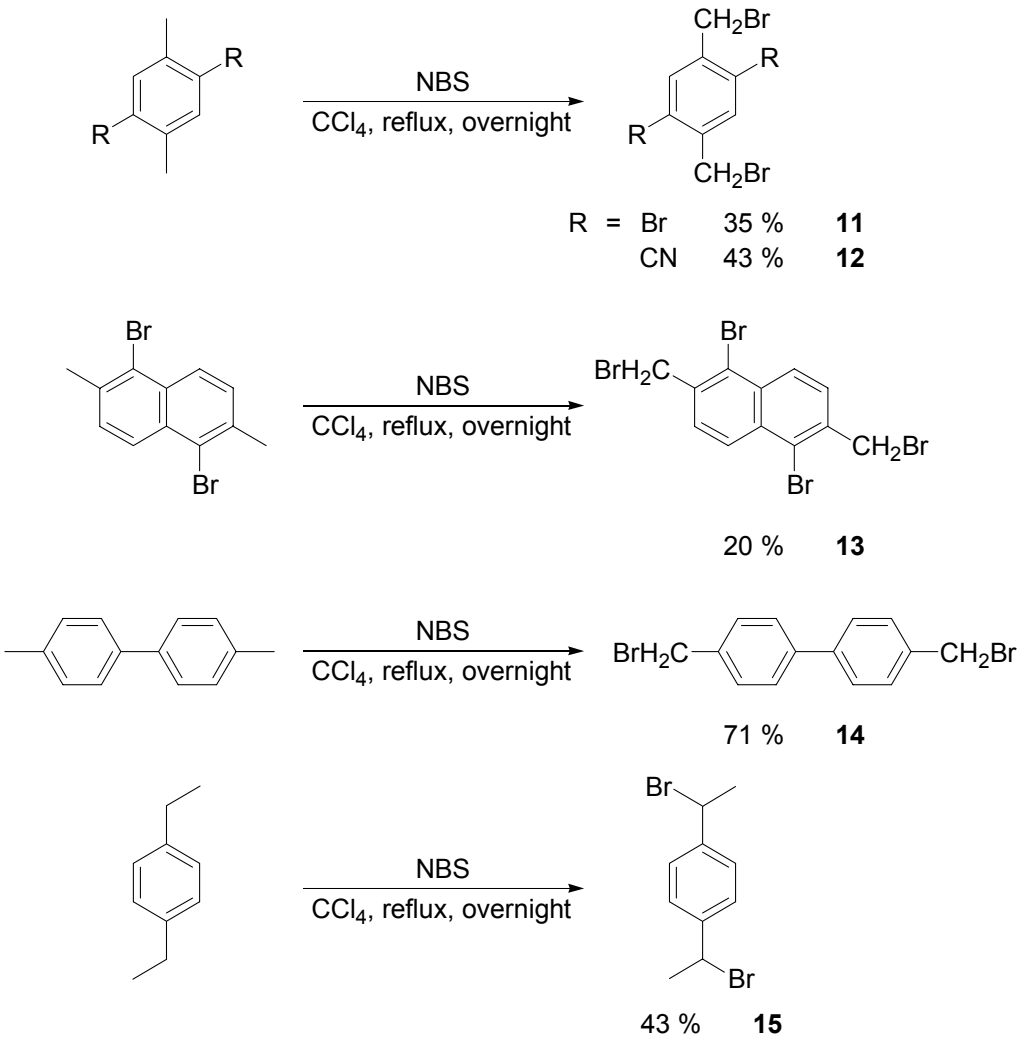

Scheme 2-5: NBS bromination of a series of methyl- and ethyl-substituted aromatic compounds.

Compound **11** has been prepared in Ref. 14 in significantly higher yield (71 %) than the one reported in the present work. Reports have been made[15,16] of the preparation of **12**, but no yields or NMR data have been provided for this compound. The syntheses of **13**, **14** and **15** have also previously been described in Ref. 17-19, 20-23 and 24, respectively. 1,4-bis-bromomethyl-2,5-dimethoxy-benzene (**16**) was prepared as shown in Scheme 2-6, where 1,4-dimethoxybenzene was bromo-methylated, according to the procedure given in Ref. 25.

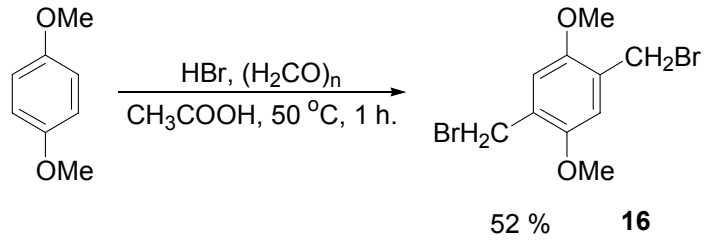

Scheme 2-6: Bromomethylation of 1,4-dimethoxybenzene

1,5-Dibromo-2,6-dimethyl-naphthalene was prepared by first assembling the naphthalene ring in a condensation with the grignard reagent of 1-chloromethyl-4-methyl-benzene and 4,4-dimethoxy-butan-2-one and afterwards brominating the resulting 2,6-dimethyl-naphthalene.

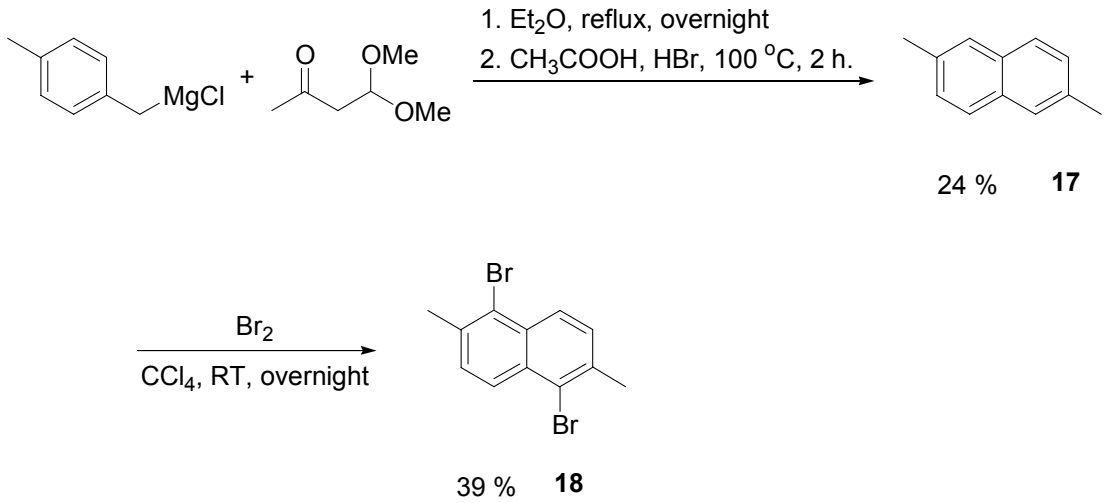

Scheme 2-7: Preperation of 1,5-dibromo-2,6-dimethyl-naphthalene.

The only report of the syntheses of 2,6-dimethyl-naphthalene using the condensation reaction depicted in Scheme 2-7 was made by Kochetkov *et al.*[26] in 1955 but no NMR data were available in the literature for this compound. They claimed that the use of HBr in the reaction results in lower yield as opposed to using a 3:2 mixture of H_2SO_4:H_3PO_4. However, their reported yield of 27 % does not deviate significantly from the yield of 24 % obtained in the present work, where HBr was used.

2,5-dicyano-*p*-xylene was prepared in a Rosenmund-von Braun reaction with 2,5-dibromo-*p*-xylene as shown in Scheme 2-8.

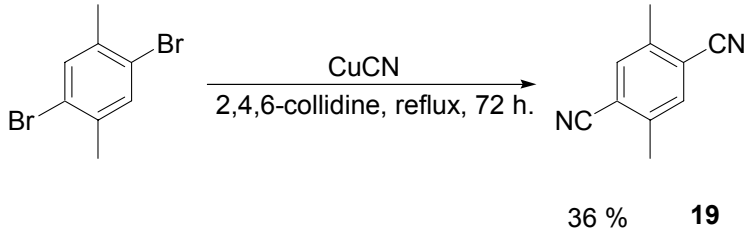

36 % **19**

Scheme 2-8: The synthesis of 2,5-dicyano-*p*-xylene

The reaction proceeded in 36 % yield which is higher than what is reported by Raposo *et al.*[27] (17 %) but somewhat lower than what Ngola *et al.* (81 %) reported.[28]

Several attempts were made to make a 4-bromomethyl aniline, which then could be converted to a phosphonate ester. NBS bromination of 4-*N,N*-dimethyl-amino-benzaldehyde was tried but the bromo-methyl compound was not be isolated. This could be due to a reaction with the formed bromine radicals and the nitrogen atom. Instead, an attempt was made to react hydroxy-methyl aniline with $[PPh_3\text{-}CBr_3]^+Br^-$ and also with $SOCl_2$, but in both cases the desired product was not isolated.

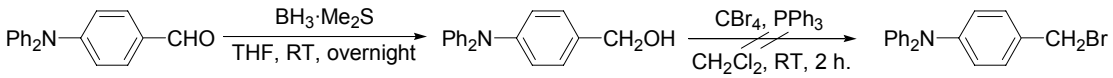

87 % **20**

Scheme 2-9: Attempt to make a bromo-methyl substituted triphenylamine.

However, a green compound was isolated from the reaction with $SOCl_2$. The ^{1}H-NMR spectrum of this compound showed broad signals, which could indicate the formation of a polymer.

2.2.3 Phosphonate esters

The bromo-methyl compounds described above were subsequently converted into phosphonate esters using the Michaelis-Arbuzov reaction as shown in Scheme 2-10.

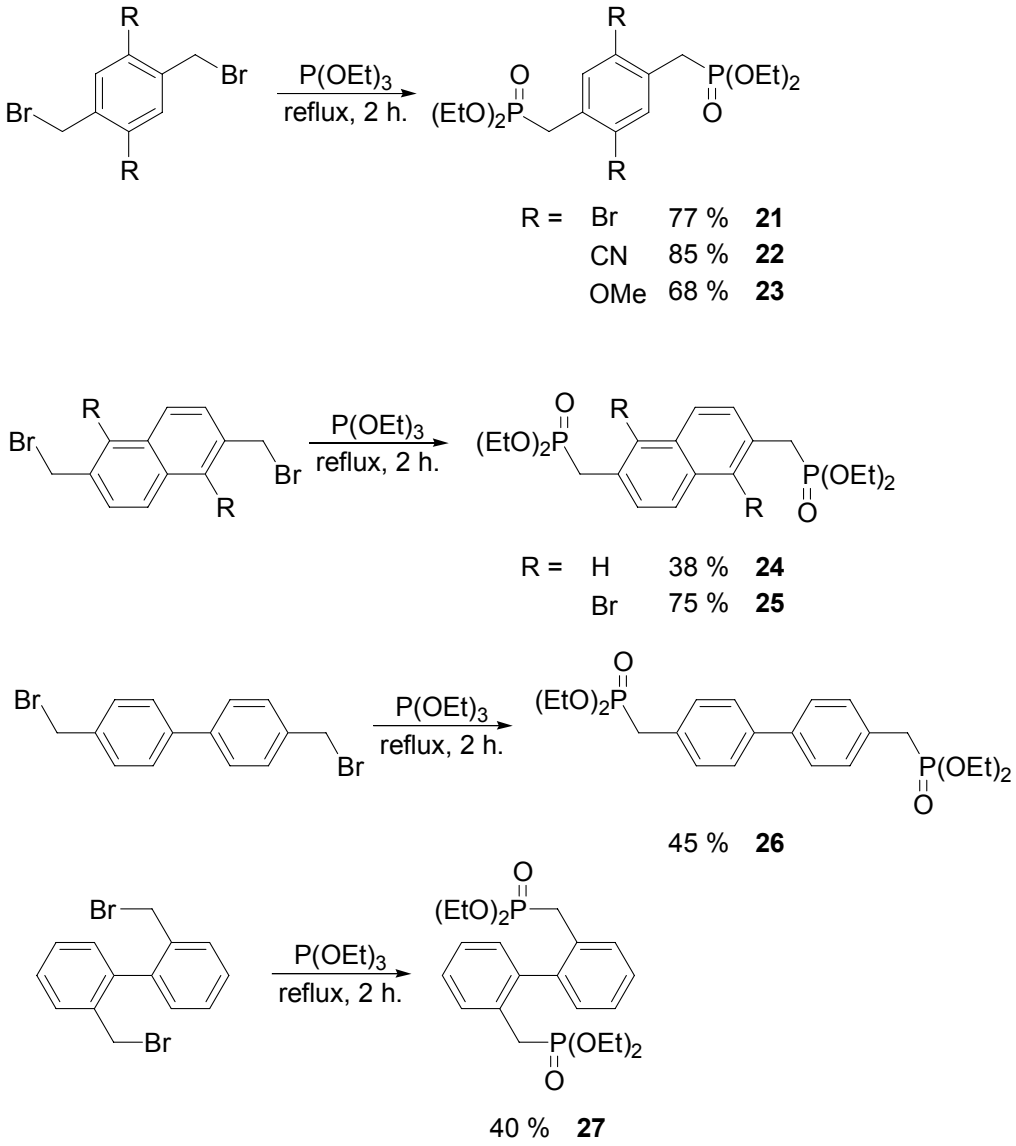

Scheme 2-10: Preperation of phosphonate esters.

The bromo-phosphonate ester (**21**) has previously been prepared by Blum and Zimmerman[14] but only in 65 % yield as opposed to the 77 % obtained in the present work. Similarly, the cyano-phosphonate ester (**22**) has previously been prepared by Wenseleers and co-workers[29] and they only obtained 65 % yield whereas the phosphonate ester was isolated in 85 % yield in the present work. However, the methoxy phosphonate ester (**23**) was reported by Brehm and co-workers[25] to have been isolated in 78 % yield and in the present work, a yield of only 68 % was obtained. The synthesis of the naphthyl-phosphonate ester (**24**) has previously been described in Ref. 30 but no yield or spectroscopic data were given. The *o*-biphenyl phosphonate ester (**27**) was prepared in significant higher yield (93 %) by Plater and

Jackson[20] than the 45 % reported in the present work. Both the synthesis and spectroscopic data have previously been given for the *p*-biphenyl phosphonate ester[31,32] (**26**) but no yield was given.

A phosphonate ester similar to **21** but with an extra methylene spacer between the ester group and the benzene ring was prepared as shown in Scheme 2-11.

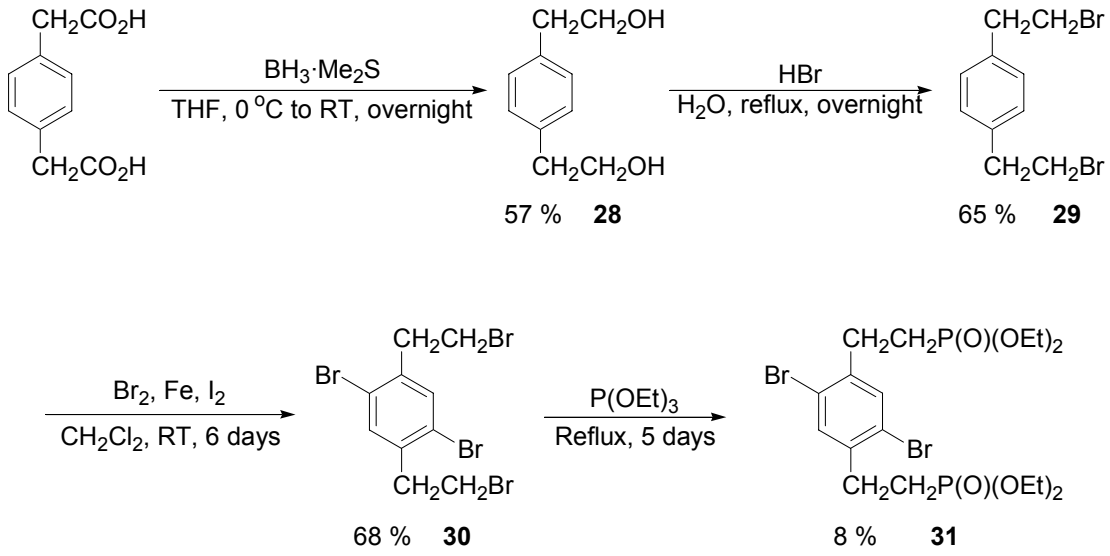

Scheme 2-11: The preparation of an "extended" phosphonate ester.

The conversion of the alcohol to the bromide and the subsequent bromination has previously been described in Ref. 33 and the yields reported for these reactions are 88 % and 94 %, respectively. The low yield of the Michaelis-Arbuzov reaction is ascribed to the fact that the bromide is un-activated towards this reaction.

2.2.4 OPV's prepared from HWE-reactions

The phosphonate esters were reacted with 4-diphenylamino-benzaldehyde to give the OPV's depicted in Scheme 2-12. Compound **32** had previously been prepared in 87 % yield by Kauffman and Moyna[1] and in 67 % by Plater and Jackson.[20] The bromo analog (**33**) was prepared in 66 % yield by Frederiksen and co-workers.[34] The cyano analog (**34**) was prepared in 51 % by Pond and co-workers[35] in a Wittig reaction using 2,5-dicyano-1,4-bis(triphenylphosphonium)benzene dibromide instead of the corresponding phosphonate ester as done in the present work. The bi-phenyl analog

(**39**) had previously been prepared in a double Heck reaction between diphenyl-(4-vinyl-phenyl)-amine and 4,4'-dibromo-biphenyl in 81 % yield.[36]

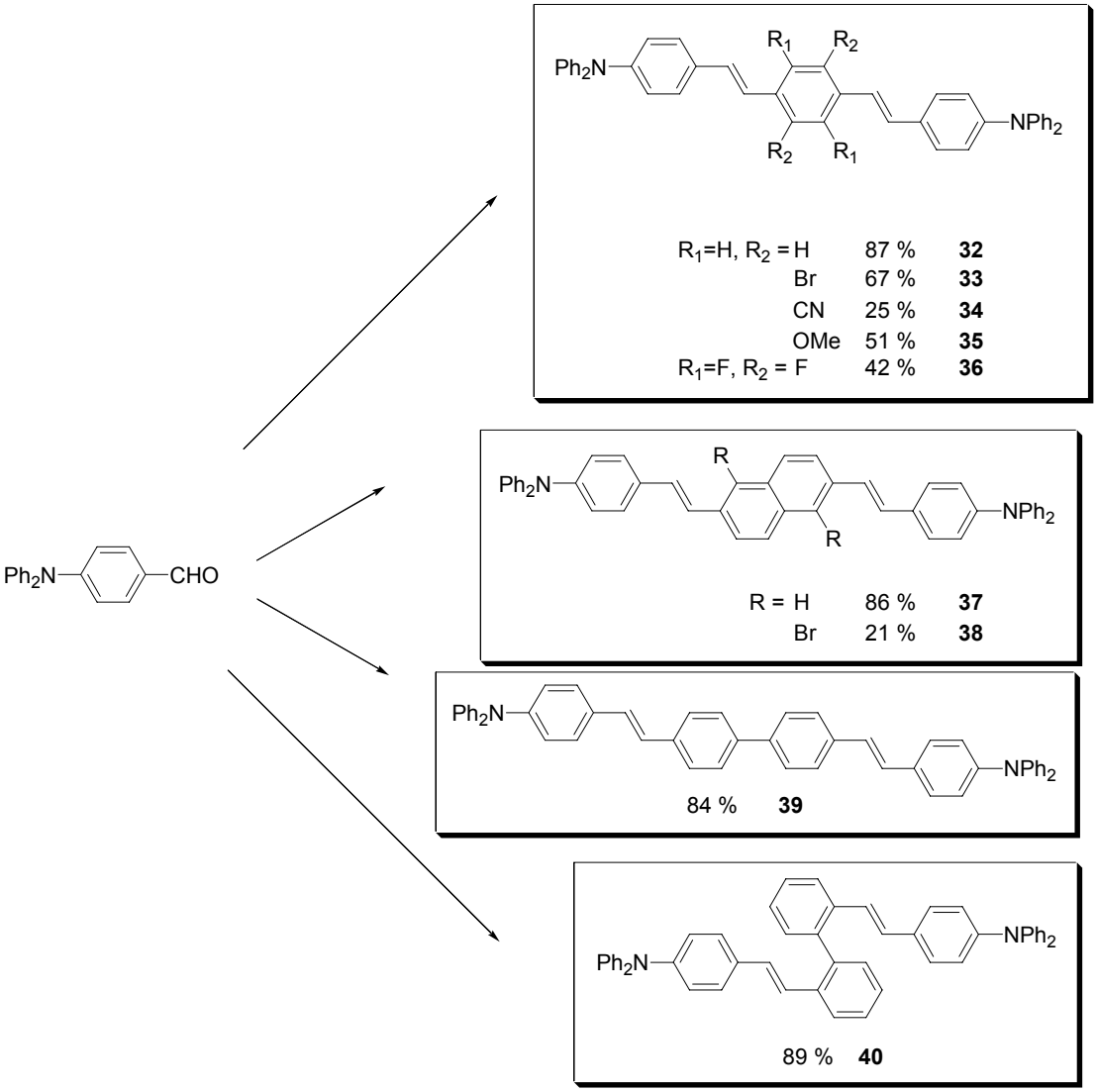

Scheme 2-12: Syntheses of OPV molecules using the HWE-reaction. In all the reactions, either DMF or THF was used as the solvent, potassium *tert*-butoxide as the base, and reaction times were typically between 1-2 hours at either reflux or RT.

Compound **34** was also prepared from **33** in a Rosenmund-von Braun synthesis but in a poor yield of only 3 %.

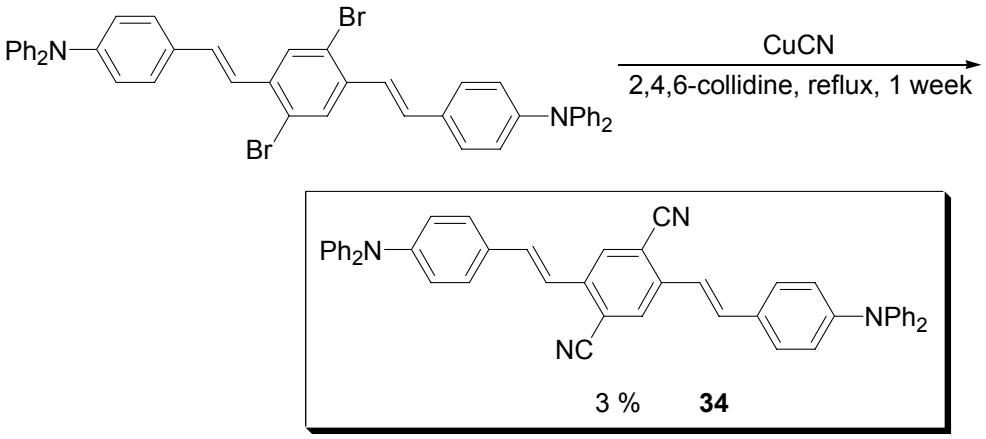

Scheme 2-13: The synthesis of **34** from **33** in a Rosenmund-von Braun reaction.

A variety of different aldehydes were then reacted with the dibromo diphosphonate ester **21** as shown in Scheme 2-14.

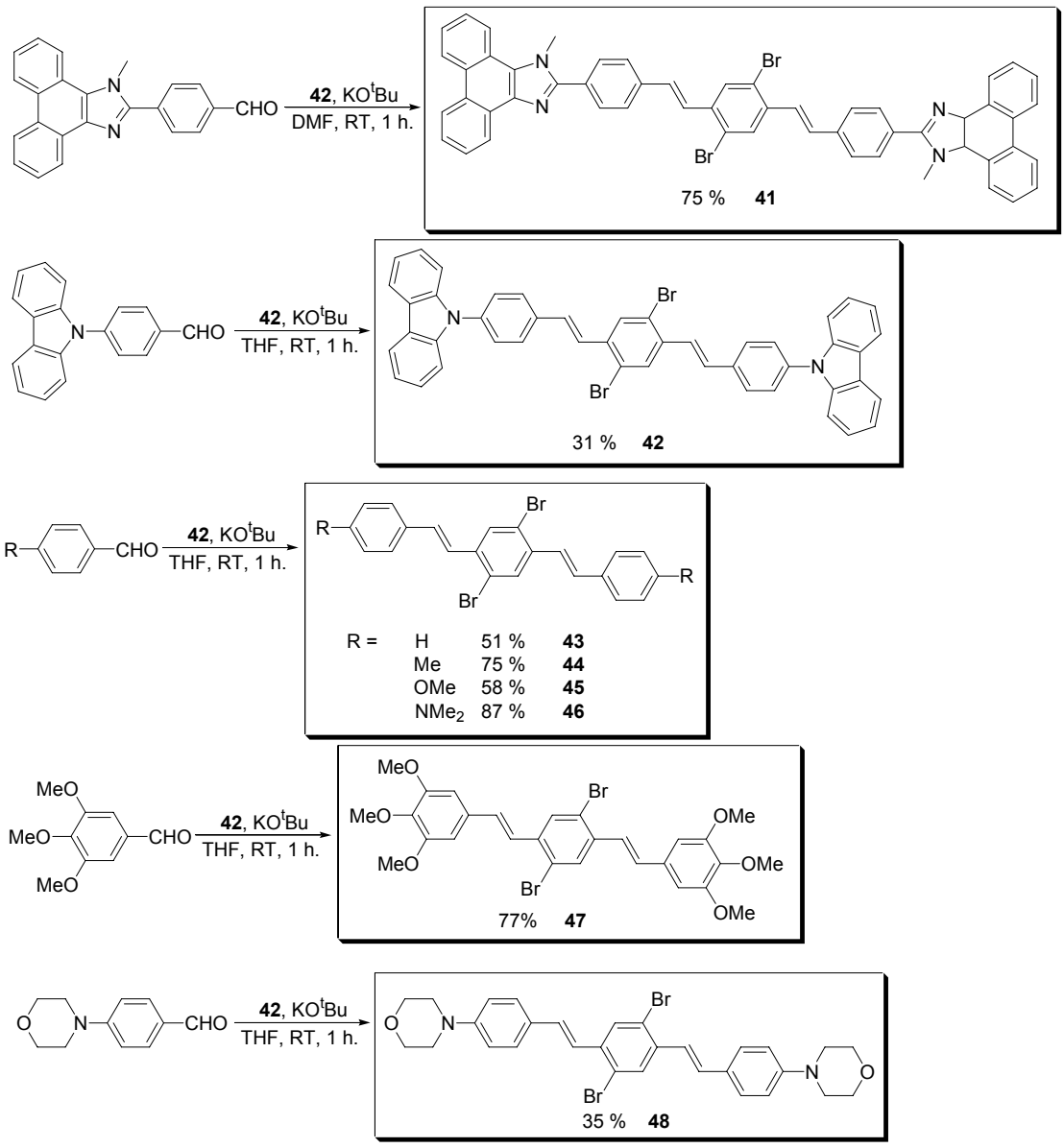

Scheme 2-14: Preparation of OPV's with different end-groups.

The solubility of the imidazole OPV (**41**) in toluene was very low and it was only possible to obtain a ^{1}H-NMR-spectrum of the compound. To increase the solubility in toluene, an attempt was made to introduce an octyl chain on the imidazole substituted benzaldehyde **5** by reacting with octyl iodide instead of methyl iodide in the *N*-alkylation step in Scheme 2-2. For a variaty of reasons,[34] toluene is the solvent of choice for many of the two-photon photophysical characterization experiments. However, it was not possible to react **3** in a Menschutkin reaction with octyl iodide.

A poly-flourinated compound (**49**) was also made (Scheme 2-15).[a] The fluorinated alkyl-chains serve as electron accepting groups resulting in a donor-acceptor-donor architecture of the molecule. But again, it was difficult to dissolve this compound in toluene.

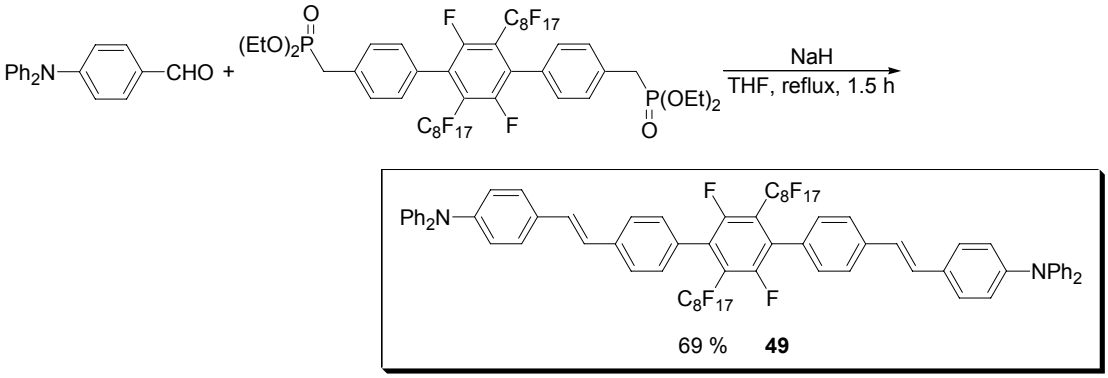

Scheme 2-15: The preparation of a poly-flourinated OPV.

2.2.5 2,5-disubstituted 1,4-dibromo-benzenes

A series of dibromo-benzenes were prepared for coupling in a Heck-reaction with diphenyl-(4-vinyl-phenyl)-amine. The synthesis of 2,5-diformyl-1,4-dibromo-benzene is shown in Scheme 2-16. In this process, 2,5-dibromo-*p*-xylene was brominated four times in 53 % yield and the resulting bromo compound (**51**) was then hydrolyzed with concentrated sulfuric acid yielding the aldehyde **52** in 71 % yield. The synthesis of this compound has previously been described in 1944 by Ruggli and Brandt[37] but no NMR data were given for this compound.

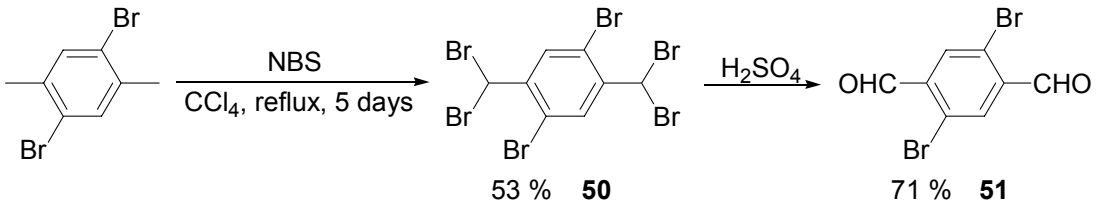

Scheme 2-16: Preparation of 2,5-diformyl-1,4-dibromo-benzene.

[a] The phosphonate ester used for making **49** was obtained as a gift from Dr. Frederik C. Krebs.

A diester and diamide were also made by converting 2,5-dibromo-terephthalic acid to the acid chloride and then reacting with either ethanol or diethylamine as shown in Scheme 2-17.

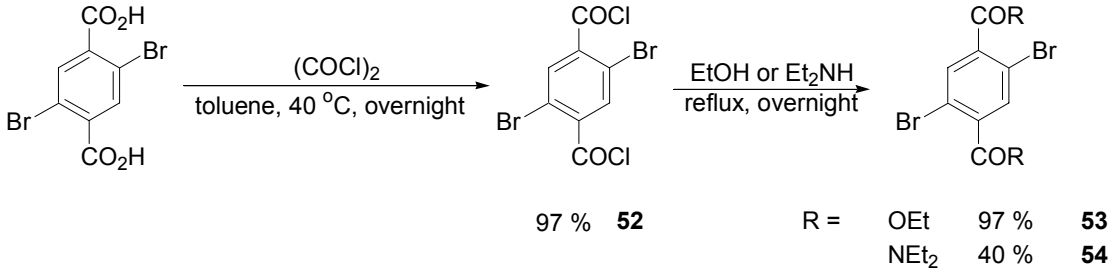

Scheme 2-17: The preparation of 2,5-diester or diamide bromo benzenes.

The conversion of the acid to the acid chloride was quantitative and so was the reaction with ethanol to form the ester. However, the reaction with diethylamine only preceded in 40 % yield. It was possible to grow crystals of the amide **54** suitable for obtaining a X-ray structure. Three ketones were also prepared using organo-cuprate chemistry by reacting the acid chloride **52** with either MeCuCNLi, ^{t}BuCuCNLi or *n*-BuCuCNLi at –78 °C (see Scheme 2-18) yielding 46 %, 59% and 52 % of methyl, *tert*-butyl and *n*-butyl-keto compounds, respectively.

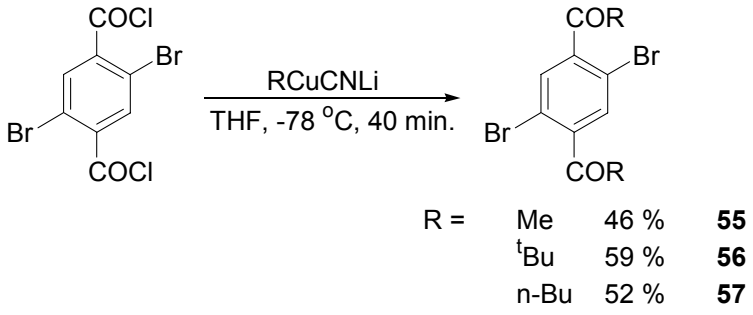

Scheme 2-18: Preparation of keto-functionalized bromo-benzenes.

The preparation of **57** has previously been decribed in Ref. 38 to proceed in 70 % yield. Crystal structures of both **55** and **56** were obtained.

2,5-dinitro-1,4-dibromo-benzene was also prepared. It is possible to nitrate 1,4-dibromo-benzene but in order to isolate the pure 2,5-dinitro compound numerous

recrystalizations are needed.[39] The bromide was instead prepared by the longer and more elaborate route shown in Scheme 2-19, which is described in Ref. 40 and 41.

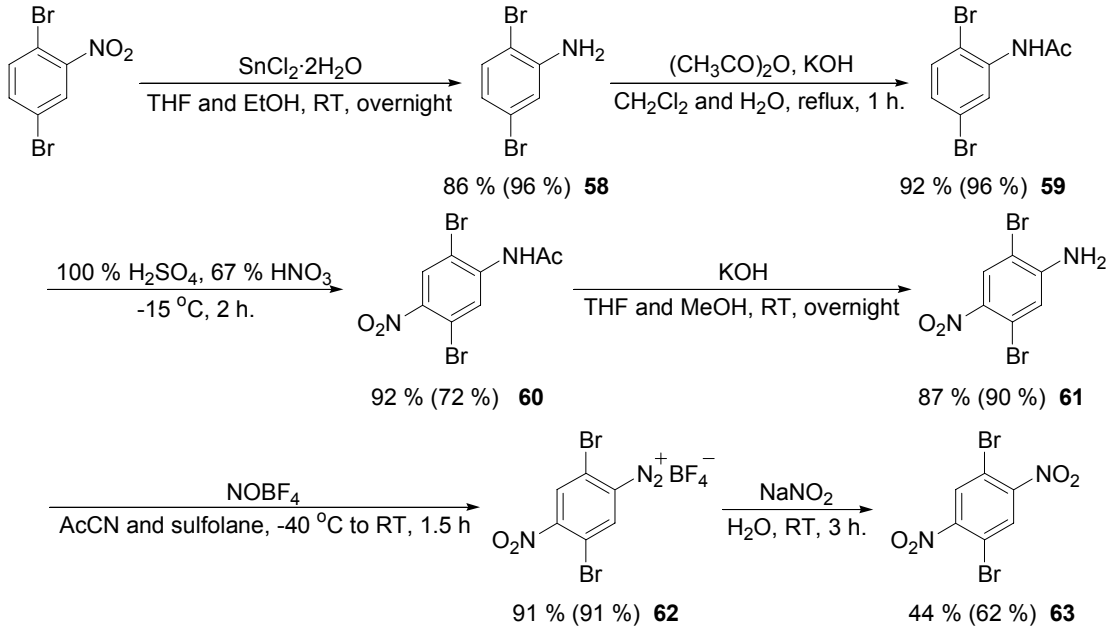

Scheme 2-19: The preparation of 2,5-dinitro-1,4-dibromo-benzene. The yields reported in Ref. 41 are given in parentheses.

The route to 2,5-dinitro-1,4-dibromo-benzene is long but the reactions are generally high yielding. The yield reported in the last step is after sublimation. Prior to sublimation the yield was 61 %. The yield reported in Ref. 41 is after sublimation. A X-ray structure of 2,5-dinitro-1,4-dibromo-benzene was obtained, which is shown in Figure 2-3. The nitro group is out of plane with the benzene ring with a dihedral angle of 59^{o} between C6, C3, N2 and O2.

A methane sulfonyl-benzene was prepared by the route shown in Scheme 2-20 using 1,4-dibromobenzene as the starting material.

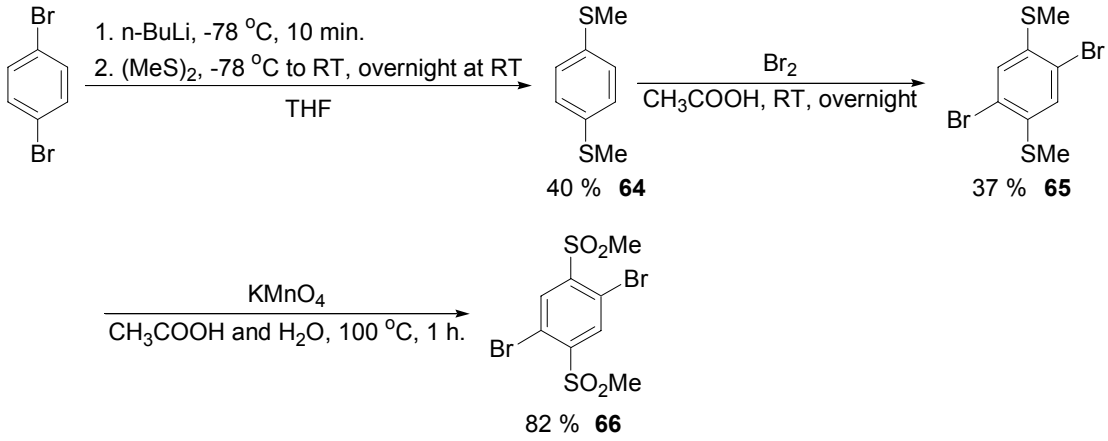

Scheme 2-20: Preparation of 1,4-dibromo-2,5-bis-methanesulfonyl-benzene.

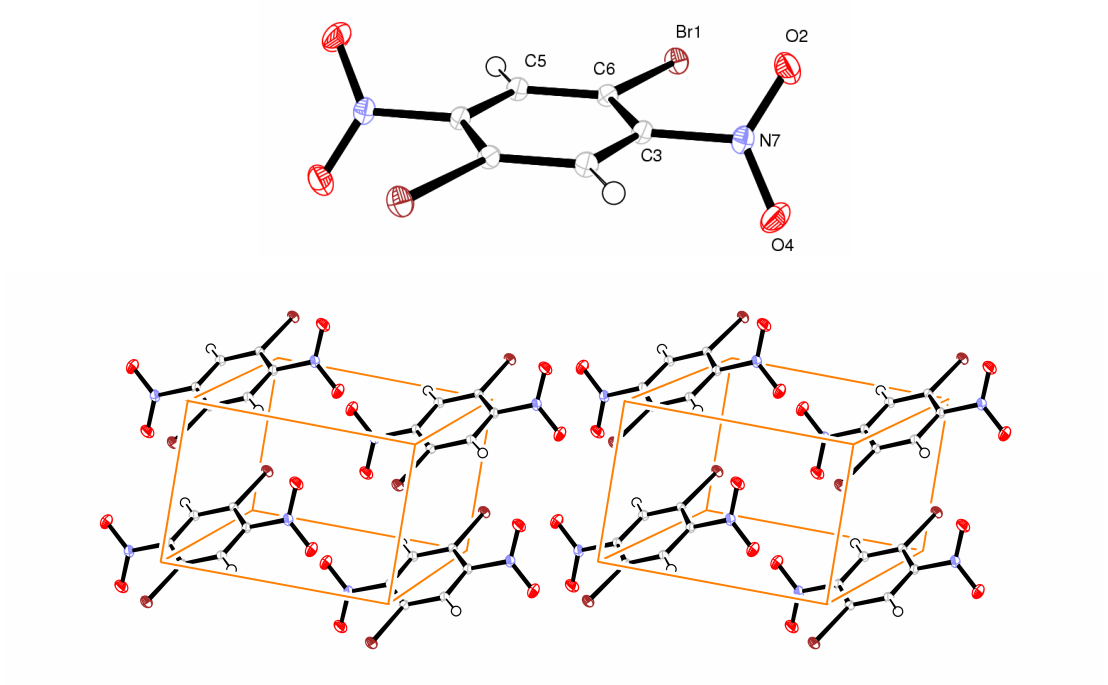

Figure 2-3: ORTEP-III plot of the 2,5-dinitro-1,4-dibromo-benzene **63** (50 % ellipsoids) and crystal packing. Hydrogens are displayed as spheres with an arbitrary radius.

A bromine-to-lithium exchange was carried out on 1,4-dibromo-benzene and by reacting with dimethyldisulfide, the methyl thio ether **64** was obtained in 40 % yield. Bromination and oxidation to the sulfonyl proceeded in 37 % and 82 % yield, respectively.

2.2.6 OPV's prepared from Heck-reactions

The 2,5-disubstituted 1,4-dibromo compounds were reacted with the diphenyl-(4-vinyl-phenyl)-amine (**2**) in a Heck reaction. There are various procedures reported for the Heck-reaction, where different sources of Pd and different phosphorous-ligands are used. The most successful phosphorous-ligand seems to be $P(^tBu)_3$, but this compound is pyroforic and needs to be handled in a glove box. However, *in situ* generation of $P(^tBu)_3$ can be done by adding a base to the air-stable HBF_4 salt of $P(^tBu)_3$ ($[(^tBu)_3PH]BF_4$). Typically an amine is used as the base and the combination of Cy_2NMe as the base, $[(^tBu)_3PH]BF_4$ and $Pd_2(dba)_3$ as the Pd-source have been reported to work well in the Heck-reaction.[42]

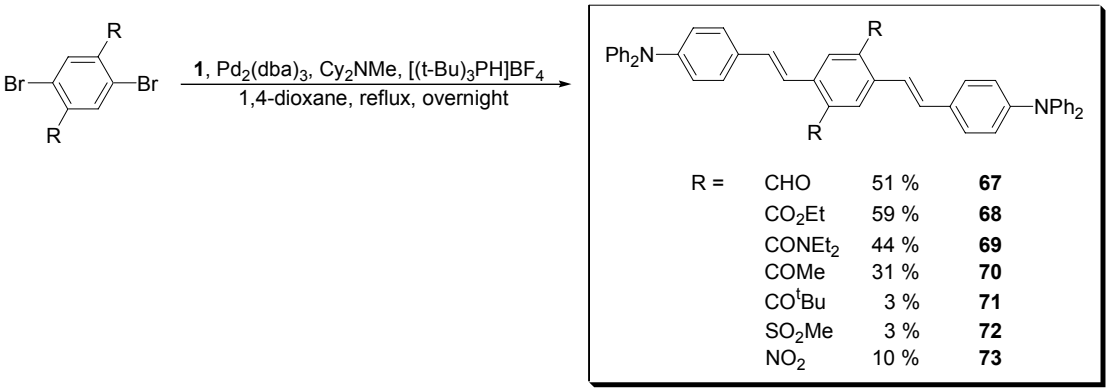

R =			
	CHO	51 %	**67**
	CO_2Et	59 %	**68**
	$CONEt_2$	44 %	**69**
	COMe	31 %	**70**
	CO^tBu	3 %	**71**
	SO_2Me	3 %	**72**
	NO_2	10 %	**73**

Scheme 2-21: OPV's prepared by using the Heck-reaction.

The yields obtained from the reaction ranged from poor (3 %) to fair (59 %). It appears that reactions with dibromo-benzenes and strong electron with-drawing (the nitro and methanesulfonyl) or sterically hindered (the *tert*-butyl ketone) groups gave the poorest yields.

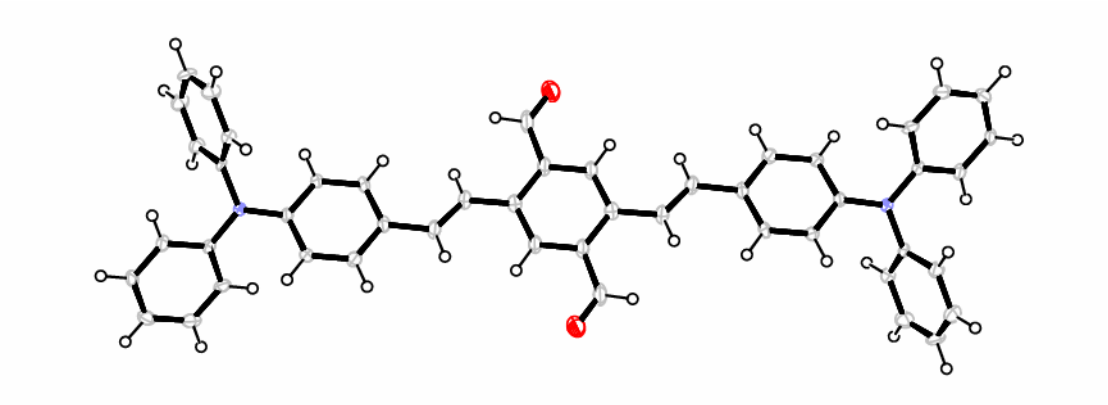

Figure 2-4: X-ray structure of **67**.

Attempts were made to convert the bromide **33** into the ketone **70** by reacting with butoxy-ethene in a Heck-reaction. If the vinyl-ether could be formed, hydrolysis should then give the methyl ketone. A similar strategy for the syntheses of methyl ketones has previously been described by Wright and co-workers.[43] However, it was not even possible to isolate the vinyl-ether. Microwave irradiation has been shown to catalyse some Pd reactions, and this was also tried but without success.

2.2.7 Extension reagents for stepwise unidirectional oligomerization

The extent of charge-transfer (CT) in a molecule depends on the distance and coupling between the donor and acceptor parts of the molecule. Varying the number of phenylene vinylene units in an OPV is an approach for studying the effect of CT on optical properties, and for this purpose, the extension reagents **81** and **82** in Scheme 2-22 were prepared.

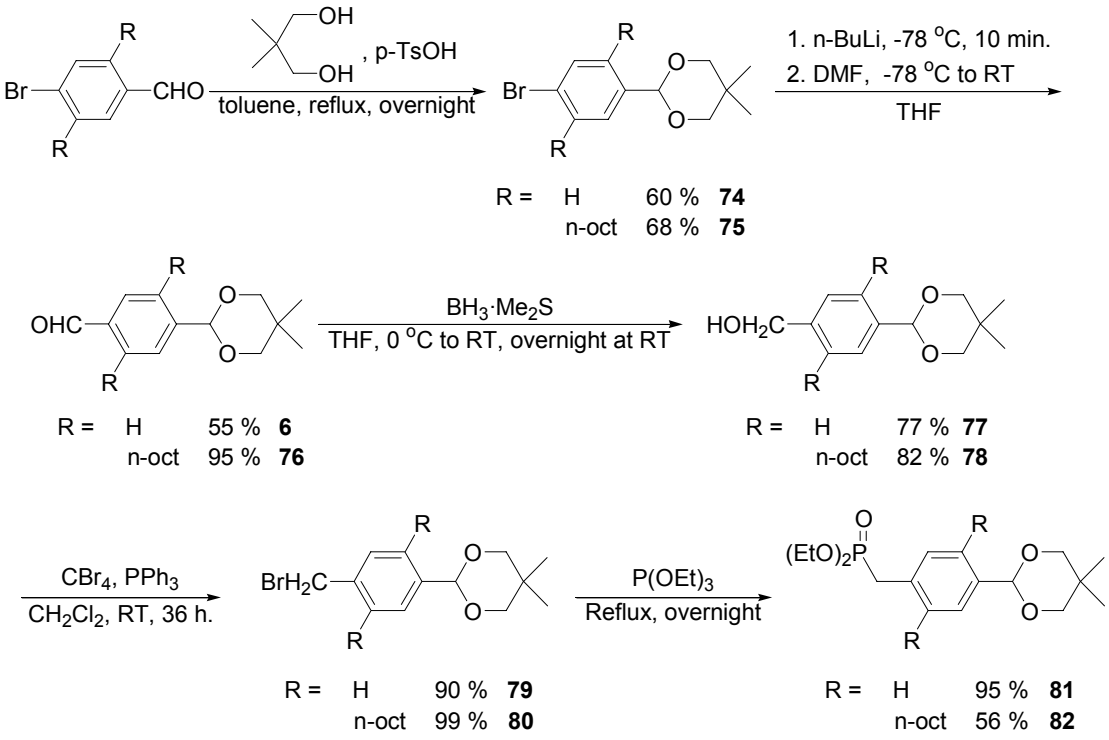

Scheme 2-22: The preparation of extension reagents for OPV synthesis.

The idea of the extension reagents is to have a phosphonate ester on one end and an acetal protected aldehyde on the other end of the benzene ring. Coupling the extension reagent to an aldehyde in a HWE reaction proceeds under basic conditions and the acetal protecting group is untouched. Once the HWE reaction is completed, acidic workup liberates the protected aldehyde resulting in an extension of the starting aldehyde with a phenylene vinylene unit. A similar strategy has been applied in Ref. 44 and 45. The reason for making an extension reagent functionalized with octyl chains is to promote solubility in solvents such as toluene. The extension reagent (with R=H) was applied to make a series of OPV's as shown in Scheme 2-23.

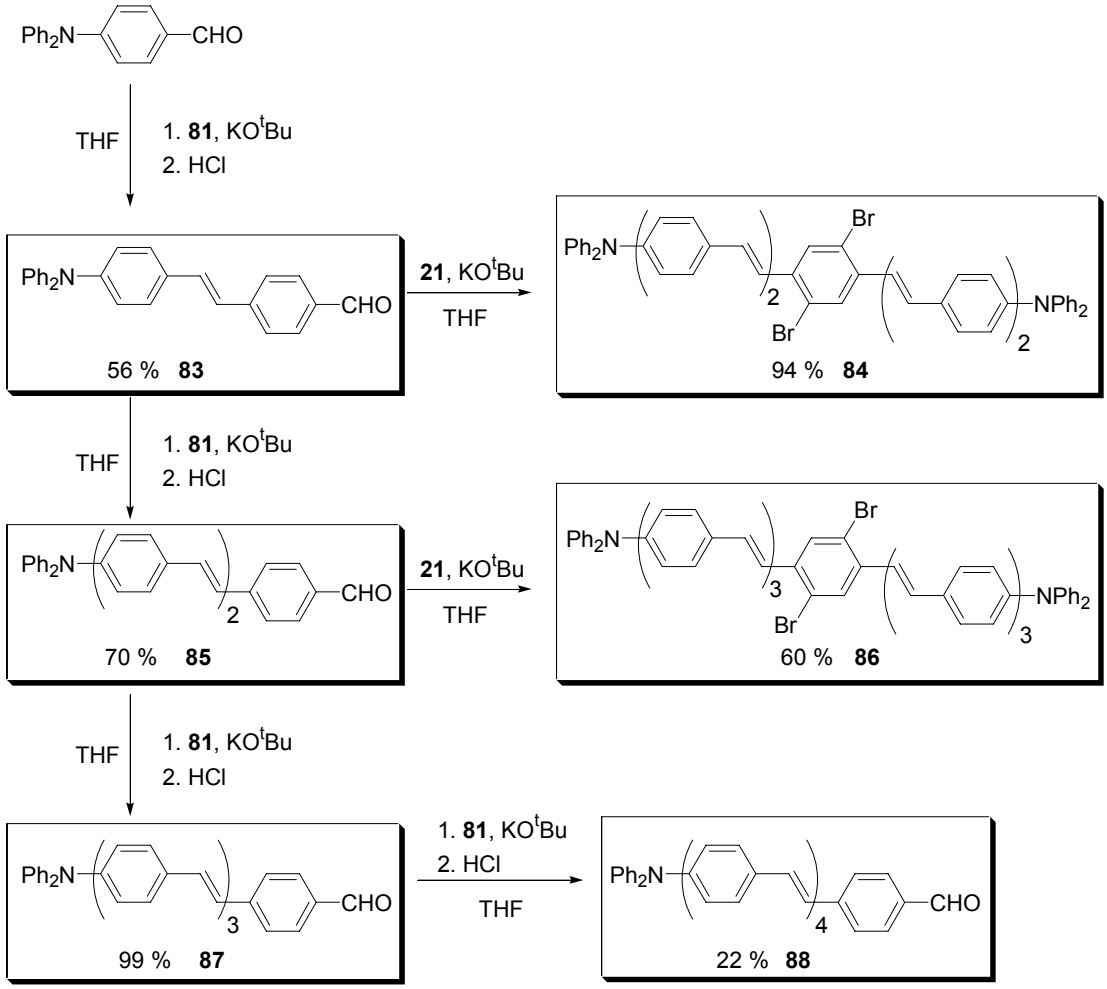

Scheme 2-23: The preparation of OPV's with varying conjugation lengths. The reaction times for the HWE-reactions were 1-2 h. at reflux, and the removal of the acetal protecting group was done by quenching the reaction with hydrochloric acid and refluxing overnight.

The solubility of the OPV's naturally decreased with an increasing number of phenylene vinylene units and it was very difficult to get **86** and **88** into solution in toluene. It was possible, however, to measure singlet oxygen quantum yields for these two compounds.

2.2.8 Knoevenagel condensations

Two compounds were made where the double bonds in the OPV were replaced with an α-β-unsaturated nitrile or ketone as shown in Scheme 2-24. The design principle for introducing electron deficient double bonds as π-linkers, is that these are less

susceptible to reactions with singlet oxygen, which should then result in an overall better photostability of the sensitizer.[46]

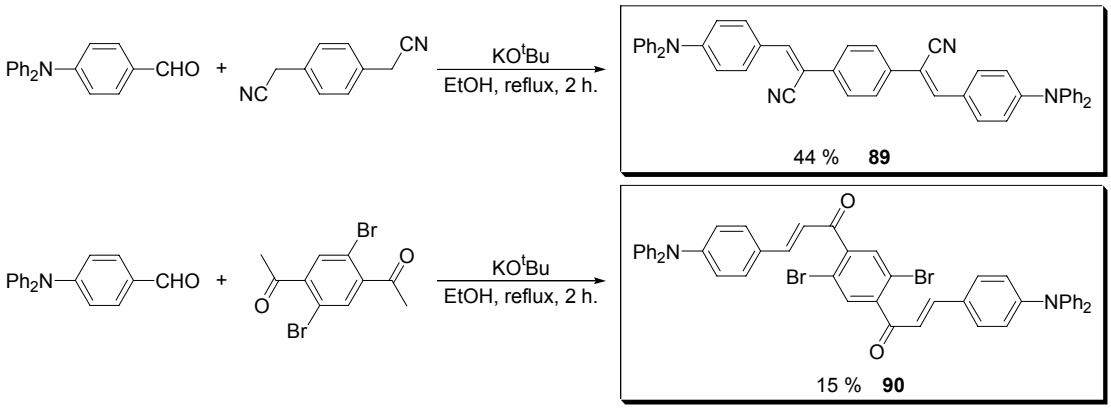

Scheme 2-24: Compounds prepared by Knoevenagel condensations.

Compound **89** has previously been prepared in 94 % yield and its crystal structure reported by Pond and co-workers.[35] Instead of using potassium *tert*-butoxide as the base in the preparation of **90**, piperidine was also tried but this did not lead to the isolation of the target molecule from the reaction mixture.

2.2.9 Acetylene analogs

Sensitizers containing alkyne moieties have been shown to be less reactive towards singlet oxygen in comparison with the equivalent sensitizers containing alkene moieties.[47] Typically, alkyne functionalities are introduced in aromatic molecules using Pd based chemistry and recently it has been shown that it is difficult to purify products containing alkyne moieties obtained from Pd catalysed reactions as Pd binds to the alkyne group.[48] Thus, the possibility of preparing acetylene analogs to some of the OPV's described above using phosphorous chemistry was investigated. It has been reported[49-52] that α-chloro or α-bromo phosphonate esters can be reacted with carbonyl groups to form a halogen substituted vinylene. A second equivalent of base can then be used for an elimination reaction thus forming the triple bond. Several α-chloro phosphonate esters were prepared as shown in Scheme 2-25 in an attempt to apply the strategy of using α-chloro phosphonate esters in preparing acetylene analogs to the OPV's described in the present work.

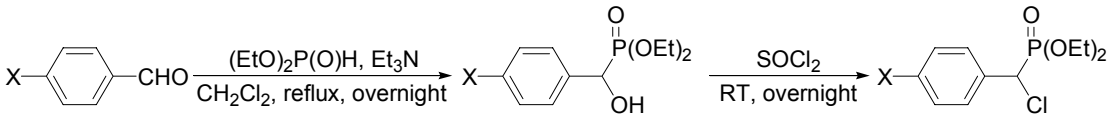

R =				R =			
	F	72 %	**91**		F	51 %	**94**
	Br	97 %	**92**		Br	71 %	**95**
	I	65 %	**93**		I	72 %	**96**

Scheme 2-25: The preparation of α-chloro phosphonate esters.

The fluoro-substituted α-chloro phosphonate ester (**94**) was reacted with 2,5-diformyl-1,4-dibromo-benzene, and the corresponding acetylene compound as shown in Scheme 2-26 was obtained. An attempt was also made to react the iodide substituted α-chloro phosphonate ester (**96**) with 2,5-diformyl-1,4-dibromo-benzene, but a number of products were obtained according, which were difficult to separate using column chromotography. The biproducts were probably formed by Ar-nucleophilic substitution with the *tert*-butoxide anion.

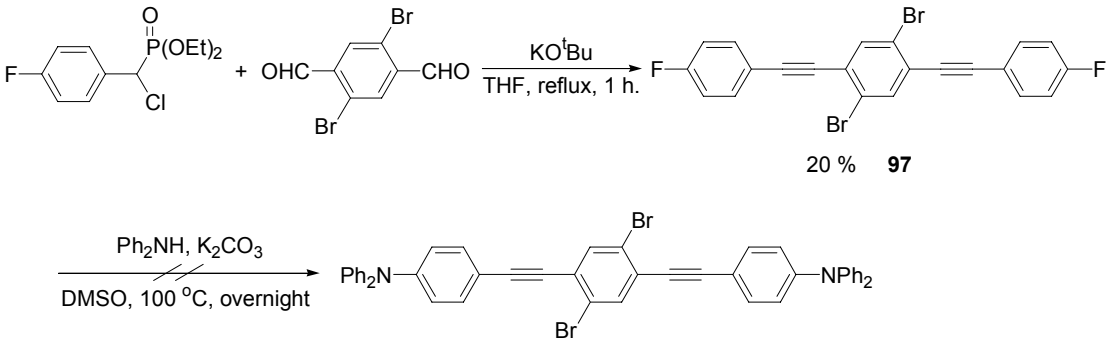

Scheme 2-26: Attempt to make the acetylene analog of **33**.

It was hoped that an Ar-nucleophilic substitution on the fluoro acetylene compound with diphenylamine could afford the acetylene analog to **33**, but this attempt was unsuccessful. As an alternative, several amino-benzaldehydes with diethyl phosphite was tried reacted with triethylamine as described for the halogen substituted benzaldehydes. It was not possible to isolate the desired α-hydroxy phosphonate esters in any of the cases. An attempt was made to react the *para*-fluoro substituted α-chloro phosphonate ester with diphenylamine in an attempt to do an Ar-nucleophilic substitution on this compound, but this also failed. Finally, the synthetic strategy was reversed, and 2,5-diformyl-1,4-dibromo-benzene was reacted with diethyl phosphite

and triethylamine (Scheme 2-27) followed by an attempt to do a substitution of the hydroxy group with chlorine.

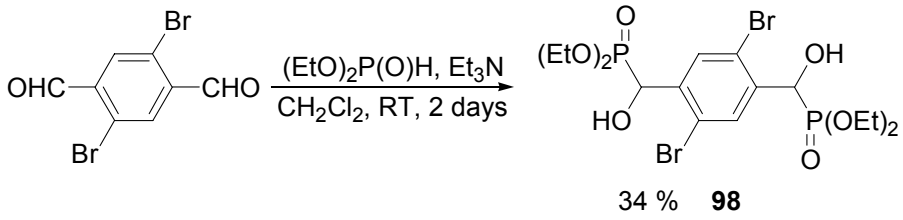

34 % **98**

Scheme 2-27: The preparation of a di-α-hydroxy phosphonate ester.

The reaction with 2,5-diformyl-1,4-dibromo-benzene and diethyl phosphite was successful, but several attempts to substitute the hydroxy group (including reacting with aqueous hydrochloric acid or thionyl chloride) failed. Some support of this finding was subsequently found in the literature,[50,51] where it was described that bulky *ortho* substituents prevents the hydroxy to halogen substitution due to sterical hindrance.

Based on the above, it was learned that even though the use of α-chloro phosphonate esters for preparing acetylene compounds has several attractable features compared to Sonogashira couplings (no inert atmosphere is needed and a Pd catalyst that could cause difficulties in the purification and cause side reactions[48] is avoided) the strategy is not feasible for preparing acetylene analogs of the OPV's described earlier.

2.3 Conclusion

The syntheses of a large number of several OPV's have been described. The key points in the synthetic routes described is the ability to introduce a variety of different substituents into the OPV framework through the use of either Wittig-based or Heck-reactions, or Knoevenagel condenations. Furthermore, it has been demonstrated how to extend the conjugation lengths of an OPV through stepwise unidirectional oligerimization reactions. Aspects of the synthesis of aromatic molecules containing alkyne moieties have also been briefly discussed.

Reference List

1. Kauffman, J. M.; Moyna, G. *J. Org. Chem.* **2003**, *68*, 839-853.
2. Monroe, B. M. *J. Phys. Chem.* **1977**, *81*, 1861-1864.
3. Wang, X. M.; Zhou, Y. F.; Yu, W. T.; Wang, C.; Fang, Q.; Jiang, M. H.; Lei, H.; Wang, H. Z. *J. Mater. Chem.* **2000**, *10*, 2698-2703.
4. Sengupta, S. *Tetrahedron Lett.* **2003**, *44*, 307-310.
5. Sengupta, S.; Sadhukhan, S. K.; Muhuri, S. *Tetrahedron Lett.* **2002**, *43*, 3521-3524.
6. Krebs, F. C.; Spanggaard, H. *J. Org. Chem.* **2002**, *67*, 7185-7192.
7. Krebs, F. C.; Jørgensen, M. *J. Org. Chem.* **2001**, *66*, 6169-6173.
8. Krebs, F. C., Personal comminication.
9. Sparks, R. B.; Combs, A. P. *Org. Lett.* **2004**, *6*, 2473-2475.
10. Wolkenberg, S. E.; Wisnoski, D. D.; Leister, W. H.; Wang, Y.; Zhao, Z. J.; Lindsley, C. W. *Org. Lett.* **2004**, *6*, 1453-1456.
11. Greenspan, P. D.; Main, A. J.; Bhagwat, S. S.; Barsky, L. I.; Doti, R. A.; Engle, A. R.; Frey, L. M.; Zhou, H. H.; Lipson, K. E.; Chin, M. H.; Jackson, R. H.; UzielFusi, S. *Bioorg. Med. Chem. Lett.* **1997**, *7*, 949-954.
12. Watanabe, M.; Nishiyama, M.; Yamamoto, T.; Koie, Y. *Tetrahedron Lett.* **2000**, *41*, 481-483.
13. Magdolen, P.; Meciarova, M.; Toma, S. *Tetrahedron* **2001**, *57*, 4781-4785.
14. Blum, J.; Zimmerman, M. *Tetrahedron* **1972**, *28*, 275-280.
15. de Diesbach, H.; Zurbriggen, G. *Helv. Chim. Acta* **1925**, *8*, 551-556.
16. Xiao, Y.; Yu, W. L.; Chua, S. J.; Huang, W. *Chem. Eur. J.* **2000**, *6*, 1318-1321.
17. Thibault, M. E.; Closson, T. L. L.; Manning, S. C.; Dibble, P. W. *J. Org. Chem.* **2003**, *68*, 8373-8378.
18. Yu, D. W.; Preuss, K. E.; Cassis, P. R.; Dejikhangsar, T. D.; Dibble, P. W. *Tetrahedron Lett.* **1996**, *37*, 8845-8848.
19. Blank, N. E.; Haenel, M. W. *Chem. Ber. /Recueil* **1983**, *116*, 827-832.
20. Plater, M. J.; Jackson, T. *Tetrahedron* **2003**, *59*, 4673-4685.

21. Shabtai, E.; Segev, O.; Beust, R.; Rabinovitz, M. *J. Chem. Soc., Perkin Trans. 2* **2000**, *6*, 1233-1241.

22. Szunerits, S.; Utley, J. H. P.; Nielsen, M. F. *J. Chem. Soc., Perkin Trans. 2* **2000**, *4*, 669-675.

23. McGimpsey, W. G.; Samaniego, W. N.; Chen, L.; Wang, F. *J. Phys. Chem. A* **1998**, *102*, 8679-8689.

24. Guo, Z. M.; Zheng, X. Z.; Thompson, W.; Dugdale, M.; Gollamudi, R. *Biorgan. Med. Chem.* **2000**, *8*, 1041-1058.

25. Brehm, I.; Hinneschiedt, S.; Meier, H. *Eur. J. Org. Chem.* **2002**, 3162-3170.

26. Kochetkov, N. K.; Nifantév, E. E.; Nesmeyanov, A. N. *Doklady Akad. Nauk S. S. S. R.* **1955**, *104*, 422-426.

27. Raposo, M. M. M.; Pereira, A. M. B.; Oliverira-Campos, A. M. F.; Shannon, P. V. R. *J. Chem. Res. Miniprint* **2000**, *4*, 528-558.

28. Ngola, S. M.; Kearney, P. C.; Mecozzi, S.; Russell, K.; Dougherty, D. A. *J. Am. Chem. Soc.* **1999**, *121*, 1192-1201.

29. Wenseleers, W.; Stellacci, F.; Meyer-Friedrichsen, T.; Mangel, T.; Bauer, C. A.; Pond, S. J. K.; Marder, S. R.; Perry, J. W. *J. Phys. Chem. B* **2002**, *106*, 6853-6863.

30. Taylor, S. D.; Dinaut, A. N.; Thadani, A. N.; Huang, Z. *Tetrahedron Lett.* **1996**, *37*, 8089-8092.

31. Agranat, I.; Rabinovitz, M.; Shaw, W. C. *J. Org. Chem.* **1979**, *44*, 1936-1941.

32. Sarker, A. M.; Ding, L. M.; Lahti, P. M.; Karasz, F. E. *Macromolecules* **2002**, *35*, 223-230.

33. Bradsher, C. K.; Hunt, D. A. *J. Org. Chem.* **1981**, *46*, 4608-4610.

34. Frederiksen, P. K.; Jørgensen, M.; Ogilby, P. R. *J. Am. Chem. Soc.* **2001**, *123*, 1215-1221.

35. Pond, S. J. K.; Rumi, M.; Levin, M. D.; Parker, T. C.; Beljonne, D.; Day, M. W.; Brédas, J. L.; Marder, S. R.; Perry, J. W. *J. Phys. Chem. A* **2002**, *106*, 11470-11480.

36. Li, C.-L.; Shieh, S.-J.; Lin, S.-C.; Liu, R.-S. *Org. Lett.* **2003**, *5*, 1131-1134.

37. Ruggli, P.; Brandt, F. *Helv. Chim. Acta* **1944**, *27*, 274-291.

38. Lamba, J. J. S.; Tour, J. M. *J. Am. Chem. Soc.* **1994**, *116*, 11723-11736.

39. Sunde, C. J.; Johnson, G.; Kade, C. F. *J. Org. Chem.* **1939**, *4*, 548-554.

40. Dirk, S. M.; Mickelson, E. T.; Henderson, J. C.; Tour, J. M. *Org. Lett.* **2000**, *2*, 3405-3406.

41. Kosynkin, D. V.; Tour, J. M. *Org. Lett.* **2001**, *3*, 993-995.

42. Netherton, M. R.; Fu, G. C. *Org. Lett.* **2001**, *3*, 4295-4298.

43. Wright, S. W.; Hageman, D. L.; McClure, L. D. *J. Heterocycl. Chem.* **1998**, *35*, 719-723.

44. Stuhr-Hansen, N.; Christensen, J. B.; Harrit, N.; Bjørnholm, T. *J. Org. Chem.* **2002**, *68*, 1275-1282.

45. Jørgensen, M.; Krebs, F. C. *J. Org. Chem.* **2004**, *69*, 6688-6696.

46. Dam, N.; Scurlock, R. D.; Wang, B. J.; Ma, L. C.; Sundahl, M.; Ogilby, P. R. *Chem. Mater.* **1999**, *11*, 1302-1305.

47. McIlroy, S. P.; Cló, E.; Nikolajsen, L.; Frederiksen, P. K.; Nielsen, C. B.; Mikkelsen, K. V.; Gothelf, K. V.; Ogilby, P. R. *J. Org. Chem.* **2005**, *70*, 1134-1146.

48. Krebs, F. C.; Nyberg, R. B.; Jørgensen, M. *Chem. Mater.* **2004**, *16*, 1313-1318.

49. Kondo, K.; Ohnishi, N.; Takemoto, K.; Yoshida, H.; Yoshida, K. *J. Org. Chem.* **1992**, *57*, 1622-1625.

50. Iorga, B.; Eymery, F.; Savignac, P. *Synthesis (Stuttgart)* **2000**, 576-580.

51. Iorga, B.; Eymery, F.; Savignac, P. *Tetrahedron* **1999**, *55*, 2671-2686.

52. Zimmer, H.; Bercz, P. J.; Maltenie, O. J.; Moore, M. W. *J. Am. Chem. Soc.* **1965**, *87*, 2777-2778.

CHAPTER 3

OLIGO PHENYLENE–VINYLENES AS TWO–PHOTON SINGLET OXYGEN SENSITIZERS

Abstract: *Photophysical studies on the molecules prepared in Chapter 2, employing the measurement of fluorescence and absorption properties, singlet oxygen quantum yields and two-photon absorption action spectra, reveals that efficient two-photon singlet oxygen sensitizers posses a moderate amount of charge-transfer character in the excited state. Charge-transfer character enhances two-photon absorption through an increase in the transition dipole moment. Too much charge-transfer, however, is counter productive as it shuts down singlet oxygen generation by providing alternative channels for excited state deactivation.*

3.1 Photophysical characterization

The molecules prepared in Chapter 2 can be divided into four groups. Two of these groups are characterized by variation of either the end- or the middle electron donor-acceptor substituents on the OPV skeleton. Another group of molecules is where the OPV conjugation length is varied, and the last group constitutes molecules where the π-linker between the benzene rings is varied. One intrinsic substituent-dependent property of all of these molecules is the extent of charge-transfer character in the excited states. This is expected to have an impact on both the singlet oxygen quantum yield and the TPA cross section, as discussed in Chapter 1. Preliminary investigations on the how to identify and subsequently quantify the extent of charge-transfer in a molecule is thus necessary in terms of discussing variations in the singlet oxygen quantum yield and TPA cross sections for the four groups of molecules.

3.2 Charge-transfer and electron donating groups

The OPV molecules discussed in this chapter were designed to have varying degrees of charge-transfer (CT) by varying the nature of the substituents in the OPV motif. One manifistation of the extent of CT character in a molecule is in the absorption spectrum. The absorption spectra of **32**, **35** and **73** are shown in Figure 3-1.

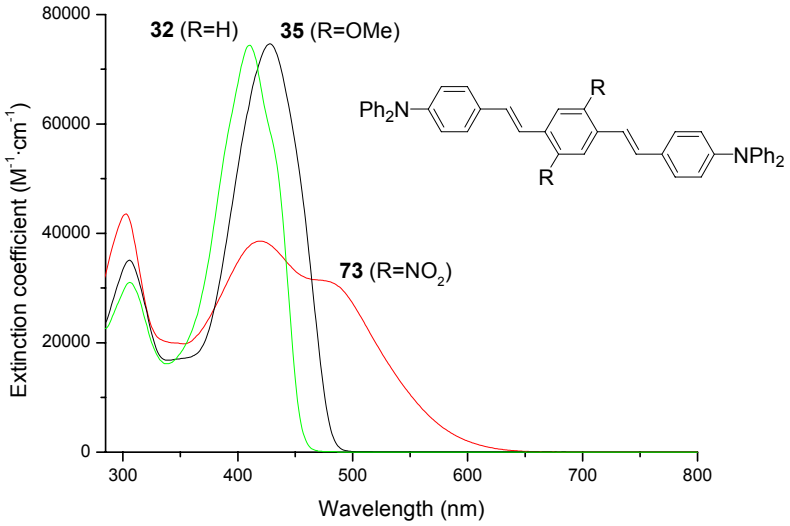

Figure 3-1: UV-VIS spectra of compounds **32**, **35** and **73** in toluene.

For **32** and **35,** only two absorption bands are observed occurring at 306 nm and 411 nm for **32** and at 306 nm and 428 nm for **35**. Compound **73** has another, red-shifted, band in the absorption spectrum (λ_{max}^{abs} at 303 nm, 420 nm and 474 nm). The absorption band at 474 nm is ascribed to a transition that populates a CT state. The two low-energy bands are even more separated in the absorption spectrum of **67** (see Figure 3-2).

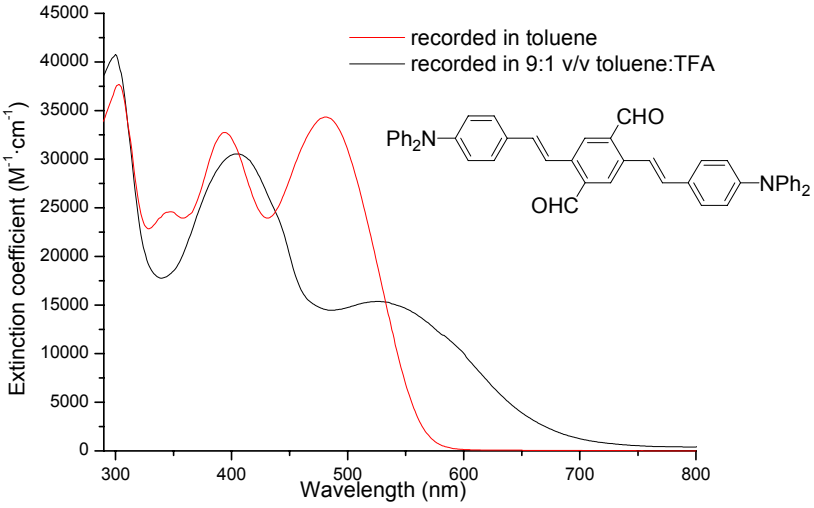

Figure 3-2: UV-VIS spectrum of **67** in toluene and in toluene with TFA.

By destroying the push-pull nature of the molecule, the band ascribed to CT should be altered. Adding trifluroacetic acid (TFA) to the solution of **67,** thus protonating the amine nitrogens and altering the electron donating capabilities of the diphenylamino group, causes a decrease of the band at 482 nm whereas a new band at 528 nm appears. The "original" spectrum can be regenerated by adding triethylamine to the solution.

Another way of determining whether a molecule has CT character is make a Lippert-Mataga plot.[1] For this analysis the fluorine analog **36** was chosen as there have been several reports[2-4] on the CT character of fluorine substituted extended aromatic molecules. A Lippert-Mataga plot is a plot of the Stokes shift as a function of the solvent polarity, where the change in Stokes shift can be quantified by applying self-consistent reaction field theory.[5,6] A result of this theory is the Lippert-Mataga equation,

$$\tilde{\nu}_a - \tilde{\nu}_f = \frac{1}{4\pi\varepsilon_0} \cdot \frac{2}{hca_w^3} \cdot \left(\mu^E - \mu^G\right)^2 \cdot \Delta f + \left(\tilde{\nu}_a^g - \tilde{\nu}_f^g\right), \tag{3.1}$$

where $\tilde{\nu}_a$ and $\tilde{\nu}_f$ are the wavenumbers for absorption and fluorescence in solution, respectively, a_w is the cavity radius of the sphere surrounding the solute, $\tilde{\nu}_a^g$ and $\tilde{\nu}_f^g$ are the wavenumbers for absorption and fluorescence in the gas phase, Δf is the reaction field factor, μ^E is the molecular dipole moment of a molecule in its excited state and μ^G is the molecular dipole moment of a molecule in its ground state. Two forms of the Lippert-Mataga equation exist, one where only the dipole moment of the solvent is taken into account and one where the polarizability of the solvent is also considered.[1] These two forms differ by the expression for the reaction field factor and the reaction field factor considering only the dipole moment of the solvent is,

$$\Delta f = \frac{\varepsilon_r - 1}{2\varepsilon_r + 1} - \frac{n^2 - 1}{2n^2 + 1}, \tag{3.2}$$

where ε_r is the relative permittivity (the dielectric constant) and n is the refractive index. When the polarizability of the solvent is taken into account the reaction field factor becomes,

$$\Delta f = \frac{\varepsilon_r - 1}{\varepsilon_r + 2} - \frac{n^2 - 1}{n^2 + 2}. \tag{3.3}$$

The solvent polarity can be varied systematically by using mixtures of two solvents and the two solvent systems (CS_2/n-heptane and CH_2Cl_2/n-heptane) was chosen for the investigations of the solvent effects on the emision wavelength of **36**. Even though **36** does not have a dipole (due to the presence of an inversion center), it does have a quadropolar moment. It has been argued that such molecules can still be described by the Lippert-Mataga equations by considering the quadropole as two dipoles.[2,4]

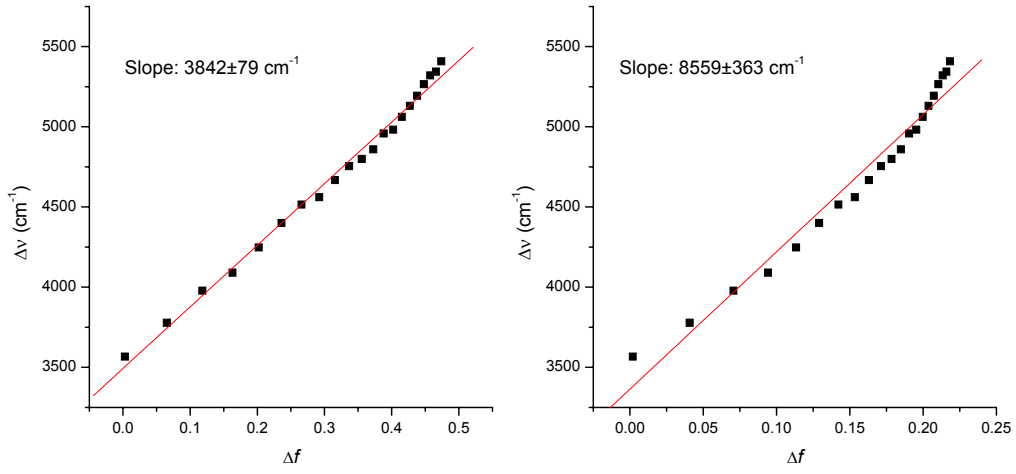

Figure 3-3: Lippert-Mataga plot using mixtures of n-heptane and CH_2Cl_2 as the solvent system. Left: The polarizability of the solvent is taken into account (Eq. (3.3)). Right: Only the dipole moment of the solvent is considered in the calculation of Δf (Eq. (3.2)).

The results of investigation of the Stokes-Shift as a function of the reaction field factor in the two solvent systems are depicted in Figure 3-3 and Figure 3-4. In the n-heptane/CH_2Cl_2 study, a better correlation was obtained when the polarizability of the solvent was taken into account. However, the slopes usually reported in the literature are calculated considering only the dipole moment of the solvent.

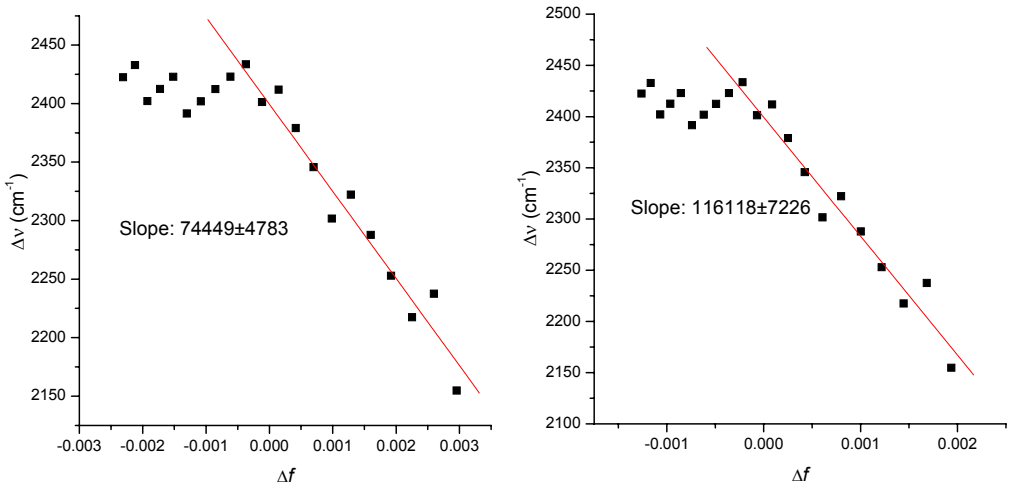

Figure 3-4: Lippert-Mataga plot using mixtures of n-heptane and CS_2 as the solvent system. Left: The polarizability of the solvent is taken into account. Right: Only the dipole moment of the solvent is considered in the calculation of Δf.

The slopes obtained from the Lippert-Mataga plots reflect the change in dipole moments between the ground and excited state (see Eq. (3.1)) and large changes are indicative of charge transfer upon excitation. In the n-heptane/CH_2Cl_2 study, a slope of approximately 8600 cm^{-1} was obtained. This value is similar to slopes obtained for a series of donor-π-acceptor molecules such as dialkylaminonaphthalene sulfonamides (10,600 cm^{-1}) and coumarines (11,300 cm^{-1}), where the excitation has been described to be of charge transfer character.[7] Although the slopes of 74,400 cm^{-1} and 120,000 cm^{-1} in the CS_2/n-heptane solvent system lead to the conclusion that excitation in **36** can be described to have charge transfer character, the data obtained have features that leads to suspicion. In this solvent system, changes in Δf are very small. Moreover, a negative slope and a systematic pattern in the data at negative values of Δf are observed.

Cyclic voltammetry was carried out on **33**, **42** and **47** in a 0.1 M Bu_4NPF_4 in CH_2Cl_2 solution. The results for **33** and **42** are shown in Figure 3-5. The reference electrode was in both cases an Ag/AgCl electrode, and the potential is reported with respect to that electrode. The working electrode was a Pt-electrode. Calibration was not done against the typically used ferrocene redox couple as it has been described to give

unreliable results for comparing the oxidation potentials of diarylamines in particular.[8] The oxidation potentials are thus reported relative to the Ag/AgCl electrode.

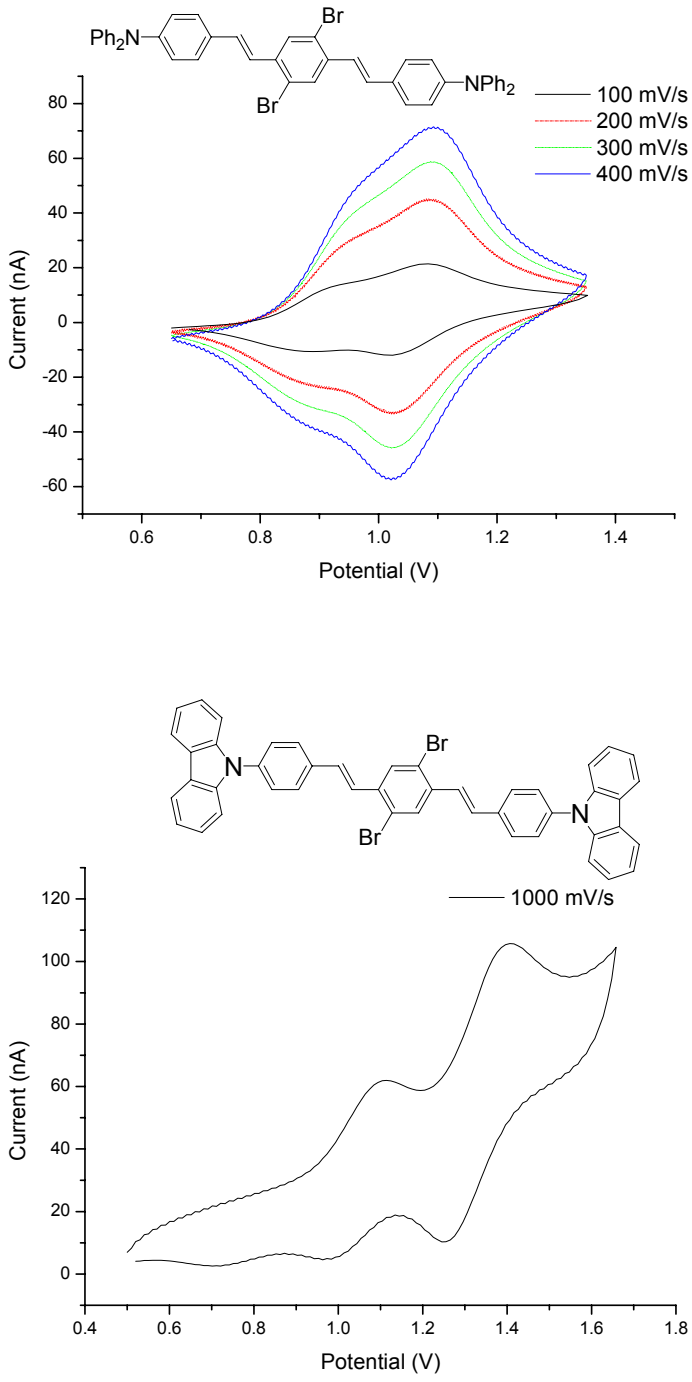

Figure 3-5: Cyclic voltammogram of **33** (top) **42** (bottom) using different scan rates and an Ag/AgCl electrode as the reference electrode.

Two partially resolved redox couples are observed for the diphenylamine **33** which were assigned to be two-step one-electron couples (the redox couples are separated by 56 mV and 59 mV, where 58 mV is required[9] for a reversible process at 298 K) corresponding to removal an electron from each triarylamine system in accordance with the observation made in Ref. 8 and 10 and for similar molecules. The presence of two redox couples indicates an electronic communication between the end groups (*i.e.* the end-groups can "see each other"). For the carbazole analog **42** two redox couples were observed, but the oxidation and reduction waves are separated by 151 mV for both couples. The failure to see reversible waves (with 58 mV separation of the two waves) was ascribed to be due to diffusion-controlled processes.[8] The cyclic voltammogram for **47** only showed one redox couple as expected, and the oxidation and reduction waves were, similar to the case of **42**, separated by 171 mV which was again ascribed to be due to diffusion controlled processes.

Table 3-1: Oxidation potentials for **33**, **42** and **47** reported relative to an Ag/AgCl working electrode.

Compound	E_{ox}/V	
33	1.07	0.89
42	1.33	1.04
47	1.20	

In terms of the electron donating capabilities for the diphenylamine, carbazole and methoxy functional groups, it is concluded (in accordance with what one would expect) that the methoxy group is the weakest donating group and the diphenylamine is the strongest.

3.3 Two-photon absorption action spectra and singlet oxygen quantum yields

In the sections above, it is illustrated that some of the molecules studied do posses pronounced CT character in the excited state. In the material that follows the non-linear optical properties of the potential singlet oxygen sensitizers is discussed.

3.3.1 The effect of varying substitution pattern in the middle ring

The one-photon properties of **36-40** and **49** are presented in Table 3-2. The UV-VIS data show absorption ranging from 375 to 428 nm with extinction coefficients between $5.6 \cdot 10^5$ $M^{-1} \cdot cm^{-1}$ and $9.5 \cdot 10^5$ $M^{-1} \cdot cm^{-1}$. In general, high fluorescence quantum yields are observed except for **38**. This finding is explained by the lack of functional groups that can promote intersystem crossing, whereas **38** has two bromine atoms. This is also reflected in the singlet oxygen quantum yields, where **38** has a Φ_Δ-value of 0.13 as opposed the rest of the compounds where the Φ_Δ-values are all below 0.10.

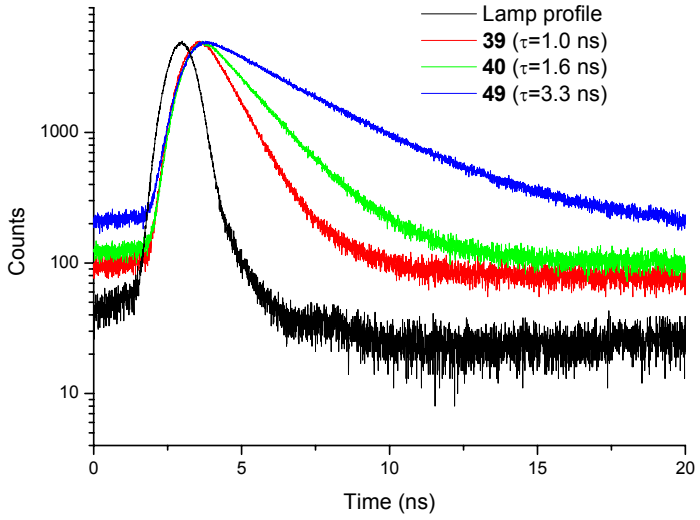

Figure 3-6: Time-resolved fluorescence from **39**, **40** and **49**.

The lifetimes of the S_1 state of the compounds were determined by time-resolved fluorescence measurements, and the decays after excitation with a 373 nm diode laser for **39**, **40** and **49** are shown in Figure 3-6. The lifetimes for **39** and **40** are very short and it was necessary to deconvolute the lamp profile from the measured decay spectra in order to extract the lifetimes. It is important to note that the lifetimes reported in the present work are overall lifetimes (thus including all deactiviation processes, not just radiative processes).

Table 3-2: One-photon properties of **36-40** and **49** in toluene. λ_{max}^{abs} is the one-photon absorption maximum. The numbers in parantheses are the logarithm of the molar extinction coefficients. λ_{max}^{em} is the fluorescence maximum, Φ_f is the fluorescence quantum yield, τ is the fluorescence lifetime, and Φ_Δ is the singlet oxygen quantum yield (determined against acridine as the standard).[a]

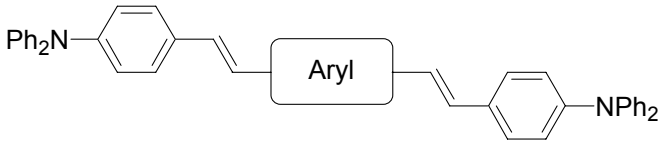

	Aryl	λ_{max}^{abs}	λ_{max}^{em}	Φ_f	τ /ns	Φ_Δ
36	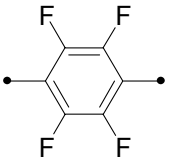	428 (4.90) 304 (4.61)	486 517	0.8	1.1	0.09
37	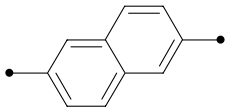	409 (4.90) 300 (4.62)	459 481	0.8	1.0	0.08
38	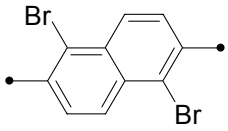	423 (4.83) 306 (4.63)	480 507	0.2	0.4	0.13
39	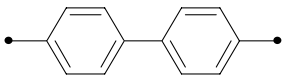	399 (4.98) 303 (4.61)	452 479	0.7	1.0	0.06
40	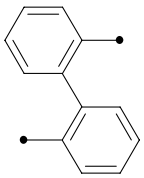	375 (4.75) 300 (4.63)	426	0.5	1.6	0.05
49	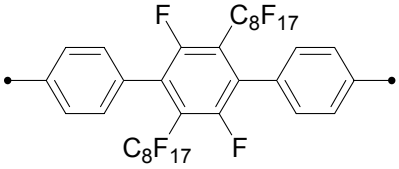	382 (4.92) 302 (4.77)	525	0.7	3.3	

Compound **49** has a significantly longer lifetime (3.3 ns) than the rest of the compounds. A lifetime of 4.4 ns (in methylene chloride) has been measured for a similar molecule in Ref. 2 adding credability to the number reported for **49**.

[a] Errors are ±10 % for all determined numbers.

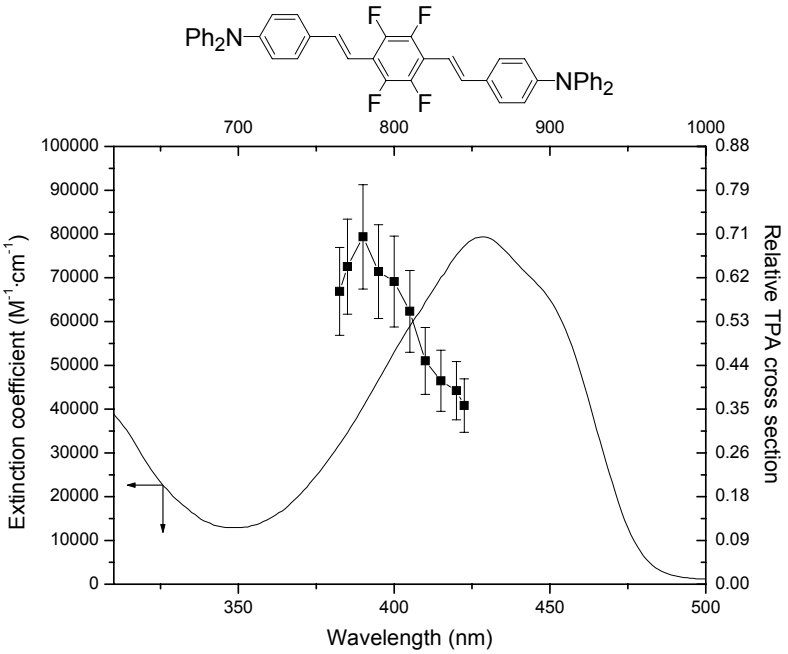

Figure 3-7: One-photon absorption and two-photon action spectra of **36** in toluene.

The UV-VIS spectra and TPA action spectra of **36**, **37** and **38** recorded in toluene are shown in Figure 3-7, Figure 3-8 and Figure 3-9, respectively.

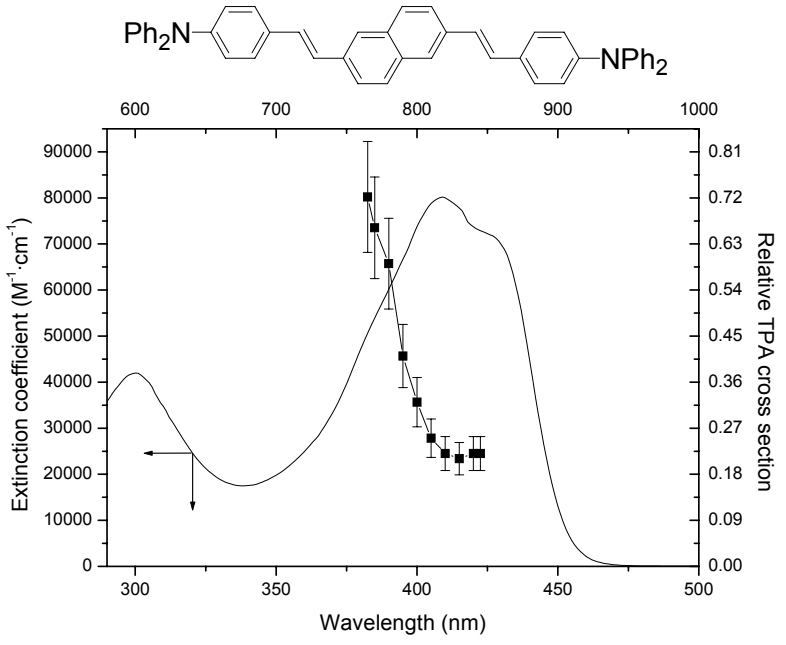

Figure 3-8: One-photon absorption and two-photon action spectra of **37** in toluene.

The TPA action spectra of **36** and **38** clearly show a maximum within the spectral range studied and in the states populated upon two-photon excitation are approximately 0.3 eV higher in energy than the states populated upon one-photon excitation. Assuming that the TPA maximum for **37** is blue shifted with a similar wavelength, the maximum should be around 740 nm, which is just outside the spectral region covered in the measurements.

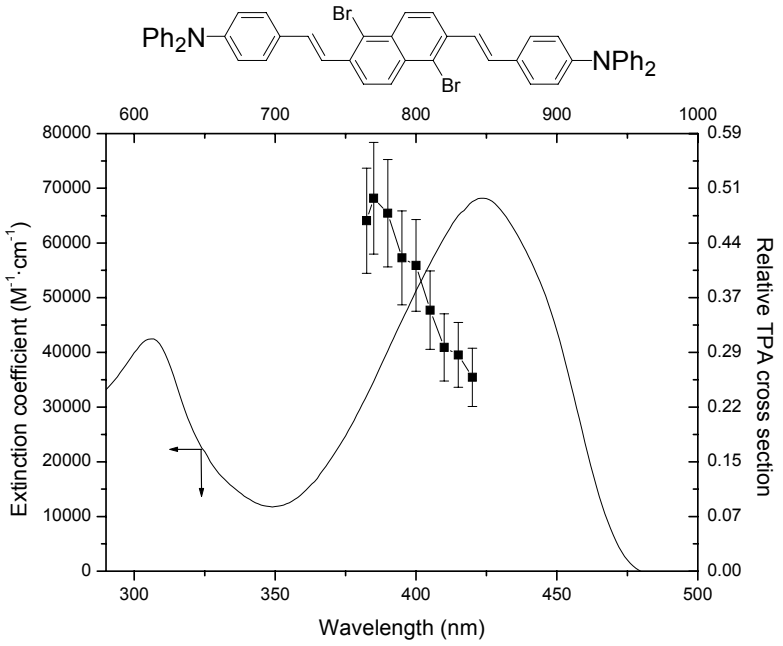

Figure 3-9: One-photon absorption and two-photon action spectra of **38** in toluene.

These compounds have an inversion center thus imposing selection rules on the excitations. In one-photon excitations, gerade-ungerade and ungerade-gerade excitations are allowed, whereas gerade-gerade and ungerade-ungerade excitations become allowed in two-photon excitation schemes.[11,12] This means that a different state is populated in the two-photon absorption process than the one populated in the one-photon absorption process. This is clearly seen from the TPA action spectra, where the excited state reached through two-photon is energetically higher placed than the state populated in the one-photon absorption process.

The relative TPA cross sections determined for **36** (0.70±0.11 at 780 nm), **37** (0.72±0.11 at 765 nm) and **38** (0.50±0.08 at 780 nm) are decent compared to the standard (**34**). However, the singlet oxygen quantum yields are not high. A given

sensitizer can be evaluated in terms of the success in producing singlet oxygen using a two-photon irradiation scheme in comparison with the standard. This comparison is done over the spectral range studied by plotting the ratio of the measured phosphorescence signals (S_Δ) at 1270 nm for the molecule under study and the standard (**34**) after correcting for the differences in concentrations. The physical value actually plotted is then $\Phi_\Delta^X \cdot \delta_{TPA}^X / \Phi_\Delta^{standard} \cdot \delta_{TPA}^{standard}$ (see Eq. (1.7)), which is done in Figure 3-10 for the three compounds.

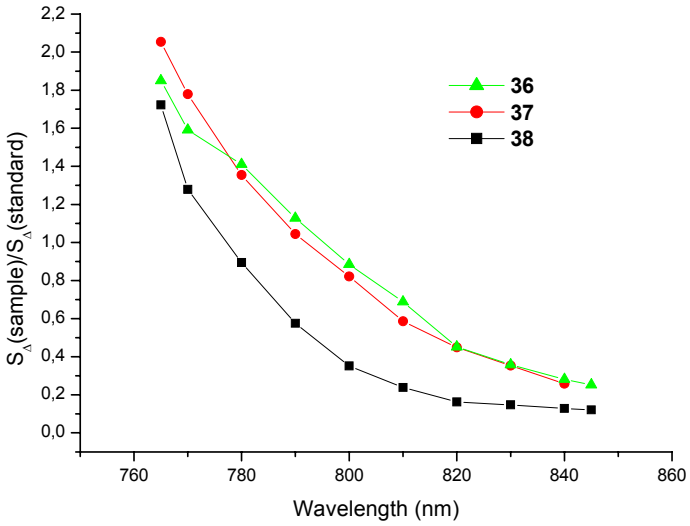

Figure 3-10: Concentration corrected phosphorescence intensities relative to **34** for **36**, **37** and **38**.

From Figure 3-10 we see that **36** and **37** can be considered to be equally good as two-photon singlet oxygen sensitizers and are better than the standard from 765 nm to 790 nm. Compound **38** is only better than the standard at 765-770 nm.

3.3.2 Electron donor and mesomeric substitution on the end-ring

In Table 3-3, the one-photon photophysical properties of **33** and **41-48** are summarized. These molecules can all be described as having the same dibromo-substituted distyryl motif but functionalized with different end-groups. It was difficult to dissolve the imidazole analog (**41**) in toluene (a 10^{-4} M solution is needed for recording the TPA action spectrum). The TPA action spectra of **33**, **42**, **46** and **47** were recorded. However, the action spectrum of **47** is not shown as the TPA

maximum is well out of the spectral range of 765-845 nm used – a relative TPA cross section of only 0.02 was measured at 765 nm. By comparing data from **47** and **45** it is seen that putting in electron donating groups at the *meta*-position has no effect on the quantum yield. However, a donating group in the *para*-position does makes a difference, which is seen by the higher singlet oxygen quantum yield of **33**, **44**, **45** and **46** in comparison to **43:** Thus a stronger electron donor gives a higher singlet oxygen quantum yield when the center phenyl ring in the OPV motif is substituted with bromine atoms.

Table 3-3: One-photon properties of **33** and **41-48** in toluene. λ_{max}^{abs} is the one-photon absorption maximum. The numbers in parantheses are the logarithm of the molar extinction coefficients. λ_{max}^{em} is the fluorescence maximum, Φ_f is the fluorescence quantum yield, τ is the fluorescence lifetime, and Φ_Δ is the singlet oxygen quantum yield (determined against acridine as the standard).[a]

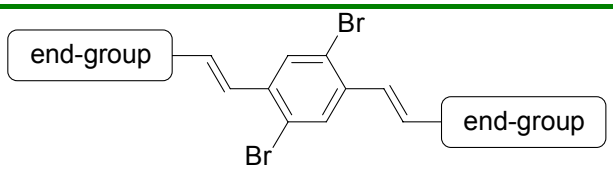

	End-group	λ_{max}^{abs}	λ_{max}^{em}	Φ_f	τ /ns	Φ_Δ
33	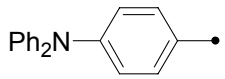	425 (4.80) 303 (4.60)	492 524	0.3	0.7	0.46
41	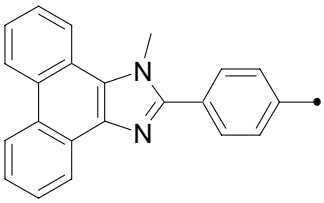	397 (4.50) 304 (4.13)	475 504	0.5	0.6	
42	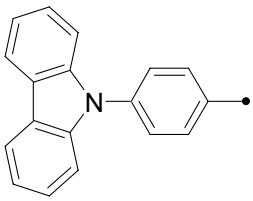	383 (4.67) 343 (4.50) 330 (4.43) 293 (4.58)	450 477	0.2	0.4	0.26
43	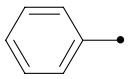	356 (4.69)	404 428	0.1	0.3	0.16
44		362 (4.76)	412 437	0.2	0.3	0.23
45	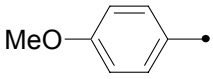	373 (4.68)	427 453	0.2	0.3	0.23
46	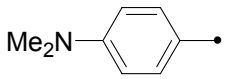	416 (4.72)	490 519	0.2	0.4	0.39

[a] Errors are ±10 % for all determined numbers.

47	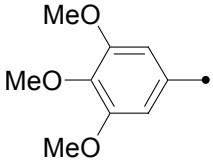				0.23
48	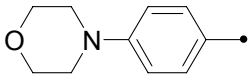	398 (4.60)	486	0.2	0.5

The TPA action spectrum of **33** in toluene is shown in Figure 3-11. The two-photon absorption maximum occurs at 780 nm with a relative cross section of 0.51±0.07. A relative value of 0.62±0.09 has previously been determined.[13]

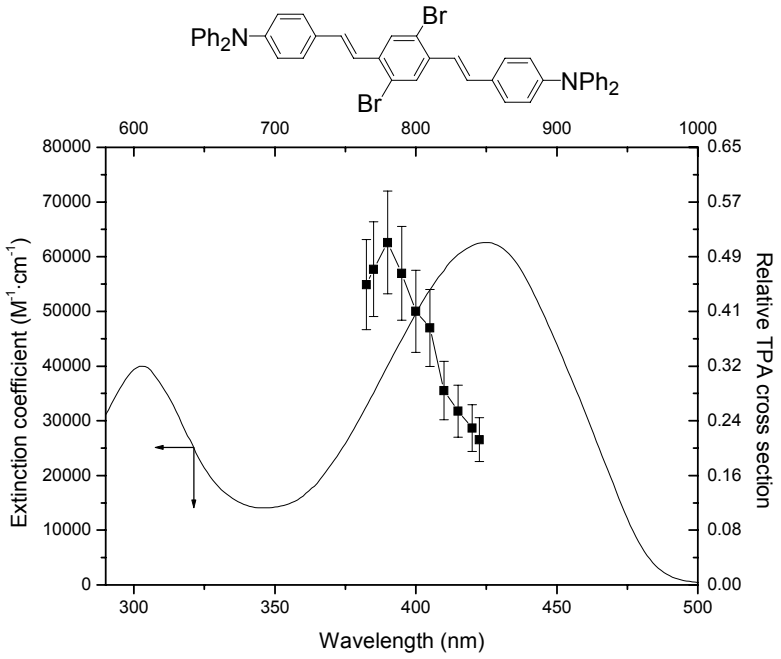

Figure 3-11: One-photon absorption and two-photon action spectra of **33** in toluene.

The two-photon state is ~0.3 eV higher in energy than the one-photon state, similar to **36** and **38**. Assuming that the TPA maximum is blue shifted for **46** by approximately 40 nm (one-photon scale), the TPA maximum is expected to be around 750 nm for the dimethylamino analog (**46**) which means that the measured relative cross section around 765 nm (0.23±0.03) is close to the maximum.

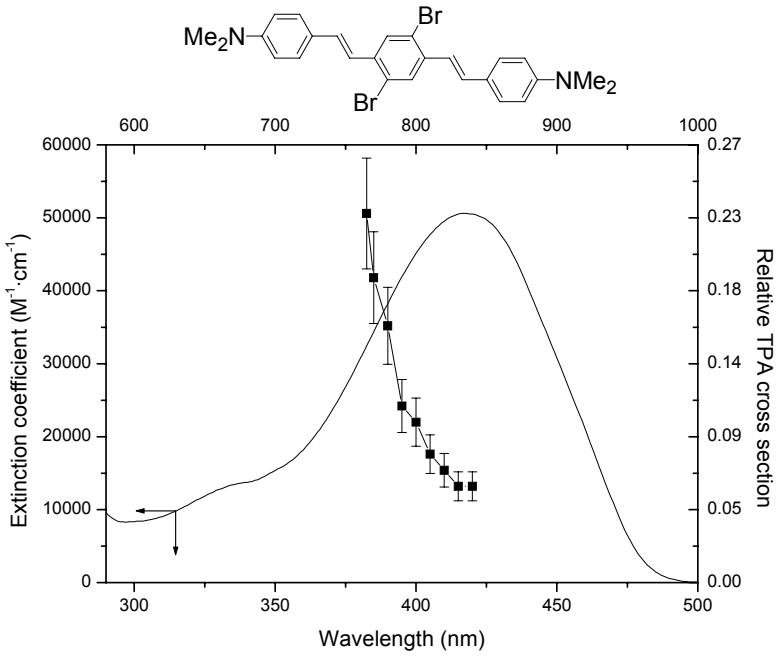

Figure 3-12: One-photon absorption and two-photon action spectrum of **46**.

It is expected that the carbazole analog **42** posesses a longer conjugation length than **33** and should, as such, have a larger TPA cross section. However, the electron donating capability of the carbazole group is weaker than the diphenylamino group, which is seen from the oxidation potentials in Table 3-1.

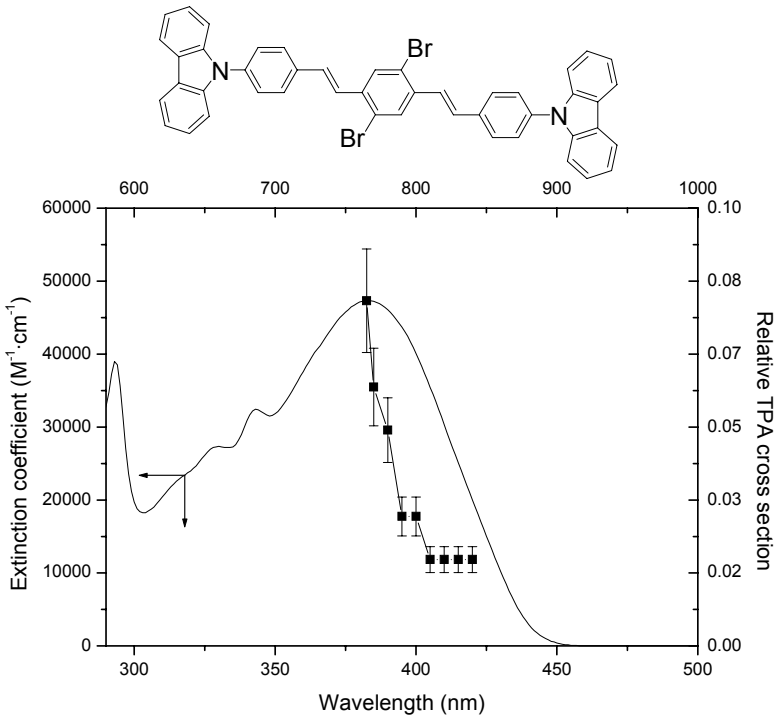

Figure 3-13: One-photon absorption and two-photon action spectrum of **42**.

The data presented so far indicates that it is the electron donating properties of the end-group that influences not just the TPA cross section and maximum, but also the singlet oxygen quantum yield. Note for example, that the carbazol analog has a low singlet oxygen quantum yield of 0.23 in comparison to the diphenyl analog (0.45). The TPA cross sections are also significantly lower for the carbazole analog within the spectral range studied (see Figure 3-13).

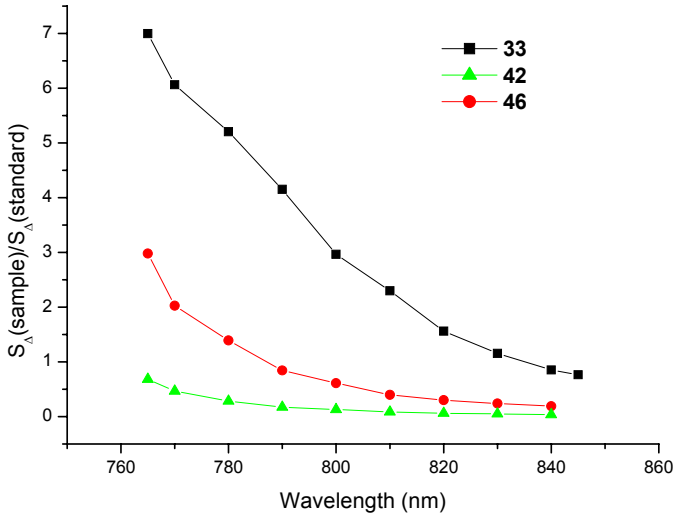

Figure 3-14: Concentration and singlet oxygen quantum yield corrected phosphorescence intensities of **33**, **42** and **46**.

The two-photon singlet oxygen efficiencies of **33**, **32** and **46** are plotted in Figure 3-14, where it is apparent that **33** is the most efficient sensitizer.

3.3.3 Functional groups as alternatives to bromine atoms for promoting intersystem crossing

On the basis of the data presented thus far, the diphenylamino end-group and the bromine atoms on the central aryl ring seem to be the best donor-acceptor pair in the OPV template. The obvious thing to do next is to study different electron accepting groups as alternatives to the bromine atoms. As discussed in Chapter 1, carbonyl groups can promote intersystem crossing as they have non-bonding π-orbitals. Furthermore, the electron accepting properties of a carbonyl group can be adjusted by having the carbonyl group present as *e.g.* an ester or an aldehyde. The one-photon properties of a series of OPV's with different functional groups on the center aryl ring are presented in Table 3-4.

Table 3-4: One-photon properties of **32**, **34**, **35** and **67-73** in toluene. λ_{max}^{abs} is the one-photon absorption maximum. The numbers in parantheses are the logarithm of the molar extinction coefficients. λ_{max}^{em} is the fluorescence maximum, Φ_f is the fluorescence quantum yield, τ is the fluorescence lifetime, and Φ_Δ is the singlet oxygen quantum yield (determined against phenalen-1-one as the standard).[a]

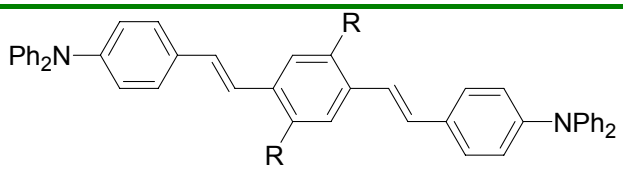

	R	λ_{max}^{abs}	λ_{max}^{em}	Φ_f	τ /ns	Φ_Δ
33	Br	425 (4.80) 303 (4.60)	492 524	0.3	0.7	0.46
32	H	410 (4.87) 306 (4.49)	458 486	0.9	1.1	0.08
34	CN	472 (4.87) 304 (4.63)	531	0.6	1.5	0.13
35	OMe	428 (4.87) 306 (4.55)	484 513	0.8	1.1	0.11
67	CHO	480 (4.61) 394 (4.59) 347 (4.47) 303 (4.63)	601	0.4	2.6	0.15
68	CO_2Et	429 (4.79) 305 (4.64)	516	0.7	1.6	0.17
69	$CONEt_2$	416 (4.87) 302 (4.56)	475 504	0.8	1.1	0.09
70	COMe	431 (4.65) 302 (4.58)	556	0.03	0.2	0.02
71	CO^tBu	419 (4.78) 303 (4.76)	481 511	0.1	0.4	0.04
72	SO_2Me	454 (4.78) 306 (4.60)	534	0.6	1.5	0.06

[a] Errors are ±10 % for all determined numbers.

73	NO_2	419 (4.59) 303 (4.64)	-	0.0	-	0.00

All the singlet oxygen quantum yields for these compounds are poor. It also appears that the singlet oxygen quantum yield decreases with increasing electron acceptor strength of the substituents. It is difficult to find a physical parameter that can be used to easily describe the amount of CT for the compounds in this particular series. Several reports have been made where the chemical shift of certain nuclei have been used for evaluating the amount of CT in the compounds under study.[14,15] However, for the compounds in the present work it is only the protons on the center ring that are distinguishable from the rest of the signals in the ^{1}H-NMR spectrum. The chemical shift of these protons cannot be considered as a good measure of the CT character in the molecule either because there is a functional group placed in *ortho*-position relative to these protons. Thus the chemical shift of these protons not only reflects the CT character in the molecule, but also the shielding from the nearby functional group. Another parameter that is often used is the oxidation potential of the compound but these have not been measured for all the compounds.

The discussion in the following will instead be based on the qualitative ordering of the functional groups in terms of their electron accepting properties. The functional groups are ordered as $CONR_2$<COOR<COR<CHO<CN<SO_2R<NO_2, where R is an alkyl group (with the nitro group as the most electron withdrawing). If the singlet oxygen quantum yields are then compared for the ester, aldehyde, cyano, methanesulfone and the nitro analogs, a drop from 0.17 (for the ester analog, **68**) to 0.00 (for the nitro analog, **73**) is observed, and from these data, it is concluded that the singlet oxygen quantum yield drops with an increasing amount of CT character in the molecule.

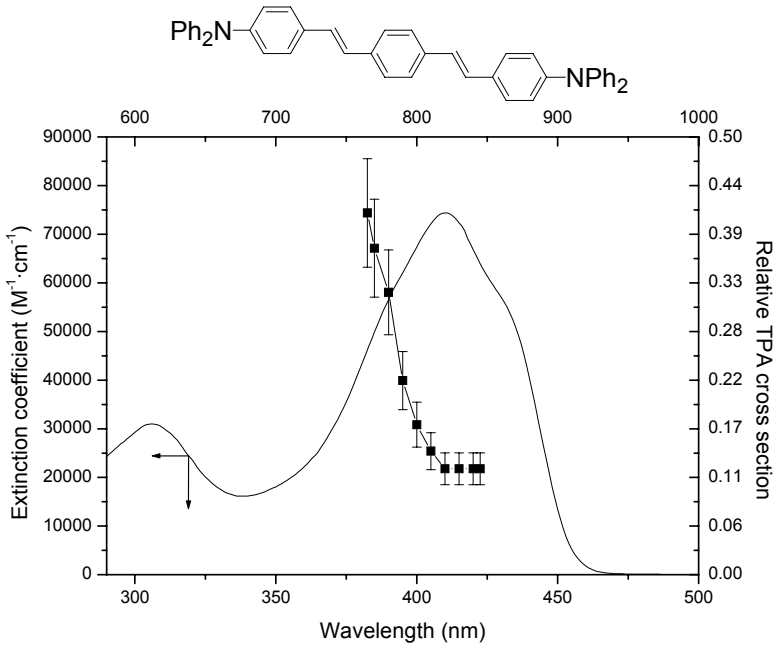

Figure 3-15: One-photon absorpion and two-photon action spectra of **32** in toluene.

The TPA action spectrum of **32** is shown in Figure 3-15. A one-photon absorption maximum occurs at 410 nm. The data suggest a TPA maximum around 740 nm, just outside the studied spectral range. The relative cross section at 765 nm is 0.41±0.06.

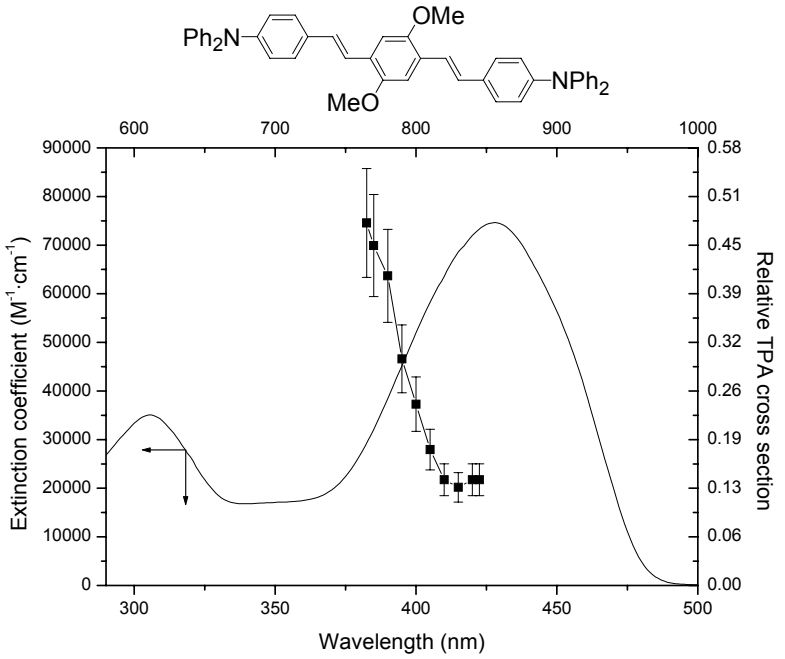

Figure 3-16: One-photon absorption and two-photon action spectra of **35**.

The one-photon absorption maximum of **35** occurs at 428 nm, and the data imply a TPA maximum around 775 nm. Thus, we assume that the relative cross section of 0.48±0.07 measured at 765 nm is close to the TPA maximum.

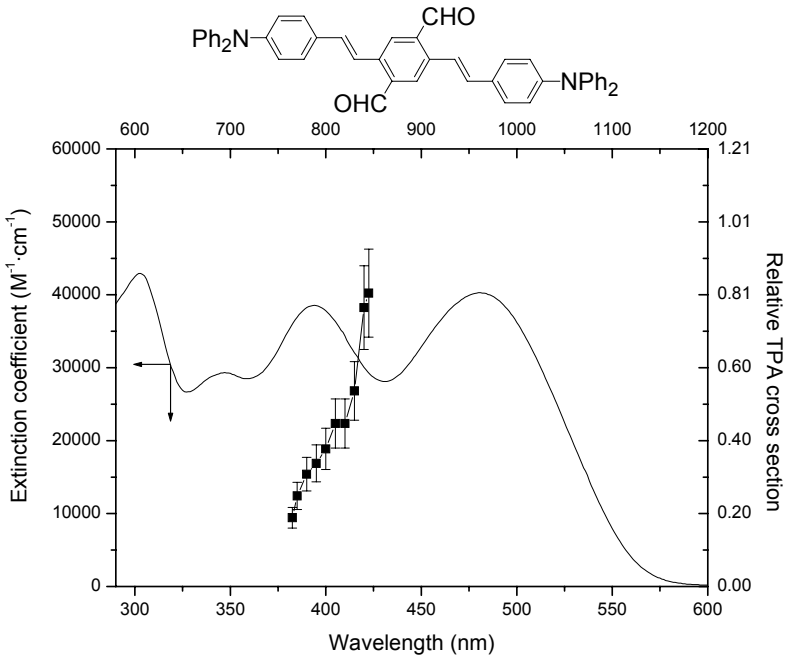

Figure 3-17: One-photon absorption and two-photon action spectra of **67**.

The TPA action spectrum of the aldehyde analog (**67**) is shown in Figure 3-17 and here it is seen that the TPA maximum is above 845 nm. The relative cross section measured at 845 nm is 0.81±0.12, which is a decent cross section. In the action spectrum of the ester functionalised OPV (**68**), the TPA maximum falls within the spectral range studied and occurs at 780 nm with a relative cross section of 0.71±0.11. A maximum at 840 nm is seen with a relative cross section of 0.42±0.06. The spectrum looks similar to the action spectrum of the standard (**34**), which also has two maxima in the action spectra – one at 845 nm and one at 885 nm.

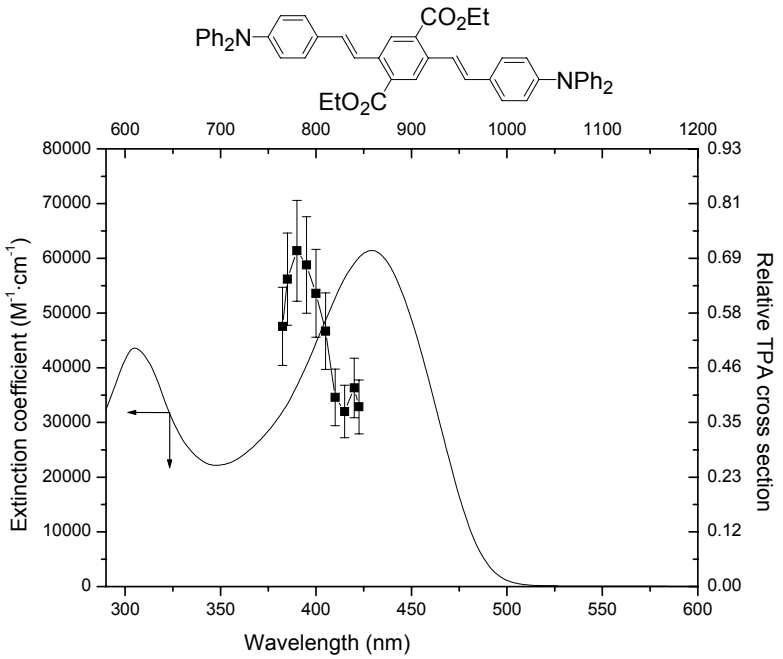

Figure 3-18: One-photon absorption and two-photon action specta of **68**.

The TPA spectrum of the amide (**69**) is shown in Figure 3-19 and TPA maxima are observed at 770 nm with a relative cross section of 0.52±0.08 and at 840 nm with a relative cross section of 0.19±0.03, similar to the ester analog (**68**).

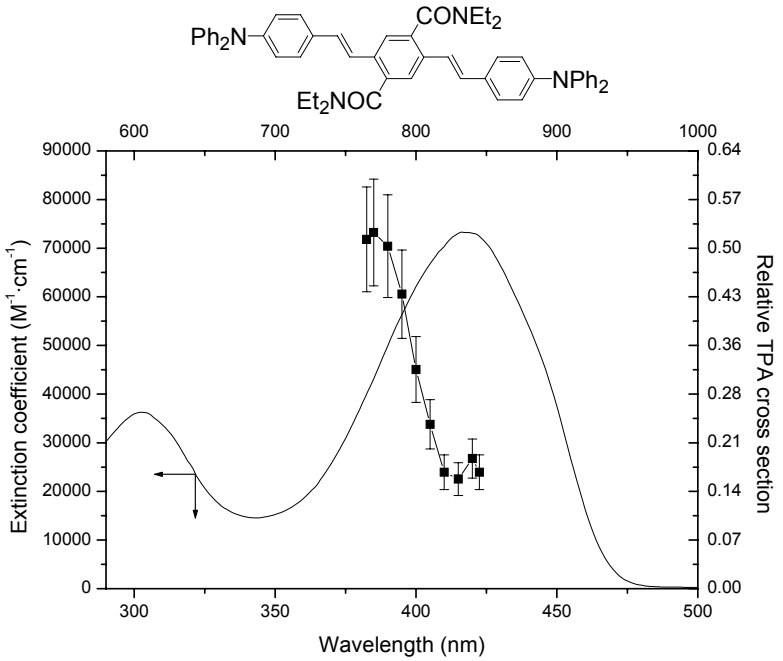

Figure 3-19: One-photon absorption and two-photon action spectra of **69**.

In the TPA action spectrum of the methyl-ketone (**70**) the data suggest two maxima; One occurring at 780 nm (0.64±0.10) and the other at 840 nm (0.59±0.09). The two relative cross sections are nearly equal as opposed to the other compounds where the maximum occurring at 840 nm has a significantly smaller cross section than the maxima occurring at shorter wavelength.

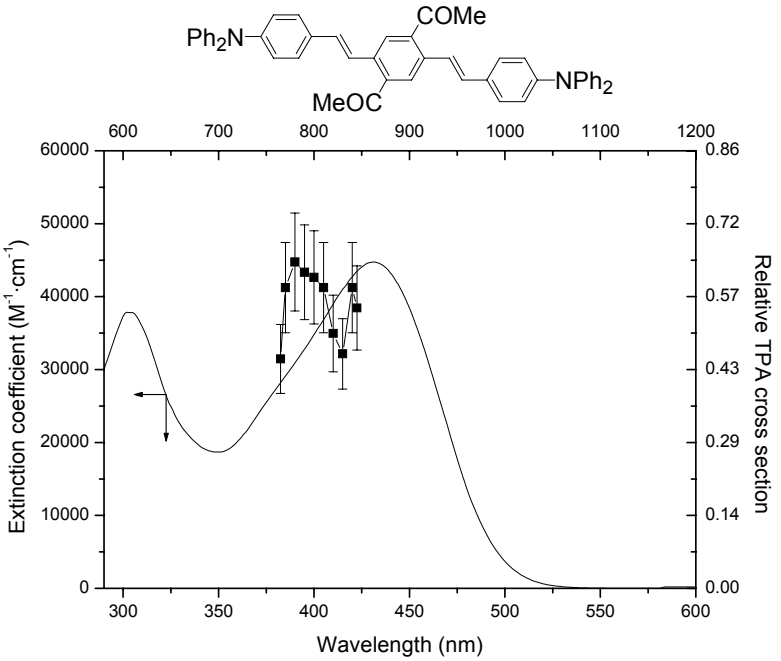

Figure 3-20: One-photon absorption and two-photon action spectra of **70**.

Two maxima are also observed in the TPA action spectrum of the *tert*-butyl ketone (**71**, see Figure 3-21), occurring at 770-780 nm and at 840 nm with relative cross sections of 0.37±0.06 and 0.15±0.02, respectively.

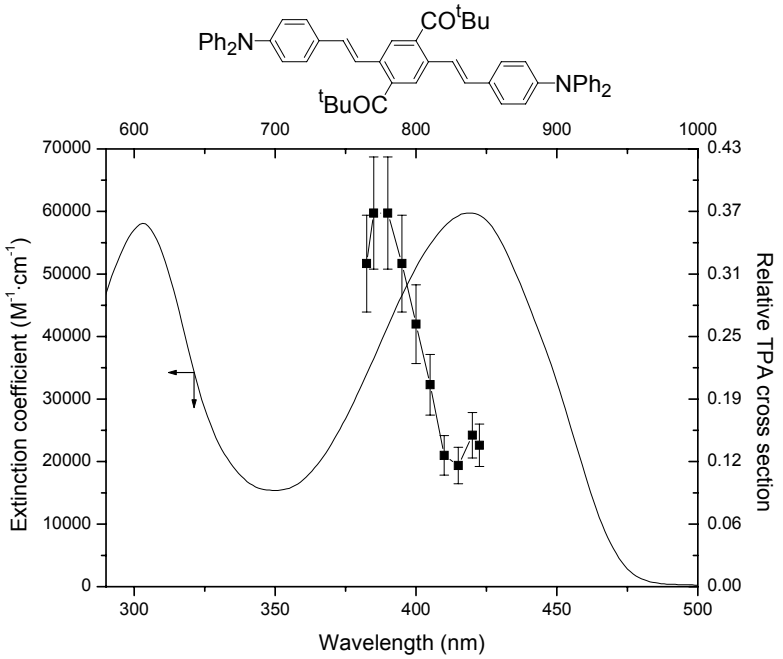

Figure 3-21: One-photon absorption and two-photon action spectra of **71**.

The cross sections measured for the compounds discussed above are all less than those observed for the standard. This is also what we would expect according to the molecular design principles for the TPA cross section described in Chapter 1; An increased amount of CT in the molecule gives an increased TPA cross section, and neither the ketone, ester, amide or aldehyde are stronger electron accepting groups than the cyano group. Thus it is reasonable that the standard molecule possesses the highest amount of CT character in comparison to **67**-**71**.

The methane sulfonyl group is a stronger electron accepter group than the cyano group, and **72** would then be expected to have a higher TPA cross section than the standard. This is indeed observed in the TPA data for **72** (see Figure 3-22) at 840 nm where a relative cross section of 1.46±0.22 is observed. A ratio of 1.37 has been measured by Strehmel and co-workers[4] for the TPA cross sections of an ethane sulfonyl compound as compared the corresponding cyano analog (see Chapter 1). The electron donating groups in the compound studied by Strehmel were dimethylamino groups as opposed to the diphenylamino group present in **34** and **72**.

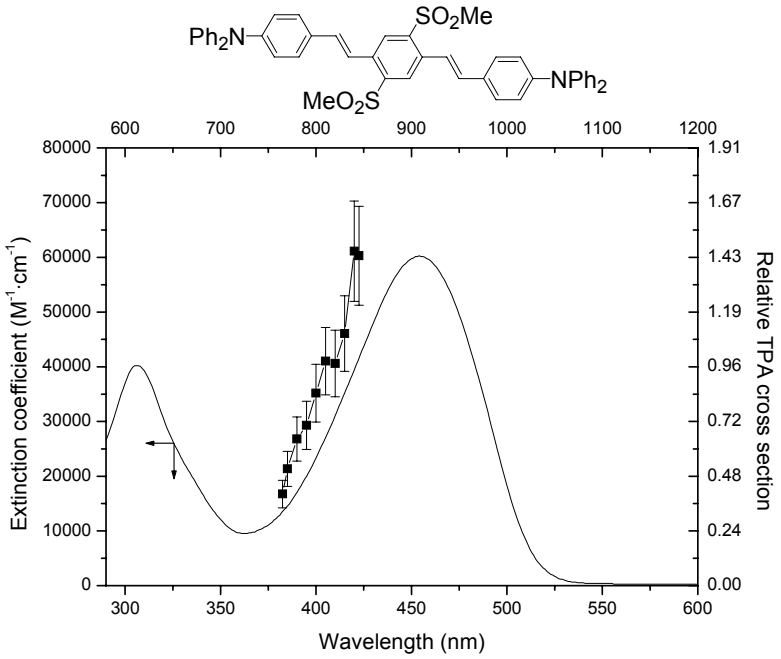

Figure 3-22: Two-photon action spectrum of compound **93**.

The two-photon singlet oxygen efficiencies are plotted in Figure 3-23 for **32**, **35**, **67-71**.

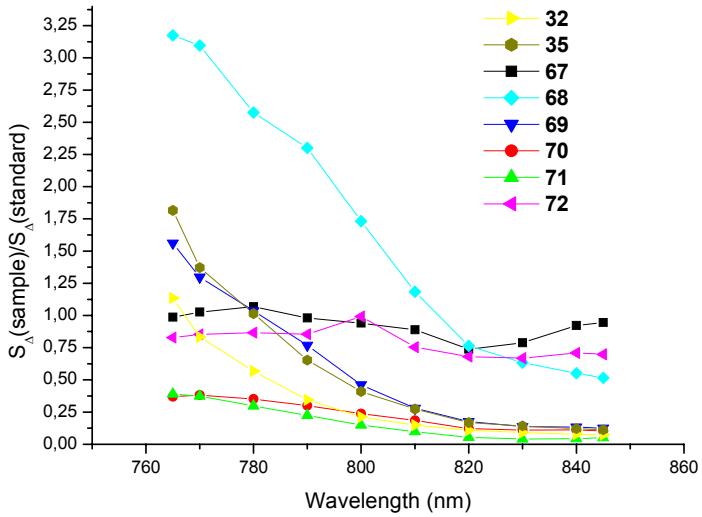

Figure 3-23: Concentration and singlet oxygen quantum yield corrected phosphorescence intensities of **32**, **35** and **67-72**.

The only compound with a noteworthy efficiency compared to the standard is **68**. However, the TPA action spectrum of **67** shows that the cross sections are increasing as the wavelength is increased, whereas the cross sections decrease for of **68**. This is also reflected in the efficiencies (Figure 3-23), where **67** is seen to be a better sensitizer than **68** above 820 nm.

3.3.4 The use of conjugation length to control the CT character

As discussed in Chapter 1, the singlet oxygen quantum yield is expected to decrease in an increase in the CT character of the senstizer. This is indeed observed with the OPV data obtained thus far. To continue the study of potentially pertinent variables, the photophysical properties of **1**, **83**, **85**, **87** and **88** were also investigated. These compounds have a donor-acceptor architecture and the donor and acceptor groups are separated by a variable number of phenylene vinylene units. Charge-transfer can be described in terms of coupling between the HOMO and LUMO of an electron donating and accepting group. Thus, increasing the distance between the donor and acceptor group should give a decreased CT character in the molecule as the mixing between the HOMO's and LUMO's of the two groups is decreased.[16,17]

The one-photon photophysical properties of the compounds are listed in Table 3-5.

Table 3-5: One-photon properties of the OPV's with varying number of phenylene-vinylene units. λ_{max}^{abs} is the one-photon absorption maximum. The numbers in parantheses are the logarithm of the molar extinction coefficients. λ_{max}^{em} is the fluorescence maximum, Φ_f is the fluorescence quantum yield, τ is the fluorescence lifetime, and Φ_Δ is the singlet oxygen quantum yield (determined against phenalen-1-one as the standard).[a]

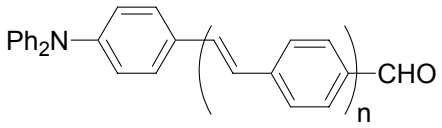

	n	λ_{max}^{abs}	λ_{max}^{em}	Φ_f	τ /ns	Φ_Δ
1	n = 0	357 (4.36) 292 (4.00)	448	0.7	3.6	0.19
83	1	404 (4.58) 303 (4.46)	481	0.6	1.7	0.04
85	2	413 (4.80) 314 (4.46)	513	0.7	1.6	0.08
87	3	416 (4.85) 316 (4.50)	517	0.8	1.3	0.08
88	4	408 (3.96) 324 (3.86)				0.05

The singlet oxygen quantum yields seems to decrease with an increasing distance (and thereby a decreasing CT character) between the diphenylamino group and the aldehyde. This finding suggests that a certain amount of CT character in the molecule is necessary to facilitate a decent singlet oxygen quantum yield. The one-photon absorption maxima, the emission maxima and the fluorescence quantum yield increase with the number of phenylene-vinylene units whereas the fluorescence lifetimes drop up to the number of four phenylene-vinylene units. The OPV with four phenylene-vinylene units has a lower one-photon absorption maximum than the

[a] Errors are ±10 % for all determined numbers.

preceeding OPV in the series indicating that the π-framework is no longer fully conjugated along the chain.

The TPA action spectra of **1**, **83** and **85** were recorded. The action spectra are shown in Figure 3-24.

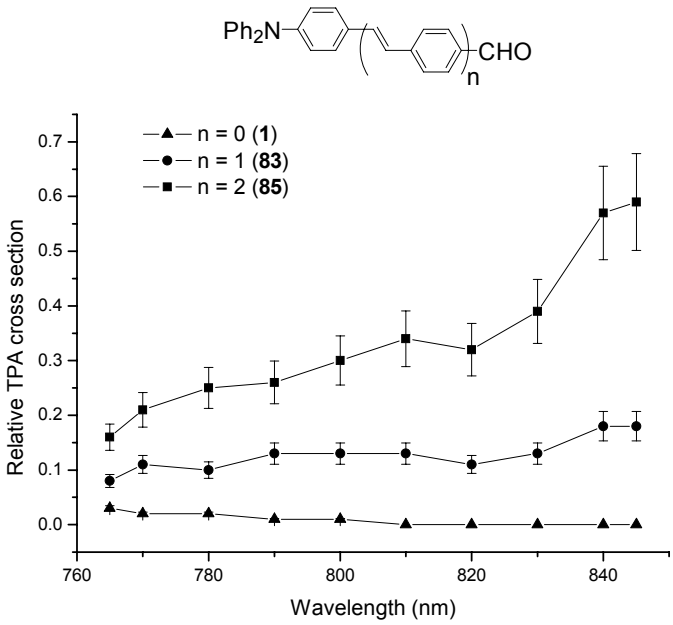

Figure 3-24: TPA action spectra of **1**, **83** and **85** in toluene.

From the TPA action spectra above it is observed, that even though the extent of CT decreases with increasing chain length, the TPA cross section increase. This finding supports what is discussed in Chapter 1 regarding conjugation length and non-linear optical properties.

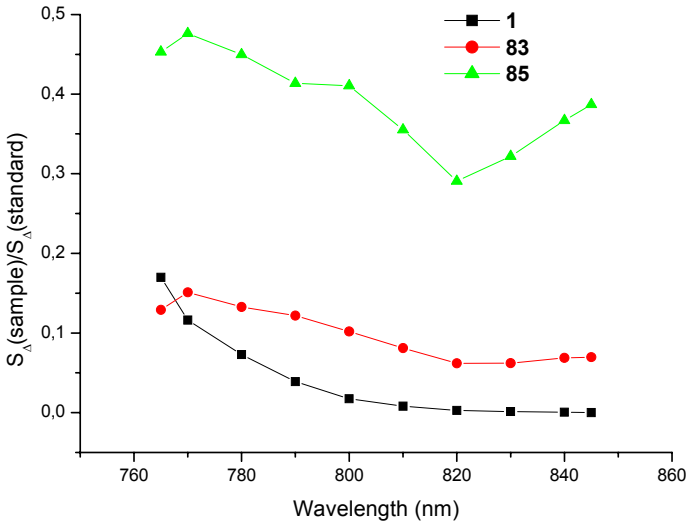

Figure 3-25: Concentration corrected phosphorescence intensities of **1**, **83** and **85**.

From the two-photon singlet oxygen efficiencies an increase in efficiency is observed by increasing the chain length. This is interpreted as with **68** that a balanced amount of CT character in the molecule facilitates a high efficiency as the amount of CT decreases gradually (due to a large seperation between the donor and acceptor part in the molecule) with the chain length as the TPA cross sections rises (due to longer conjugation length).

3.3.5 Varying π-linkers

A problem typically encountered when dealing with organic chromophores in non-linear optical measurements is the stability (or lack thereof) of the chromophores upon irradiation particularly when using a focussed laser beam. The compounds presented in the present work nearly all have double bonds, which are susceptible to attack by singlet oxygen. Electron rich double bonds react more readily with singlet oxygen than electron poor ones.[18,19] To this end, the stability of **33** versus the stability of the corresponding acetylene analog to **33** was investigated. The stability experiments were performed by irradiating sensitizer solutions (which also contained C_{60}) with a 600 nm laser beam. At 600 nm, neither **33** and the acetylene analog absorbs any light so generation of singlet oxygen occurs from the C_{60} triplet state. The degradation products from **33** and the acetylene analog do not absorb either above 600 nm (shorter

conjugation length) and furthermore C_{60} generates singlet oxygen in high yield making this compound ideally suited for stability experiments.

The relative changes in absorbances at λ_{max}^{abs} for both compounds were plotted as a function of elapsed irradiation time. The results are shown in Figure 3-26.

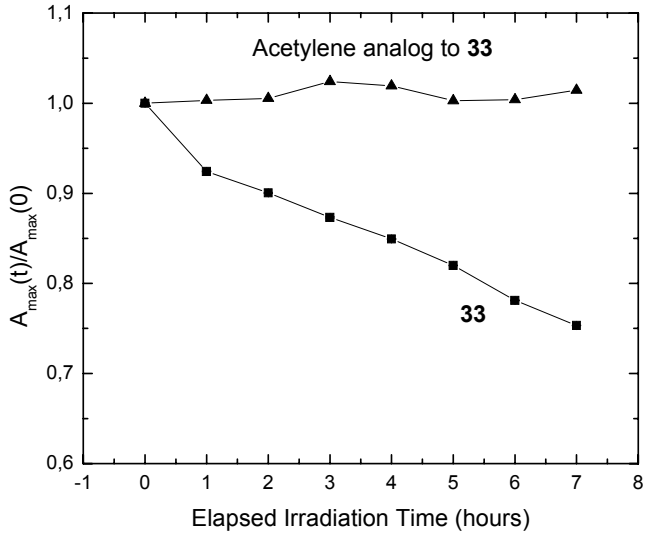

Figure 3-26: Relative absorbance changes as a function of elapsed irradiation time.

The stability experiments clearly show that the double bonds were more readily attacked by singlet oxygen that the triple bonds. Another way of inducing stability is to have electron poor double bonds, and for this reason **89** and **90** were prepared. The singlet oxygen quantum yields **89**, **90**, **84** and **86** are presented in Table 3-6. The purpose of introducing other π-linkers in the OPV skeleton is not only to introduce better stability but also to study the impact on the TPA cross section and the singlet oxygen quantum yields.

Table 3-6: Singlet oxygen quantum yields (determined in toluene with phenalen-1-one as the standard) of the compounds with varying π-linkers.[a]

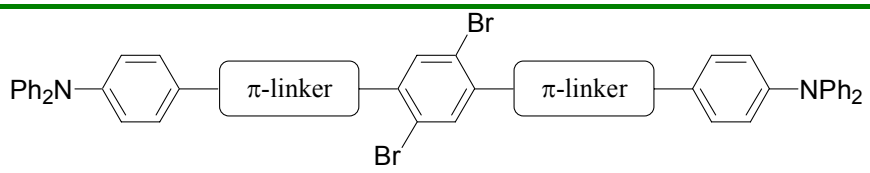

	π-linker	Φ_Δ
89	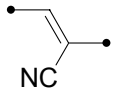	0.01
90	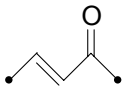	0.31
84	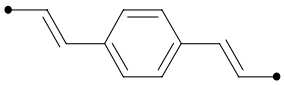	0.20
86	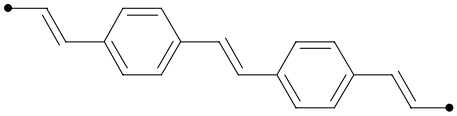	0.24

From the quantum yields, an extension of the distance between the diphenylamino groups and the bromine atoms by placing extra phenylene vinylene π-linkers is seen to cause a decrease in the singlet oxygen quantum yield. This finding is in accordance with the singlet oxygen quantum yield data for **1**, **83**, **85**, **87** and **88**, where an increasing distance between the diphenylamino group and the aldehyde functionality also resulted in a decrease in the singlet oxygen quantum yield. The singlet oxygen quantum yield of **89** is somewhat low, and its two-photon absorption properties were not investigated. Compounds **84** and **86** were not soluble enough in toluene to make a 10^{-4} M solution. The TPA action spectrum of **90** was recorded, however, and the data are shown in Figure 3-27.

[a] Errors are ±10 % for all determined numbers.

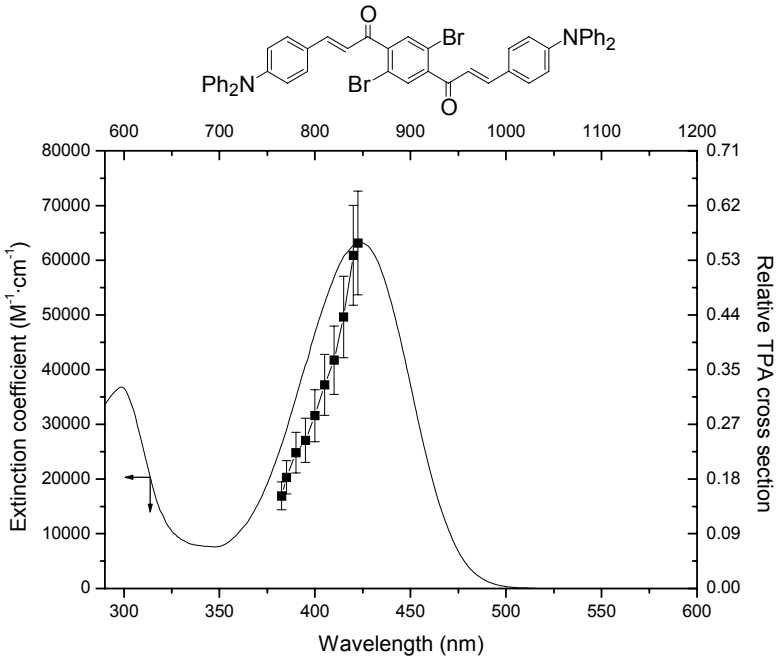

Figure 3-27: One-photon absorption and TPA action spectra of **90** in toluene.

The TPA cross sections measured for **90** were pretty good, and since the compound also has a decent singlet oxygen quantum yield it would serve well as a two-photon singlet oxygen sensitizer in a range of applications. What is interesting about this compound is that it confirms one of the molecular design principles discussed in Chapter 1; Introducing more functional groups (than the ones already present in the molecule) to promote intersystem crossing has no effect, inasmuch as an increase in the measured singlet oxygen quantum yield of **90** (0.31) in comparison with **33** (0.46) is not observed. Furthermore, the two-photon absorption maximum appears to occur at a longer wavelength than twice the one-photon absorption maximum, which is unlike the other compounds investigated in the present work. This is explained in terms of the parity of the lowest singlet state. In all the other cases discussed above, the state populated upon two-photon absorption (an ungerade state) was placed energetically higher than the state populated upon one-photon absorption (a gerade state). The parity of the two lowest states are seen to change in **90** as the lowest state is now a gerade state (populated upon two-photon irradiation) and the next state is then an ungerade state (populated upon one-photon irradiation).

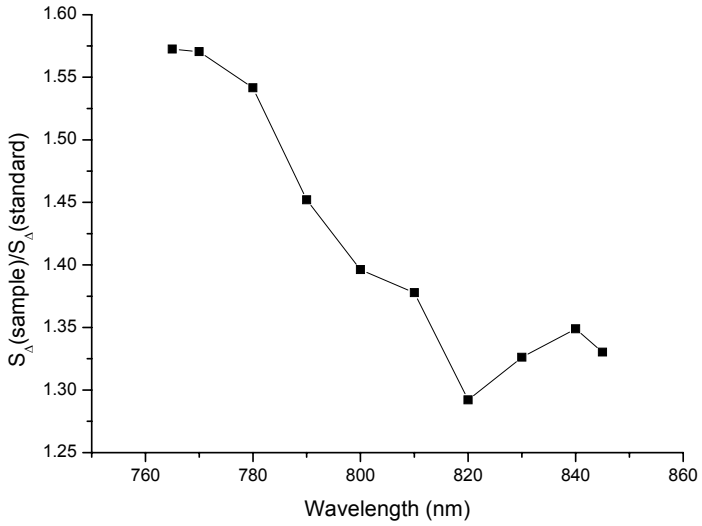

Figure 3-28: Concentration corrected phosphorescence intensities of **90**.

The two-photon singlet oxygen efficiency of **90** is plotted in Figure 3-28, where the efficiency is seen to be better than the standard at all wavelengths.

3.3.6 Triplet-triplet absorption

Triplet-triplet absorption spectra for **33** and **46** in toluene were recorded and these are shown in Figure 3-29. The purpose of doing triplet-triplet absorption spectra is to investigate whether the sensitizer has a triplet-triplet absorption in the region generally used for irradiation as this would then "disqualify" the sensitizer under certain conditions; In two-photon experiments performed with a nanosecond pulsed laser, the triplet state could be excited by another photon within the pulse envelope. Thus attempts to quantify absorption cross sections would be misleading.

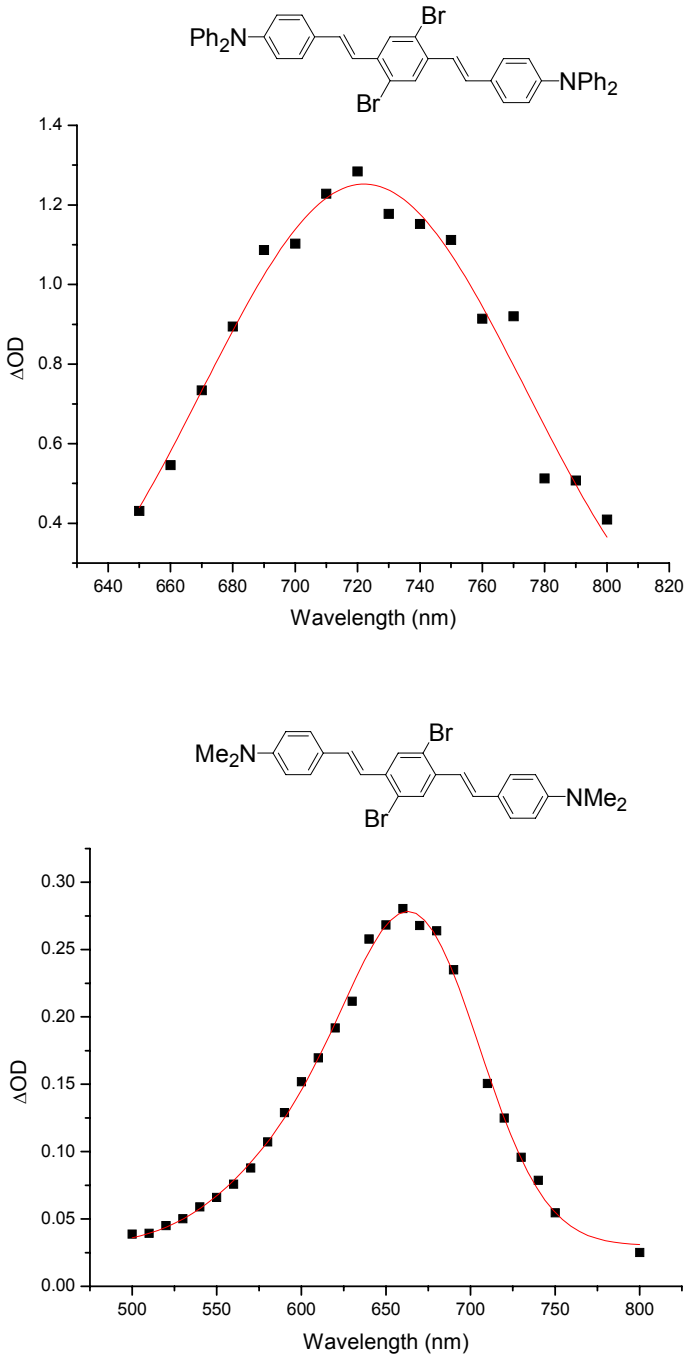

Figure 3-29: Triplet-triplet absorption spectra of **33** (top) and **46** (bottom) recorded in toluene.

The diphenylamino analog **33** has a T_1-T_n maximum of approximately 720 nm and has a tail extending out to above 800 nm rendering this molecule unsuited for nano-second experiments. A maximum occurs at 650 nm in the triplet-triplet absorption spectrum of **46** and it is noted that almost no absorption occurs at 765 nm and above making these molecule suitable for two-photon singlet oxygen sensitization. Triplet-

triplet absorption spectra were only recorded for these two molecules but in order to thoroughly establish that the other molecules discussed are efficient two-photon singlet sensitizers, triplet-triplet absorption spectra should be recorded for those as well

3.4 Conclusion

Singlet oxygen quantum yields are very much dependent on the amount of charge-transfer in the OPV chromophore. Too much CT opens up the possibility for decay processes that do not lead to singlet oxygen generation in agreement with Ref. 20, 21 and 22. Furthermore, we found that simply introducing more and more functional groups to promote intersystem crossing does not result in higher singlet oxygen quantum yield.

The TPA cross section is dependent on both the charge-transfer character within the molecule and the conjugation length; A higher degree of charge-transfer induced by strong electron donor and acceptor groups gives higher TPA cross sections Larger conjugation lengths also results in higher TPA cross sections.

Finally, stability issues can cause some problems inasmuch as electron rich double bonds reacts with singlet oxygen. Such stability problems can be solved by replacing the double bonds with triple bonds.

Reference List

1. Reichardt, C. *Solvents and Solvents Effects in Organic Chemistry*; 3 ed.; Wiley: Weinheim, 2003.
2. Krebs, F. C.; Spanggaard, H. *J. Org. Chem.* **2002**, *67*, 7185-7192.
3. Strehmel, B.; Sarker, A. M.; Malpert, J. H.; Strehmel, V.; Seifert, H.; Neckers, D. C. *J. Am. Chem. Soc.* **1999**, *121*, 1226-1236.
4. Strehmel, B.; Sarker, A. M.; Detert, H. *ChemPhysChem* **2003**, *4*, 249-259.
5. Nielsen, C. B.; Sauer, S. P. A.; Mikkelsen, K. V. *J. Chem. Phys.* **2003**, *119*, 3849-3870.
6. Nielsen, C. B.; Mikkelsen, K. V.; Sauer, S. P. A. *J. Chem. Phys.* **2001**, *114*, 7753-7760.
7. Jager, W. F.; Volkers, A. A.; Neckers, D. C. *Macromolecules* **1995**, *28*, 8153-8158.
8. Koene, B. E.; Loy, D. E.; Thompson, M. E. *Chem. Mater.* **1998**, *10*, 2235-2250.
9. Koryta, J.; Dvořák, J.; Boháèková, V. *Electrochemistry*; Methuen and Co: London, 1970.
10. Wong, K. T.; Hung, T. H.; Kao, S. C.; Chou, C. H.; Su, Y. O. *Chem. Commun.* **2001**, 1628-1629.
11. McClain, W. M. *Acc. Chem. Res.* **1974**, *7*, 129-135.
12. McClain, W. M. *J. Chem. Phys.* **1971**, *55*, 2789-2796.
13. Frederiksen, P. K. "The Two-Photon Photosensitized Production of Singlet Oxygen," 2003, Ph. D. dissertation, University of Aarhus
14. Lin, T. C.; He, G. S.; Prasad, P. N.; Tan, L. S. *J. Mater. Chem.* **2004**, *14*, 982-991.
15. Wang, X. M.; Zhou, Y. F.; Yu, W. T.; Wang, C.; Fang, Q.; Jiang, M. H.; Lei, H.; Wang, H. Z. *J. Mater. Chem.* **2000**, *10*, 2698-2703.
16. Turro, N. J. *Modern Molecular Photochemistry*; University Science Books: Sausalito, 1991.
17. Klessinger, M.; Michl, J. *Excited States and Photochemistry of Organic Molecules*; VCH Publishers, Inc.: New York, 1995.
18. Foote, C. S., Valentine, J. S., Greenberg, A., and Liebman, J. F. Ed. *Active Oxygen in Chemistry*; Chapman and Hall: London, 1995.

19. Dam, N.; Scurlock, R. D.; Wang, B. J.; Ma, L. C.; Sundahl, M.; Ogilby, P. R. *Chem. Mater.* **1999**, *11*, 1302-1305.

20. McGarvey, D. J.; Szekeres, P. G.; Wilkinson, F. *Chem. Phys. Lett.* **1992**, *199*, 314-319.

21. Kristiansen, M.; Scurlock, R. D.; Iu, K. K.; Ogilby, P. R. *J. Phys. Chem.* **1991**, *95*, 5190-5197.

22. Frederiksen, P. K.; McIlroy, S. P.; Nielsen, C. B.; Nikolajsen, L.; Skovsen, E.; Jørgensen, M.; Mikkelsen, K. V.; Ogilby, P. R. *J. Am. Chem. Soc.* **2005**, *127*, 255-269.

CHAPTER 4

TWO–PHOTON SINGLET OXYGEN GENERATION IN WATER

Abstract: *The synthesis and characterization of a series of water-soluble singlet oxygen sensitizers has been undertaken. Two approaches were used for achieving water-solubility: An ionic and a non-ionic approach. In the ionic approach, salts of pyridine, benzathiazole and piperazine were used. In the non-ionic approach, oligo-ethylene glycol units were used to achieve water-solubility. Stability issues of the sensitizers are also addressed and, finally, it is shown that the sensitizers developed can indeed generate singlet oxygen in water upon two-photon excitation.*

4.1 Introduction

For many biological applications, it is important to have singlet oxygen sensitizers that are water-soluble. Complications arise when singlet oxygen is to be generated in water using a two-photon irradiation scheme.[1] In the previous chapter it was demonstrated that the CT character of a molecule facilitates a large TPA cross section but is counter productive in singlet oxygen generation. The CT character of a molecule is more pronounced in polar solvents (such as water) and in order to make an efficient two-photon singlet oxygen sensitizer for water applications, a precise amount of CT character has to be present in the molecule in order to give both a high TPA cross section and a decent singlet oxygen quantum yield. In search of a suitable sensitizer, several water-soluble molecules with a varying amount of CT character controlled by the nature of the substituents in the molecule were prepared. Two different strategies for achieving water solubility were utilized: An ionic and a non-ionic approach. The functional groups used were oligo-ethylene glycol units for the non-ionic approach and salts of pyridine, benzothiazole, sulfonic acid or 1-methyl-piperazine for the ionic approach. Because these groups are also attached to the π-system of the chromophore, their electron donating or accepting properties influences the extent of CT character in the molecule. Most of the sensitizers prepared in the present work are also functionalized with bromine atoms serving as (weak) electron acceptors and used to facilitate intersystem crossing to the triplet state.

4.2 Preparation of the sensitizers

An oligomer with three ethylene glycol units end-capped with a methyl group (from hereon denoted as MTEG) was chosen for the syntheses of water-soluble ethylene glycol functionalized OPV's. In the construction of thses OPV's MTEG-substituted benzaldehydes were prepared from hydroxy-substituted benzaldehydes and tosylated triethylene-glycol mono-methyl ether in a S_N2 reaction using potassium carbonate as the base and DMF as the solvent (see Scheme 4-1). All of the MTEG substituted benzaldehydes were made from commercially available hydroxy-substituted benzaldehydes, except 3,4,5-tri-hydroxy-benzaldehyde. Only two methods have been reported for preparing this latter compound: Rosenmund and co-workers[2,3] original work on gallous acid and a newer route[4] from the acetyl protected acid by reduction to the alcohol with diborane and reoxidation with pyridinium dichromate. An alternative to the Rosenmund reduction was attempted using $(Ph_3P)_2CuBH_4$ as the reducing agent (see Scheme 4-2), which proceeded in moderate yield (56%).

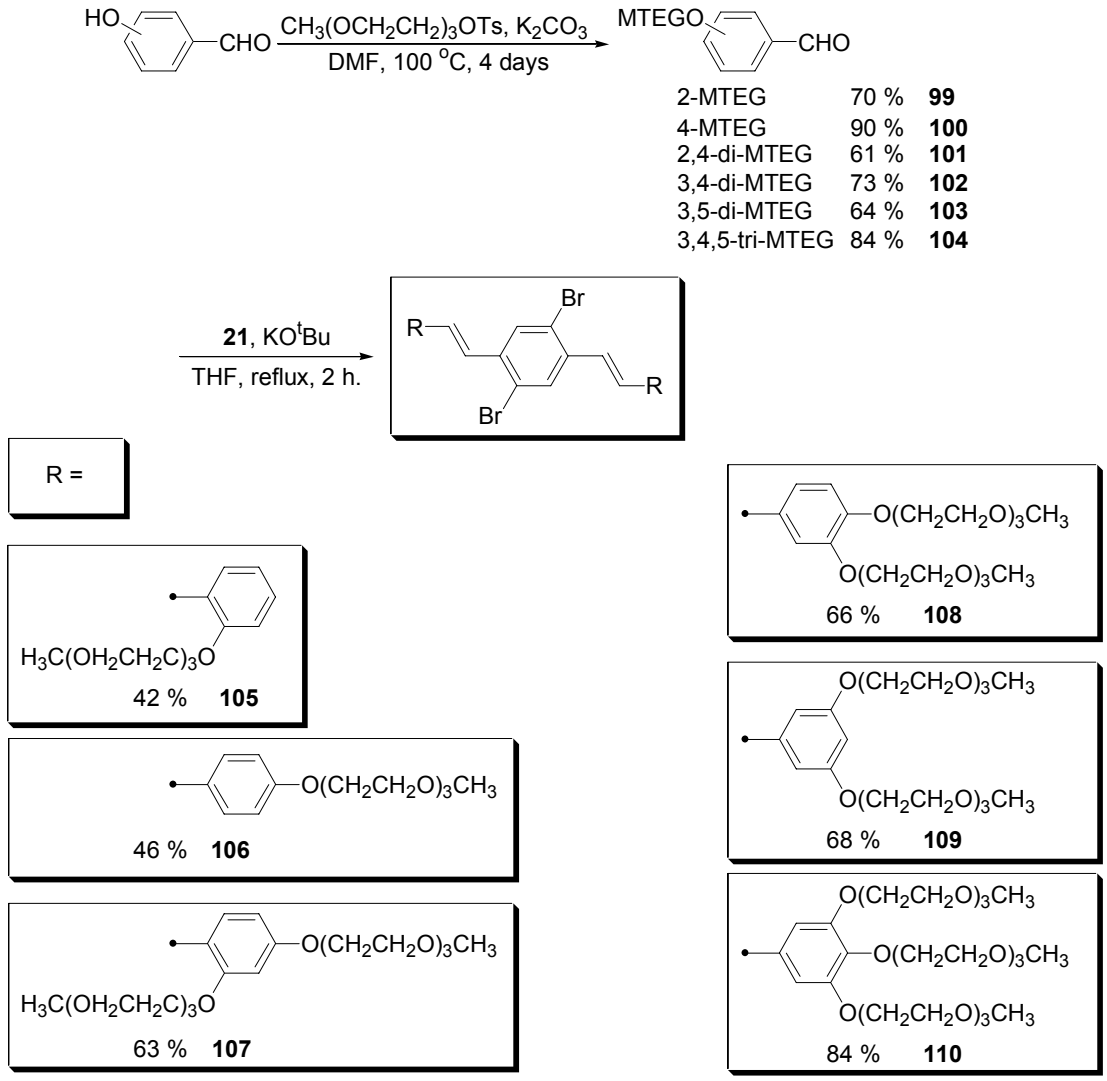

Scheme 4-1: The syntheses of a series of MTEG-OPV's.

However, a more practical way of preparing the aldehyde (without using chromic reagents and in a more atom economical way) is to reduce the acetyl protected gallous acid with $BH_3 \cdot Me_2S$ to the alcohol and then reoxidizing to the aldehyde using a Swern oxidation[5] (see Scheme 4-2, 50 % overall yield). The acetyl groups were then removed as described in Ref. 2 and 3 with sodium methoxide in methanol. Tri-hydroxy-benzaldehyde is an important building block in many applications, such as in the synthesis of certain dendrimers,[6] and many biological active compounds contain a tri-hydroxy functionalized substitution pattern.

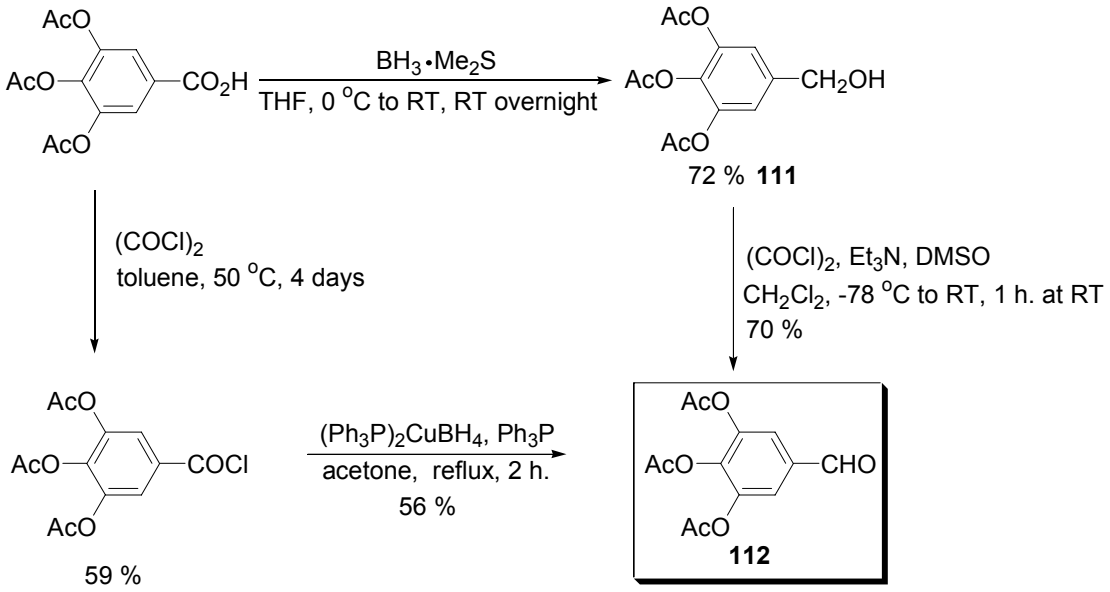

Scheme 4-2: Preparation of 3,4,5-trihydroxy-benzaldehyde.

The non-ionic MTEG-substituted OPV's were then prepared from the MTEG-substituted benzaldehydes by a HWE reaction with the diphosphonate ester **21** in THF using potassium tert-butoxide as the base (see Scheme 4-1). The yields for the HWE reaction were all fair to good (44-84 %). Instead of using an alkoxy group as the electron donating group, an amino-derivitized analog to the MTEG-OPV compounds discussed above (**115**) was prepared as shown in Scheme 4-3. In this case, the commercially available 2,2'-(phenylazanediyl)-diethanol was protected with acetyl groups and was then formylated using the Vilsmeier-Haack reaction. The acetyl groups were then removed and the resulting free alcohols were deprotonated with sodium hydride and reacted with tosylated mono-methyl ether triethylene glycol in a S_N2 reaction. The resulting aldehyde **114** was then reacted with the phosphonate ester **21** in a HWE-reaction. The yield of the HWE-reaction for the preparation of **115** was relatively low which were ascribed to the workup, where the compound was difficult to eluate from the column material.

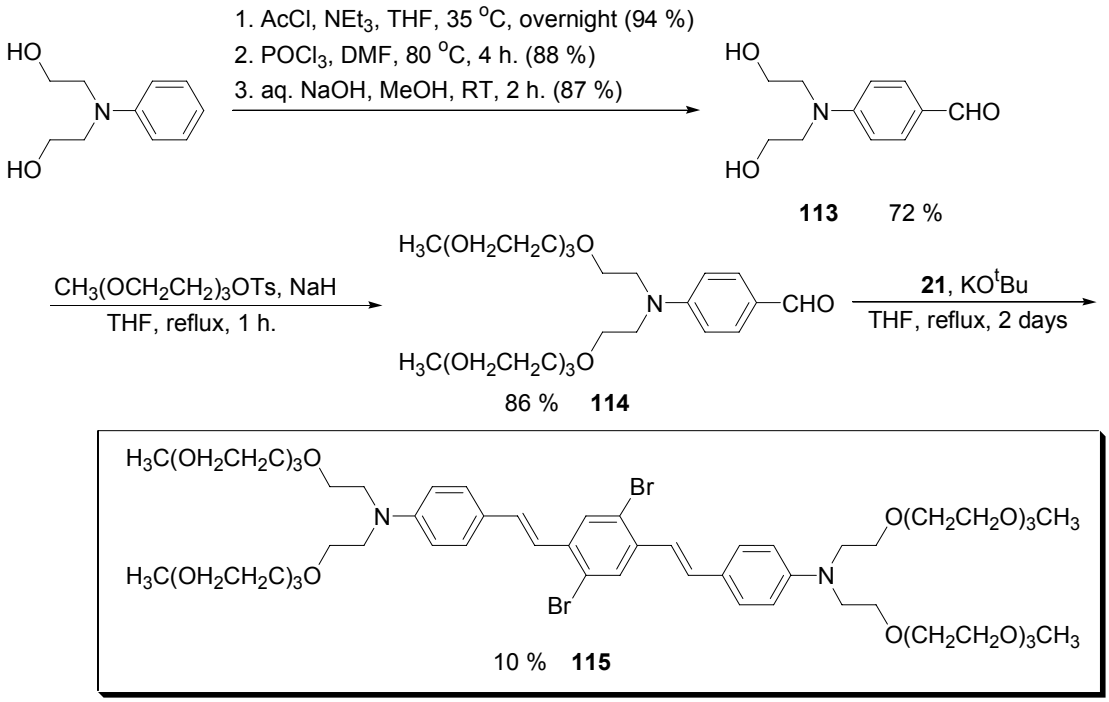

Scheme 4-3: Preparation of a MTEG-substituted OPV with an amino-group as the electron donating end-group.

Before arriving at the synthetic scheme shown in Scheme 4-3, a variety of other attempts were made to make analogs to **115**. In an early strategy, the OPV was assembled prior to introducing the functional groups that imparts water solubility. The TBDMS protecting group was used instead of the acetyl group in the preparation of protected 4-[bis-(2-hydroxy-ethyl)-amino]-benzaldehyde and kept on during the HWE reaction. The protecting groups were then removed from the isolated OPV using TBAF in THF giving the tetra-alcohol **120** in 90 % yield (from the TBDMS protected alcohol). Functionalization of the free alcohol groups with di-BOC-protected ornithine was tried using the DCC and HOPT based coupling scheme typically used for assembling peptides (Scheme 4-4). Removal of the BOC groups with hydrochloric acid should then give the hydrochloride salt of the amino acid functionalized OPV.

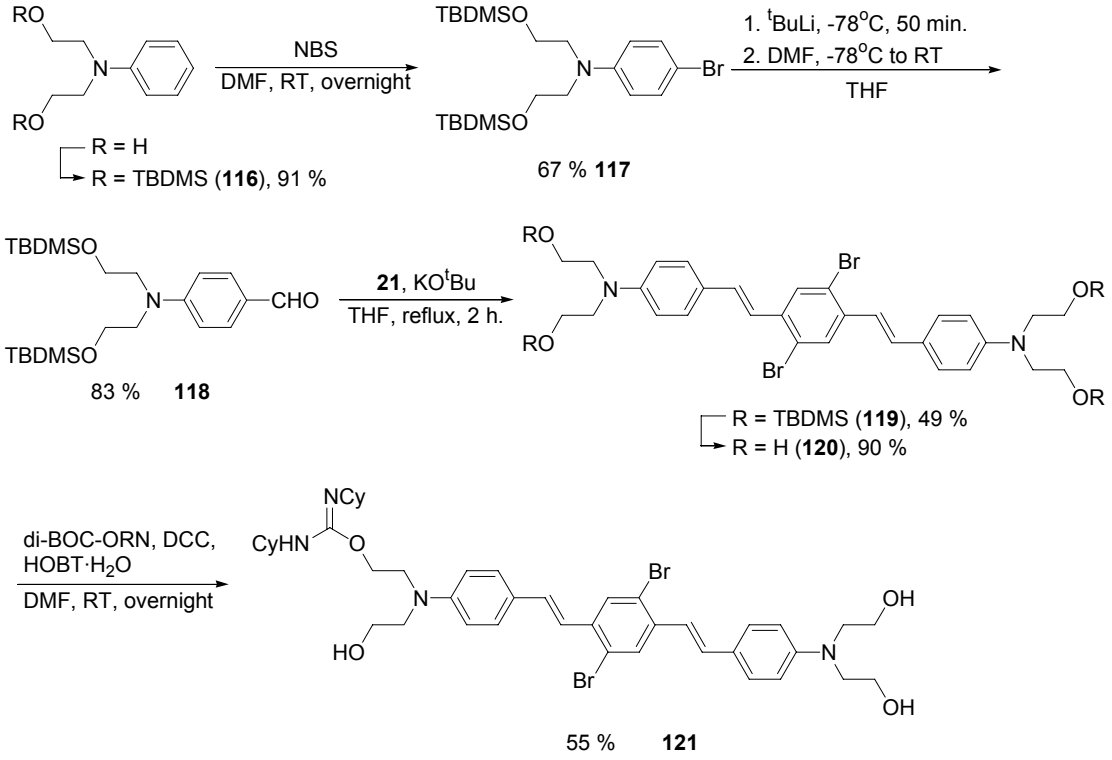

Scheme 4-4: Attempt to make an aminoacid functionalized OPV.

The DCC coupling reagent is used for activating the amino acid, but in this case the alcohols were significantly more reactive than the acid resulting in the isolation of **121**. The ^{1}H-NMR spectrum of this compound is depicted in Figure 4-1.

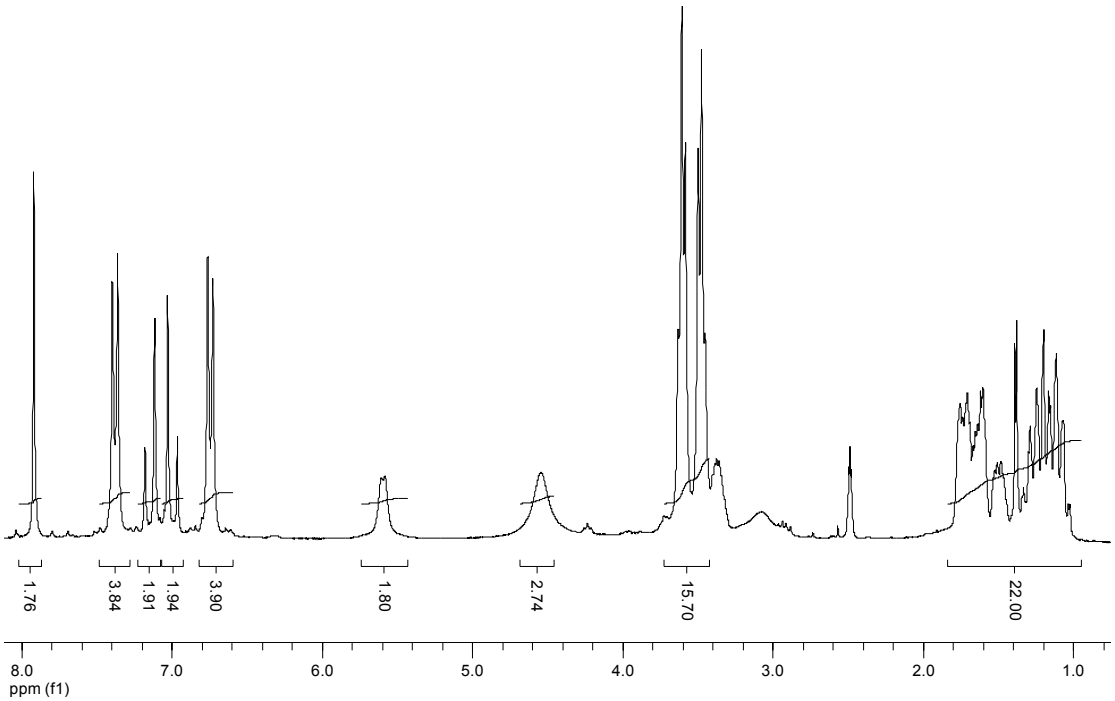

Figure 4-1: ^{1}H-NMR(DMSO, 300 K) of **121**.

This problem has previously been described and other reagents, such as TFFH, can be used for activating the acid. By reacting the acid with TFFH, the acid flouride is obtained which can be isolated or reacted *in situ* with the alochol. This strategy was tried in an attempt to synthesize **122** (see Scheme 4-5), but the ^{1}H-NMR spectrum of amino acids are typically "messy" and it was difficult to establish the purity of this compound. Instead, **113** was reacted with the corresponding acid of MTEG giving **123**.

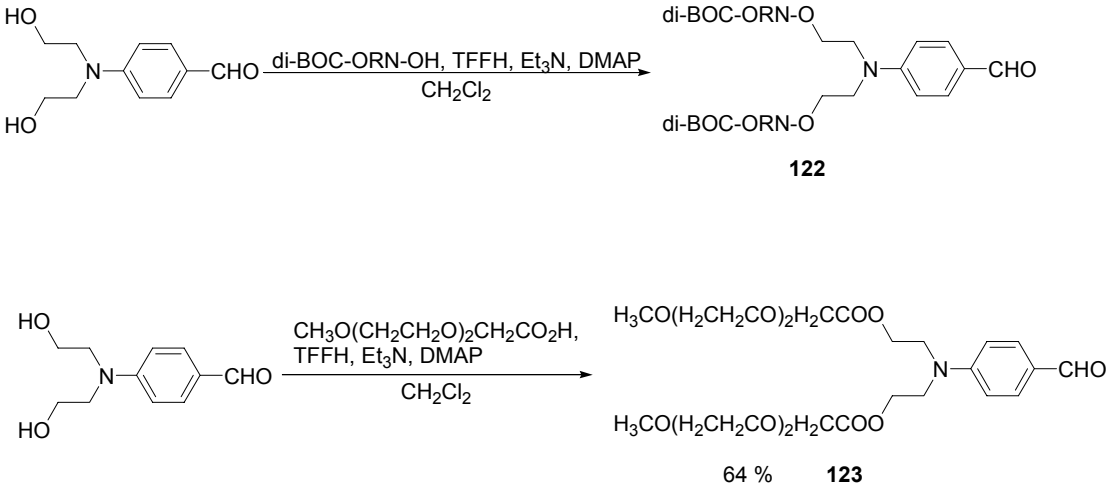

Scheme 4-5: Aldehydes obtained from coupling of **118** with di-BOC protected ornithine or $CH_3O(CH_2CH_2O)_2CH_2CO_2H$ using TFFH.

The aldehyde **123** was reacted with the phosphonate ester **21** but TLC showed the formation of multiple products (possibly due to reactions with the ester group) that were difficult to isolate, and this strategy was abandond and the strategy shown in Scheme 4-3 was used instead.

In the ionic approach, an OPV substituted with sulfonic acid groups was investigated. The acid was prepared by a HWE reaction with the phosphonate ester **125** and 2,5-diformyl-1,4-dibromo-benzene (**51**) as shown in Scheme 4-6. The phosphonate ester **125** was prepared by brominating toluene-4-sulfonic acid methyl ester and then converting the obtained 4-bromomethyl-benzenesulfonic acid methyl ester (**124**) into the phosphonate ester (**125**) using the Michaelis-Arbuzov reaction. In this reaction, the methyl sulfonic ester transesterified forming the ethyl ester, which was later hydrolyzed during workup after the HWE reaction. The mono potassium salt of the sulfonic acid was isolated.

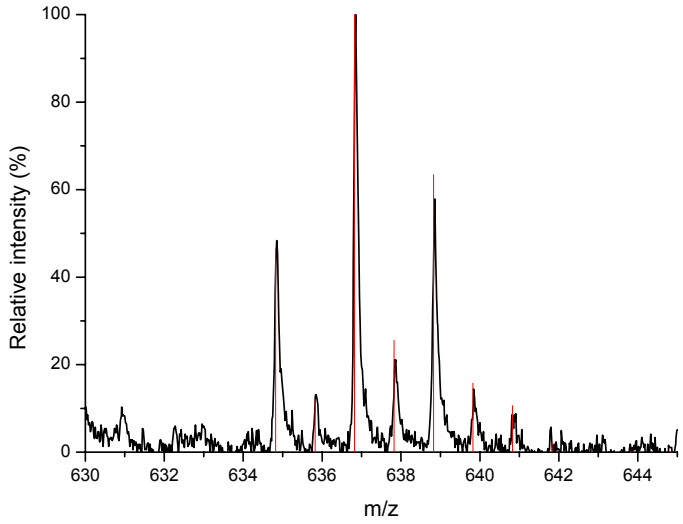

Figure 4-2: MALDI-TOF spectrum, with the spectrometer run in negative ion mode, of the sulfonic acid **147**. The red bars are the theoretical isotopic distribution of the ion $C_{22}H_{14}Br_2KO_6S_2^-$.

The isolation of the mono-potasium salt was confirmed by MALDI-TOF, where the section of the spectrum containing the $C_{22}H_{14}Br_2KO_6S_2^-$-ion is shown in Figure 4-2. The theoretical isotopic distribution is also shown, and a good agreement is observed.

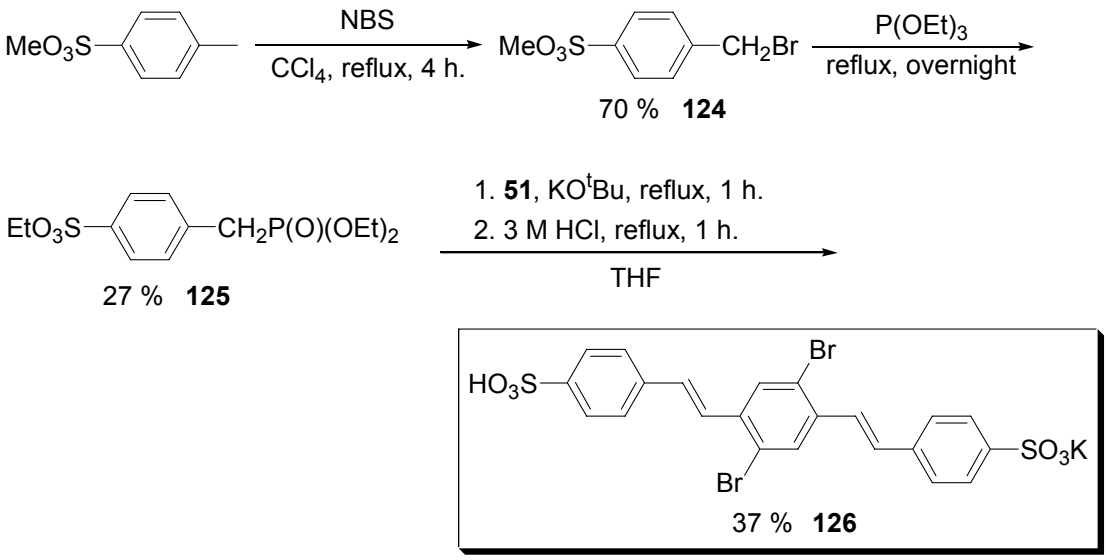

Scheme 4-6: The preparation of a sulfonic acid functionalized OPV.

The typical way of introducing sulfonic acid functionalities on an aromatic ring is by direct sulfonation with HSO_3Cl or reacting with SO_3 in concentrated sulfuric acid.

There are not viable strategies for functionalizing acid sensitive molecules. The approach shown in Scheme 4-6 constitutes a mild method for introducing the sulfonic acid functionality and is the first report on introducing sulfonic acids using the HWE-reaction. However, the sulfonic acid derivatized OPV (**126**) turned out to be very sparingly soluble in water. It was, however, possible to get enough into solution in a 1 M sodium hydroxide solution to record an absorption spectrum.

Salts of *N*-methyl-pyridinium, 1,1-dimethyl-piperazinium and *N*-methyl-benzothiazolium can also be used to facilitate water solubility. It was decided to use the HWE reaction for making the OPV's with benzothiazole units and, to this end, the phosphonate ester shown in Scheme 4-7 was prepared. An A-π-D-π-A architecture using methoxy groups as donors was employed in the design of **131** (see Scheme 4-8). Attempts were made to condense *N*-methyl-benzothiazolium iodide with 2,5-dimethoxy-terephthtalic aldehyde but it was not possible to isolate **131** using this approach. Benzothiazolium derivatives are normally prepared by a Knoevenagel condensation with a *N*-methyl-benzothiazolium salt, but some problems are usually encountered using this strategy as two benzothiazole molecules can condense with one aldehyde.[7] Also, problems have been reported with attempting to condense benzothiazole salts with ortho-substituted benzaldehydes.[7]

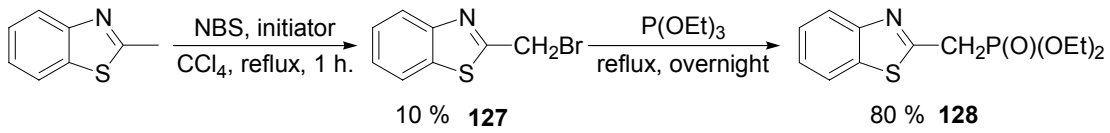

Scheme 4-7: Preparation of a benzothiazole phosphonate ester. The initiator used for the NBS bromination was AIBN.

Using the approach outlined in Scheme 4-8, the problems observed in the condensation reactions with *N*-methyl-benzothiazolium salts were avoided. The benzothiazole unit is, in itself, electron accepting. The methoxy group was chosen as the electron donating group in the benzothiale OPV's and **129** was prepared and subsequently reacted with the phosphonate ester **128**.

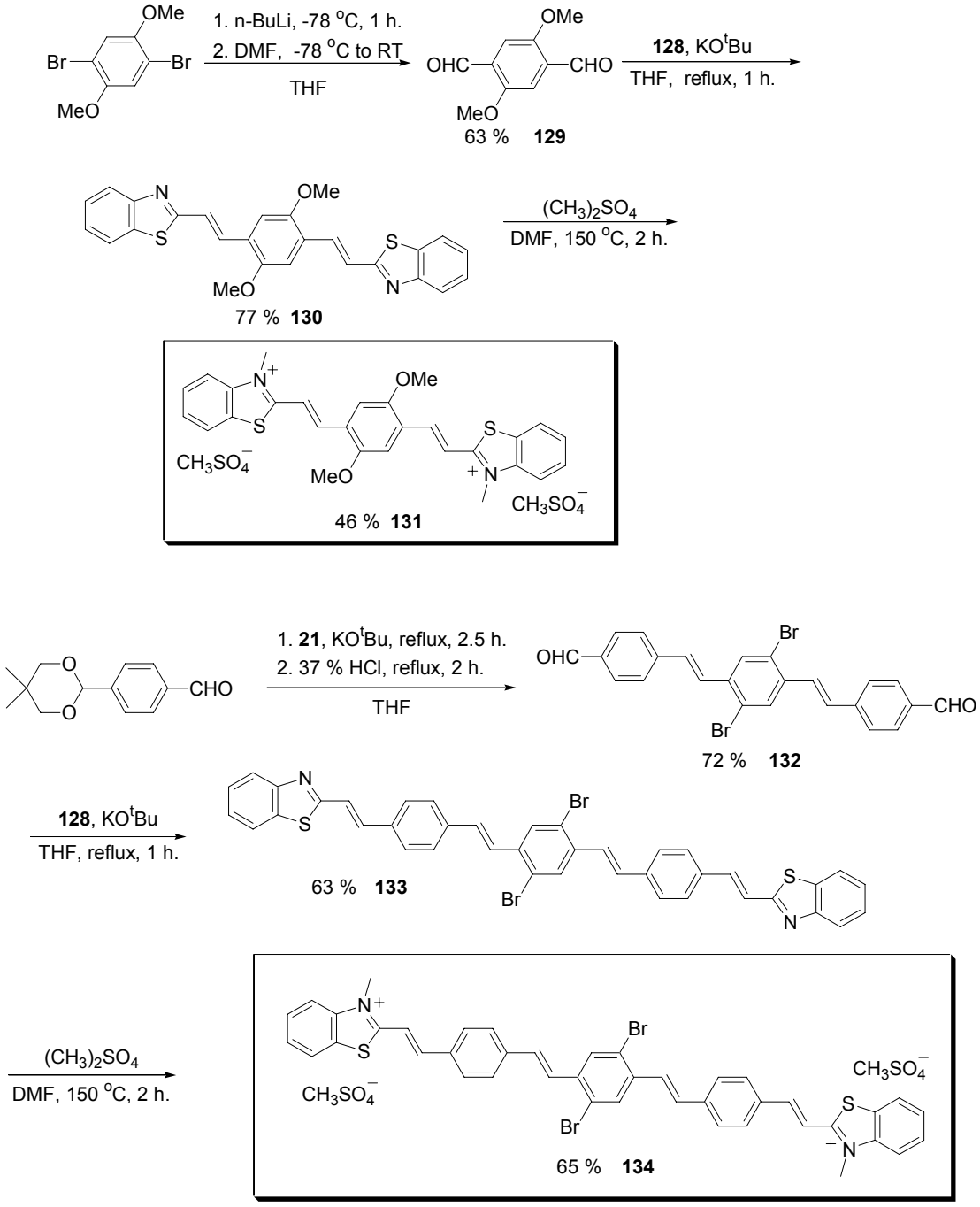

Scheme 4-8: Preparation of two benzathiazole OPV's and their corresponding salts.

In an attempt to prepare a sensitizer with a longer conjugated bridge between the terminal electron acceptors and one that would have a larger probability for intersystem crossing, **134** was made as shown in Scheme 4-8. This compound was prepared using the aldehyde end-capped OPV (**132**). The latter was made by reacting monoacetal-protected terephthtalaldehyde with **21** and then hydrolyzing the acetal protecting groups off during workup. Compound **133** was then prepared by reacting

the dialdehyde **132** with the phosphonate ester **128**. The salts **131** and **134** were finally made by heating solutions of **130** or **133** with dimethyl sulfate in DMF. Crystal structures of both **130** and **131** were obtained.

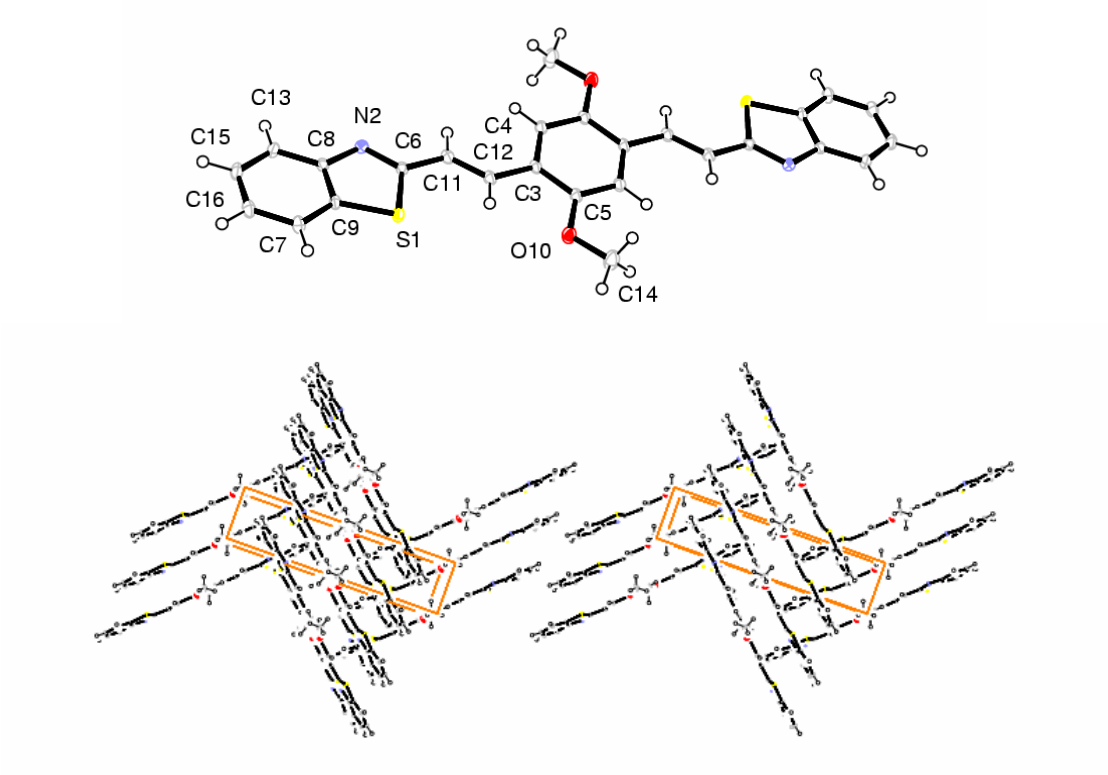

Figure 4-3: X-ray structure of **130** and crystal packing (in stereo view).

Selected bond-lengths and angles are listed in Table 4-1, and these show that there is some change in the bond-length alternation around the double bonds as a result of *N*-methylation inasmuch as the single bonds becomes shorter and the double bonds themselves become longer.

Table 4-1: Selected bond-lengths in **130** and **131**.

130		**131**	
C8-C9	1.4039(16)	C11-C14	1.402(3)
N2-C8	1.3917(15)	N22-C14	1.400(3)
S1-C9	1.7305(11)	S1-C11	1.733(2)
N2-C6	1.3046(14)	N22-C25	1.329(3)
S1-C6	1.7586(12)	S1-C25	1.717(2)
C6-C11	1.4501(16)	C25-C30	1.443(4)
C11-C12	1.3397(16)	C30-C17	1.344(3)
C3-C12	1.4608(16)	C8-C17	1.451(3)

Bond-length alternation is typically used as a measure of the CT character in a donor-acceptor molecule (see Ref. 8), and the changed alternation in **131** as compared to **130** indicates that the CT character of the benzothiazole OPV skeleton is changed by *N*-methylation. This is also expected because an increase in positive charge at the end-benzothiazole rings is obtained as a result of the methylation (a full positive charge is now present).

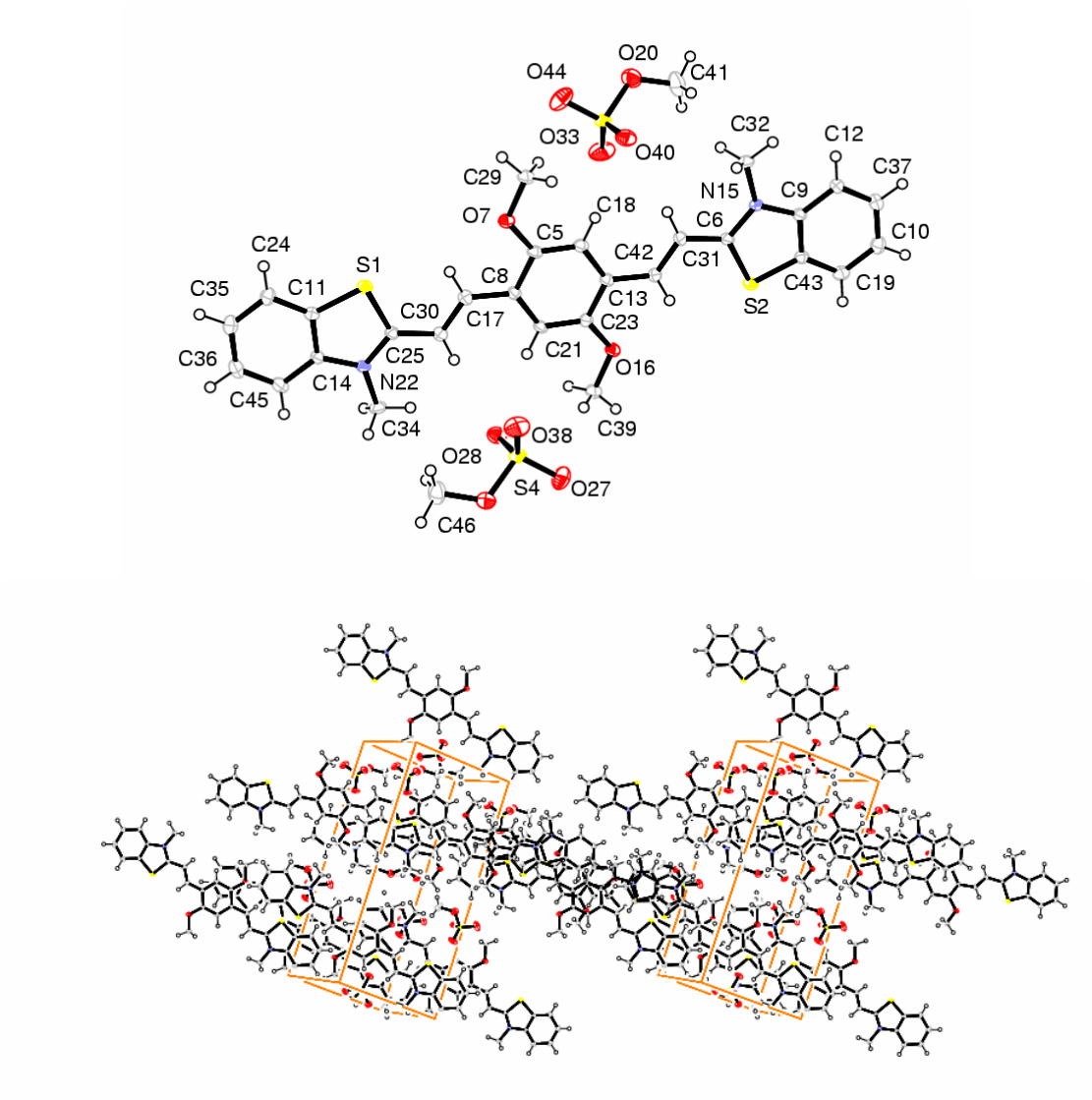

Figure 4-4: X-ray structure of **131** and crystal packing (in stereo view).

The pyridinium salts **140**, **141**, **142** and **143** were prepared by reacting the appropriate phosphonate ester (see Scheme 4-9) with 4-pyridine-carboxaldehyde (Scheme 4-10). The pyridine-OPV's obtained from these HWE-reactions were then converted to the *N*-methyl-pyridinium salts by reacting with them with dimethyl sulfate in DMF.

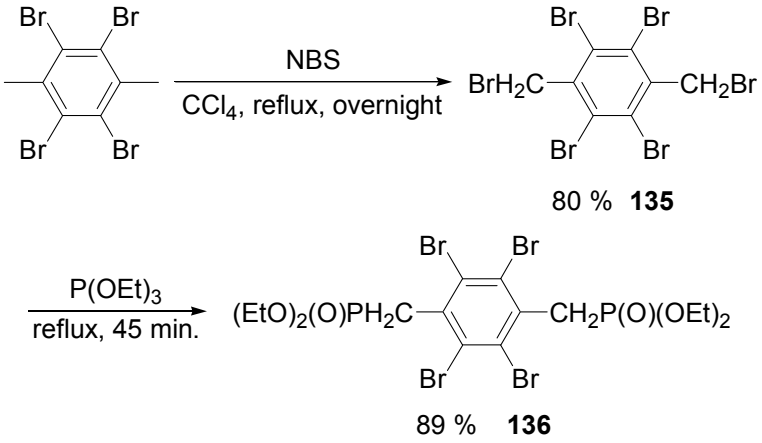

Scheme 4-9: Preparation of a tetra-bromo substituted phosphonate ester.

Compound **138** was also reacted with methyl iodide in a Menschutkin reaction giving the iodide **142** in order to investigate the effect of having different counterions in the salt.

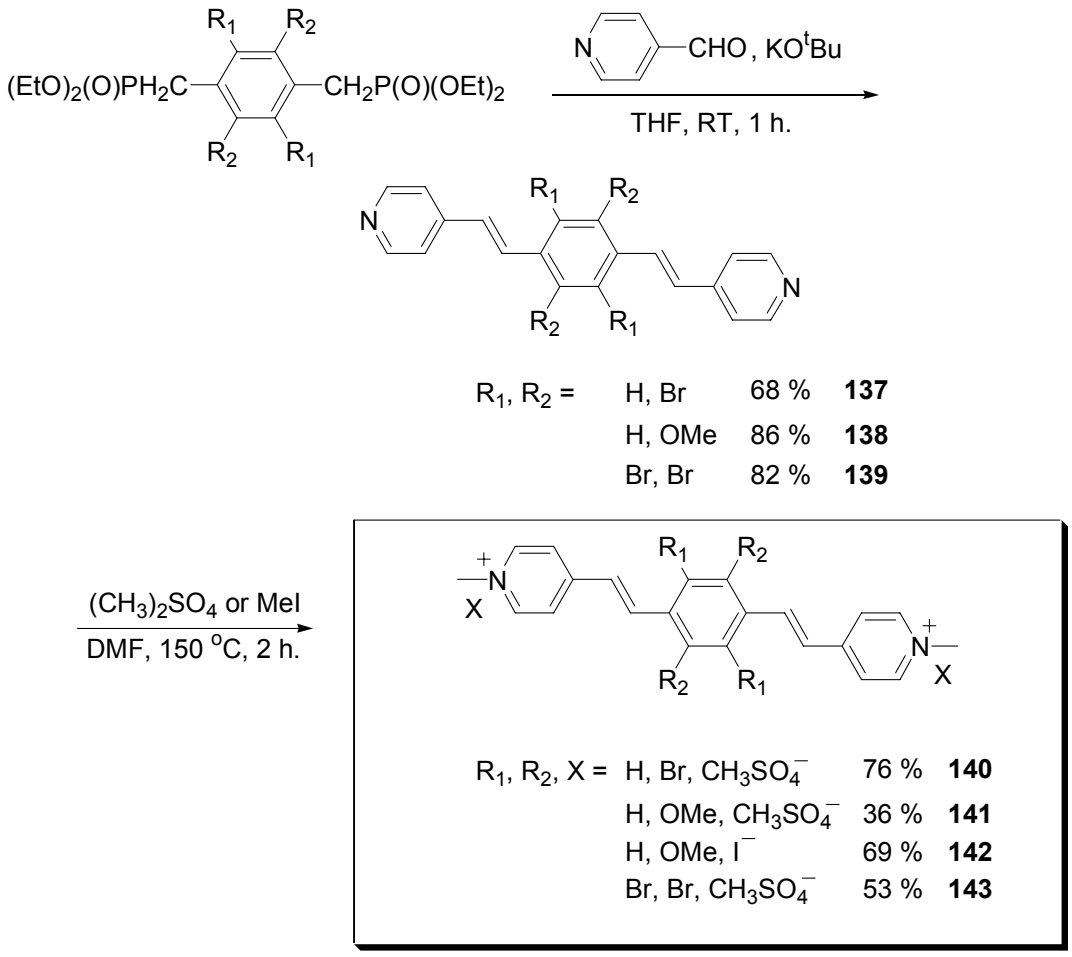

Scheme 4-10: Preparation of pyridine-OPV's and their salts.

A crystal structure of **143** was obtained (see Figure 4-5). The structure shows that the end-pyridine rings are almost completely perpendicular to the tetra-bromo substituted center ring and the double bonds are also distorted from planarity with the center ring. A dihedral angle of 152° for C21, C17, C9 and C20 and a dihedral angle of –108° for C9, C20, C7 and C13 were determined from the structure.

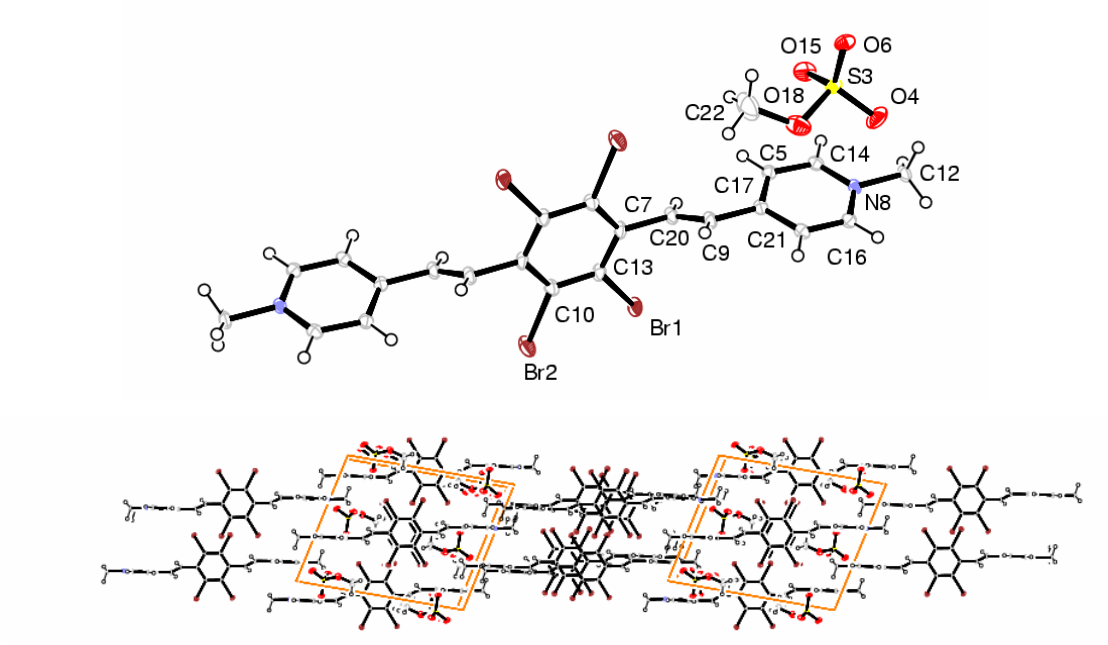

Figure 4-5: ORTEP-III plot (50 % ellipsoids) of the crystal structure of **143** including only one $CH_3SO_4^-$ counter ion. Hydrogens are showed as spheres with an arbitrary radius.

The crystallographic data are presented in Appendix C. A somewhat large peak difference (1.392 eÅ^{-3}) is observed close to the bromine atoms and this is ascribed to the problems associated with emperical absorption corrections when the crystal morphology is a thin plate and contains strong absorbers similar to what is reported by Krebs and Spanggaard.[9]

In the salts prepared in Scheme 4-8 and Scheme 4-10 the cationic site is an integral part of the chromophore. An attempt was also made to prepare a compound where the cationic site is isolated from the π-conjugated system of the sensitizer (see Scheme 4-11). To this end, the aldehyde **144** was prepared in a reaction with 4-fluoro-benzaldehyde and piperazine. The aldehydes were then reacted with the phosphonate ester **21**.

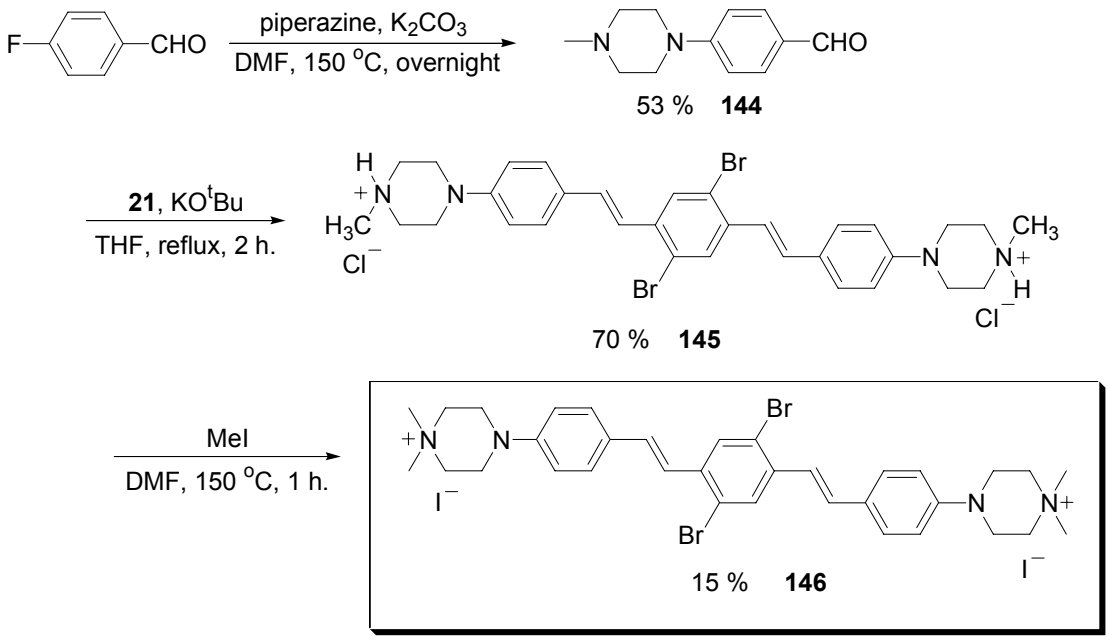

Scheme 4-11: Preparation of an 1,1-dimethyl-piperazine OPV.

The HWE reaction was quenched with hydrochloric acid, which lead to the isolation of the dihydrochloride **145** in the reaction of **144** with **21**. Interestingly, this dihydrochloride could be reacted with methyl iodide and the 1,1-dimethyl-piperazinium salt (**146)** was isolated.

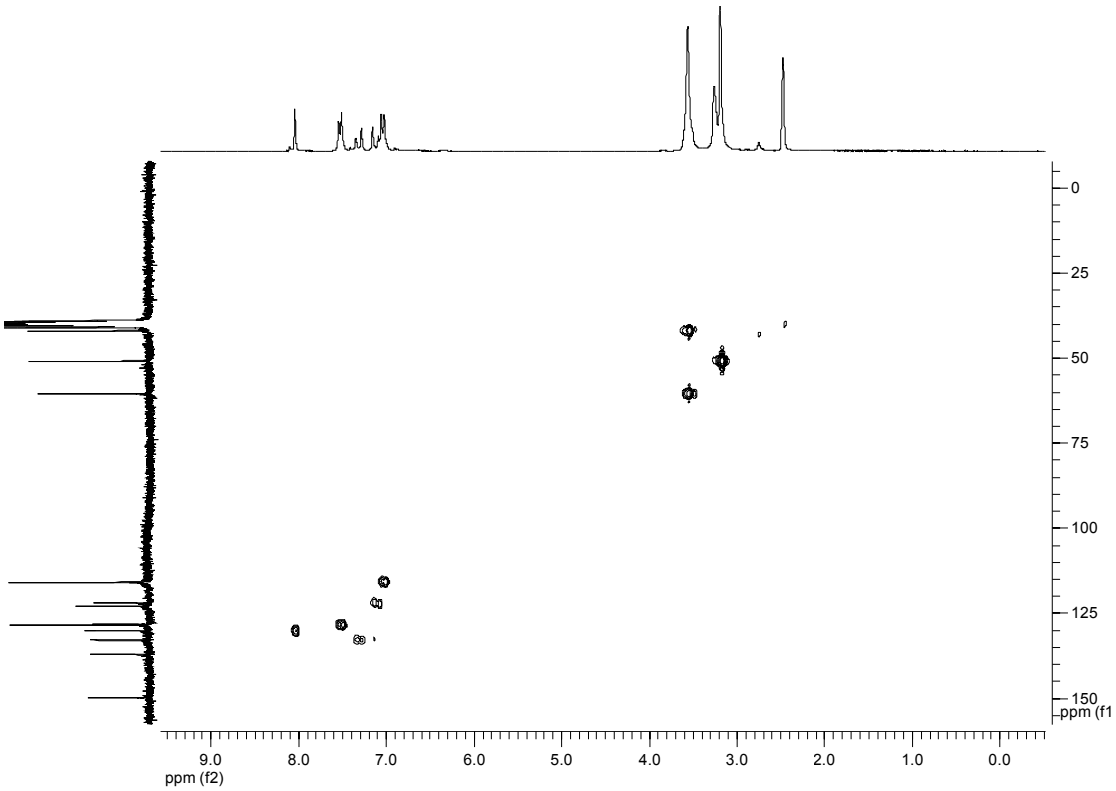

Figure 4-6: HMQC spectrum of **146** in DMSO recorded at 300 K.

In principle, the Menschutkin reaction with methyliodide can result in the methylation of either of the two different amine functionalities in **146,** but NMR only showed one type of methyl groups in accordance with what is expected from the structure of **146**. A HMQC spectrum was recorded for **146** and is shown in Figure 4-6. The multiplet at 3.64-3.47 ppm in the ^{1}H-NMR spectrum is assigned to methylene protons and they integrate to 16 protons. The singlet at 3.19 ppm (which integrate to 12 protons) in the ^{1}H-NMR spectrum is assigned to the protons on the methyl groups. From the HMQC-spectrum it is seen that these protons are positioned on chemically identical carbon atoms (see Figure 4-6). Methylation with dimethylsulfate was also tried but the isolated product was not air stable.

4.3 Photophysical characterization

4.3.1 One-photon properties

Photophysical data determined for the compounds prepared in the present work are summarized in Table 4-2, Table 4-3 and Table 4-4.

Table 4-2: Photophysical data for the compound prepared in the present work. λ_{max}^{abs} is the absorption maximum. Values of log(ε), where ε is the extinction coefficient, are given in parentheses. Φ_f is the fluorescence quantum yield, τ is the fluorescence lifetime.[a]

Compound	Solvent	λ_{max}^{abs} /nm	τ/ns	Φ_f
105	Toluene	354 (4.37)	0.2	0.13
106	Toluene	370 (4.62)	0.2	0.12
107	Toluene			
	Water			
108	Toluene	364		
	Water	348		
109	Toluene	352		
	Water	337		
110	Toluene	362		
	Water	347		
115	Toluene	426, 335		
	Water	418, 352		
126	Toluene	338 (3.67)	0.3	0.13
	1 M NaOH	280		
131	Water	491 (4.65), 395 (4.51)	1.9	0.19
134	Water	509		
138	Toluene	397 (4.48), 326 (4.38)	1.9	0.01
140	Water	360 (4.49)		0.01
141	Water	446 (4.60), 360 (4.48)	1.5	0.15
142	Water	445 (4.82), 358 (4.71)	1.6	0.15
143	Water	315 (4.53)		0.00
146	Water	364 (4.39)	1.0	0.08

[a] Errors are ±10 for all determined numbers.

All the MTEG-substituted OPV molecules (**105-110** and **115**) and the OPV salts with two bromine atoms on the central aromatic ring (**126**, **134**, **140**, **143** and **146**) have a single broad one-photon absorption band between ~ 300 and 400 nm (Figure 4-7). On the other hand, the compounds with comparatively strong electron donating methoxy groups on the central aromatic ring (*i.e.*, **131**, **141** and **142**) have a second discrete absorption band whose maximum is red-shifted with respect to that of the first band (Figure 4-7). This second band is ascribed to a transition that populates a comparatively low-lying CT state.

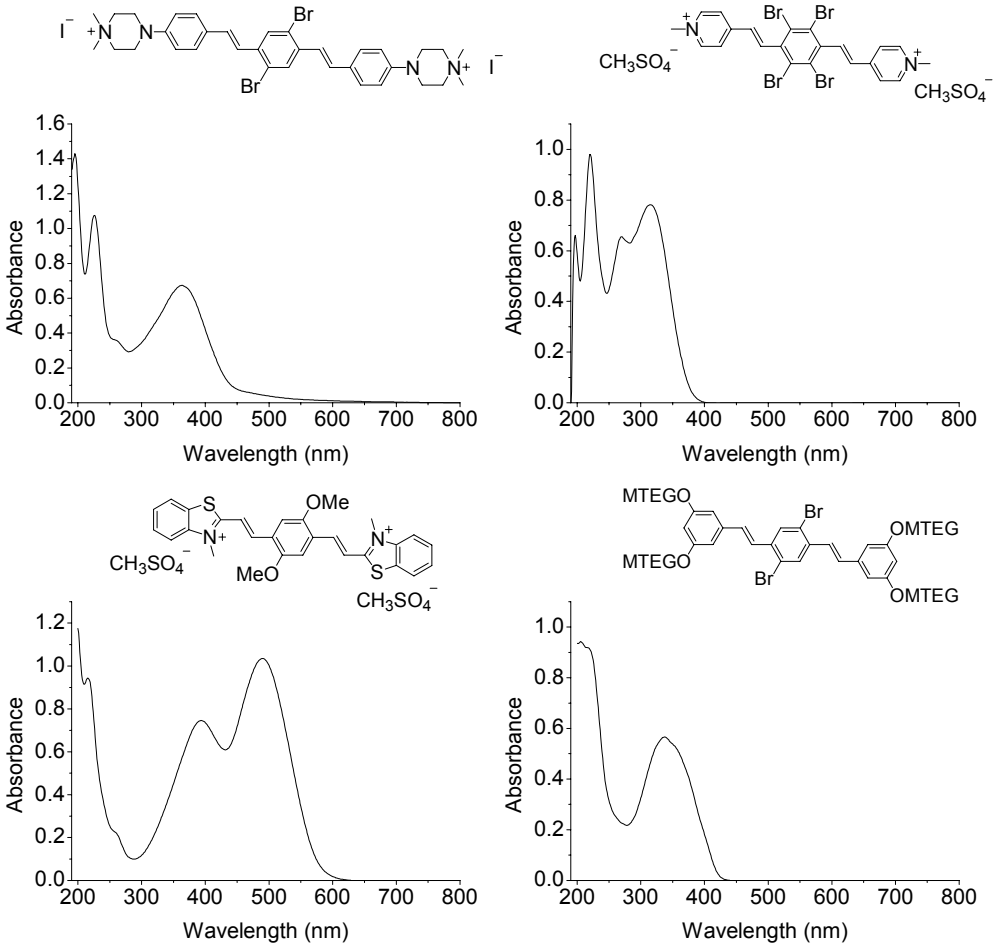

Figure 4-7: UV-VIS spectra of **109**, **131**, **143** and **146**. All of the spectra were recorded in water.

Due to the difficulties of getting **134** into solution in water an extinction coefficient for this compound could not be determined accurately and the absorption maximum reported in Table 4-2 for this compound may be a value for an aggregated species.

This is consistent with the broad absorbance spectral profile observed. The piperazine salt **146** absorbs at 364 nm and bearing in mind that the MTEG-amino analog absorbs above 400 nm, it is concluded that the cationic site draws charge trough an orbital overlap from the pendant aniline nitrogen significantly reducing the amount of CT in the aromatic ring system.

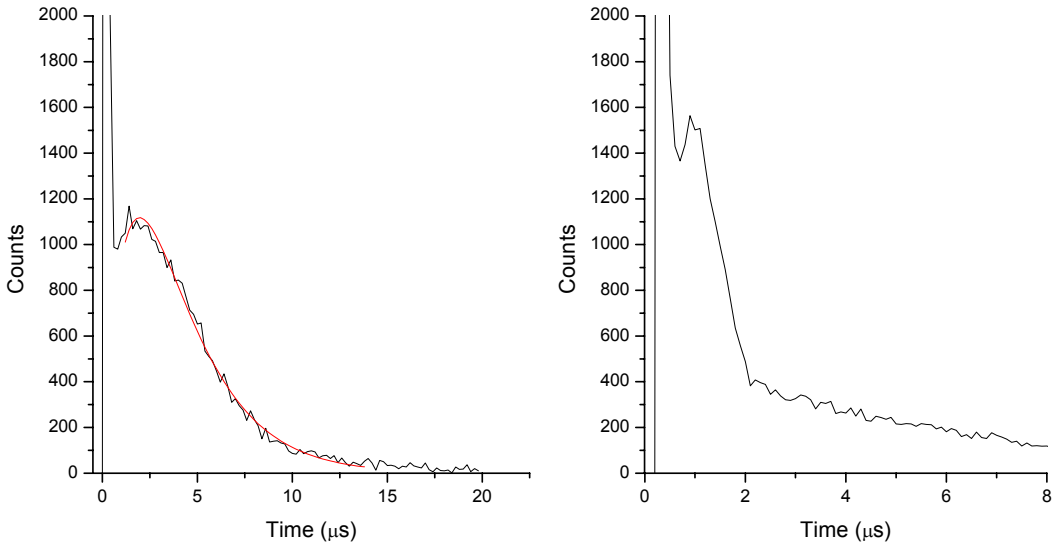

Figure 4-8: Time-resolved phosphorescence signal from singlet oxygen at 1270 nm using **107** as the photosensitizer in H_2O. Left: Low laser-power (i.e. 0.4 mW). Right: High laser-power (i.e. 4 mW) The intense "spike" preceding the singlet oxygen signal is due to a combination of sensitizer fluorescence, scattered laser light, and luminescence from the optics used.

The optical detection of singlet oxygen in water is more difficult than in solvents such as toluene due to the significantly shorter lifetime of singlet oxygen in water (approximately 3.5 μs as opposed to 30 μs in toluene).[10] Also, the rate constants for oxygen's radiative transitions are small in water.[11]

The singlet oxygen quantum yields determined in the present work were determined by monitoring the singlet oxygen phosphorescence at 1270 nm upon irradiation of the sensitizer in a one-photon experiment (see Ref. 1 for more details). The kinetics of triplet state photosensitized production of singlet oxygen are described in Scheme 4-12.

$$O_2(X^3\Sigma_g^-) \xrightarrow[T_1]{k_{form}} O_2(a^1\Delta_g) \xrightarrow{k_{decay}} O_2(X^3\Sigma_g^-)$$

Scheme 4-12: Singlet oxygen is first formed by quenching the photosensitizer triplet state with ground state oxygen occurring with rate constant k_{from}. The formed singlet oxygen molecules then decays to the ground state with rate constant k_{decay}.

The concentration of singlet oxygen will evolve in time according to,

$$(3) \qquad \left[O_2(a^1\Delta_g)\right]_t = \frac{k_{form}\left[O_2(X^3\Sigma_g^-)\right]}{k_{decay} - k_T}\left[T_1\right]_0\left(e^{-k_T t} - e^{-k_{decay} t}\right),$$

where k_T is the rate constant that expresses all channels for the decay of the photosensitizer triplet state, including the oxygen dependent bimolecular channel $k_{form}[O_2(X^3\Sigma_g^-)]$, and $[T_1]_0$ is the initial concentration of sensitizer triplet state. In a typical aqueous system the rate constants k_{decay} and k_T will be roughly equal, and as a consequence, the time evolution of the singlet oxygen signal observed in a time-resolved phosphorescence experiment should appear as the difference of two exponential functions, showing distinct rising and falling components. In Figure 4-8, the time-resolved phosphorescence intensity measured at 1270 nm is shown for **107** in water with a low and a high laser power. Both the raising and falling components are clearly seen in the decay spectra. In H_2O, the value of k_{decay} is approximately[12] 0.29 μs^{-1} and a value of 0.39±0.02 μs^{-1} was obtained by fitting expression (3) to the low-energy decay spectrum in Figure 4-8. At high laser energy, the time-resolved singlet oxygen phosphorescence signal shows an increased deviation from first order single exponential kinetics as shown in Figure 4-8. This behavior has previously been described, and has been interpreted to reflect the photoinduced production of a transient species that can quench singlet oxygen and whose lifetime is somewhat shorter than that of singlet oxygen.[1,13] The quencher is likely formed in competition with the production of singlet oxygen as a consequence of the interaction between the triplet state sensitizer and oxygen.[13,14] This interpretation is supported by the observation of transient luminescence signal at 1200 nm with a lifetime of approximately 1 μs.

Table 4-3: Singlet oxygen quantum yields for the MTEG-substituted OPV's in toluene and water.[a]

	Compound	Φ_Δ	
		Toluene	Water
105	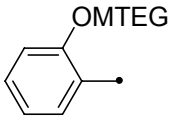	0.33	
106	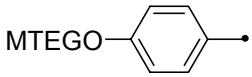	0.35	
107	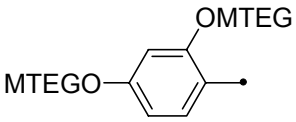	0.32	0.20
108	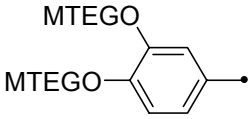	0.26	0.14
109	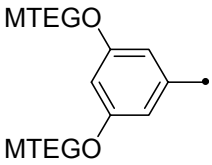	0.18	0.10
110	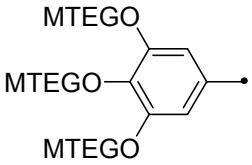	0.35	0.14
111	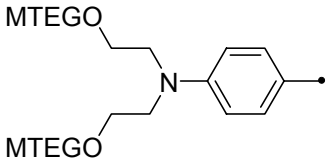	0.33	0.11

All the compounds where the ionic groups are an integral part of the sensitizer have small singlet oxygen quantum yields. In contrast, the non-ionic, MTEG-substituted sensitizers produce singlet oxygen in greater yield (see Table 4-3 and Table 4-4). For MTEG-substituted molecules an appreciable solvent effect on Φ_Δ was observed

[a] Errors are ±10 for all determined numbers.

indicating that singlet oxygen is more efficiently produced in toluene than it is in the more polar solvent water. These data are consistent with the thesis that significant CT character in a sensitizer and/or sensitizer-oxygen complex can adversely affect singlet oxygen yields by providing an independent pathway for the deactivation of sensitizer excited states that competes with energy-transfer to $O_2(X^3\Sigma_g^-)$.

Table 4-4: Singlet oxygen quantum yields of the ionic sensitizers.[a]

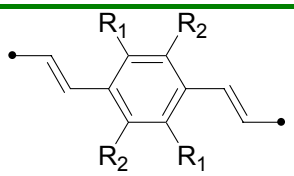

Compound		Φ_Δ	
		Toluene	Water
126 (R_1, R_2=H, Br)	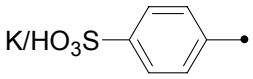	0.22	
131 (R_1, R_2=H, OMe)	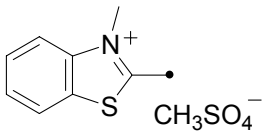		0.01
138 (R_1, R_2=H, OMe)	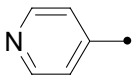	0.31	
140 (R_1, R_2=H, Br)	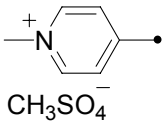		0.03
141 (R_1, R_2=H, OMe)	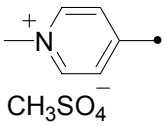		0.03
142 (R_1, R_2=H, OMe)	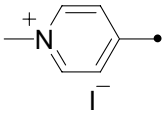		0.02
143 (R_1, R_2=Br, Br)	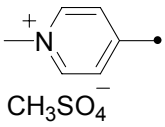		0.00
146 (R_1, R_2=Br, Br)	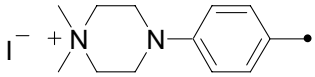		0.00

[a] Errors are ±10 for all determined numbers.

The addition of positively charged electron-withdrawing substituents to each end of the π system adversely affects the singlet oxygen yield (see Table 4-4). This is seen not only in the comparison between the MTEG- and ionic *N*-methylated species, but also in the comparison between the ionic *N*-methylated species and the corresponding non-methylated amines. For example, the pyridine-terminated OPV **138** has a Φ_Δ value of 0.30, whereas the corresponding *N*-methylpyridyl-terminated OPVs **141** and **163** both have a singlet oxygen Φ_Δ value of 0.02. Similarly, Φ_Δ values for the amino-terminated OPV **136** are noticeably larger than Φ_Δ values for the corresponding *N*-methylated **140** and **146**. In this discussion, it is also important to note that the singlet oxygen quantum yield can be influenced by many features of a given sensitizer, not just the extent of CT character. For example, a key parameter is the relative energy of the sensitizer triplet state,[15] and this energy is certainly expected to change upon methylation of an amine whose lone pair electrons are an integral part of the chromophore. Within the MTEG-substituted series, the singlet oxygen quantum yields consistently reflect the substitution pattern of the pendant ether. Thus, for compounds in which the alkoxy groups are *ortho* and/or *para* to the vinyl-ether moiety, the singlet oxygen yield is comperatively large. In contrast, for the compounds in which the alkoxy groups are *meta* to the vinyl moiety, the singlet oxygen yield is noticeably smaller. These observations are consistent with the expectation that, in contrast to the effect of withdrawing electron density from the chromophore (vide supra), electron donating groups cause an increase in the singlet oxygen quantum yield.

4.3.2 Stability issues

Although the water soluble MTEG-substituted molecules produced singlet oxygen in moderate yields, these molecules were unfortunately not particularly stable upon irradiation in aereated H_2O. This is illustrated in Figure 4-9 for **115**, where the absorption spectrum of a freshly prepared solution of **115** was recorded and compared to the absorption spectrum taken after the sample was left in the sunlight for a few hours.

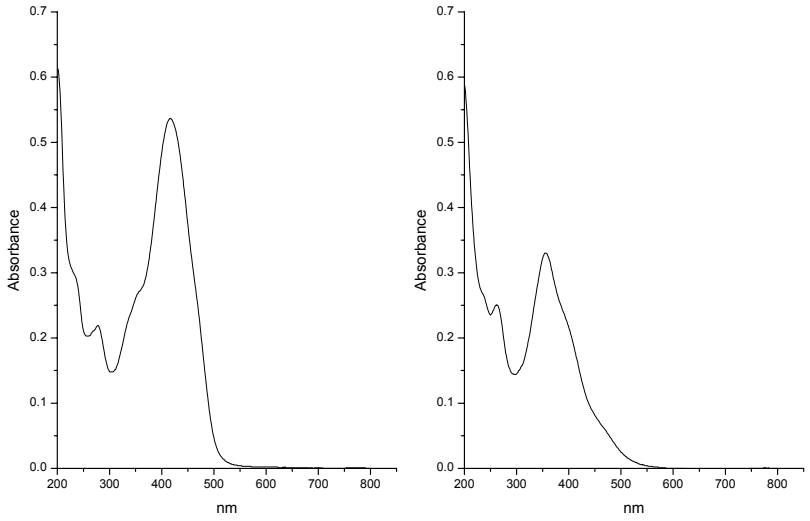

Figure 4-9: UV-VIS spectra of **115** in water. Left: Freshly prepared sample. Right: Recorded after the sample was exposed to sunlight for a few hours.

This stability issue was investigated further by independently irradiating samples of **108** and **115** in both water (H_2O and D_2O) and toluene with a 400 nm 30 mW laser in 1 min. intervals and recording the absorption spectrum of the sample in between each irradiation period. The absorption spectra for these experiments performed in H_2O are presented in Figure 4-10.

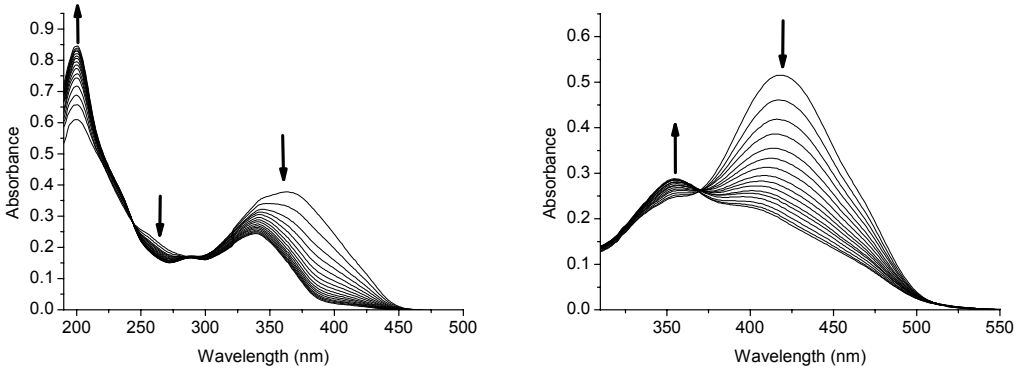

Figure 4-10: UV-VIS absorption spectra of two MTEG-substituted sensitizers recorded as a function of elapsed exposure to 400 nm light in aerated H_2O (CW laser operated at 30 mW, irradiated spot size ~5 mm in diameter). Arrows on the respective spectra indicate whether the absorbance increases (up arrow) or decreases (down arrow) upon prolonged irradiation. Spectra were recorded at 1 min intervals during irradiation. Left: **108**. Right: **115**.

In both cases, the degradation reactions involved appear to shorten the chromophore as seen by a decrease in the intensity of the longest wavelength absorption band. Moreover, distinct isosbestic points in the spectra indicate that, under the conditions of these experiments, only one degradation product is formed in each case. Despite the apparent similarities in the data shown in Figure 4-10, however, the kinetics for **108** and **115** were different.

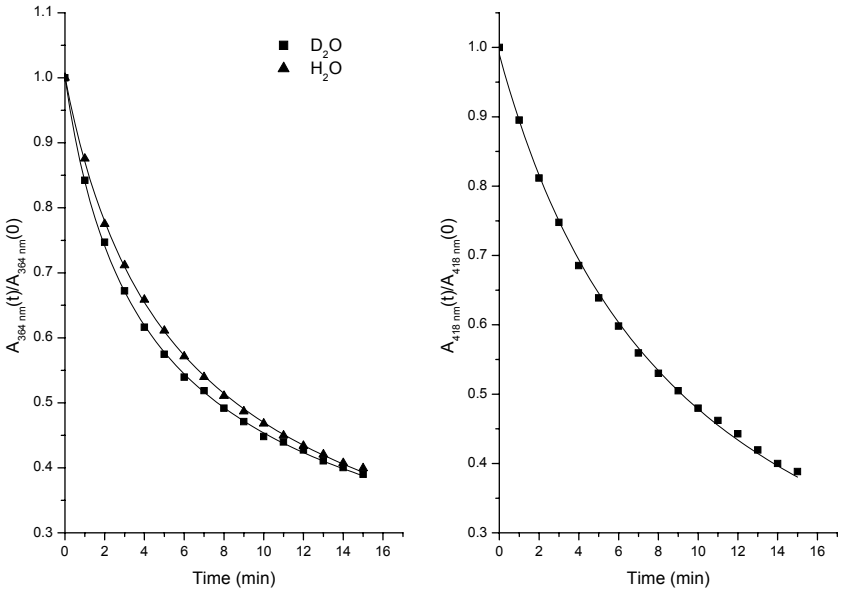

Figure 4-11: Photoinduced changes in aqueous solutions of **108** (left) and **115** (right) monitored by recording the absorbance of the solutions at either 364 nm (**108**) or 418 nm (**115**) as a function of the elapsed photolysis time at 400 nm.

In Figure 4-11 the photoinduced changes of aqueous solutions of **108** and, independently, **115** are shown. The overall rate for the degradation of **108** is seen to be greater in D_2O than in H_2O. Because the lifetime of singlet oxygen is longer in D_2O than it is in H_2O,[11] such data are generally interpreted to indicate that singlet oxygen is involved in the degradation process. In contrast, a D_2O/H_2O solvent isotope effect was not observed in the photo-induced changes of a solution of **115**. Thus, for these two compounds it appears that different reactions may be involved in the degradation process. In support of this, the decay of **108** did not follow either first- or second-order kinetics over the reaction period, whereas **115** followed second-order kinetics over a comparatively long period of irradiation. It is possible that the

destruction of **108** could be a singlet oxygen-mediated oxygenation of a double bond linking the aromatic rings.[16,17] However, **115** has amines that could potentially be oxidized in a reaction not involving singlet oxygen which, in turn, could likewise alter the chromophore and hence the absorption profile of the molecule.

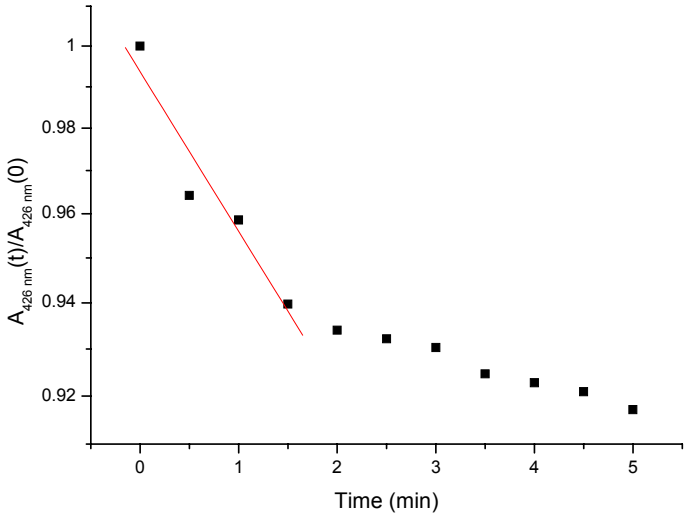

Figure 4-12: Photo-induced changes in a toluene solution of **115** as monitored by recording the absorbance of a solution at 426 nm as a function of the elapsed photolysis time at 400 nm.

To illustrate the potential complexity of these degradation reactions, data recorded for **115** in toluene are shown in Figure 4-12 and a pronounced difference from the data recorded in water is observed.

4.3.3 Two-photon properties

The two-photon action spectra for **115** and **130** recorded in toluene are shown in Figure 4-13 and Figure 4-14.

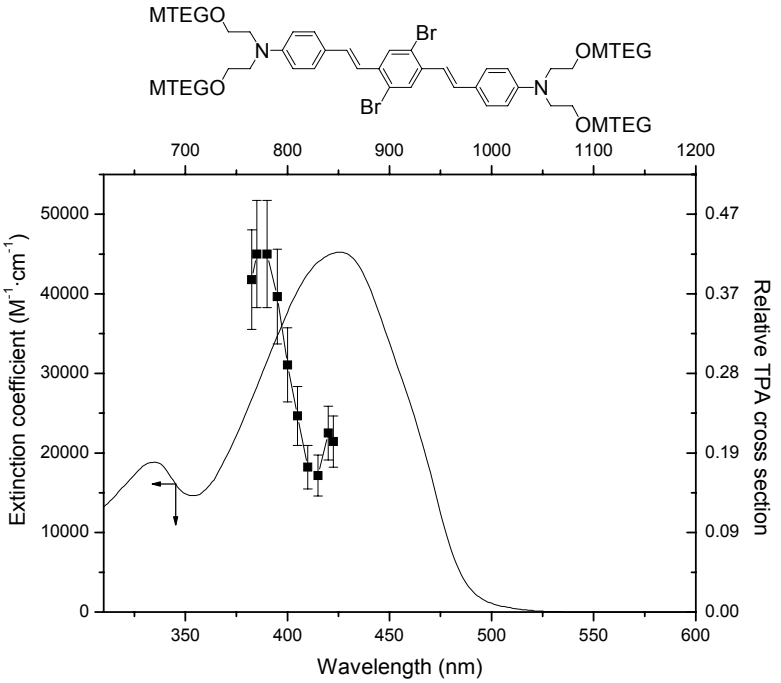

Figure 4-13: One-photon absorption and two-photon action spectra of **115** in toluene.

The two-photon action spectra of **115** show a maximum at 775 nm similar to **33**, but **115** aslo appears to have a maximum at 840 nm, which **33** does not have. Only the tail of an absorption band is seen in the two-photon action spectrum of **130**.

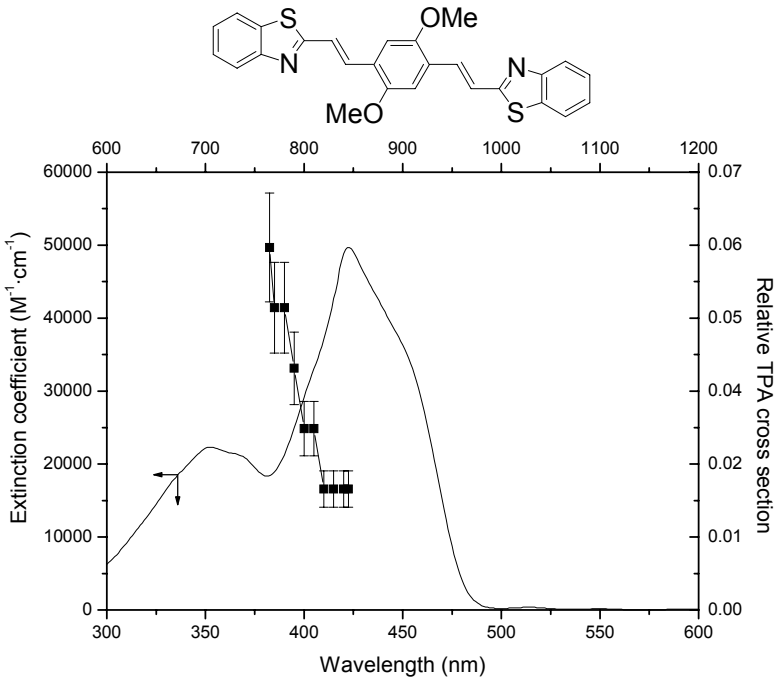

Figure 4-14: One-photon absorption and two-photon action spectra of **130** in toluene.

It remains to be demonstrated that singlet oxygen can be produced in water using one of the developed sensitizers in a two-photon process. For this purpose **115** was chosen because it has a two-photon absorption maximum within the spectral range studied. Two-photon sensitization of singlet oxygen in water was only demonstrated at 800 nm. Experiments were performed in both D_2O and H_2O. As required for a process of two-photon excitation, the intensity of the singlet oxygen phosphorescence signals observed scale according to the square of the power of the irradiating laser (Figure 4-15).

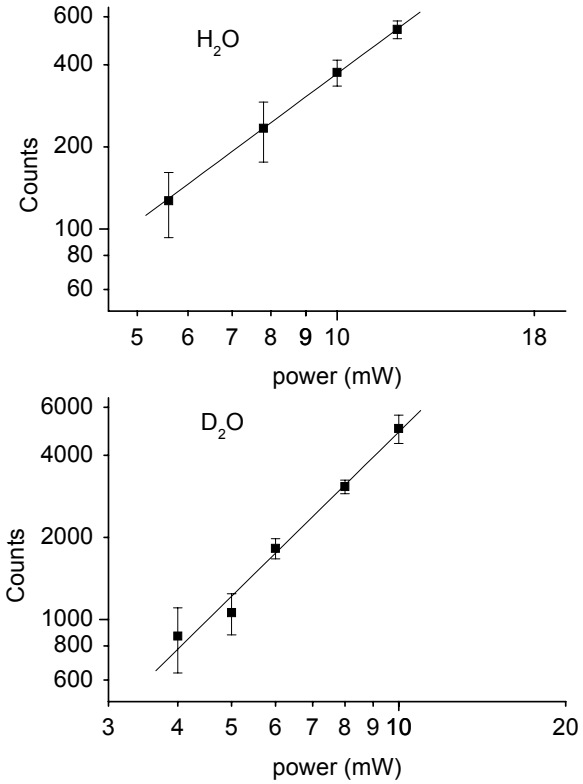

Figure 4-15: Double logarithmic plot of the singlet oxygen phosphorescence intensity against the average laser power incident on the sample. These data were recorded upon 800 nm irradiation of aqueous solutions of **115**. Top: Experiments performed in H_2O with 0.44 mM of **115**. A slope of 2.1 ± 0.4 was obtained. Bottom: Experiments performed in D_2O with 0.38 mM of **115**. A slope of 2.0 ± 0.2 was obtained.

Thus, it has been demonstrated that singlet oxygen in water can indeed be produced upon two-photon excitation of an OPV sensitizer with an electron-donor-acceptor architecture.

4.3.4 Solvent effects on the singlet oxygen quantum yield

The decrease in singlet oxygen quantum yield observed when changing solvent from toluene to water leaves the question whether a systematic change as a function of some solvent parameter can be observed. One solvent parameter is the polarity defined in Chapter 3. The singlet oxygen quantum yield was measured for **115** in six different solvents (toluene, 1,4-dioxane, $CHCl_3$, THF, 1-propanol and water) and the singlet oxygen quantum yield is plotted against the solvent polarity in Figure 4-16.

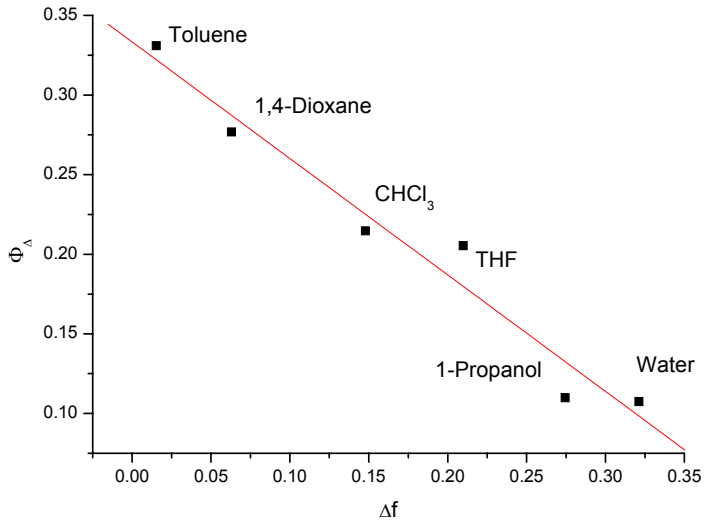

Figure 4-16: A Lippert-Mataga type plot of the singlet oxygen quantum yield (determined using the sodium salt of 1-oxo-1H-phenalene-2-sulfonic acid as the standard) for **115**.

A linear relation between the quantum yield and the solvent polarity is observed similar to a Lippert-Mataga plot. Usually, such a relation is indicative of a change in energies of the electronic states as predicted by reaction field theory. The change in electronic state energies can be viewed upon as a result of changes in the CT character in the molecule. In particular the increase in charge-character as a function of an increase in solvent polarity is in fact described in the literature.[18] From the results in Figure 4-16 it is then suggested that the poor quantum yields observed in water for the compounds discussed in the present chapter is due to changes in the CT character of the compounds upon changing solvent.

4.4 Conclusion

It has been shown that singlet oxygen can be generated from a water-soluble sensitizer with a donor-acceptor OPV architecture. Two different approaches were used to achieve water solubility, where an OPV was functionalised with oligo ethylene glycol chains in the non-ionic approach and salts of pyridine, benzothiazole, *N*-methyl-piperazine or sulfonic acids were used in the ionic approach. The most successful sensitizer prepared was the tetra oligo ethylene glycol substituted OPV with a 2,4-substitution pattern on the end-benzene rings. The success of this

compound is ascribed to a precise amount of charge-transfer in the compound. Stability of the sensitizer is an important aspect of a successful singlet oxygen sensitizer and this has been addressed and shown to be a complex issue. Furthermore, the ionic sensitizers with an appreiciable amount of charge transfer character generated singlet oxygen with low quantum efficiency in water, and this is believed to be caused by CT-mediated competive pathways present for deactivation of sensitizer-excited states. The difficulties of making singlet oxygen sensitizers that absorb above 400 nm have been addressed, and in order to achieve absorption maxima above this wavelength relatively long conjugation lengths are required. To make such large organic molecules water-soluble, it is necessary to have a significant number of hydrophilic groups present in the molecule.

Reference List

1. Frederiksen, P. K.; McIlroy, S. P.; Nielsen, C. B.; Nikolajsen, L.; Skovsen, E.; Jørgensen, M.; Mikkelsen, K. V.; Ogilby, P. R. *J. Am. Chem. Soc.* **2005**, *127*, 255-269.

2. Rosenmund, K. W.; Zetzsche, F. *Chem. Ber. /Recueil* **1918**, *51*, 594-602.

3. Rosenmund, K. W.; Pfannkuch, E. *Chem. Ber. /Recueil* **1922**, *55*, 2357-2372.

4. Schmidt, U.; Wild, J. *Liebigs Ann. Chem.* **1985**, *9*, 1882-1894.

5. Mancuso, A. J.; Swern, D. *Synthesis (Stuttgart)* **1981**, 165-185.

6. Brouwer, A. J.; Mulders, S. J. E.; Liskamp, R. M. J. *Eur. J. Org. Chem.* **2001**, 1903-1915.

7. Jørgensen, M.; Krebs, F. C. *J. Org. Chem.* **2004**, *69*, 6688-6696.

8. Wang, X. M.; Zhou, Y. F.; Yu, W. T.; Wang, C.; Fang, Q.; Jiang, M. H.; Lei, H.; Wang, H. Z. *J. Mater. Chem.* **2000**, *10*, 2698-2703.

9. Krebs, F. C.; Spanggaard, H. *J. Org. Chem.* **2002**, *67*, 7185-7192.

10. Schweitzer, C.; Schmidt, R. *Chem. Rev.* **2003**, *103*, 1685-1757.

11. Wilkinson, F.; Helman, W. P.; Ross, A. B. *J. Phys. Chem. Ref. Data* **1995**, *24*, 663-1021.

12. Egorov, S. Y.; Kamalov, V. F.; Koroteev, N. I.; Krasnovsky, A. A.; Toleutaev, B. N.; Zinukov, S. V. *Chem. Phys. Lett.* **1989**, *163*, 421-424.

13. Gorman, A. A.; Rodgers, M. A. J. *J. Am. Chem. Soc.* **1986**, *108*, 5074-5078.

14. Kristiansen, M.; Scurlock, R. D.; Iu, K. K.; Ogilby, P. R. *J. Phys. Chem.* **1991**, *95*, 5190-5197.

15. Schmidt, R.; Shafii, F.; Schweitzer, C.; Abdel-Shafi, A. A.; Wilkinson, F. *J. Phys. Chem. A* **2001**, *105*, 1811-1817.

16. Dam, N.; Scurlock, R. D.; Wang, B. J.; Ma, L. C.; Sundahl, M.; Ogilby, P. R. *Chem. Mater.* **1999**, *11*, 1302-1305.

17. Scurlock, R. D.; Wang, B. J.; Ogilby, P. R.; Sheats, J. R.; Clough, R. L. *J. Am. Chem. Soc.* **1995**, *117*, 10194-10202.

18. Gould, I. R.; Boiani, J. A.; Gaillard, E. B.; Goodman, J. L.; Farid, S. *J. Phys. Chem. A* **2003**, *107*, 3515-3524.

CHAPTER 5

EFFECT OF ACID–BASE EQUILIBRIA ON SINGLET OXYGEN GENERATION

Abstract: *A singlet oxygen sensitizer is protonated in order to investigate the impact this chemical change of the sensitizer will have on the singlet oxygen quantum yield. Systematic changes of the singlet oxygen quantum yield are observed upon protonating the sensitizer, which may reflect changes in triplet state energy levels and/or a changes in the charge-transfer character of the sensitizer.*

5.1 Introduction

The amount of CT character in the sensitizer molecules described in the previous chapters has been controlled by variation of the substituents in the molecule. Another way of controlling the CT character in the molecule is to protonate the amine nitrogens in the amine functional groups that serve as electron donors.

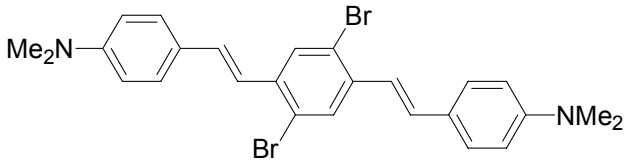

46

Figure 5-1: The structure of the sensitizer used to study the effect of acid-base equilibria on singlet oxygen quantum yields.

For this study, **46** was chosen. These experiments were performed in toluene using trifluoroacetic acid (TFA) as the proton source. The singlet oxygen quantum yields were then determined as a function of the amount of TFA added to the system. A NMR titration in $CDCl_3$ was also carried out in order to determine whether both amine functionalities are protonated at once or if they are protonated step-wise. Equilibrium constants for these acid-base reactions can be deduced from both the toluene and $CDCl_3$ experiments. The determined equilibrium constants can then be compared to see if the change from a non-polar to a polar solvent causes the changes as predicted from simple chemical principles.

Relatively little work is presented in the literature about the effect of protonating basic sites on a singlet oxygen sensitizer,[1-4] where only rate constants for other processes governing singlet oxygen has been measured. These rate constants were then used to estimate the singlet oxygen quantum yield and a sigmoidal dependence of the singlet oxygen quantum yield on pH in the sample was found. Thus, direct measurements of the effect of protonating basic sites on the sensitizer in singlet oxygen generation have not previously been addressed. In the present work the singlet oxygen quantum yields were measured directly.

5.2 Singlet oxygen quantum yields in acidic solutions

A titration was carried out on **46** in $CDCl_3$, where TFA was used for protonating the amine nitrogens. The titration was followed using NMR. In all the measurements, the formal concentration of the sensitizer was kept constant and the chemical shift of the *N*-methyl groups was monitored and plotted against the ratio between the amount of TFA (in moles) and sensitizer (in moles). The results are presented in Figure 5-2.

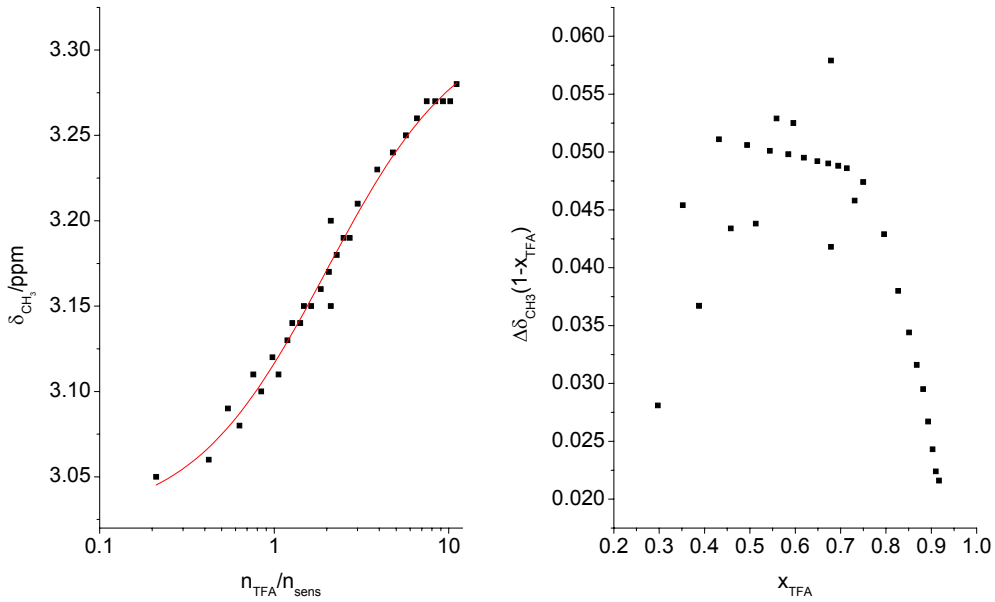

Figure 5-2: Left: Chemical shift of the CH_3-protons in compound 67 as a function of n_{TFA}/n_{sens}, where n_{TFA} is the amount of TFA (in moles) and n_{sens} is the amount of sensitizer (in moles). Right: Job-plot for the titration.

The Job-plot obtained from the NMR-titrations indicate that both amine nitrogens are protonated at the same time during the titration because a maximum around 2/3 is observed in the Job-plot.[5] From the inflection point in the sigmoidal fit to the experimental data in Figure 5-2, an equilibrium constant for the protonation shown in Scheme 5-1 was determined to be 2.0±0.2.

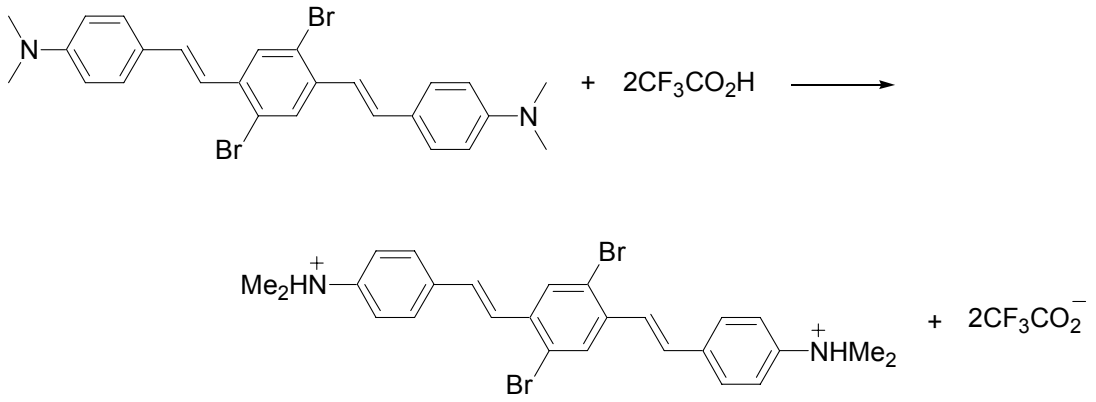

Scheme 5-1: Protonation equilibrium for **46**. An equilibrium constant was determined to 2.0±0.2 for the $CDCl_3$ experiments.

Direct measurements of singlet oxygen quantum yields were measured as a function of the amount of TFA in a toluene solution of **46** where the formal concentration of the sensitizer was identical in all measurements. Absorption spectra were recorded for each sample as a function of added TFA and representative examples are presented in Figure 5-3, where it is noticed that an isosbestic point is not present.

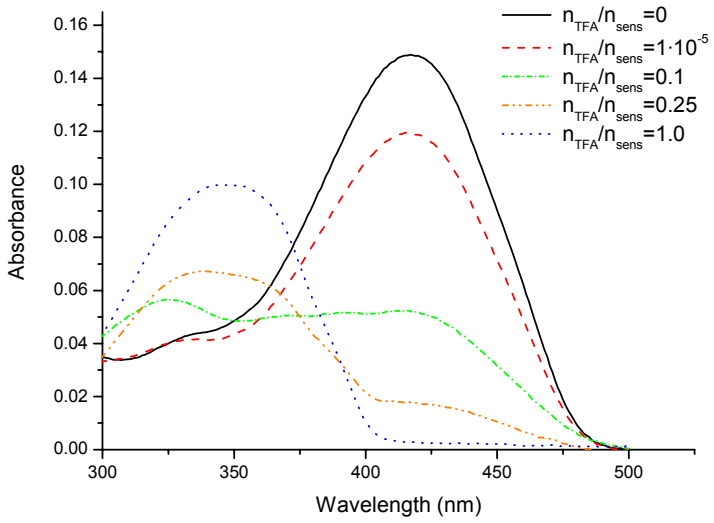

Figure 5-3: Selected absorption spectra of solutions with different n_{TFA}/n_{sens} ratios. An isosbestic point is not observed.

The singlet oxygen quantum yields were measured at two different wavelengths (355 and 416 nm) and the results are presented in Figure 5-4. The quantum yields measured at 355 nm show a nice sigmoidal dependence on the ratio between the amount of TFA and sensitizer (both in moles).

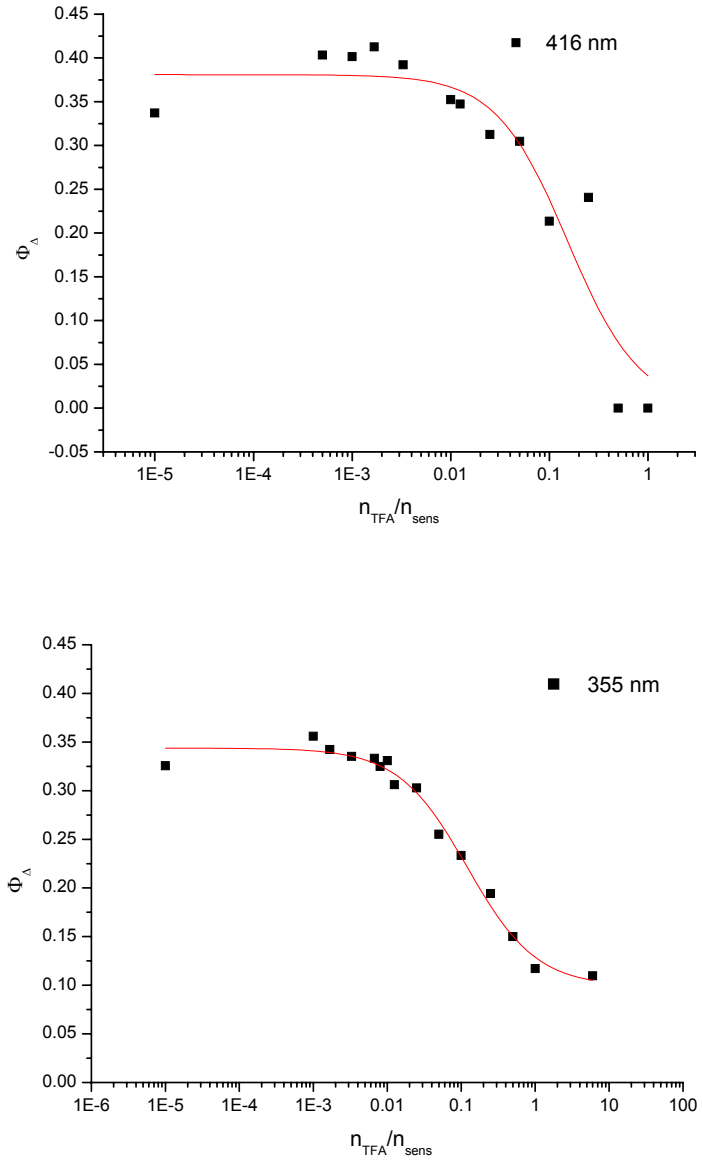

Figure 5-4: Singlet oxygen quantum yields as a function of the ratio between the amount of TFA and sensitizer.

The equilibrium constant for the reaction in Scheme 5-1 was determined to be 0.12±0.02 from the quantum yields determined at 355 nm and 0.15±0.04 from the quantum yields determined at 416 nm (infered from the inflection points in the sigmoidal fits). The two numbers are an order of magnitude lower than the equilibrium constant determined in $CDCl_3$ using the NMR titration technique. This finding is explained by the polarity of solvents used. Toluene is a non-polar solvent whereas $CDCl_3$ is a polar solvent. The equilibrium in Scheme 5-1 is expected to be

"drawn to the product side" by increasing the solvent polarity as the charged species are better solvated and this is also what is observed. Thus the protonation of the sensitizer behaves as expected.

The sigmoidal dependence shown in Figure 5-4 can be interpreted in terms of the sensitizer singlet-triplet energy difference changes occuring upon protonation of the amines. An increasing energy gap between the S_1 and T_1 states should result in a lower triplet quantum yield and thereby also a lower singlet oxygen quantum yield (see Chapter 1). However, a phenomenalical approach is to view the changes in singlet and triplet state energies as a result of a changing donor-strength of the amine end-groups. Upon protonating the amines, the lone pairs on the nitrogen atoms cannot be delocalised into the aromatic π-system in the sensitizer. The effect of this change is a decrease in charge density in the vicinity of the bromine atoms, which again causes a decrease in the triplet quantum yield as the bromine atoms are responsible for intersystem crossing due to the heavy atom effect discussed in Chapter 1. Irrespective of the underlying mechanism behind the changes in the singlet oxygen quantum yield it is important to realize that it is evident that an acid-base equilibrium is responsible for the changes observed. However, it is not evident that the change in singlet oxygen quantum yields follows a nice sigmoidal curve as a function of the amount of TFA present similar to a standard acid-base titration inasmuch as an isosbestic point is not observed in the absorption spectra. The absence of an isosbestic point means that at least three chromophores are present in the solution upon adding TFA to the solution.

5.3 Conclusion

The lone-pairs on the amine-groups in **46** are somewhat delocalised into the aromatic π-system. By protonating these lone-pairs, the amino-group becomes less potent as an electron-donating group and the extent of CT can be controlled in the molecule. A titration carried out by increasing the amount of TFA present in a solution of **46** reveals that the singlet oxygen quantum yield drops as a function of the amount of the TFA present in the solution. This can be due to both changes in the triplet-energy levels in the sensitizer but also due to an altered amount of CT character in the molecule. These results are important for the development of sensitizers that are to be

used in biological applications, as the pH in cells may vary dependent on the nature of the cell.

Reference List

1. Burt, C. D.; Moore, D. E. *Photochem. Photobiol.* **1987**, *45*, 729-739.

2. Bagno, O.; Soulignac, J. C.; Joussotdubien, J. *Photochem. Photobiol.* **1979**, *29*, 1079-1081.

3. Pottier, R.; Bonneau, R.; Joussotdubien, J. *Photochem. Photobiol.* **1975**, *22*, 59-61.

4. Bonneau, R.; Pottier, R.; Bagno, O.; Joussotdubien, J. *Photochem. Photobiol.* **1975**, *21*, 159-163.

5. Connors, K. A. *Binding Constants - The Measurement of Molecular Complex Stability*; Wiley: New York, 1987.

CHAPTER 6

PORPHYRINS: SYNTHESIS AND CHARACTERIZATION

Abstract: *Porphyrins have interesting photophysical properties and are also known to make singlet oxygen in high yields. The synthesis and characterization of porphyrins with a donor-acceptor substitution pattern was investigated.*

6.1 Introduction

Porphyrins have several attractive features with respect to singlet oxygen generation inasmuch as they have a very high one-photon absorption coefficient (approximately 500,000 $M^{-1}\cdot cm^{-1}$) around 420 nm (the Sóret band). Many porphyrins are good singlet oxygen sensitizers with quantum yields above 0.70 and, for these reasons, porphyrins are often used as sensitizers for PDT.[1-7] Porphyrins are also good candidates for two-photon singlet oxygen sensitization, and this warrants an investigation as to whether porphyrins can be designed to have high TPA cross sections following the design principles discussed in Chapter 1 and in Ref. 8-10.

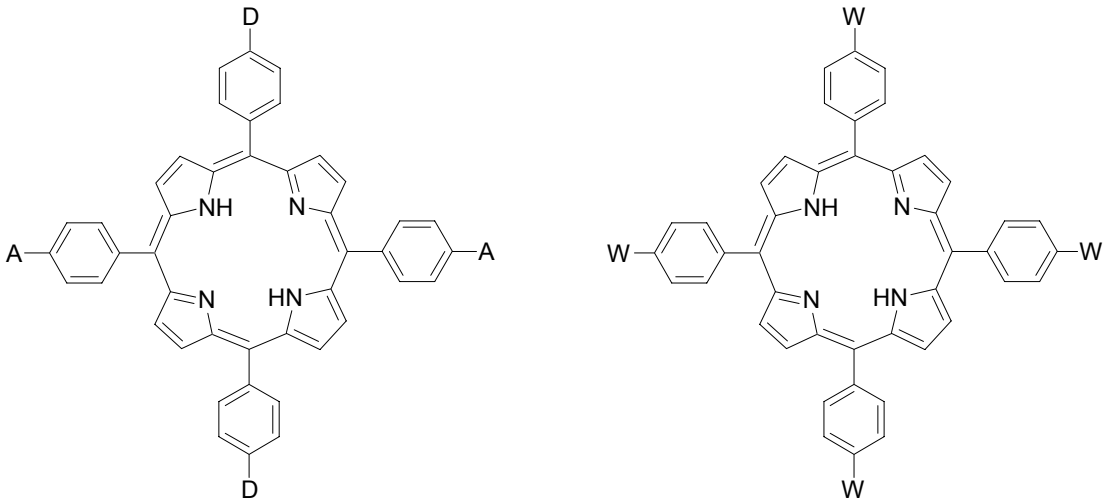

Chart 6-1: General structures of the target molecules. A and D are electron accepting and donating groups respectively, and W is a functional group imparting water solubility.

Water soluble two-photon singlet oxygen sensitizers are also of interest and to this end the possibility of making a porphyrin functionalized with extended conjugated water soluble functional groups was investigated. General structures of the two types of target molecules are shown in Chart 6-1.

6.2 Preparation of porphyrins

The porphyrin skeleton depicted in Figure 6-1 can be functionalized in a variety of different positions. Typically the 5, 10, 15 and 20-positions (the *meso* or β-positions) are functionalized with aryl rings and further substitutions on these aryl rings are used as "handles" for making chemistry on the porphyrins.

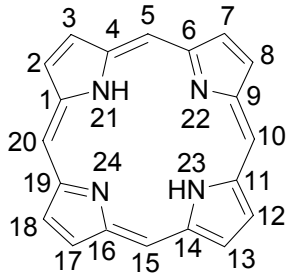

Figure 6-1: Numbering in the porphyrin skeleton.

Several groups have reported that positions 5, 10, 15 and 20 can be lithiated when positions 2, 3, 7, 8, 12, 13, 17 and 18 are blocked (*i.e.* 2, 3, 7, 8, 12, 13, 17, 18-octaethyl-porphin) and reacted with electrophiles.[11-19] Symmetrical *meso*-substituted porphyrins can be synthesized by condensing an aldehyde with pyrrole using a Lewis acid or TFA as the catalyst. Oxidation with either chloranil or DDQ then gives the porphyrin ring system (Scheme 6-1).[20]

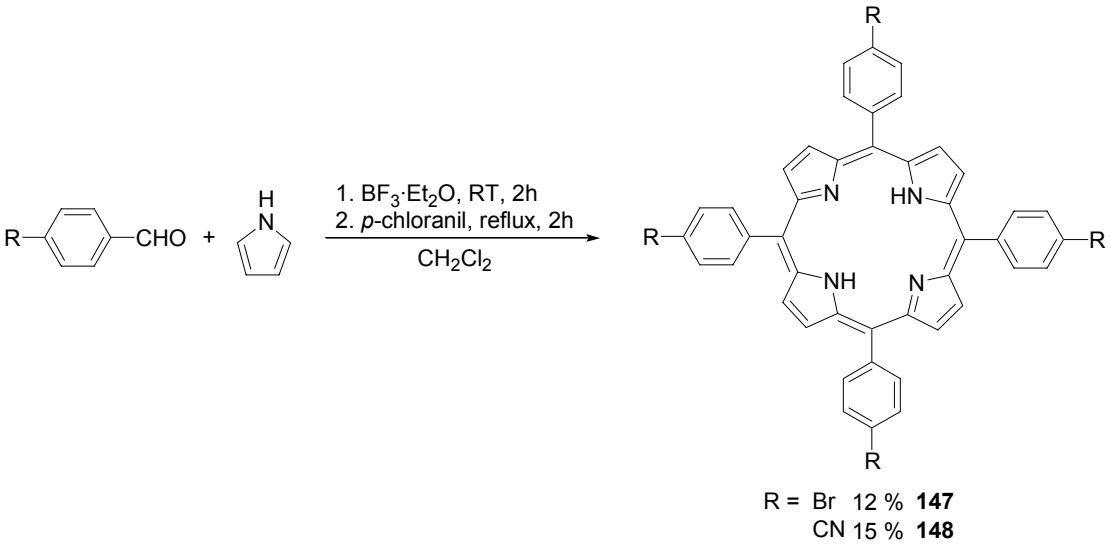

Scheme 6-1: Synthesis of symmetrical porphyrins using the procedure described above.

Attempts were made to make a water-soluble symmetrical porphyrin where water solubility should be achieved through a pyridinium salt. TMPyP have been shown to be a good singlet oxygen sensitizer with a reasonable TPA cross section. However, a larger conjugation length is wanted in order to obtain a larger TPA cross section. Both of these requirements could be realized in the pyridinium salt of the porphyrin depicted in Scheme 6-3. To this end, 4-pyridin-4-yl-benzaldehyde was synthesized. Nicolaou and coworkers have reported the synthesis of this compound by oxidizing 4-*p*-tolyl-pyridine with IBX.[21] 4-*p*-tolyl-pyridine was first prepared in a Suzuki-reaktion with 4-chloro-pyridine hydrochloride and *p*-tolylic acid but it was not possible to oxidize 4-*p*-tolyl-pyridine to the aldehyde using IBX (Scheme 6-2).

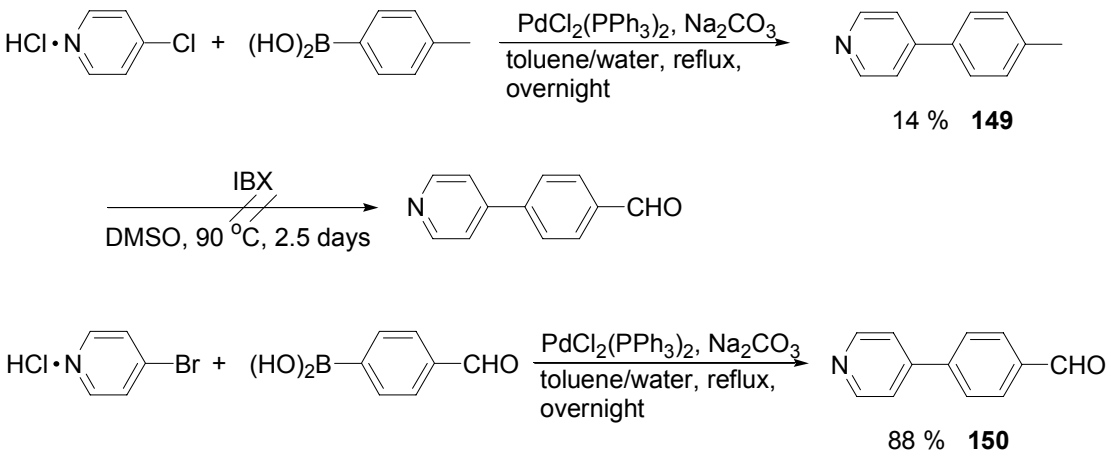

Scheme 6-2: The synthesis of 4-pyridin-4-yl-benzaldehyde using the Suzuki reaction.

Instead, 4-pyridin-4-yl-benzaldehyde was prepared in a Suzuki reaction with 4-bromo-pyridine hydrochloride and 4-formyl-phenylboronic acid in 88 % yield.

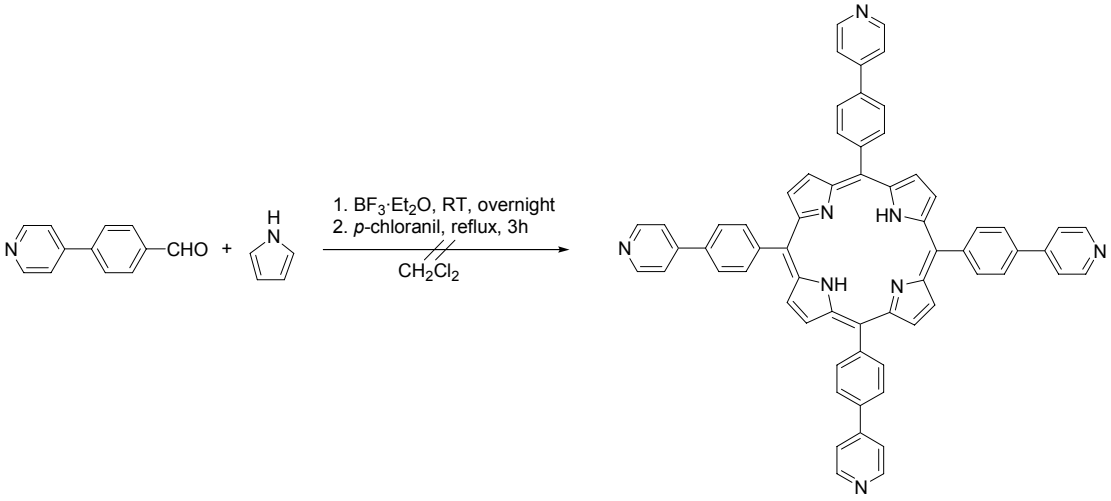

Scheme 6-3: Attempt to make a pyridine-substituted porphyrin using procedure described above.

However, it was not possible to react the 4-pyridin-4-yl-benzaldehyde with pyrrole using the procedure described above (see Scheme 6-3).

Usymmetrical porphyrins were prepared, where the 5, 15 and 10, 20-positions have the same substituents, respectively, resulting in a *trans*-A_2B_2 substitution pattern. Such porphyrins are prepared by first making a dipyrromethane and then condensing it with an aldehyde and finally oxidizing to the porphyrin with either p-chlor-anil or DDQ. In the present work, two dipyrromethanes were prepared as illustrated in Scheme 6-4 and porphyrins were made from these dipyrromethanes.

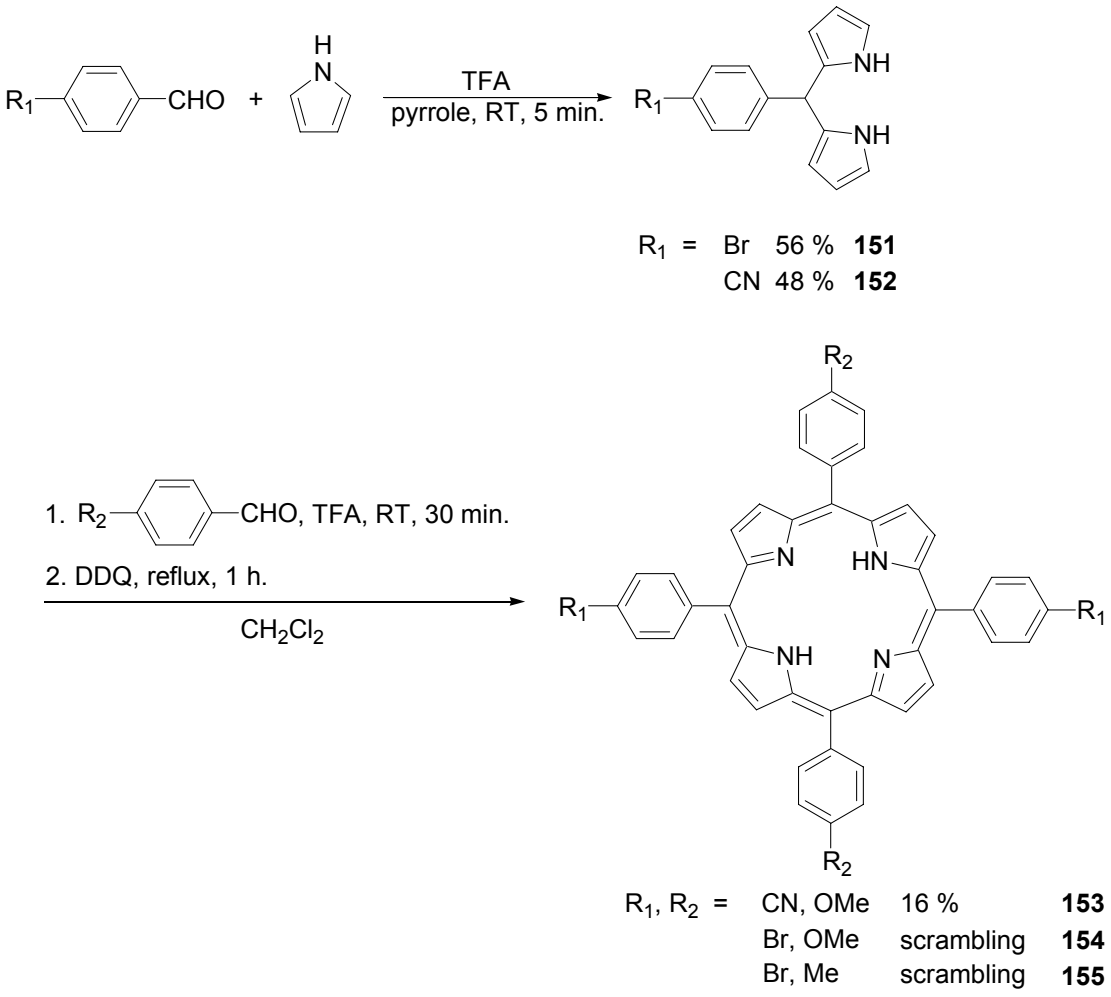

Scheme 6-4: The preparation of trans-substituted porphyrins.

Several reports have been made in the literature about scrambling of the *meso* substituents in attempts to make *trans*-A_2B_2 substituted porphyrins using condensations with dipyrromethanes and aldehydes followed by oxidation resulting in a mixture of up to six different porphyrins.[22] It has also been reported that different salts can promote condensations between the aldehyde and pyrrole. The addition of salts should in some cases also prevent scrambling of the *meso* substituents (*e.g.* NH_4Cl).[22] Preparations where dipyrromethanes of electron deficient benzaldehydes (such as 5-(2, 3, 4, 5, 6-penta-fluoro-phenyl)-dipyrromethane), sterically hindered dipyrromethanes (such as 5-(3,5-di-*tert*-butyl-phenyl)-dipyrromethane) or even dipyrromethane itself, were used, have been reported to proceed without scrambling.[23] This is in accordance with what is observed for the porphyrins prepared as described in Scheme 6-4. Scrambling of the *meso*-substitutents occurred in the synthesis where

the 5-(4-bromo-phenyl)-dipyrromethane was reacted with either anisaldehyde or tolulaldehyde, which was proven by MALDI-TOF (see Figure 6-2).

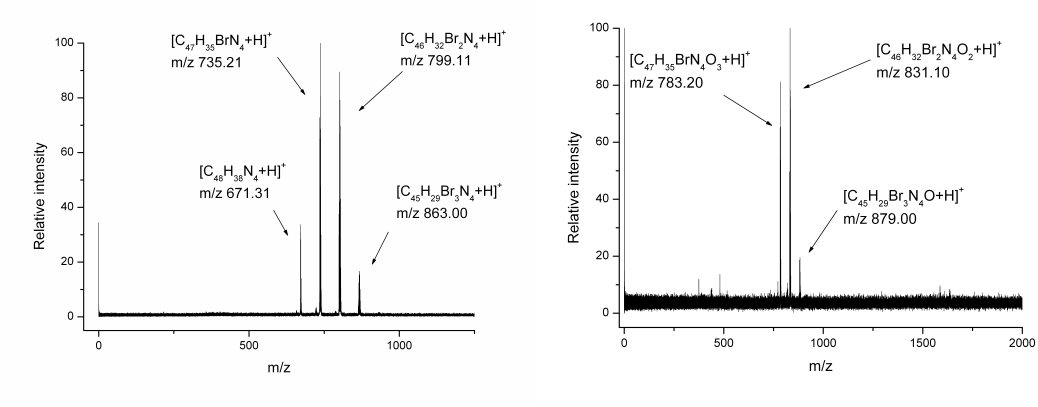

Figure 6-2: MALDI-TOF spectra of the mixture of porphyrins obtained from reacting 5-(4-bromo-phenyl)-dipyrromethane with either tolulaldehyde (left, **155**) and anisaldehyde (right, **154**).

The masses corresponding to A_2B_2-substituted porphyrins could originate from both the *trans*- and *cis*-isomer of the porphyrin. The mixture of porphyrins obtained from the reaction with 5-(4-bromo-phenyl)-dipyrromethane and anisaldehyde was also analysed with HPLC chromatography (see Figure 6-3).

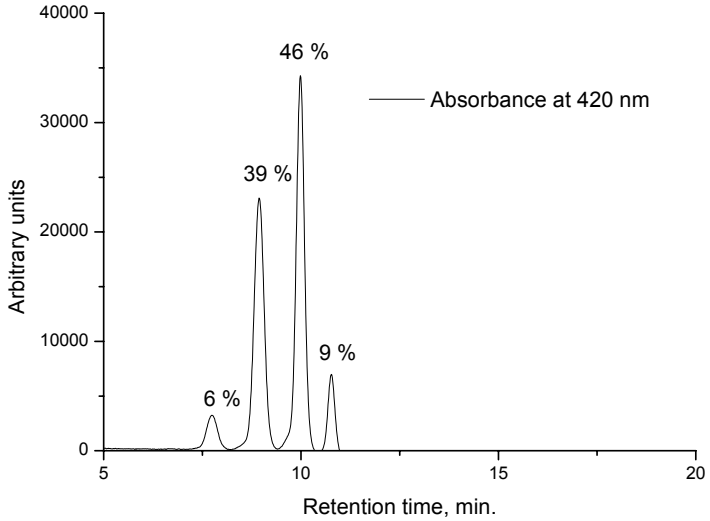

Figure 6-3: HPLC chromatogram of a solution of the mixture of porphyrins obtained from reacting 5-(4-bromo-phenyl)-dipyrromethane with anisaldehyde (**154**). The absorbance at 420 nm was monitored as a function of the retention time.

Four peaks were observed in the chromatogram but only three peaks were observed in the MALDI-TOF spectrum. The peaks were almost perfect Gaussian shaped demonstrating that each peak only contains one component. From the chromatogram the distribution of the porphyrins was determined to 6 %, 39 %, 46 % and 9 %.

The NH-part of the ^{1}H-NMR spectra for each or the porphyrin mixture is shown in Figure 6-4.

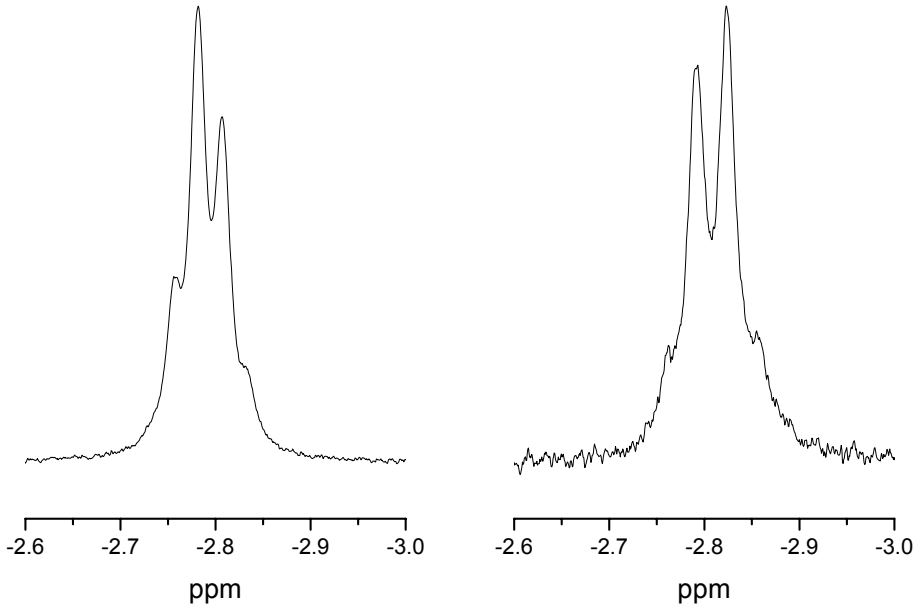

Figure 6-4: ^{1}H-NMR of the NH-region of the spectra of the porphyrin mixtures. Left: Bromo and methyl substitution pattern (**155**). Right: Bromo and methoxy substitution pattern (**154**).

In the ^{1}H-NMR-spectrum of the bromo-methyl-porphyrin mixture, four peaks are observed in accordance to what is observed in the MALDI-TOF spectrum. The signal from –2.72 to –2.86 ppm was fitted with four Lorentzian functions (as shown in Figure 6-5). The chemical shift of the N-H protons is –2.76 for TTP and –2.86 for **147** indicating that an increasing number of bromine substituents cause an up-field shift of the N-H protons. From these data, the distribution of the different porphyrins could be determined to 5 % of the porphyrin with three bromine atoms, 33 % with two bromine

atoms, 48 % with one bromine atom and 14 % of the porphyrin with zero bromine atoms.

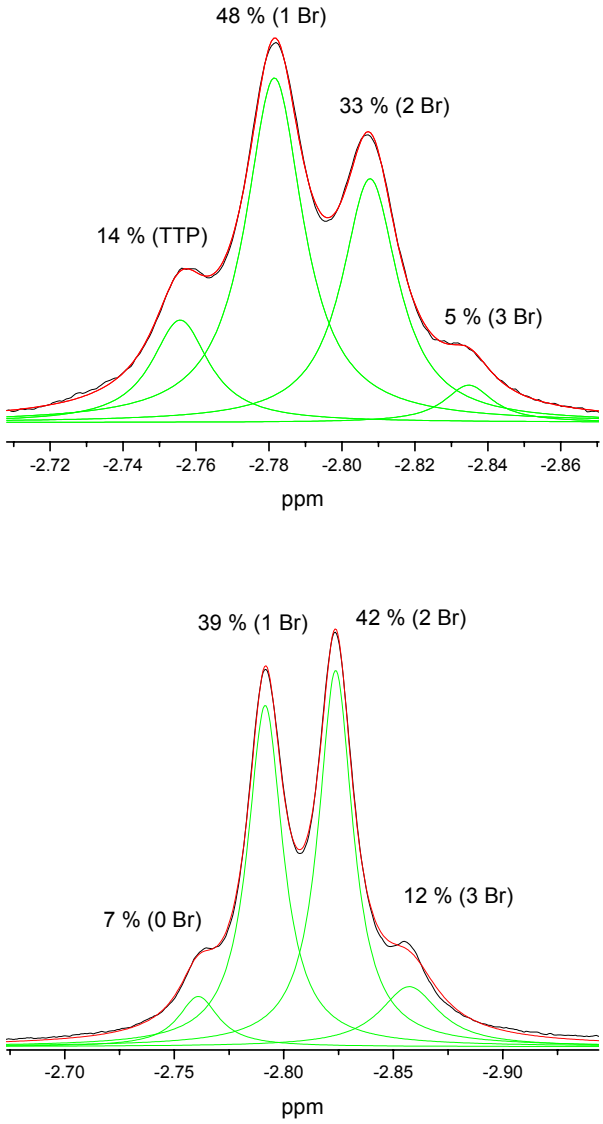

Figure 6-5: Four Lorentzian functions were fitted to the N-H part of the ^{1}H-NMR-spectrum of **155** (top) and **154** (bottom).

The distribution of porphyrins determined from the ^{1}H-NMR-spectrum of the bromo-methoxy-porphyrin is 7 %, 39 %, 42 % and 12 % in good agreement with the distribution determined from the HPLC results.

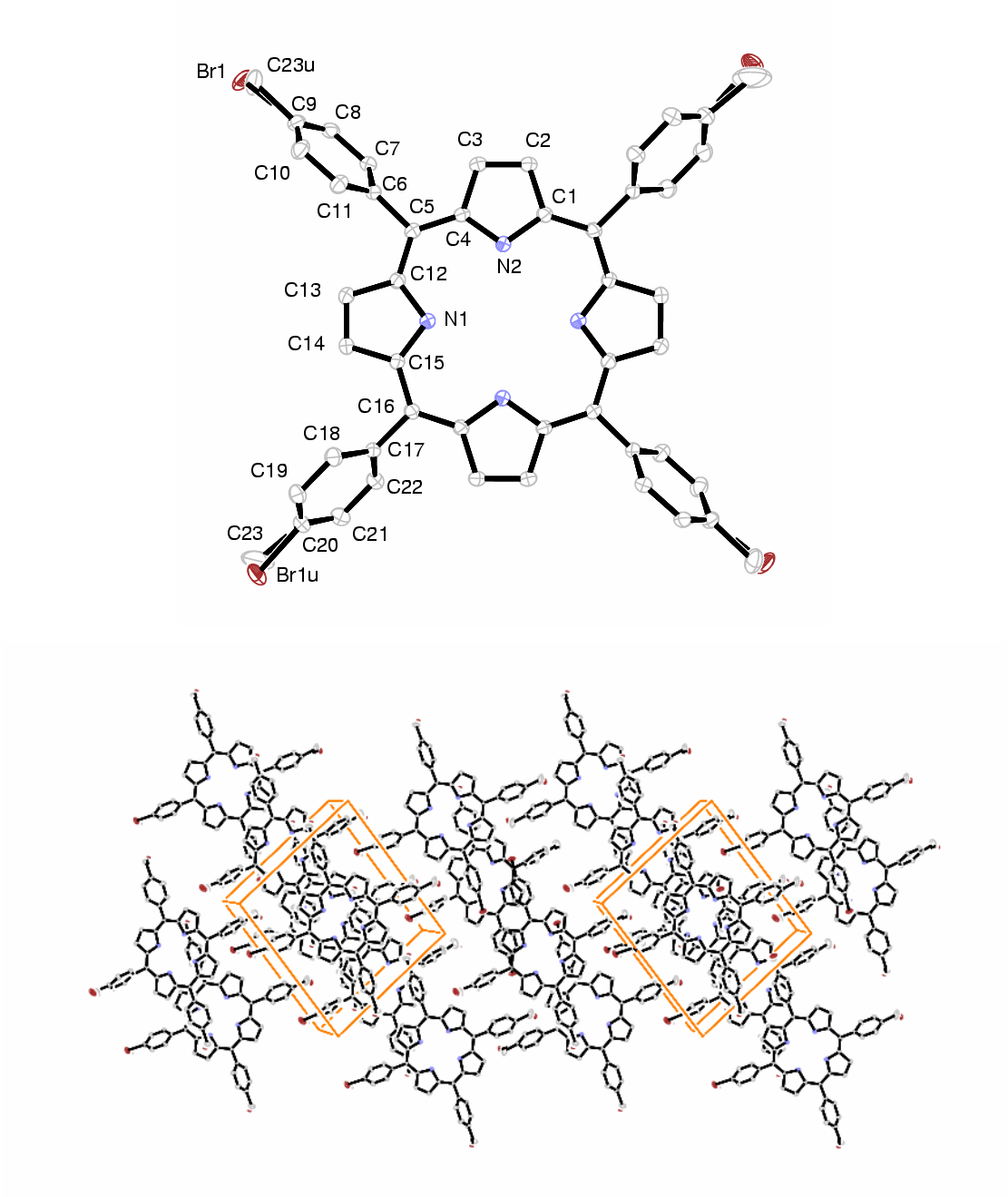

Figure 6-6: X-ray structure and crystal packing (stereo view) of the mixture of **155**.

Due to the similar size of a bromine atom and a methyl group it was possible to grow crystals of the mixture of **155** suitable for x-ray crystallography. A disordered model was used to solve the structure (shown in Figure 6-6).

6.3 Photophysical studies

UV-VIS and fluorescence spectra were recorded (in toluene) for a series of porphyrins (R_1, R_2=H, Br; H, CN and H, CHO, see Scheme 6-4). All of them have fluorescence maxima at 654 and 720 nm irrespective of the substituent pattern on the *meso* aryl rings. The absorption spectra shows the characteristic B(0,0) (or Sóret) band at 422 nm and the four Q-bands at 515 nm ($Q_y(1,0)$), 551 nm ($Q_y(0,0)$), 592 nm ($Q_x(1,0)$) and at 649 nm ($Q_x(0,0)$) for all the investigated porphyrins. Apparently, the UV-VIS and fluorescence data do not reveal any substituent effect (of changing substituents on the meso aryl ring) on the optical properties consistent with what is reported in the litterature.

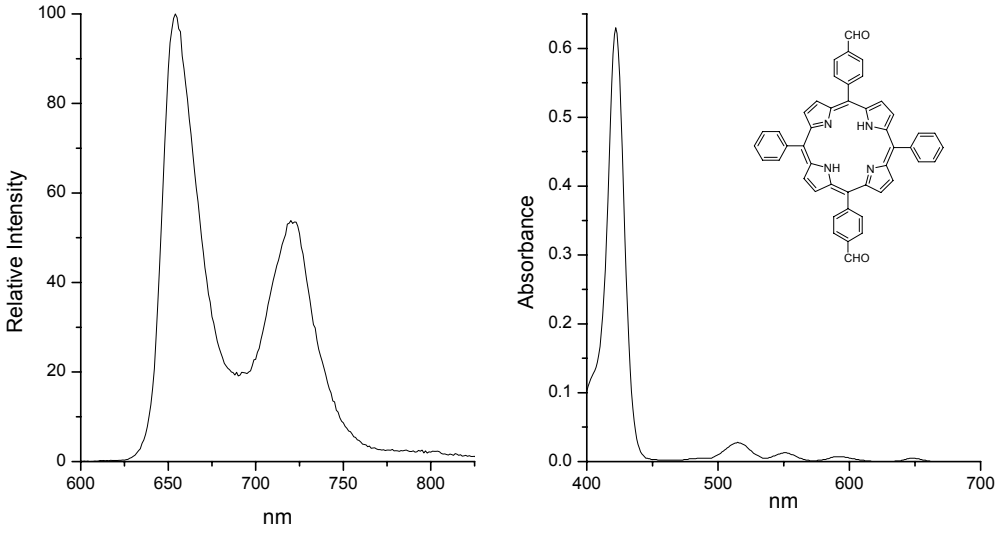

Figure 6-7: Fluroescence (left, excitation with 421 nm) and UV-VIS spectrum (right) of the depicted porphyrin. Both spectra were recorded in toluene.

Singlet oxygen quantum yields were measured for **147**, **148**, TPP and TTP (see Table 6-1).

Table 6-1: Singlet oxygen quantum yields measured in toluene (acridine as the standard). The molecular framework to which R refers is depiced in Scheme 6-1.[a]

R	Φ_Δ
H (TPP)	0.72
CH_3 (TTP)	0.80
Br	1.07
CN	0.75

The quantum yields are high as expected for a porphyrin molecule. It is also seen that there is a little effect of changing the R group from H to a strong electron acceptor such as the cyano group. However, bromine substitution seems to have a significant effect and this can be explained in terms of spin-orbit coupling as discussed in Chapter 1; Introducing a heavy atom into a molecule can promote intersystem crossing from the S_1 state to the triplet manifold due to spin-orbit coupling.

Measurements on **147** were carried out in toluene using femtosecond laser pulses and the intensity of the singlet oxygen phosphorescence signal was monitored as a function of the laser power (see Chapter 1). If singlet oxygen is generated in a two-photon process, the intensity of the singlet oxygen phosphorescence signal should increase quadratically with the laser power. In a double logarithmic plot, the singlet oxygen phosphorescence signal (I_Δ) should then be linearally dependent on the laser power with a slope of 2.

[a] Errors are ±10 % for all determined numbers.

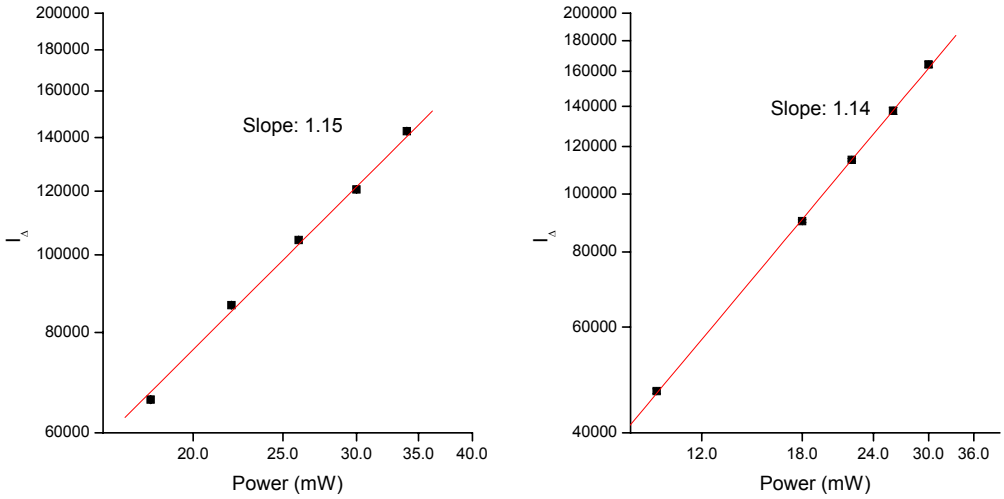

Figure 6-8: Double logarithmic plots of the singlet oxygen phosphorescence signal (I_Δ) as a function of the laser power using wavelengths of 765 nm (right) and 801 nm (left). Slopes in the vicinity of one indicating one-photon generation of singlet oxygen was observed in both cases.

The power dependencies measured at the wavelengths 765 and 801 nm are presented in Figure 6-8. In both cases a quadratic dependence was not observed. Several experiments, where singlet oxygen phosphorescence was measured generated from solutions with different porphyrins in various concentrations were carried out but despite these efforts, it was not possible to generate singlet oxygen in a two-photon irradiation scheme using a porphyrin as the photosensitizer. A possible explenation for this finding could be that the Q-bands extend to the infrared so that a one-photon band is actually present in the spectral range used for the two-photon experiments.

6.4 Conclusion

Porphyrins are currently used as one-photon singlet oxygen sensitizers in PDT. In the present work, the difficulties in using porphyrins as photosensitizers for two-photon singlet oxygen generation is described. One major difficulty is the preparation of pure porphyrins, as scrambling of the substitutents often take place in the synthesis. Furthermore there seems to be little or no substituent effects on the electronic properties upon *meso* substitution making it difficult to obtain large TPA cross sections using donor-acceptor architectures as described in Chapter 1. Reports have

been made, however, that there are substituent effects upon functionalizing porphyriazines (the porphyriazine skeleton is shown in Chart 6-2); Enhancement of the two-photon absorption cross section has been observed by functionalizing porphyrazines with electron-accepting substitutents.[24]

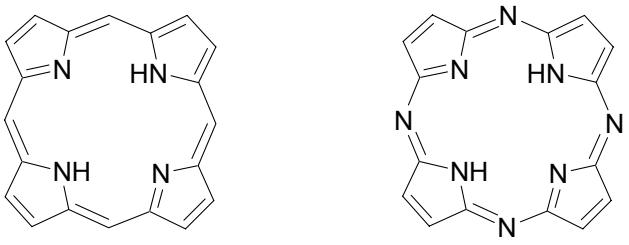

Chart 6-2: The porphyrin- (left) and the porphyrazine-skeleton (right).

These findings can be explained in the geometries of the *meso*-phenyl substituted porphyrins as both computational and X-ray studies indicate that the phenyl rings are perpendicular to the porphin ring. Thus no overlap between the π-orbitals on the *meso*-phenyl ring and the porphin core can take place thereby diminishing the effect of changing substituents on the meso-phenyl ring. Placing substituents directly on the porphyrazine core can result in substituent effects as the π-orbitals on the substituent can efficiently overlap with the porphyrazine core. Problems in observing true two-photon behaviour were faced, as singlet oxygen could not be generated using a porphyrin sensitizer in a two-photon irradiation scheme.

Reference List

1. Brown, J. E.; Brown, S. B.; Vernon, D. I. *J. Soc. Dyers Colour.* **1999**, *115*, 249-253.

2. Cox, G. S.; Krieg, M.; Whitten, D. G. *J. Am. Chem. Soc.* **1982**, *104*, 6930-6937.

3. Cox, G. S.; Bobillier, C.; Whitten, D. G. *Photochem. Photobiol.* **1982**, *36*, 401-407.

4. Sharman, W. M.; Allen, C. M.; van Lier, J. E. *Drug Discovery Today* **1999**, *4*, 507-517.

5. Fuchs, J.; Thiele, J. *Free Radical Biology and Medicine* **1998**, *24*, 835-847.

6. Derosa, M. C.; Crutchley, R. J. *Coord. Chem. Rev.* **2002**, *233*, 351-371.

7. Nyman, E. S.; Hynninen, P. H. *J. Photochem. Photobiol. B* **2004**, *73*, 1-28.

8. Albota, M.; Beljonne, D.; Brédas, J. L.; Ehrlich, J. E.; Fu, J. Y.; Heikal, A. A.; Hess, S. E.; Kogej, T.; Levin, M. D.; Marder, S. R.; McCord-Maughon, D.; Perry, J. W.; Rockel, H.; Rumi, M.; Subramaniam, C.; Webb, W. W.; Wu, X. L.; Xu, C. *Science* **1998**, *281*, 1653-1656.

9. Rumi, M.; Ehrlich, J. E.; Heikal, A. A.; Perry, J. W.; Barlow, S.; Hu, Z. Y.; McCord-Maughon, D.; Parker, T. C.; Rockel, H.; Thayumanavan, S.; Marder, S. R.; Beljonne, D.; Brédas, J. L. *J. Am. Chem. Soc.* **2000**, *122*, 9500-9510.

10. Zojer, E.; Beljonne, D.; Kogej, T.; Vogel, H.; Marder, S. R.; Perry, J. W.; Brédas, J. L. *J. Chem. Phys.* **2002**, *116*, 3646-3658.

11. Feng, X. D.; Bischoff, I.; Senge, M. O. *J. Org. Chem.* **2001**, *66*, 8693-8700.

12. Senge, M. O.; Kalisch, W. W.; Bischoff, I. *Chem. Eur. J.* **2000**, *6*, 2721-2738.

13. Feng, X. D.; Senge, M. O. *J. Chem. Soc., Perkin Trans. 1* **2001**, 1030-1038.

14. Krattinger, B.; Callot, H. J. *Eur. J. Org. Chem.* **1999**, 1857-1867.

15. Setsune, J.; Yazawa, T.; Ogoshi, H.; Yoshida, Z. *J. Chem. Soc., Perkin Trans. 1* **1980**, 1641-1645.

16. Krattinger, B.; Callot, H. J. *Tetrahedron Lett.* **1998**, *39*, 1165-1168.

17. Krattinger, B.; Callot, H. J. *Tetrahedron Lett.* **1996**, *37*, 7699-7702.

18. Shea, K. M.; Jaquinod, L.; Smith, K. M. *J. Org. Chem.* **1998**, *63*, 7013-7021.

19. Jiang, X. Q.; Nurco, D. J.; Smith, K. M. *Chem. Commun.* **1996**, 1759-1760.

20. Rao, P. D.; Dhanalekshmi, S.; Littler, B. J.; Lindsey, J. S. *J. Org. Chem.* **2000**, *65*, 7323-7344.

21. Nicolaou, K. C.; Baran, P. S.; Zhong, Y. L. *J. Am. Chem. Soc.* **2001**, *123*, 3183-3185.

22. Wallace, D. M.; Leung, S. H.; Senge, M. O.; Smith, K. M. *J. Org. Chem.* **1993**, *58*, 7245-7257.

23. Cammidge, A. N.; Ozturk, O. *Tetrahedron Lett.* **2001**, *42*, 355-358.

24. Drobizhev, M.; Karotki, A.; Kruk, M.; Mamardashvili, N. Z.; Rebane, A. *Chem. Phys. Lett.* **2002**, *361*, 504-512.

CHAPTER 7

TRIPLET–STATE PROPERTIES FROM GAS PHASE EXPERIMENTS

Abstract: *Gas-phase experiments have been carried out on a series of ionic molecules with the potential use as singlet oxygen sensitizers. Triplet lifetimes and quantum yields were determined for these ions using a unique experimental setup. These experiements provide results that complement the results presented in the previous chapters for solution phase experiments and add a different perspective to the study of intrinsic photophysical properties pertinent to singlet oxygen generation. The triplet quantum yields measured are upper limits, but they help elucidate the lack of singlet oxygen generation of the ionic molecules in water.*

7.1 Introduction

The triplet quantum yield of a potential singlet oxygen sensitizer is an important property to know, as singlet oxygen generation typically occurs from the sensitizer triplet state.[1] However, triplet quantum yields can be difficult to measure accurately in a solution phase experiment.[2] Despite the fact that all the experiments described up to now have been done in the solution phase, a fundamental understanding of the intrinsic molecular properties for the isolated molecule (in the gase phase) would be helpful. This will add a different perspective to the development of singlet oxygen sensitizers. For some of the ionic water-soluble sensitizers discussed in chapter 4 that generate singlet oxygen in poor yield, it would be interesting to know the triplet quantum yield. This would then provide different insight into the features that influence the photosensitized production of singlet oxygen.

Recently, it has been demonstrated that triplet quantum yields and lifetimes can be determined from storage ring experiments.[3,4] In these experiments, an electrospray ion source is used for ionising the molecule and the ion chosen for experimental scrutiny is selected in a bending magnet and led into the storage ring. Thus the triplet properties are measured for a charged molecule. Fortunately, the ionic sensitizers of concern here already possess a charge meaning that the ion investigated in the gas-phase is the same molecular entity found in the solution phase.

7.2 Experimental setup

Two kinds of experiments were done for the gas-phase measurements. First a MIKE (Mass-analysed Ion Kinetic Energy) spectrum of the ions was obtained in order to identify the neutrals formed upon dissociation. Once this was established the compounds could be subjected to storage ring experiments.

7.2.1 MIKE-experiments

A detailed description of the experimental setup for the sector instrument used for the MIKE-experiments is given in Ref. 5 and 6. A schematic along with pictures of the instrument is shown in Figure 7-1. The samples were dissolved in a 1:1 CH_2Cl_2:MeOH mixture or a 1:20 AcCN: CH_3COOH mixture and electrosprayed. The ions were then accelerated to a translational kinetic energy of either 50 keV (single charged ions) or 100 keV (doubly charged ions).

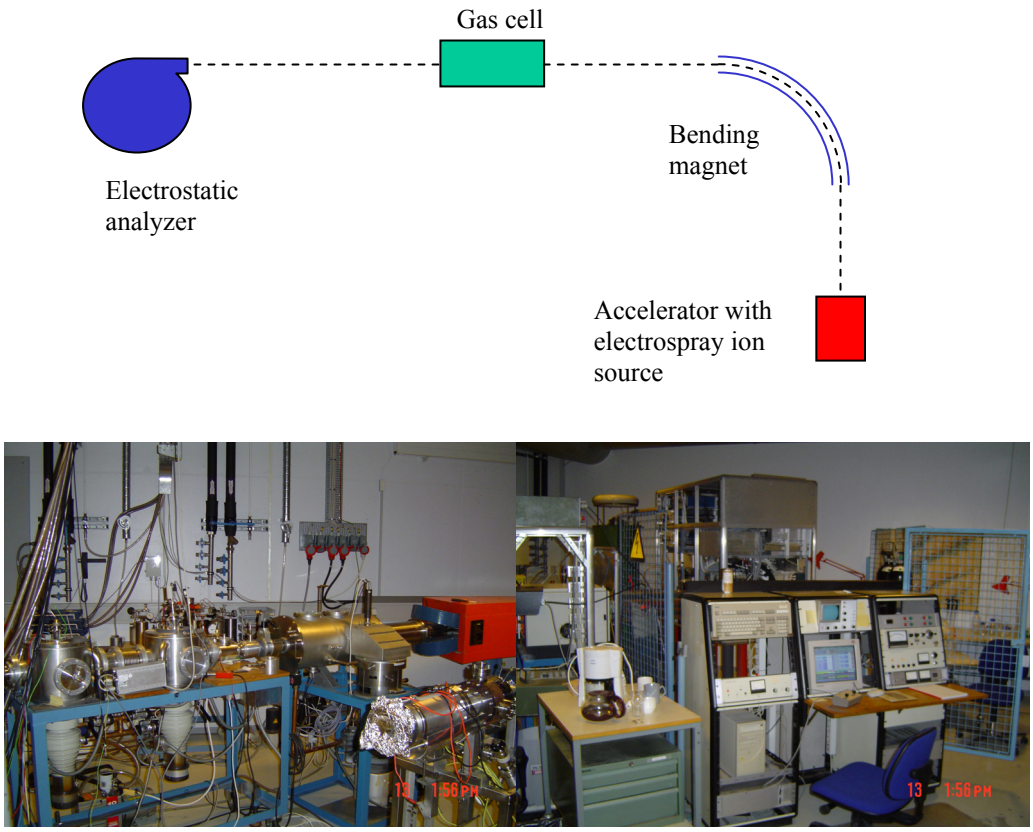

Figure 7-1: A schematic (top) and pictures of the accelerator instrument.

The ions were led into a gas cell where they where collisionally activated with He gas and the fragments formed upon dissociation of these excited ions were analysed with an electrostatic analyser that scanned the kinetic energy of the fragment ions.

7.2.2 Storage ring experiments

The triplet state properties were determined from experiments carried out with the electrostatic storage ring ELISA.[7-9] The samples were dissolved in a 1:1 CH_2Cl_2:MeOH mixture and electrosprayed. The ions were then accumulated in a 22-pole ion trap in which they were thermalized by collisions with He at room temperature. Ions were extracted from the trap after about 0.1 s and accelerated to either 22 keV (single charged ions) or 44 keV (doubly charged ions). The ions chosen for experiments were selected with a bending magnet, injected into ELISA and stored. An ion bunch contained about 10^4 ions. A schematic and pictures of the storage ring ELISA is shown in Figure 7-2.

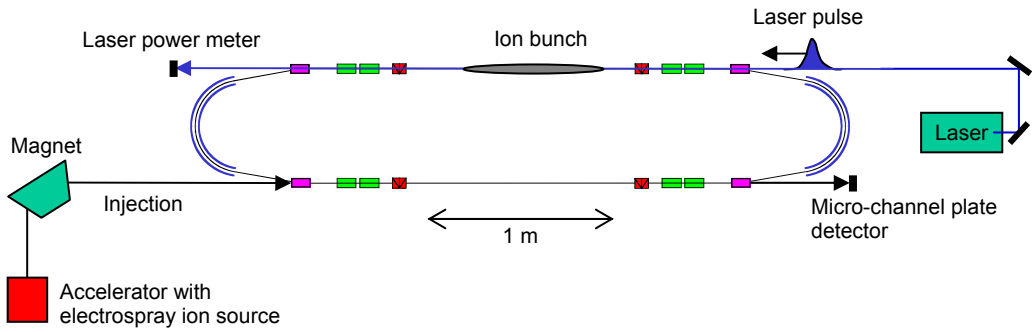

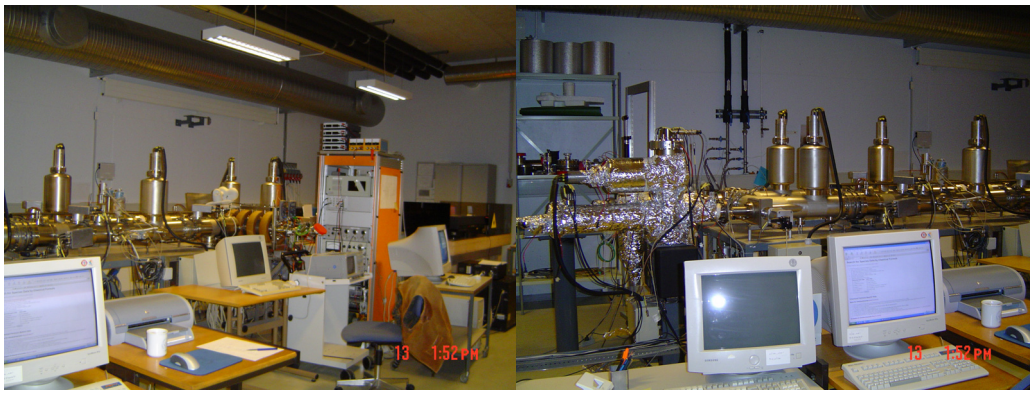

Figure 7-2: A schematic (top) and pictures of the ELISA storage ring.

Metastable decay and collisions with residual gas in the ring led to the production of neutral fragments. The details of fragmentation and detection are described elsewhere. Briefly, the neutrals were counted by a multichannel plate detector when they were formed in the middle of the ring on the side of the injection port (see Figure 7-2). The ions were irradiated with 390 nm laser light light at a 10 Hz repetition rate on the back side of the storage ring. After injection, initiation occurred after a time-delay of 60 ms to ensure that all metastable ions had decayed. The neutrals formed from the (delayed) dissociation of the photoexcited "hot" ions were detected with the multichannel plate detector. The fragments formed are detected after half a revolution time meaning that any rapid dissociation processes on the excited-singlet state potential energy surface cannot be identified. Radiative deexcitation, fluorescence or phosphorescence, lead to "cold" ions that do not dissociate and these processes are not detected either.

The ions examined in the current investigation are shown in Figure 7-3.

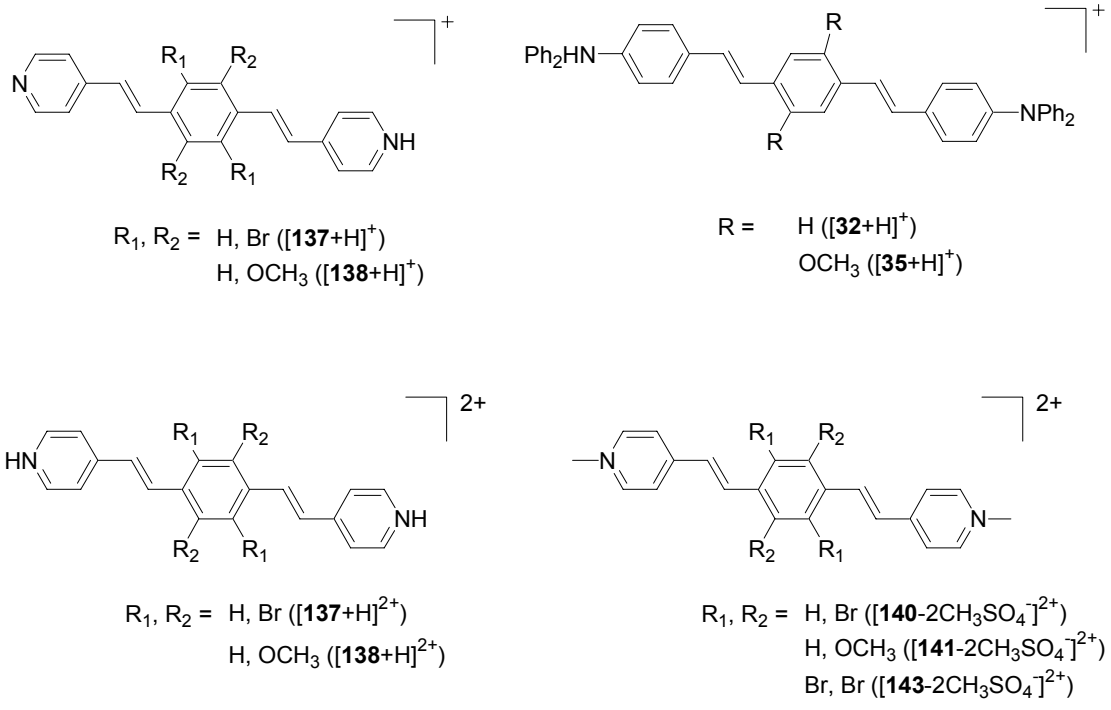

Figure 7-3: The structure of the ions investigated in the present work.

7.3 High-energy MIKE-spectra

The fragmentation spectra of the ions [**32**+H]$^+$ and [**35**+H]$^+$ are shown in Figure 7-4. In both spectra, loss of Ph occurs and Ph_2N is also lost from the ion [**32**+H]$^+$. In both

spectra, a narrow peak at half the mass-to-charge ratio is observed and these are assigned to the doubly charged ions formed upon collisional electron detachment.

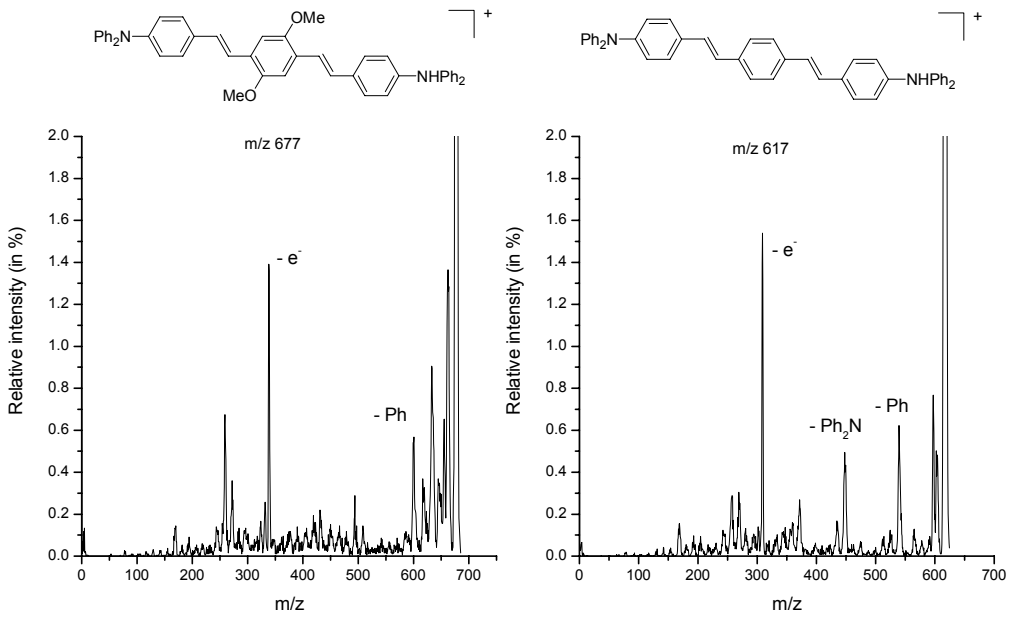

Figure 7-4: MIKE-spectra of the ions $[\mathbf{32}+H]^+$ and $[\mathbf{35}+H]^+$. The ions had a kinetic energy of 50 keV and the collision gas was He.

The high-energy MIKE-CID (CID: Collisional Induced Dissociation) spectra of the ions $[\mathbf{140}\text{-}2CH_3SO_4^-]^{2+}$ and $[\mathbf{143}\text{-}2CH_3SO_4^-]^{2+}$ are shown in Figure 7-5.

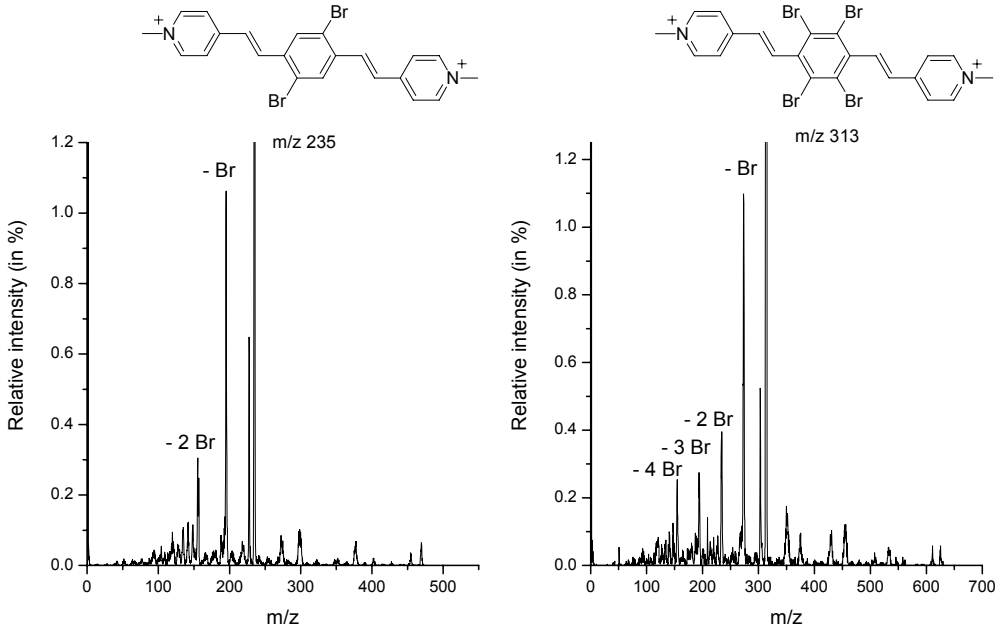

Figure 7-5: High-energy MIKE-CID spectra of the ions [**140**-$2CH_3SO_4^-$]$^{2+}$ and [**143**-$2CH_3SO_4^-$]$^{2+}$. The ions had a kinetic energy of 100 keV.

The principal dissociation channels for these ions is the loss of bromine atoms on the center ring and, in the case of [**143**-$2CH_3SO_4^-$]$^{2+}$, the sequential loss of all four bromine atoms could actually be observed. Similarly, for the high-energy MIKE-CID spectrum of the ion [**141**-$2CH_3SO_4^-$]$^{2+}$, a single methoxy substituent is lost from the molecular ion upon collisional activation. In the spectra of the ions [**140**-$2CH_3SO_4^-$]$^{2+}$, [**141**-$2CH_3SO_4^-$]$^{2+}$ and [**143**-$2CH_3SO_4^-$]$^{2+}$, no signal corresponding to electron detachement was identified. In the single and double charged ions, [**137**+2H]$^{2+}$, [**137**+H]$^+$, [**138**+2H]$^{2+}$ and [**138**+H]$^+$, it was only possible to identify a signal in the spectra of [**138**+H]$^+$ that could be assigned to electron detachment.

7.4 ELISA experiments

An example of a decay spectrum obtained from the storage ring experiments is shown in Figure 7-6 for the ion [**140**-$2CH_3SO_4^-$]$^{2+}$.

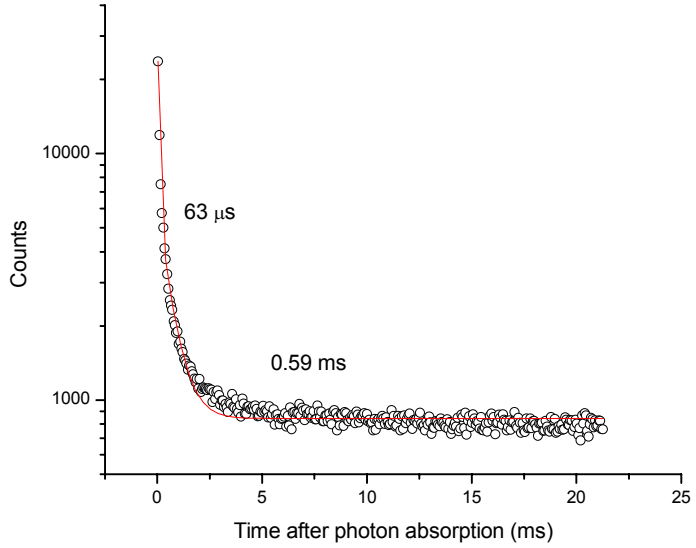

Figure 7-6: Time spectrum for the decay of [**140**-2$CH_3SO_4^-$]$^{2+}$ after 390 nm photon absorption using an energy of 1.01 mJ/pulse. A second order exponential decay is fitted to the experimental points.

In the present experiments, it is sufficient to represent the data with a biexponential fitting function. The deviation from the fit is likely due to the finite width of the internal energy distribution since an energy spread gives a spread in lifetime. Nevertheless, as described below and as outlined in published reports, all that is necessary is distinguish a fast from a slow decay component. The spacing between the points is the ion revolution time and in the case of [**140**-2$CH_3SO_4^-$]$^{2+}$ is 61.9 μs.

To interpret the biexponential decay observed, the Jablonsky diagram in Figure 7-7 is considered (in accordance with the model presented in Ref. 4,10 and 9). Initially, N ions are excited to singlet states S_1 and S_n through both one- and two-photon processes. It is then assumed that, after relaxation, aN ions populate the S_1 state and bN ions populate the T_1 state (thus a+b=1). Dissociation to produce detectable neutrals occurs from these two states. The first dissociation mechanism is internal conversion (assumed to occur fast) from the S_1 state to a vibrationally excited S_0 state that then dissociates with the rate constant k. In the second mechanism, rate-limiting intersystem crossing must first occur to populate the vibrationally excited S_0 state with the rate constant k_{TS}. Dissociation can then occur with a rate constant k.

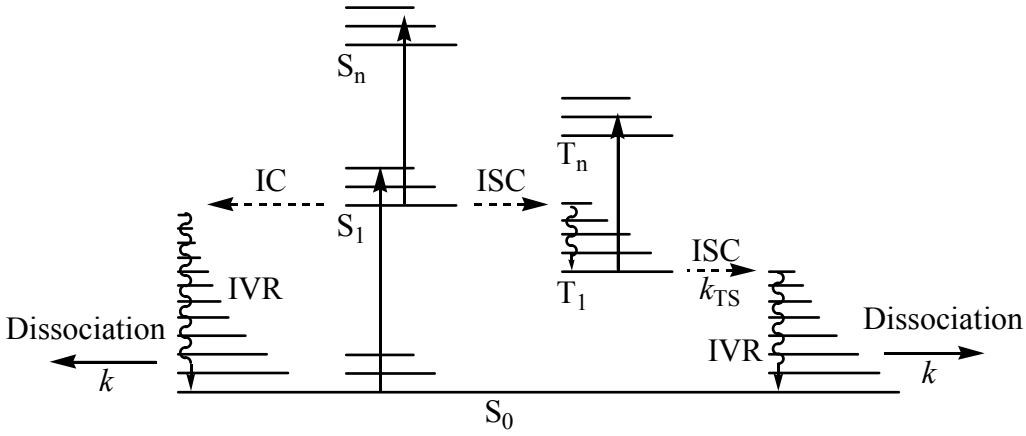

Figure 7-7: Jablonsky diagram illustrating the photophysical processes occurring during the ELISA experiments. IC: Internal conversion, IVR: Internal vibrational redistribution, ISC: Intersystem crossing.

The reaction channels for dissociation lead to the following differential equations,

(7.1) $$\frac{dn}{dt} = k \cdot n_{S_0^*}$$

(7.2) $$\frac{dn_{S_0^*}}{dt} = -k \cdot n_{S_0^*} + k_{TS} \cdot n_{T_1}$$

(7.3) $$\frac{dn_{T_1}}{dt} = -k_{TS} \cdot n_{T_1},$$

where n is the number of detected neutrals, $n_{S_0^*}$ is the number of ions populating the vibrational excited S_0 state (S_0^*) and n_{T_1} is the number of ions populating the T_1 state as a function of time (t). Since the internal conversion from the S_1 state to the vibrationally excited S_0 is assumed to occur almost instantaneously, the initial condition becomes $n_{T_1} = bN$ and $n_{S_0^*} = aN$ at t=0. This model of the processes occurring during the experiments leads to the expression for the number of neutrals detected as a function of time,

(7.4) $$n(t) = \left(aN - \frac{bNk_{TS}}{k - k_{TS}} \right) e^{-kt} + bN \frac{k}{k - k_{TS}} e^{-k_{TS}t} + c,$$

where c is a constant describing background counts from collision induced dissociation. The triplet quantum yield is then given as $b/(a+b)$ (or simply just b). The ratio, γ, of the pre-exponential factors in Eq. (7.4) then gives,

$$\gamma = \frac{bN\dfrac{k}{k-k_{TS}}}{\left(aN-\dfrac{bNk_{TS}}{k-k_{TS}}\right)+\dfrac{bNk}{k-k_{TS}}} = \frac{b}{a+b}\frac{k}{k-k_{TS}}. \tag{7.5}$$

From this ratio we obtain the triplet quantum yields as,

$$\Phi_T = \gamma\left(1-\frac{k_{TS}}{k}\right). \tag{7.6}$$

The short- and long-lived components in the decay spectra of the ion [**140**-$2CH_3SO_4^-$]$^{2+}$ both show a one-photon dependence on the laser-power. However, some of the compounds investigated have different photon dependencies for the short- and long-lived components and it is therefore necessary to extrapolate the γ-ratio to zero photon energy, as this value is then the one-photon limit. The γ-ratio follows the following expression as a function of the pulse energy,

$$\gamma = \frac{\gamma_0\left(1-\sigma_T E\right)}{1-\left(1-\gamma_0\right)^2\sigma_{S_0^*}E}, \tag{7.7}$$

where E is the pulse energy, γ_0 is the γ-ratio at zero pulse energy, σ_T is the absorption cross section of the triplet state and $\sigma_{S_0^*}$ is the absorption cross section of vibrationally excited ground state ions.

Having established the physics behind the observed decay spectra, accurate lifetimes were then determined by adding all the decay spectra recorded at different powers and fitting a biexponential decay to this sum-spectrum. The resulting sum-spectrum and corresponding fit is depicted in Figure 7-8.

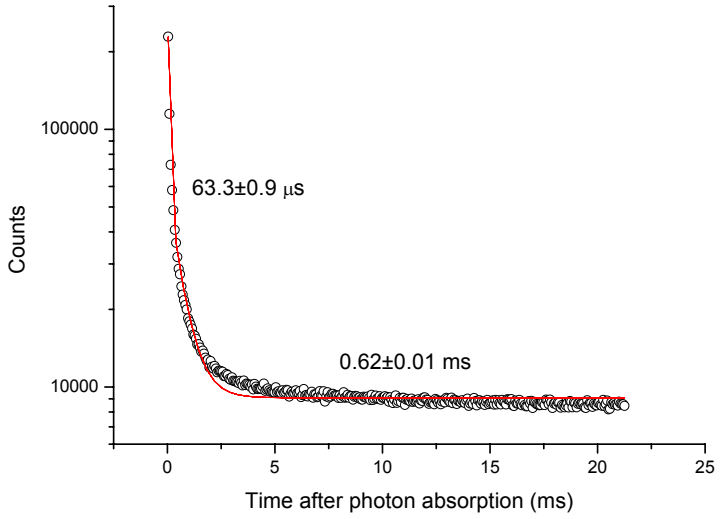

Figure 7-8: The sum-spectrum for the ion [**140**-2$CH_3SO_4^-$]$^{2+}$.

The lifetimes obtained by considering the sum of all the decay spectra are seen to deviate a bit from the lifetimes obtained from the fit to a single spectrum (see Figure 7-6 and Figure 7-8). The pre-exponential factors for the exponential components in each spectrum were determined by fitting a second order exponential decay with fixed lifetimes using the lifetimes determined from the sum-of-spectra.

Activation of the ion by the laser beam can occur in a multiphoton scheme and, in order to determine the number of photons absorbed in the process, the pre-exponential factors for the short- and long-lived component were plotted as a function of the laser power. An example of such a plot is given in Figure 7-9 for the pre-exponential factors obtained from the decay spectra of the ion [**140**-2$CH_3SO_4^-$]$^{2+}$.

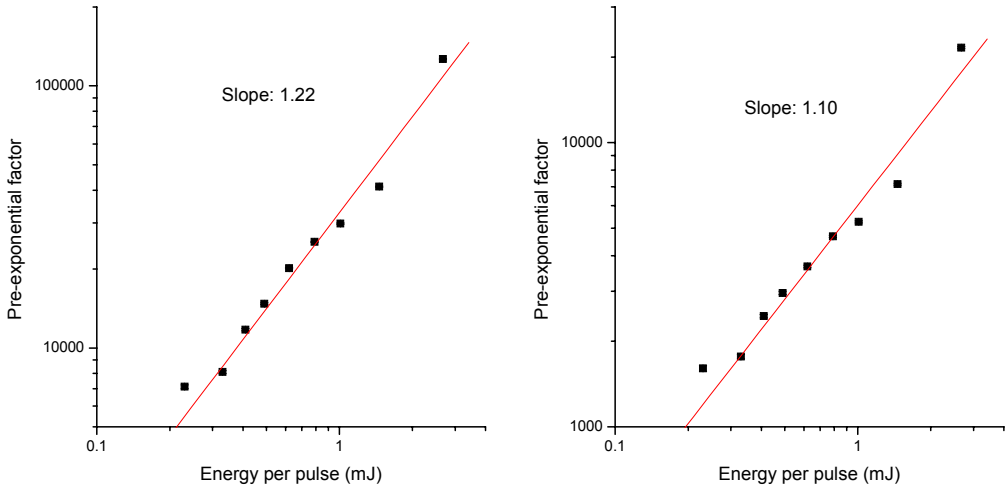

Figure 7-9: Double-logarithmic plots of the short- (left) and long-lived (right) component pre-exponential factors for the decay spectra of the [**140**-2$CH_3SO_4^-$]$^{2+}$ ion.

The data show some curvature and a slope of 1.22 for a straight line fitted to the experimental data for the short-lived component indicates that two-photon absorption processes also occur.

The γ-ratio at zero photon energy is then used for calculating the triplet quantum yield; At zero photon energy only one-photon absorption processes are considered. An example of a γ-ratio plot is given for the ion [**140**-2$CH_3SO_4^-$]$^{2+}$ in Figure 7-10.

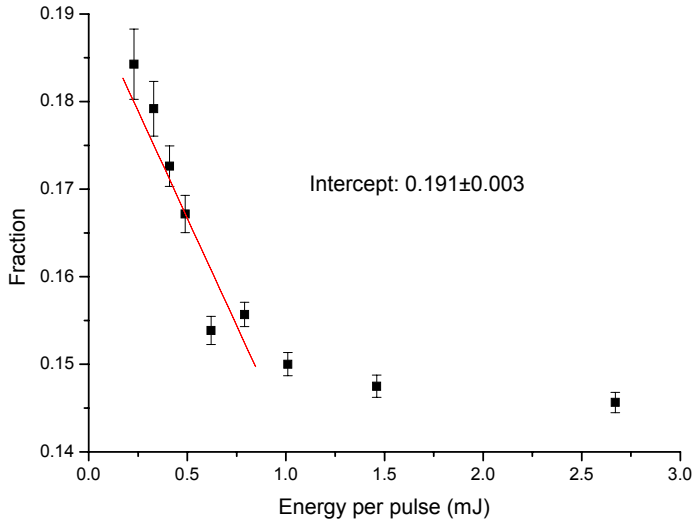

Figure 7-10: The γ-ratio for the decay spectra of [**140**-$2CH_3SO_4^-$]$^{2+}$.

From the γ-ratio of 0.191±0.003 determined in Figure 7-10 and from the lifetimes given in Figure 7-8 a triplet quantum yield of 0.171±0.003 is determined for the ion [**140**-$2CH_3SO_4^-$]$^{2+}$. The triplet quantum yield and lifetimes were determined for all the other ions studied using the same procedure as described above and the results are given in Table 7-1.

Table 7-1: Triplet quantum yields (Φ_T), triplet lifetimes (τ_T) and lifetimes of the dissociating excited S_0 state (τ).

Ion	τ/μs	τ_T/ms	Φ_T
[**140**-2$CH_3SO_4^-$]$^{2+}$	66.3±0.9	0.62±0.01	0.171±0.003
[**141**-2$CH_3SO_4^-$]$^{2+}$	39.0±0.6	0.69±0.02	0.143±0.003
[**143**-2$CH_3SO_4^-$]$^{2+}$	60.7±0.9	1.08±0.05	0.143±0.008
[**137**+2H]$^{2+}$	51.5±0.5	0.39±0.01	0.079±0.003
[**137**+H]$^{+}$	39.0±0.6	1.72±0.05	0.129±0.008
[**138**+2H]$^{2+}$	51.4±0.6	0.71±0.07	0.32±0.06
[**138**+H]$^{+}$	76.1±0.8	0.65±0.02	0.209±0.004
[**32**+H]$^{+}$	49.3±0.3	0.46±0.03	0.27±0.05

The triplet quantum yields determined are upper limits, which means that if processes such as fluorescence occur the actual triplet quantum yield will be less than the value reported in Table 7-1. In Chapter 4, the fluorescence quantum yield of [**141**-2$CH_3SO_4^-$]$^{2+}$ was determined to 0.15 in water and the fluorescence quantum yields of [**140**-2$CH_3SO_4^-$]$^{2+}$ and [**143**-2$CH_3SO_4^-$]$^{2+}$ are virtually zero in water. The triplet quantum yields then decreases in the series [**140**-2$CH_3SO_4^-$]$^{2+}$, [**143**-2$CH_3SO_4^-$]$^{2+}$ and [**141**-2$CH_3SO_4^-$]$^{2+}$, where [**140**-2$CH_3SO_4^-$]$^{2+}$ has the highest triplet quantum yield.

In terms of the heavy atom effect discussed in Chapter 1, it is expected that the triplet quantum yield of [**143**-2$CH_3SO_4^-$]$^{2+}$ should be higher than the value for [**140**-2$CH_3SO_4^-$]$^{2+}$ but this is not observed. The crystal structure of **143** suggests that the end-pyridine rings are almost completely perpendicular to the center benzene ring. A more planar structure is expected for **140** and **141** meaning that the difference in the triplet quantum yield of [**140**-2$CH_3SO_4^-$]$^{2+}$ and [**143**-2$CH_3SO_4^-$]$^{2+}$ not only reflects different substituents but also different geometries of the ions.

Non-bonding π-electrons can contribute to the triplet quantum yield according to El-Sayed's selection rules discussed in Chapter 1. An experimental evidence for this is seen in the triplet quantum yields of the ions [**137**+2H]$^{2+}$ and [**137**+H]$^{+}$, where the doubly charged ion has a lower triplet quantum yield (0.079) in comparison to the single charged ion (0.129). The same trend is not observed for the ions [**138**+2H]$^{2+}$

and [**138**+H]$^+$ but this is explained in terms of the fluorescence properties of **138**: A fluorescence quantum yield that increases in the series **138,** [**138**+H]$^+$ and [**138**+2H]$^{2+}$ could explain this discrepancy.

7.5 Conclusion

The triplet properties of a series of ions were measured using a unique technique. Some of the ions correspond to the cationic species used in the water experiments discussed in Chapter 4, where salts of pyridine-OPV's were investigated as potential singlet oxygen sensitizers. In the present chapter it is shown that the ions have fairly low triplet quantum yields in the gas phase. It is important to point out that the values measured in the present chapter are gas-phase values and cannot simply be projected onto the solution phase properties of the corresponding salts. However, the values determined for the investigated ions do point to the explanation that the lack of singlet oxygen generation for the corresponding salts in water might be due to a low triplet quantum yield.

Reference List

1. Schweitzer, C.; Schmidt, R. *Chem. Rev.* **2003**, *103*, 1685-1757.

2. Bensasson, R. V.; Land, E. J.; Truscott, T. G. *Flash photolysis and pulse radiolysis: Contributions to the chemistry of biology and medicine*; Pergamon: Oxford, 1983.

3. Nielsen, C. B.; Forster, J. S.; Ogilby, P. R.; Nielsen, S. B. *J. Phys. Chem. A* **2005**, *In press*.

4. Calvo, M. R.; Andersen, J. U.; Hvelplund, P.; Nielsen, S. B.; Pedersen, U. V.; Rangama, J.; Tomita, S.; Forster, J. S. *J. Chem. Phys.* **2004**, *120*, 5067-5072.

5. Boltalina, O. V.; Hvelplund, P.; Jørgensen,T. J. D.; Larsen, M. C.; Larsson, M. O.; Sharoitchenko, D. A. *Phys. Rev. A* **2000**, *6202*.

6. Larsson, M. O.; Hvelplund, P.; Larsen, M. C.; Shen, H.; Cederquist, H.; Schmidt, H. T. *Int. J. Mass. Spec.* **1998**, *177*, 51-62.

7. Nielsen, S. B.; Andersen, J. U.; Hvelplund, P.; Liu, B.; Tomita, S. *J. Phys. B: At., Mol., Opt. Phys.* **2004**, *37*, R25-R56.

8. Møller, S. P. *Nuclear Instruments & Methods in Physics Research Section A-Accelerators Spectrometers Detectors and Associated Equipment* **1997**, *394*, 281-286.

9. Andersen, J. U.; Andersen, L. H.; Hvelplund, P.; Lapierre, A.; Møller, S. P.; Nielsen, S. B.; Pedersen, U. V.; Tomita, S. *Hyperfine Interact.* **2003**, *146*, 283-291.

10. Andersen, J. U.; Hvelplund, P.; Nielsen, S. B.; Tomita, S.; Wahlgreen, H.; Møller, S. P.; Pedersen, U. V.; Forster, J. S.; Jørgensen, T. J. D. *Rev. Sci. Instrum.* **2002**, *73*, 1284-1287.

CHAPTER 8

THEORETICAL CONSIDERATIONS

Abstract: *Theoretical predictions of molecular non-linear optical properties are typically done by applying a truncated sum-over-states expression. A full sum-over-states is implicitly carried out by applying response theory, and recently such calculations have received attention and have been used as a predictive tool. In the present work calculations are carried out on water and small aromatic molecules in order to evaluate the accuracy of the ab initio response methods typically used for evaluating non-linear optical properties. The purpose of carrying out these calculations is also to evaluate the requirements necessary, in terms of level of theory and basis set requirements, for obtaining accurate two-photon absorption cross sections*

8.1 Introduction

One of the molecular properties pertinent to two-photon singlet oxygen sensitization using donor-acceptor type molecules is the TPA cross section. Several groups have demonstrated that TPA cross sections can be calculated for comperatively large molecules, and the results can be used to determine in a relative sense which molecules will have a largest TPA cross section.[1-6] Claims have even been made that absolute numbers can be obtained from such calculations.[3] Most of the methods used in these studies are low-level *ab initio* or semiemperical methods. The purpose of the present work is to validate the methods available for calculating TPA cross sections, which is done by calculating the cross sections for a series of small molecules (water and small aromatic molecules) using sophisticated *ab initio* methods.

8.2 The two-photon absorption cross section

The TPA cross section is given as,[7,8]

$$\delta = \frac{\pi^2 e^4}{c^2 \varepsilon_0^2 h^2} \omega^2 \left| \sum_i \frac{\left\langle \Psi_f \left| \vec{\mu} \right| \Psi_i \right\rangle \left\langle \Psi_i \left| \vec{\mu} \right| \Psi_g \right\rangle}{\omega_i - \omega} \right|^2 g(2\omega)$$

$$= \frac{\pi^2 e^4}{c^2 \varepsilon_0^2 h^2} \omega^2 g(2\omega) \left(\frac{1}{30} \sum_{a,b} \left(2S_{a,a} S_{b,b}^* + 4S_{a,b} S_{b,a}^* \right) \right) \quad (8.1)$$

$$= 4\pi^2 \alpha^2 g(2\omega) \omega^2 \left(\frac{1}{30} \sum_{a,b} \left(2S_{a,a} S_{b,b}^* + 4S_{a,b} S_{b,a}^* \right) \right)$$

where ω is the energy corresponding to the laser frequency, ω_i is the excitation energy from the ground state (*g*) to the *i*'th (intermediate) state, $g(2\omega)$ is the band shape function, $\vec{\mu}$ is the dipole operator, $\left\langle \Psi_f \left| \vec{\mu} \right| \Psi_i \right\rangle$ is the dipole matrix element between the final state (Ψ_f) and the intermediate state (Ψ_i), S_{ab} are the two-photon tensor elements (S_{ab}^* is the complex conjugate to S_{ab}), Ψ_i is the ground state, α is the fine structure constant, and *a* and *b* designate the x, y or z axes in the cartesian coordinate system. The S_{ab} tensor elements are defined as,[7,8]

$$S_{ab} = \sum_i \frac{\left\langle \Psi_g \left| \vec{\mu}_a \right| \Psi_i \right\rangle \left\langle \Psi_i \left| \vec{\mu}_b \right| \Psi_f \right\rangle}{\omega_i - \omega} + \frac{\left\langle \Psi_g \left| \vec{\mu}_b \right| \Psi_i \right\rangle \left\langle \Psi_i \left| \vec{\mu}_a \right| \Psi_f \right\rangle}{\omega_i - \omega}, \quad (8.2)$$

where $\vec{\mu}_a$ is the *a* component of the dipole operator $\vec{\mu}$.

A large number of theoretically determined TPA cross sections have been accumulated in the literature, and most of these are the results of *ab initio* calculations with modest basis sets or semiemperical calculations (see for example Ref. 9). To investigate the accuracy of calculated TPA cross sections, the TPA cross section for water has been calculated. In this case excitations to the first electronic state in each of the irreducible representations in the C_{2v} point group were performed using the highly correlated coupled-cluster methods and the correlation consistent basis sets of Dunning and co-workers.[10-12] The purpose of using the Dunning basis sets is that they are constructed to converge when the basis set is increased. In the series of basis sets with increasing size cc-pVDZ, cc-pVTZ, cc-pVQZ, cc-pV5Z and cc-pV6Z, a convergence profile should be obtained within the model used (*e.g.* a coupled-cluster method such as CCSD) for the molecular property calculated. A similar series of the basis sets listed above is designated aug-cc-pVXZ, which are expanded versions with diffuse basis functions added to improve the description of diffuse electronic states

(from hereon X denotes D, T, Q etc.). The basis set series d-aug-cc-pVXZ and t-aug-cc-pVXZ have even more diffuse functions. Calculations with the cc-pCVXZ and aug-cc-pCVXZ basis sets have also been performed. These basis sets have core valence functions, which are supposed to provide a more accurate description of the core electrons (such as the electrons in the 1s-orbitals) when calculations are carried out with correlated methods. The methods used for the calculations are the random phase approximation (RPA) and the coupled-cluster based methods (singles (CCS), singles with non-iterative doubles (CC2) and singles and doubles (CCSD)).[13] The results obtained using these methods are listed in the order of expected accuracy,[14-16] where the CCSD method is the most accurate (and includes the most dynamical electron correlation) and the RPA method is the least accurate (and includes no dynamical electron correlation). In all the calculations the water molecule was placed in the yz-plane and we used the geometry R_{OH}=0.95903 Å and $\angle_{HOH}$=104.654 . In previous TPA cross section calculations of water, He, Ne and Ar a gaussian band shape function has been used with a maximum of $2\pi t_0$.[17-19] This function is also applied for the calculations of the TPA cross sections of water in the present work.

8.3 Results

The $^1A_1$ state is taken as an example in illustrating the difficulties of obtaining converged cross sections. The cross-sections as a function of the basis sets used are plotted in Figure 8-1 for the RPA, CCS, CC2 and CCSD methods. The cross-sections calculated with the aug-cc-pVXZ basis sets seem to diverge when calculated with all the methods (see Figure 8-1) for the $^1A_1$ state. However, convergence seems to be obtained with the d-aug-cc-pVXZ basis set series.

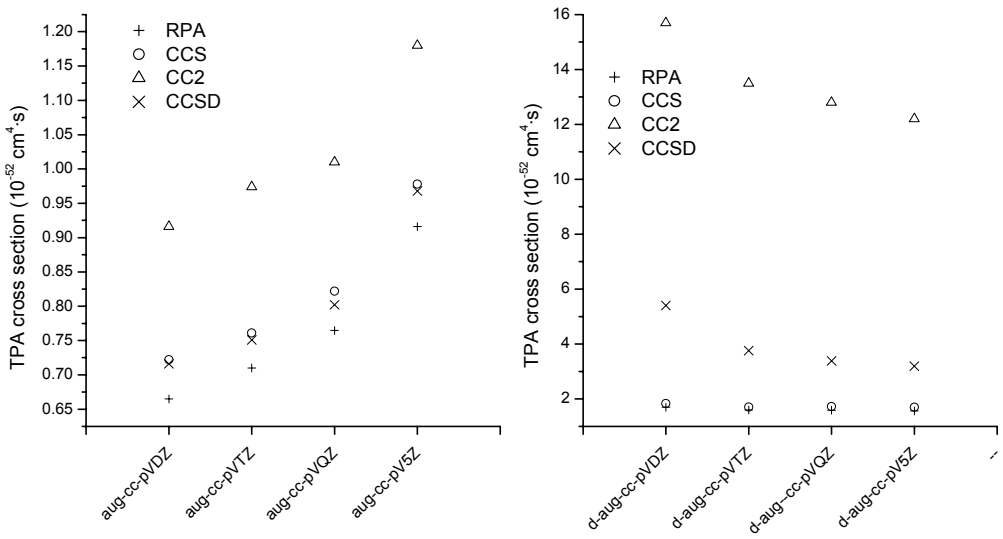

Figure 8-1: TPA cross sections for water calculated using the RPA and the coupled-cluster methods with the aug-cc-pVXZ basis set series (left) and with the d-aug-cc-pVXZ basis set series (right).

The cross sections calculated with the d-aug-cc-pV5Z basis set are expected to be the most accurate numbers and the results for the cross sections of the $^1A_1$, $^1B_1$, $^1B_2$ and $^1A_2$ states calculated with the RPA, CCS, CC2 and CCSD methods are presented in Table 8-1. These numbers are similar to the theoretically determined numbers presented in Ref. 17.

Table 8-1: Two-photon absorption maximum (nm) and cross sections (in 10^{-52} cm^4·s) calculated with the d-aug-cc-pV5Z basis set for water.

	$^1A_1$		$^1B_1$		$^1B_2$		$^1A_2$	
	λ	δ	λ	δ	λ	δ	λ	δ
RPA	228	1.56	287	0.15	200	0.05	240	1.81
CCS	228	1.70	285	0.18	200	0.04	240	1.96
CC2	261	12.2	338	0.33	236	0.00	276	3.60
CCSD	249	3.19	322	0.24	220	0.00	262	2.96

The two-photon action spectrum for water have been investigated experimentally by Nikogosyan and co-workers[20-22] where they measured the two-photon absorption

coefficients, β^{abs}, at different wavelengths. The two-photon absorption coefficient at a given wavelength is in general related to the cross sections through the relation,[23]

$$\delta = \frac{\hbar\nu\beta^{abs}}{N} = \frac{\hbar\nu\beta^{abs}M_w}{N_A\rho} \tag{8.3}$$

where N is the number density of the liquid studied, ν is the frequency of the laser light used, M_w is the molecular weight of the liquid studied, N_A is Avogrados number, and ρ is the density of the liquid studied. The number density of water is $3.343\cdot10^{28}$ m^{-3} at 298 K and the values reported for the two-photon absorption coefficients of water were $1.0\cdot10^{-12}$ mW^{-1} at 266 nm, $7\cdot10^{-13}$ mW^{-1} at 281 nm, $6\cdot10^{-13}$ mW^{-1} at 289 nm, $4.5\cdot10^{-13}$ mW^{-1} at 300 nm and $4\cdot10^{-13}$ mW^{-1} at 316 nm obtained by using a picosecond laser setup.[21] These numbers corresponds to cross sections of $3.6\cdot10^{-52}$ $cm^4\cdot s$ at 266 nm, $2.5\cdot10^{-52}$ $cm^4\cdot s$ at 281 nm, $2.1\cdot10^{-52}$ $cm^4\cdot s$ at 289 nm, $1.6\cdot10^{-52}$ $cm^4\cdot s$ at 300 nm and $1.4\cdot10^{-52}$ $cm^4\cdot s$ at 316 nm. Later on, an absorption coefficient of $1.9\cdot10^{-12}$ mW^{-1} at 282 nm was measured using a femtosecond laser system,[22] which corresponds to a cross section of $6.8\cdot10^{-52}$ $cm^4\cdot s$. Absorption coefficient values of $1.8\cdot10^{-11}$ mW^{-1} at 266 nm ($6.4\cdot10^{-51}$ $cm^4\cdot s$) and $2.3\cdot10^{-10}$ mW^{-1} at 264 nm ($8.2\cdot10^{-50}$ $cm^4\cdot s$) have also been reported.[20] These reported values deviate by 2 orders of magnitude from each other. An explanation for this spread in the experimentally determined cross sections is suggested in Ref. 20 and 21, where changes in the pulse durations are suggested to cause deviations in the measured absorption coefficients. The deviation in the experimental determined cross sections makes it difficult to assess the accuracy of the theoretical determined numbers. However, it is possible to compare trends in the available data. The measured absorption coefficients from Ref. 21 includes five wavelengths and are plotted in Figure 8-2 along with the experimentally determined one-photon absorption cross section from Ref. 24 and the calculated TPA cross sections (CCSD/d-aug-cc-pV5Z values). A correlation between the measured and the calculated cross sections is observed, as the experimental determined TPA cross sections increase with decreasing wavelength similar to the calculated TPA cross section. It is noteworthy that there appear to be a one-photon transition that is not two-photon allowed.

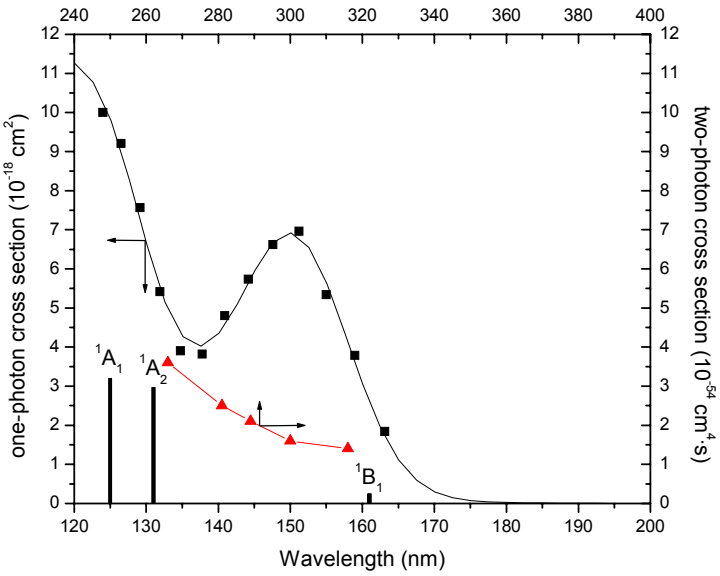

Figure 8-2: One-photon absorption cross sections of water (from Ref. 24, black) fitted with two gaussian functions and two-photon absorption cross sections (from the absorption coefficients in Ref. 21, red) as a function of wavelength. The calculated TPA cross sections (CCSD/d-aug-cc-pV5Z) are also shown

As it appears to be difficult to obtain accurate absolute TPA cross section by means of theoretical methods, it was investigated whether it is possible to obtain accurate relative values. To this end, a series the TPA cross sections for a series of small organic molecules were calculated.

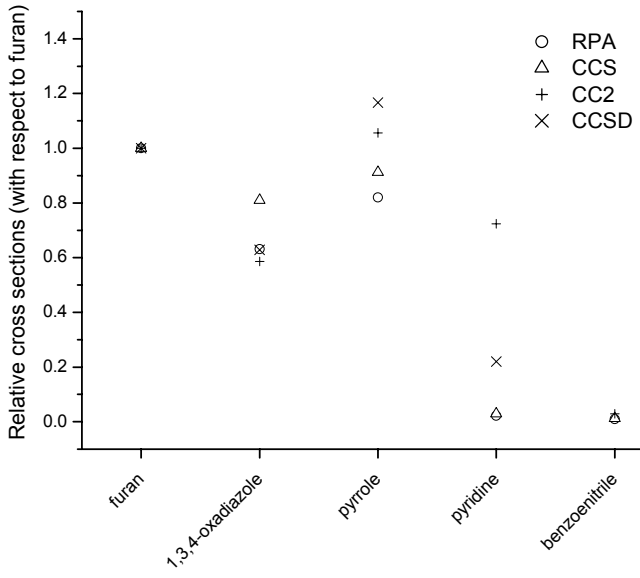

Figure 8-3: Relative TPA cross sections (with respect to furan) for a series of organic molecules. In all the calculations the aug-cc-pVDZ basis set and experimental geometries were used.

Calculated relative cross sections for two-photon excitation to the $^1A_1$ electronic state for a series of organic molecules with C_{2v} symmetry were obtained using the RPA, CCS, CC2 and CCSD methods with the aug-cc-pVDZ basis set and the relative values (with respect to furan) are plotted in Figure 8-3. Experimental geometries were used for all the molecules.[25-29] Within each method (*e.g.* RPA), the same ordering of the relative values for the series of molecules is observed as in the other methods but the same ratio for the relative values is not observed in between the methods.

8.4 Conclusion

The conclusions from the calculations done on liquid water, is that is very difficult to obtain trustworthy TPA cross sections as very large basis sets are needed. Some explanation for this finding can be found in the expression for the TPA cross section, which contains a summation over all intermediate states. The intermediate states can be considered as superposition of real states and this means that it is necessary to have an accurate description of all real states. High lying electronic states are typically very diffuse (*e.g.* Rydberg states) and accurate calculations on these states therefore requires the use of diffuse basis functions in accordance with the results above.

However, calculations using low-level methods like the RPA method can be used for qualitatively to decide whether a given sensitizer will have a better two-photon absorption cross section in comparison to another molecule, but the ratio between the cross section for the molecules is not a reliable number.

Reference List

1. Frederiksen, P. K.; McIlroy, S. P.; Nielsen, C. B.; Nikolajsen, L.; Skovsen, E.; Jørgensen, M.; Mikkelsen, K. V.; Ogilby, P. R. *J. Am. Chem. Soc.* **2005**, *127*, 255-269.

2. McIlroy, S. P.; Cló, E.; Nikolajsen, L.; Frederiksen, P. K.; Nielsen, C. B.; Mikkelsen, K. V.; Gothelf, K. V.; Ogilby, P. R. *J. Org. Chem.* **2005**, *70*, 1134-1146.

3. Poulsen, T. D.; Frederiksen, P. K.; Jørgensen, M.; Mikkelsen, K. V.; Ogilby, P. R. *J. Phys. Chem. A* **2001**, *105*, 11488-11495.

4. Rumi, M.; Ehrlich, J. E.; Heikal, A. A.; Perry, J. W.; Barlow, S.; Hu, Z. Y.; McCord-Maughon, D.; Parker, T. C.; Rockel, H.; Thayumanavan, S.; Marder, S. R.; Beljonne, D.; Brédas, J. L. *J. Am. Chem. Soc.* **2000**, *122*, 9500-9510.

5. Zojer, E.; Beljonne, D.; Kogej, T.; Vogel, H.; Marder, S. R.; Perry, J. W.; Brédas, J. L. *J. Chem. Phys.* **2002**, *116*, 3646-3658.

6. Cronstrand, P.; Luo, Y.; Ågren, H. *J. Chem. Phys.* **2002**, *117*, 11102-11106.

7. McClain, W. M. *Acc. Chem. Res.* **1974**, *7*, 129-135.

8. McClain, W. M. *J. Chem. Phys.* **1971**, *55*, 2789-2796.

9. Pond, S. J. K.; Rumi, M.; Levin, M. D.; Parker, T. C.; Beljonne, D.; Day, M. W.; Brédas, J. L.; Marder, S. R.; Perry, J. W. *J. Phys. Chem. A* **2002**, *106*, 11470-11480.

10. Dunning, T. H. *J. Chem. Phys.* **1989**, *90*, 1007-1023.

11. Kendall, R. A.; Dunning, T. H.; Harrison, R. J. *J. Chem. Phys.* **1992**, *96*, 6796-6806.

12. Woon, D. E.; Dunning, T. H. *J. Chem. Phys.* **1993**, *98*, 1358-1371.

13. Christiansen, O.; Jørgensen, P.; Hättig, C. *Int. J. Quantum Chem.* **1998**, *68*, 1-52.

14. Christiansen, O.; Koch, H.; Jørgensen, P. *J. Chem. Phys.* **1995**, *103*, 7429-7441.

15. Christiansen, O.; Koch, H.; Jørgensen, P. *Chem. Phys. Lett.* **1995**, *243*, 409-418.

16. Koch, H.; Christiansen, O.; Jørgensen, P.; Olsen, J. *Chem. Phys. Lett.* **1995**, *244*, 75-82.

17. Thomsen, C. L.; Madsen, D.; Keiding, S. R.; Thøgersen, J.; Christiansen, O. *J. Chem. Phys.* **1999**, *110*, 3453-3462.

18. Hättig, C.; Christiansen, O.; Jørgensen, P. *J. Chem. Phys.* **1998**, *108*, 8355-8359.

19. Sundholm, D.; Rizzo, A.; Jørgensen, P. *J. Chem. Phys.* **1994**, *101*, 4931-4935.

20. Dragomir, A.; McInerney, J. G.; Nikogosyan, D. N.; Ruth, A. A. *IEEE J. Quantum Electron.* **2002**, *38*, 31-36.

21. Nikogosyan, D. N.; Oraevsky, A. A.; Rupasov, V. I. *Chem. Phys.* **1983**, *77*, 131-143.

22. Reuther, A.; Laubereau, A.; Nikogosyan, D. N. *J. Phys. Chem.* **1996**, *100*, 16794-16800.

23. Sutherland, R. *Handbook of nonlinear optics*; Marcel Dekker, Inc.: New York, 1996.

24. Heller, J. M.; Hamm, R. N.; Birkhoff, R. D.; Painter, L. R. *J. Chem. Phys.* **1974**, *60*, 3483-3486.

25. Mata, F.; Martin, M. C.; Sørensen, G. O. *J. Mol. Struct.* **1978**, *48*, 157-163.

26. Sørensen, G. O.; Mahler, L.; Rastrupa, N. *J. Mol. Struct.* **1974**, *20*, 119-126.

27. Nygaard, L.; Nielsen, J. T.; Sørensen, G. O.; Steiner, P. A.; Rastrupa, J.; Hansen, R. L. *J. Mol. Struct.* **1972**, *12*, 59-69.

28. Casado, J.; Nygaard, L.; Sørensen, G. O. *J. Mol. Struct.* **1971**, *8*, 211-224.

29. Nygaard, L.; Nielsen, J. T.; Kirchhei, J.; Maltesen, G.; Rastrupa, J.; Sørensen, G. O. *J. Mol. Struct.* **1969**, *3*, 491-506.

APPENDIX A

PYRENE FUNCTIONALIZED GOLD NANO PARTICLES

Abstract: *Electronic interactions between a metal surface and an organic molecule are expected to cause a significant change in the non-linear optical properties of the organic molecule. For this reason, colloid particles of gold with pyrene moieties attached to the gold surface were made. These nano particles have been characterized by several experimental techniques such as NMR and UV-VIS, and their properties are discussed with respect to potential applications in non-linear optics.*

A.1 Introduction

Functionalized nano particles have interesting optical properties resulting from the interaction between the metal colloid particle and the attached chromophore.[1] The goal persued in the present work is to make molecules or assemblies of molecules with high TPA cross sections and high singlet oxygen quantum yields. Reports have been given[2-8] where large non-linear optical properties have been described for functionalized nano particles due to an enhancement of the non-linear properties caused by the surface plasmon on the nano particle, and one goal of the present work has been to investigate whether a high TPA cross section and a high singlet oxygen quantum yield can be obtained by functionalizing nano particles with singlet oxygen sensitizers.

A.2 Surface plasmons

UV-VIS spectroscopy of Au colloid particles reveals a broad absorption band around 500 nm, which is ascribed to a surface plasmon absorption band.[9,10] A plasmon is a charge density wave and can be understood in terms of a simple model; The electron density is oscillating or changing position on the surface of the colloid particle thereby creating an electric field. An oscillating charge density can be brought to oscillate with a higher frequency and, since this occurs at an atomic level, the charge density oscillations can be considered to be a quantized oscillation with discrete energy levels.[11] Thus the absorption band in the UV-VIS spectrum corresponds to exciting the “charge density oscillator”.

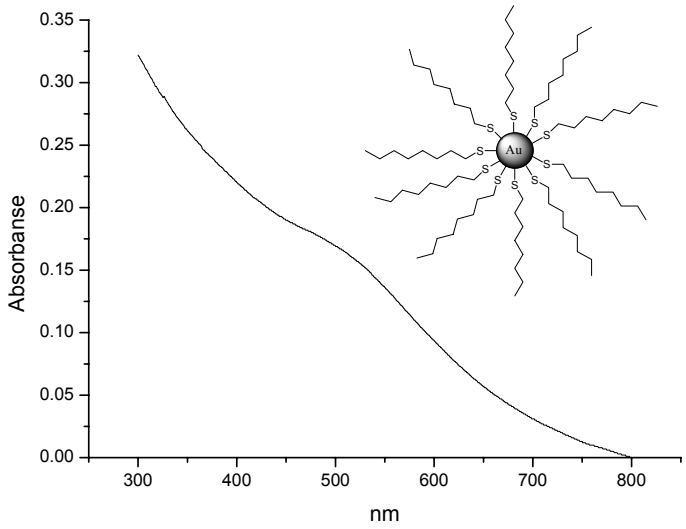

Figure A-1: Absorption spectrum of octylthio-stabilized Au nano-particles. The absorbance was set to zero at 800 nm.

The UV-VIS spectrum depicted in Figure A-1 shows that the absorbance is increasing with decreasing wavelength which is due to Reileigh scattering of the colloid partices; Spherical colloid particles have diameters ranging from 1-50 nm (Au nano particles are typically spherical whereas Ag nano particles are ellipsoidal).[1,12] A surface plasmon is observed in Figure A-1 at ~510 nm.

In surface enhanced Raman scattering, the molecule subjected to experimental study is placed on a metal substrate. Laser light focused on the substrate then generates a surface plasmon, which creates large local fields resulting in amplifications of the Raman scattering. It is believed that such large local fields can generate enhanced nonlinear optical responses and experimental evidence for this claim has been provided for aromatic molecules deposited on Ag surfaces.[2-8] It has also been suggested that the geometry of the surfaces plays an important role; Periodic lattices can support travelling plasmon waves over comparatively large distances, whereas in ellipsoidal particles, for example, the surface plasmon is forced to move in a confined region of space, determined by the geometry of the particle, thus creating large local fields.[13,14] The local fields on ellipsoidal surfaces should also be larger than on spherical surfaces. In particular, the TPA cross section measured by fluorescence of

the two-photon excited chromophore has been shown to increase by several orders of magnitude when the chromophore is anchored to an Ag fractal surface.[13] Organic chromophores attached with an alkyl spacer to a colloidal metal particle can be considered as an adsorbate on a metal surface. Both theoretical and experimental studies suggests that the S_1-state of the chromophore is quenched through space by the metal core.[14,15] If the chromophore is strongly interacting with the metal core, transfer of charge from the chromophore to the metal can occur.[14,15] The observed enhancement of non-linear optical properties measured using fluorescence techniques[13,16] indicates that local field effects can enhance the TPA cross section to a greater extent than the metal core can quench the S_1-state.

In the present work, the TPA cross section is determined by measuring the intensity of singlet oxygen phosphorescence, as discussed previously, and therefore a singlet oxygen sensitizer is needed as the chromophore. Pyrene was chosen for three reasons: Pyrene has a singlet oxygen quantum yield of 0.71 in benzene and the preperation of pyrene functionalised Au nano particles is described in the literature.[17] Furthermore, pyrene fluoresces so that singlet oxygen experiments can be complemented with fluorescence experiments. Boal and Rotello[17] have prepared the colloid particles depicted in Figure A-2 for use in guest-host chemistry and the synthetic route was adopted from their work to prepare pyrene functionalised Au nano particles, where the pyrene is attached to the colloid particle with alkyl chains of varying length.

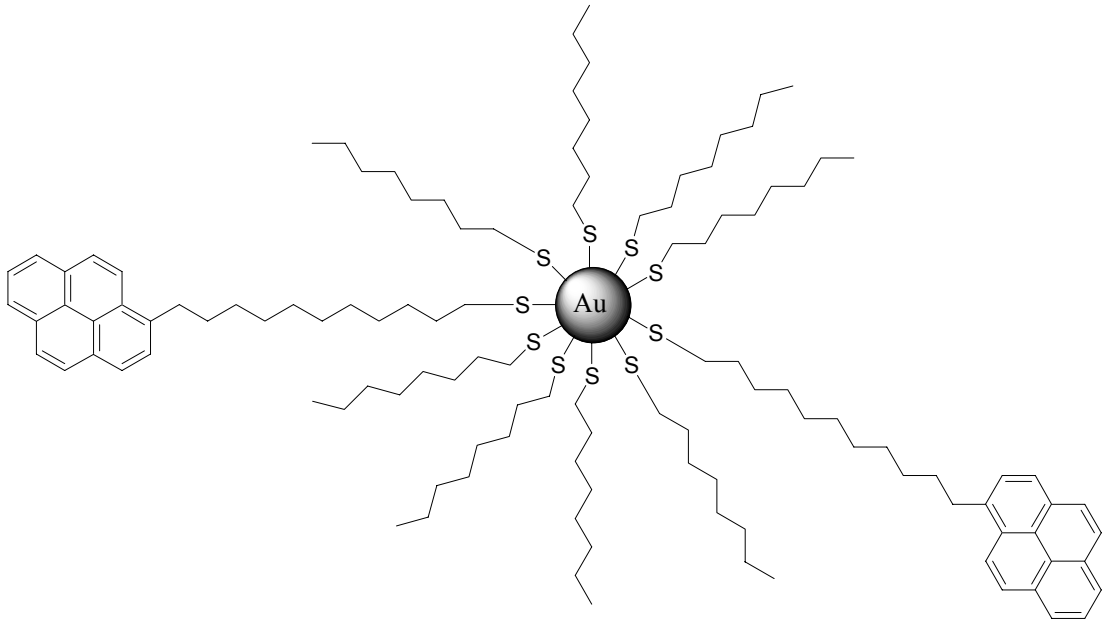

Figure A-2: Pyrene and diacyldiaminopyridine functionalized nano particles prepared by Boal and Rotello.

A.3 Preperation of pyrene functionalized nano particles

The synthetic route followed for preparing the nano particles is depicted in Scheme A-1.

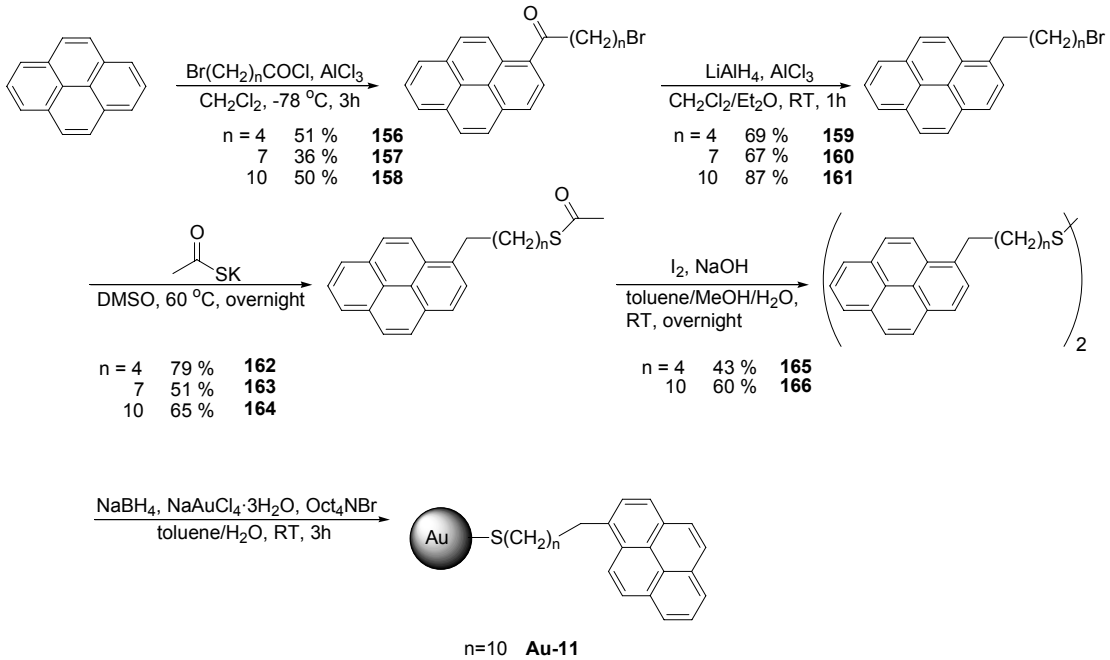

Scheme A-1: The preperation of colloid Au particles functionalized with pyrene. The Au particle and the pyrene moiety are separated with an alkyl chain with various lengths.

Pyrene was reacted with a bromine end-functionalized aliphatic acid chloride in a Friedel-Crafts reaction run at –78 °C in methylene chloride. In this reaction, the 1-position on pyrene is specifically acylated. The keto-functionality is then removed in an alene reduction using aluminium lithium hydride and aluminium trichloride in methylene chloride run at room temperature. The bromine atoms were then substituted with potassium thiourea in a S_N2 reaction run in DMSO and the disulfide was made by oxidizing the thiourea derivatives with iodide. Boal and Rotello did not specify an oxidizing agent in this reaction, and it was not possible to reproduce their results using their reported procedure for the preparation of **166** from **164**. The colloid particles were made by reducing the appropriate disulfide with sodium borohydride in the prescence of Au^{III} in a water-toluene two-phase solvent system and tetraoctylammonium bromide as the phase transfer catalyst. The number of chromophores bonded to the particles was estimated by elemental analysis.

A.4 Physical properties of the nano particles

A H-NMR spectrum the prepared colloid particles is shown in Figure A-3. Broad bands due to high rotational time for the colloids are seen both in the aromatic and the aliphatic regions of the spectrum making it impossible to deduce any structural information. The ^{13}C-NMR spectra show similar behaviour.

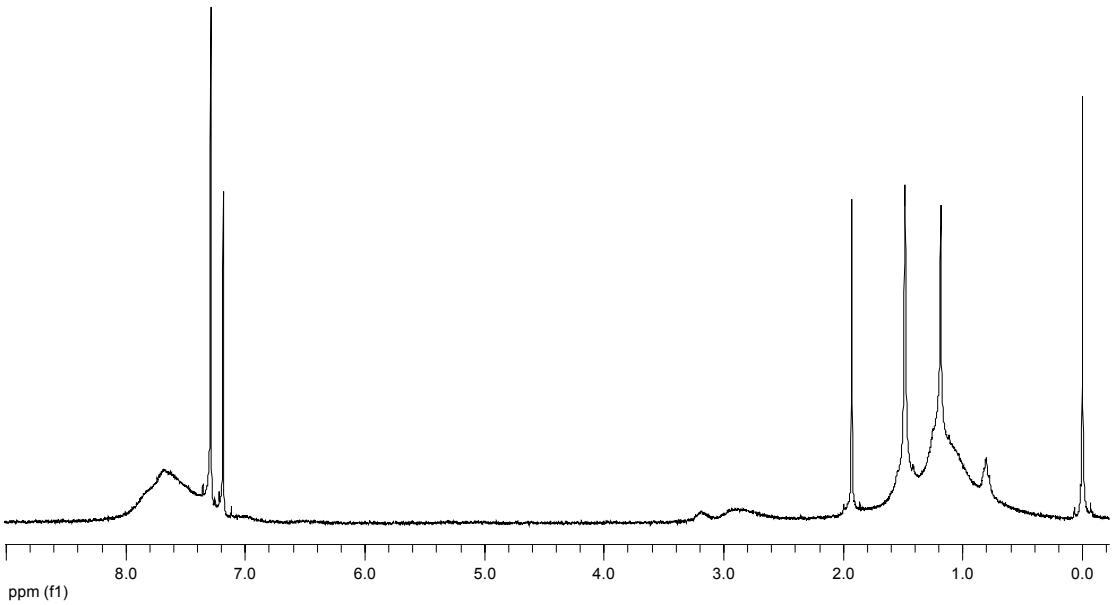

Figure A-3: ^{1}H-NMR spectrum of crude Au-pyrene colloid particles. Residual peaks from $CHBrCl_2$ and CH_3CN are present in the spectrum at 7.19 and 1.95 ppm, respectively.

An important physical property of the colloid particles is their shape and size distribution. Au colloid particles are described in the literature to be spherical.[1] The particles prepared in the present work was characterized by TEM-microscopy and SAXS measurements in order to determine the colloid's shape and size. Indeed, the particles were found to be spherical by TEM-microscopy (see Figure A-4) and the TEM-images suggest diameters of these spherical particles of approximately 2 nm.

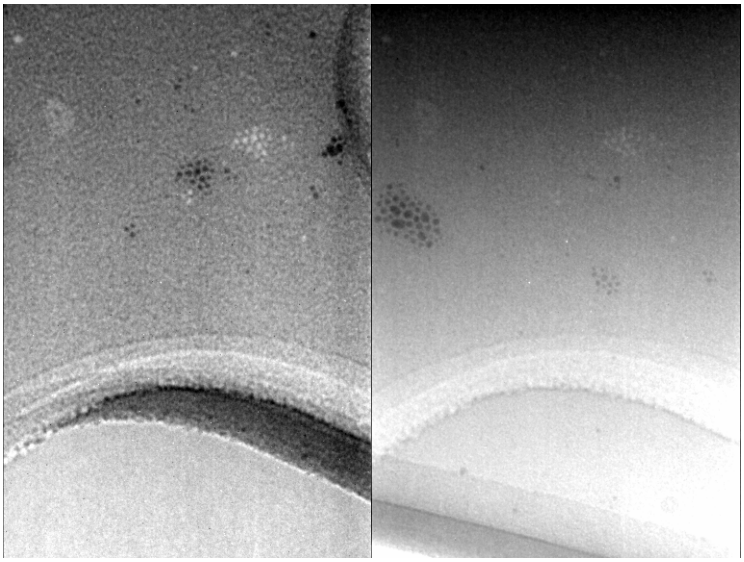

Figure A-4: TEM pictures of the **Au-11** colloid particles. The scale of each picture is 319 nm x 213 nm.

High-resolution TEM pictures were also taken of the particles, and an example is shown in Figure A-5. From this picture, the layered structure of the Au atoms in each Au nano particle is clearly seen. It was not possible to determine the crystal lattice observed in each particle so an accurate length-scale could not be determined for this picture.

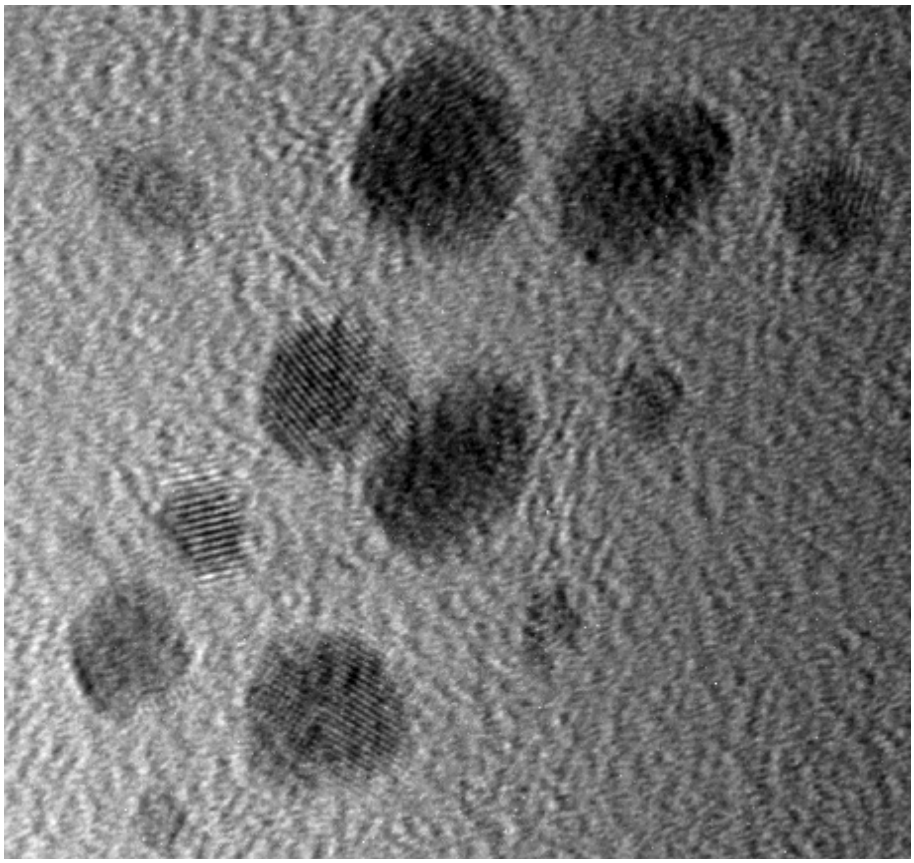

Figure A-5: High-resolution TEM image of the colloid particles. The layered structure of the Au atoms is clearly seen.

SAXS data were also recorded for the **Au-11** colloid particles dissolved in toluene, and by fitting a spherical size distribution to these data a volume size distribution (shown in Figure A-6) was obtained.

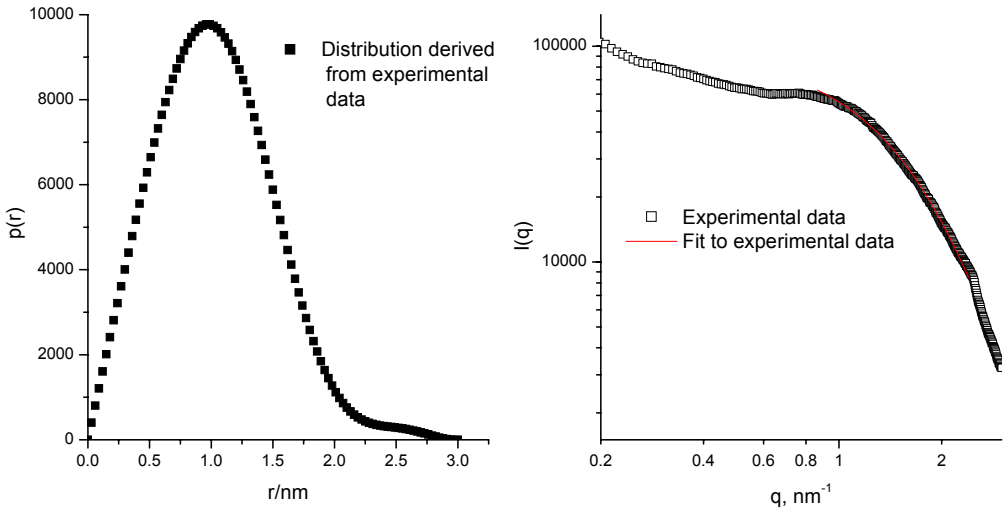

Figure A-6: Volume size distrubtion as a function of the sphere radius of the colloid particles in toluene (left) and the integrated intensity from the SAXS measurements (right).

From these measurements, a mean average diameter of the particles was determined to approximately 2 nm. Diameters of colloidal particles of 1-50 nm, and even larger, have been reported in the literature,[1] and also procedures for controlling the size distribution has been given.[1,18] Further characterization of the colloid particles was done by XPS measurements, and the resulting spectra are shown in Figure A-7. The characteristic peaks corresponding to the ejection of the $4f_{7/2}$, $4f_{5/2}$, $4d_{5/2}$ and the $4d_{3/2}$ electrons in Au are observed at binding energies identical to reported literature values for pure (chemical non-modified) Au.[19]

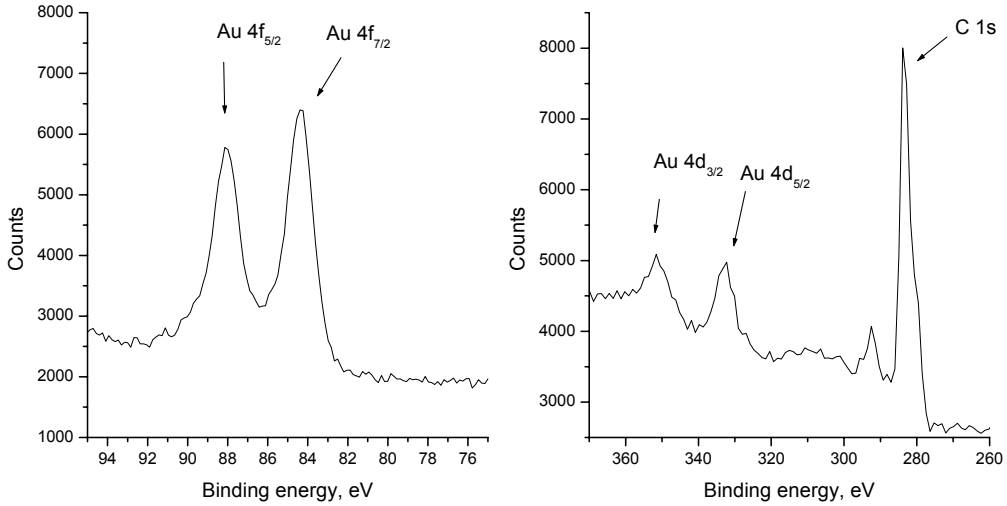

Figure A-7: XPS spectra of the **Au-11** colloid particles.

The UV-VIS and fluorescence spectra of **Au-11** are depicted in Figure A-8 along with a UV-VIS spectrum of pyrene.

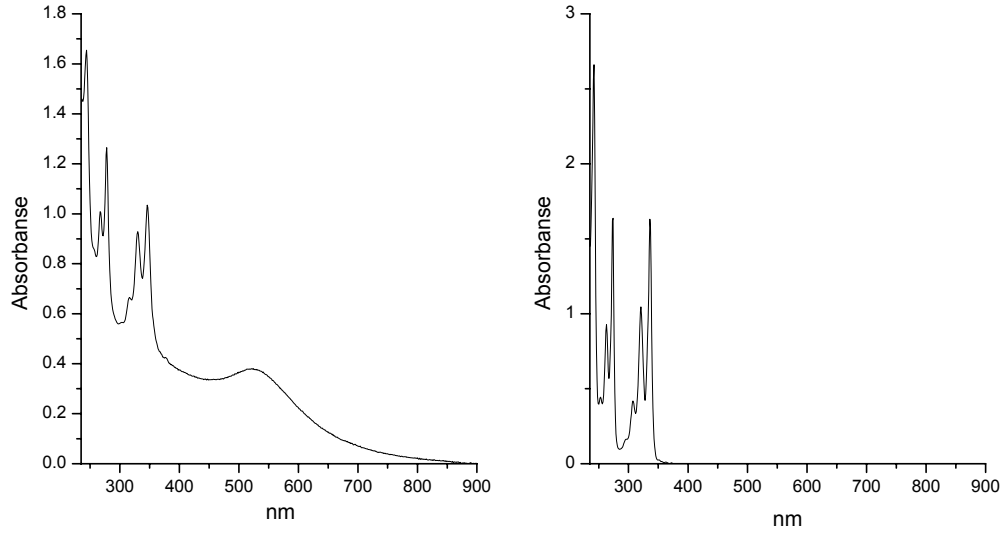

Figure A-8: UV-VIS spectra of **Au-11** (left) and pyrene (right) in methylene chloride.

The surface plasmon in the UV-VIS spectrum of **Au-11** is observed at 531 nm. Absorption bands originating from pyrene itself occur at almost the same wavelengths as the absorption bands of non-Au-bonded pyrene.

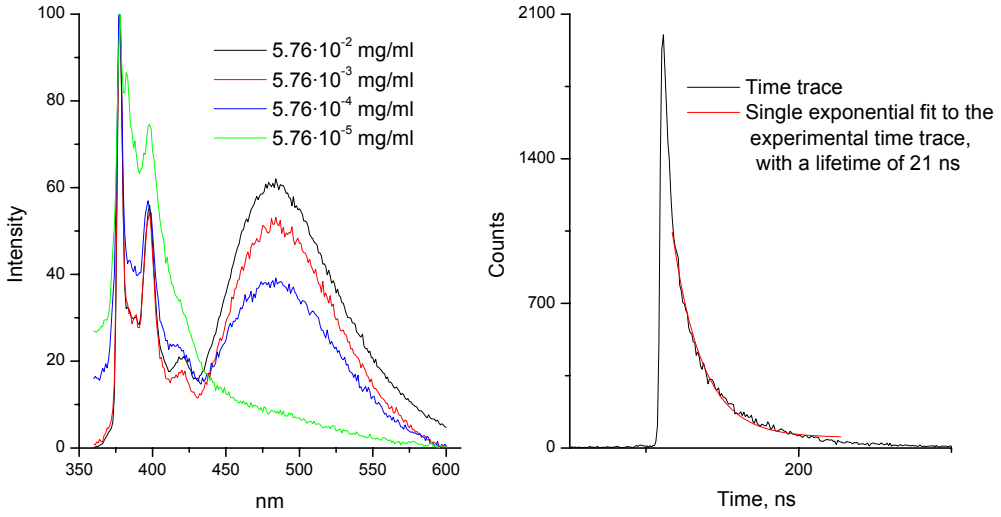

Figure A-9: Steady state fluorescence spectra and decay of **Au-11** in methylene chloride. The excitation wavelength was 355 nm and the decay spectrum was recorded by monitoring fluorescence at 380 nm. The samples were air saturated.

Fluorescence from the Au particles, apart from the fluorescence from pyrene itself, was not observed. In the fluorescence spectra of **Au-11** fluorescence from the pyrene excimer at 484 nm was observed and the intensity of this band could be intensified or reduced by either concentrating or diluting the sample. A lifetime of 21 ns was found for pyrene functionalized Au particles in air saturated methylene chloride. Similar values have been reported in the literature for the fluorescence lifetime of pyrene in air saturated solutions without any other chemical species.[20] Emmision maxima occuring at 378 and 398 nm for **Au-11** were observed, and "pure" pyrene emits at 374 and 395 nm and has the same emision profile as the **Au-11** particles. This finding indicates that no interaction is occurring between the Au-particle core and the attached pyrene moiety.

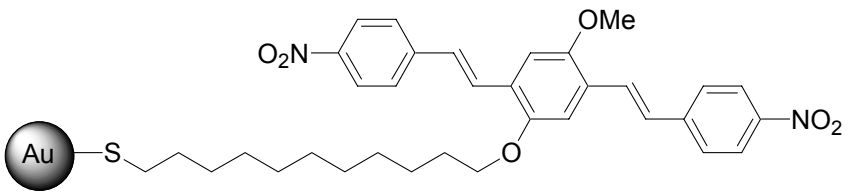

Figure A-10: Colloid particles prepared by Stellacci and coworkers for studying the effect of surface plasmons on the TPA cross sections.

Experiments were done in order to detect singlet oxygen generated from two-photon excited **Au-11** colloid particles using the nano-second laser setup described in Ref. 21 and 22, but it was not possible to detect phosphorescence from singlet oxygen due to interference from scattered light. Stellacci and coworkers[23] recently prepared the colloid particles depicted in Figure A-10 and measured the TPA cross section of these particles by monitoring fluorescence from the attached chromophore. They also concluded that no electronic interaction occurs between the chromophore and the metal core as the TPA cross section of the colloid particles was determined to be the number of chromophores attached to the particle times the TPA cross section of a single chromophore.

A.5 Conclusion

The results presented above support what is already reported in the literature that the TPA cross section can not be enhanced by a nearby Au surface plasmon. Pyrene functionalized Ag particles were not made due to the experience with the Au particles. In order to detect singlet oxygen phosphorescence a 1270 nm bandpass filter is placed in front of the detector and too much scattered light in the room causes a high background signal making it difficult to detect the weak phosphorescence signal from singlet oxygen. Stability is also an issue inasmuch as the Au-S bond is not stable and the attached chromophores will eventually come off the metal core. Preparing functionalized nano particles is thus not the choice for making a sensitizer with a high TPA cross section and a high singlet oxygen quantum yield.

Reference List

1. Daniel, M. C.; Astruc, D. *Chem. Rev.* **2004**, *104*, 293-346.

2. Kamat, P. V. *J. Phys. Chem. B* **2002**, *106*, 7729-7744.

3. Wokaun, A.; Bergman, J. G.; Glass, A. M.; Heritage, J. P.; Liao, P. F. *IEEE J. Quantum Electron.* **1981**, *17*, 104.

4. Glass, A. M.; Wokaun, A.; Heritage, J. P.; Bergman, J. G.; Liao, P. F.; Olson, D. H. *Phys. Rev. B* **1981**, *24*, 4906-4909.

5. Bergman, J. G.; Chemla, D. S.; Liao, P. F.; Glass, A. M.; Pinczuk, A.; Hart, R. M.; Olson, D. H. *Opt. Lett.* **1981**, *6*, 33-35.

6. Glass, A. M.; Liao, P. F.; Bergman, J. G.; Olson, D. H. *Opt. Lett.* **1980**, *5*, 368-370.

7. Wokaun, A.; Bergman, J. G.; Heritage, J. P.; Glass, A. M.; Liao, P. F.; Olson, D. H. *Phys. Rev. B* **1981**, *24*, 849-856.

8. Kamat, P. V.; Barazzouk, S.; Hotchandani, S. *Angew. Chem. Int. Ed. Engl.* **2002**, *41*, 2764-2767.

9. Alvarez, M. M.; Khoury, J. T.; Schaaff, T. G.; Shafigullin, M. N.; Vezmar, I.; Whetten, R. L. *J. Phys. Chem. B* **1997**, *101*, 3706-3712.

10. Alvarez, M. M.; Khoury, J. T.; Schaaff, T. G.; Shafigullin, M.; Vezmar, I.; Whetten, R. L. *Chem. Phys. Lett.* **1997**, *266*, 91-98.

11. Ashcroft, N. W.; Mermin, N. D. *Solid state Physics*; Holt-Saunders International Editions: Japan, 1981.

12. Link, S.; El Sayed, M. A. *J. Phys. Chem. B* **1999**, *103*, 8410-8426.

13. Wenseleers, W.; Stellacci, F.; Meyer-Friedrichsen, T.; Mangel, T.; Bauer, C. A.; Pond, S. J. K.; Marder, S. R.; Perry, J. W. *J. Phys. Chem. B* **2002**, *106*, 6853-6863.

14. Avouris, P.; Persson, B. N. J. *J. Phys. Chem.* **1984**, *88*, 837-848.

15. Ipe, B. I.; Thomas, K. G.; Barazzouk, S.; Hotchandani, S.; Kamat, P. V. *J. Phys. Chem. B* **2002**, *106*, 18-21.

16. Clark, H. A.; Campagnola, P. J.; Wuskell, J. P.; Lewis, A.; Loew, L. M. *J. Am. Chem. Soc.* **2000**, *122*, 10234-10235.

17. Boal, A. K.; Rotello, V. M. *J. Am. Chem. Soc.* **2000**, *122*, 734-735.

18. Hostetler, M. J.; Wingate, J. E.; Zhong, C. J.; Harris, J. E.; Vachet, R. W.; Clark, M. R.; Londono, J. D.; Green, S. J.; Stokes, J. J.; Wignall, G. D.; Glish, G. L.; Porter, M. D.; Evans, N. D.; Murray, R. W. *Langmuir* **1998**, *14*, 17-30.

19. Moulder, J. F.; Stickle, W. F.; Sobol, P. E.; Bomben, K. D. *Handbook of X-Ray Photoelectron Spectroscopy*; Perkin-Elmer Corporation: Minnesota, 1992.

20. Wang, T. X.; Zhang, D. Q.; Xu, W.; Yang, J. L.; Han, R.; Zhu, D. B. *Langmuir* **2002**, *18*, 1840-1848.

21. Frederiksen, P. K.; Jørgensen, M.; Ogilby, P. R. *J. Am. Chem. Soc.* **2001**, *123*, 1215-1221.

22. Poulsen, T. D.; Frederiksen, P. K.; Jørgensen, M.; Mikkelsen, K. V.; Ogilby, P. R. *J. Phys. Chem. A* **2001**, *105*, 11488-11495.

23. Stellacci, F.; Bauer, C. A.; Meyer-Friedrichsen, T.; Wenseleers, W.; Marder, S. R.; Perry, J. W. *J. Am. Chem. Soc.* **2003**, *125*, 328-329.

APPENDIX B

EXPERIMENTALS

Characterization techniques

Cyclic voltammetry: A standard three-electrode cell and an Autolab potentiostat was used. The measurements were carried out in a 0.1 M Bu_4NBF_4 solution with CH_2Cl_2 as the solvent. A Pt-electrode was used as the working electrode, an Ag/AgCl electrode as the reference electrode and an Au-electrode as the ground electrode.

HPLC measurements: A Shimadzu HPLC system was used with a Nucleosil C18 column (4.6x250 mm) and gradient eluation MeOH to 50 % THF and 50 % MeOH.

SAXS measurements: For a detailed description of the instrument used see Ref. 1. Toluene was used as the solvent for the measurements.

MALDI-TOF: The mass-spectra were recorded on a Bruker Reflex IV instrument with no matrix added to the samples.

TEM measurements: The TEM pictures were taken on a JEOL 3000F instrument.

Singlet oxygen quantum yield measurements: A detailed description of how these measurements were carried out is given in Ref. 2.

Single crystal X-ray crystallography: See Ref. 3 for more details of these experients.

Stability measurements: These experiments are described in more detail in Ref. 4.

Triplet-triplet absorption: A setup similar to the one described in Ref. 5 was used. The samples were excited at 355 nm and the absorbance at 355 nm was adjusted to approximately 0.3. Toluene was used as the solvent.

XPS-measurements: Details of the instrument used and sample preparation can be found in Ref. 6.

Absorption measurements: UV-VIS spectra were recorded on a Shimadzu UV-1700 instrument.

Flourescence experiments: Solutions were degassed for 15 min with argon prior to use. Data were recorded using an instrument comprised of a 450 W Xe lamp for steady-state measurements and a

diode laser for lifetime measurements. The detection system was a single-photon-counting photomultiplier tube in a peltier-cooled housing. All spectra where measured in a perpendicular geometry using 1-cm quartz cuvettes. Steady-state measurements were obtained with 1.8 nm band pass filters and corrected for wavelength dependent intensity variation of the excitation light source. Quantum yields were determined using 9,10-diphenylanthracene in cyclohexane[7] (Φ_f =1.00) as the fluorescence standard with refractive index and differential absorption corrections. In all cases, time-resolved fluorescence decay traces were single exponential and lifetimes were determined using least-squares analysis.[8] All time-resolved measurements were conducted with 7.3 nm band pass filters.

Synthesis

Metling points were uncorrected. Starting materials and reagents were purchased from commercial suppliers and were used without further purifications. All reactions were performed under an inert atmosphere of Ar. Solvents were all reagent grade and used without further purification unless otherwise is stated, except for THF which were either freshly distilled from sodium/benzophenone ketyl or obtained from a commercial vendor (anhydrous THF). Chromotographic separations using the dry column vacuum chromatography (DCVC) technique were performed on silica gel 60 (SiO_2, E. Merck, particle size 0.015-0.040 mm) using gradient elueation (stationary phase/mobile phase). Filtrations through silica plugs and flash column chromatography (FCC) separations were performed with silica gel 60 (SiO_2, 70-230 mesh). Filtrations through celite plugs were performed with Celite 545. All nuclear magnetic resonance spectra were recorded on a Bruker Avance DPX-250 instrument. Chemical shifts for the ^{1}H-NMR spectra are reported with the solvent as the reference ($CDCl_3$: δ 7.26 ppm, DMSO δ 2.50 ppm). Data are reported as follows: chemical shift, multiplicity (s=singlet, d=doublet, t=triplet, q=quartet, p=pentet, h=heptet, m=multiplet), integration and coupling constants (Hz). Chemical shifts for the ^{13}C-NMR spectra are reported with the solvent as the reference ($CDCl_3$: δ 77.0 ppm, DMSO δ 39.5 ppm). ^{19}F-NMR spectra were recorded by adding a sealed capillary with C_6F_6 to the NMR tube. Chemical shifts for the ^{19}F-NMR spectra are reported with C_6F_6 as the reference (C_6F_6 δ -163.0 ppm).

4-(*N*,*N*-Diphenylamino)-benzaldehyde[9] (1)

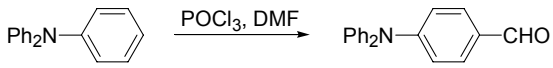

A stirred solution of Ph_3N (14.31 g, 58.33 mmol) and DMF (9.96 g, 137 mmol) was cooled to 0 ºC and $POCl_3$ (100 ml, 1.07 mol) was added dropwise. The temperature was raised to room temperature and the solution was refluxed for 45 min and poured onto ice. After neutralization with conc. NaOH (aq) the product was filtered of and purified by DCVC (n-heptane/$CHCl_3$) yielding 12.22 g (77 %) of the title compound as an light yellow solid; ^{1}H-NMR($CDCl_3$, 300 K): 9.81 (s, 1H), 7.68 (d, 2H, *J*=8 Hz), 7.39-7.29 (m, 4H), 7.22-7.12 (m, 6H), 7.01 (d, 2H, *J*=9 Hz); ^{13}C-NMR($CDCl_3$, 300 K): 190.3, 153.4, 146.2, 131.3, 129.7, 129.2, 126.3, 125.1, 119.4.

Diphenyl-(4-vinyl-phenyl)-amine[10] (2)

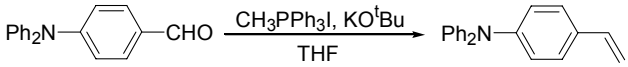

A solution of 4-(*N*,*N*-Diphenylamino)-benzaldehyde (2.03 g, 7.43 mmol) and CH_3PPh_3I of (3.24 g, 8.02 mmol) was prepared in THF (150 ml) and stirred for 15 min. under Ar atmosphere. To the solution was added KO^tBu (2.14 g, 19.1 mmol) and the reaction mixture was stirred for 1.5 h. Water was then added and the organic phase was washed with brine. The isolated organic phase was dried with $MgSO_4$ and removal of the solvent under reduced pressure left the crude product which was purified twice by DCVC (n-heptane/1,2-$C_2H_4Cl_2$) leaving 1.51 g (75 %) of the title compound as a white powder; ^{1}H-NMR($CDCl_3$, 300 K): 7.32-7.19 (m, 6H), 7.13-6.97 (m, 8H), 6.66 (dd, 1H, J_1=18 Hz, J_2=11 Hz), 5.64 (dd, 1H, J_1=18 Hz, J_2=1 Hz), 5.16 (dd, 1H, J_1=11 Hz, J_2=1 Hz); ^{13}C-NMR($CDCl_3$, 300 K): 147.7, 147.5, 136.3, 132.0, 129.2, 127.1, 124.4, 123.6, 122.9, 112.1.

2-(4-Bromo-phenyl)-1*H*-phenanthro[9,10]imidazole·AcOH (3)

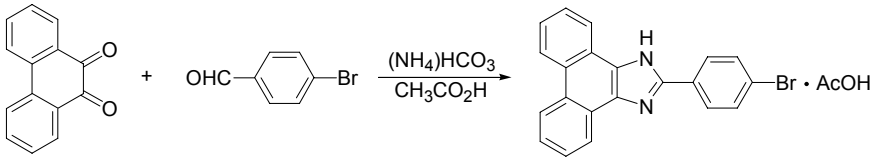

A solution of phenanthrenequinone (28.10 g, 135.0 mmol), 4-bromo-benzaldehyde (23.80 g, 128.6 mmol) and NH_4HCO_3 (21.88 g, 276.8 mmol) was prepared in glacial acetic acid (1 l). The reaction mixture was refluxed for 1 h and water (250 ml) was added. The product was filtered off the reaction mixture leaving 44.40 g (93 %) of the title compound as an off-white solid; mp 245-246 ºC; ^{1}H-NMR(DMSO, 300 K): 13.52 (bs, 1H), 11.95 (bs, 1H), 8.80 (d, 2H, *J*=8 Hz), 8.54 (d, 2H, *J*=8 Hz), 8.24 (d, 2H, *J*=8 Hz), 7.83-7.52 (m, 6H), 1.90 (s, 3H); ^{13}C-NMR(DMSO, 300 K): 172.0, 148.1, 131.9, 129.6, 128.0, 127.7, 127.1, 125.4, 123.9, 122.5, 121.9, 21.0; Anal. Calcd. for $C_{23}H_{17}BrN_2O_2$: C, 63.75; H, 3.95; N, 6.47. Found: C, 63.53; H, 3.83; N, 6.37.

2-(4-Bromo-phenyl)-1-methyl-1*H*-phenanthro[9,10]imidazole (4)

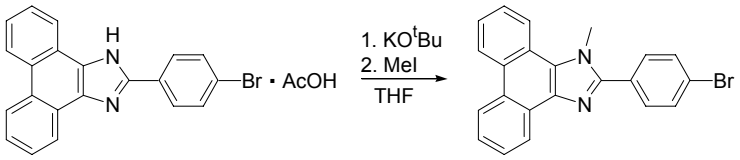

To a solution of 2-(4-Bromo-phenyl)-1*H*-phenanthro[9,10]imidazole·AcOH (9.71 g, 21.7 mmol) in THF (1 l) was added KO^tBu (7.53 g, 64.6 mmol). The reaction mixture is stirred for 20 min at RT and then MeI (11.22 g, 76.4 mmol) was added. The mixture was stirred for further 1 h at RT and water (500 ml) and $CHCl_3$ (750 ml) was added. The organic phase was collected and dried with $MgSO_4$. Evaporating the solvent off left 6.43 g (74 %) of the title compound as light yellow flakes; mp 200-201 ºC; ^{1}H-NMR($CDCl_3$, 300 K): 8.84 (d, 1H, *J*=8 Hz), 8.77 (d, 1H, *J*=8 Hz), 8.70 (d, 1H, *J*=8 Hz), 8.49-8.41 (m, 1H), 7.76-7.59 (m, 8H), 4.28 (s, 3H); ^{13}C-NMR($CDCl_3$, 300 K): 151.3, 137.5, 132.0, 131.3, 129.3, 129.2, 128.1, 127.8, 127.3, 127.2, 126.6, 125.5, 124.9, 124.4, 123.9, 123.5, 123.1, 122.5, 120.6, 36.0; Anal. Calcd. for $C_{22}H_{15}BrN_2$: C, 68.23; H, 3.90; N, 7.23. Found: C, 67.91; H, 3.83; N, 7.10.

4-(1-Methyl-1*H*-phenanthro[9,10-*d*]imidazol-2-yl)-benzaldehyde (5)

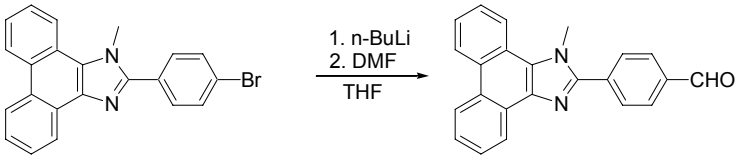

A solution of 2-(4-Bromo-phenyl)-1-methyl-1*H*-phenanthro-[9,10]imidazole (16.80 g, 43.4 mmol) in THF (1 l) was cooled to –78 ºC. To this mixture was added 1.6 M BuLi in hexane (45 ml, 72 mmol) and the reaction mixture was stirred for 1 h at –78 ºC. DMF (28 ml, 0.37 mol) was then added the mixture was allowed to warm to RT at which 1 M hydrochloric acid (100 ml) was added. The mixture was concentrated and water was added to the mixture, which was left stirring overnight. The crude product was obtained by filtration and was placed on top of a silica plug. Impurities were removed by eluating with EtOAc and the title compound was then obtained by subsequently eluating with THF. Yield 11.03 g (76 %) as a light yellow powder; mp 228-229 °C; ^{1}H-NMR($CDCl_3$, 300 K): 10.12 (s, 1H), 8.94 (d, 1H, *J*=8 Hz), 8.83 (d, 1H, *J*=8 Hz), 8.58 (d, 2H, *J*=8 Hz), 8.13-8.09 (m, 4H), 7.80-7.57 (m, 4H), 4.30 (s, 3H); ^{13}C-NMR($CDCl_3$, 300 K): 191.5, 150.9, 137.7, 136.5, 135.8, 130.3, 129.9, 129.4, 128.2, 127.3, 127.1, 126.7, 125.7, 125.2, 124.4, 123.4, 123.1, 122.6, 120.8, 36.2; Anal. Calcd. for $C_{23}H_{16}N_2O$: C, 82.12; H, 4.79; N, 8.33. Found: C, 81.05; H, 4.49; N, 8.14.

4-(5,5-Dimethyl-[1,3]dioxan-2-yl)-benzaldehyde[11] (6)

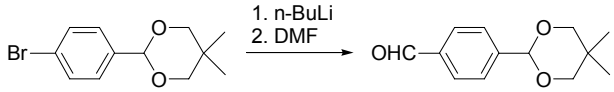

To a solution of 2-(4-Bromo-phenyl)-5,5-dimethyl-[1,3]dioxane (17.75 g, 65.5 mmol) in THF (500 ml) cooled to –78 °C was added 1.6 M n-BuLi in hexanes (45 ml, 72 mmol) and the reaction was stirred at this temperature for 10 min. DMF (11 ml, 142 mmol) was then added and the reaction was allowed to reach RT, where 37 % HCl (50 ml) was added and the reaction mixture was stirred for 2 min. The organic phase was isolated, washed with water (3x100 ml), dried ($MgSO_4$) and the solvent was removed *in vacou* leaving the crude which was recrystallized from n-heptane yielding 7.93 g (55 %) of the title compound as a white solid; ^{1}H-NMR($CDCl_3$, 300 K): 10.03 (s, 1H), 7.90 (d, 2H, *J*=8 Hz), 7.68 (d, 2H, *J*=8 Hz), 5.45 (s, 1H), 3.80 (d, 2H, *J*=11 Hz), 3.67 (d, 2H, *J*=11 Hz), 1.29 (s, 3H), 0.82 (s, 3H); ^{13}C-NMR($CDCl_3$, 300 K): 191.9, 144.6, 136.7, 129.7, 126.9, 100.7, 77.7, 30.3, 23.0, 21.8.

4'-Methyl-biphenyl-4-carbaldehyde (8),[12] general procedure

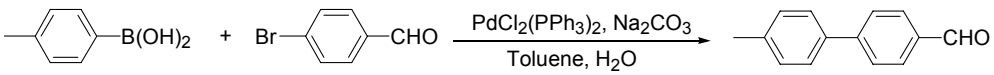

4-bromo-benzaldehyde (8.53 g, 46.1 mmol), 4-tolyl-boronic acid (11.60 g, 85.32 mmol) and $PdCl_2(PPh_3)_2$ (1.45 g, 2.07 mmol) was mixed in toluene (200 ml) and 2 M Na_2CO_3 (50 ml) and refluxed for 48 h under Ar-atmosphere. The reaction mixture was allowed to cool to RT and then filtrated. The solvent was removed under reduced pressure from the isolated organic phase leaving the crude product which was subjected to DCVC (n-heptane/EtOAc) yielding 10.24 g (83 %) of the title compound as a white compound; ^{1}H-NMR($CDCl_3$, 300 K): 10.05 (s, 1H), 7.94 (d, 2H, *J*=8 Hz), 7.74

(d, 2H, *J*=8 Hz), 7.55 (d, 2H, *J*=8 Hz), 7.29 (d, 2H, *J*=8 Hz), 2.42 (s, 3H); ^{13}C-NMR($CDCl_3$, 300 K): 191.8, 147.2, 138.5, 136.8, 135.0, 130.3, 129.7, 127.4, 127.2, 21.2.

4-Carbazol-9-yl-benzaldehyde[13] (9)

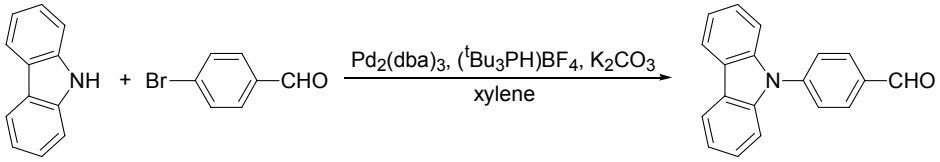

Carbazole (8.76 g, 52.4 mmol) and 4-bromo-benzaldehyde (9.65 g, 52.2 mmol) was dissolved in xylene (200 ml) and degassed with Ar. $Pd_2(dba)_3$ (0.48 g, 0.52 mmol), (^{t}Bu$_3$PH)BF_4 (0.45 g, 1.6 mmol) and K_2CO_3 (21.62 g, 156.4 mmol) was then added and the reaction mixture was refluxed overnight. After cooling to RT the reaction mixture was filtered, celite was added and the mixture was evaporated. Purification by DCVC(n-heptane/$CHCl_3$) and recrystallization from EtOH yielded 0.36 g (3%) of the title compound as a light yellow powder; ^{1}H-NMR($CDCl_3$, 300 K): 10.12 (s, 1H), 8.15 (t, 4H, *J*=8 Hz), 7.79 (d, 2H, *J*=8 Hz), 7.55-7.30 (m, 6H); ^{13}C-NMR($CDCl_3$, 300 K): 190.8, 143.4, 140.1, 134.7, 131.3, 126.8, 126.3, 124.0, 120.8, 120.5, 109.7.

4-Morpholin-4-yl-benzaldehyde[14] (10)

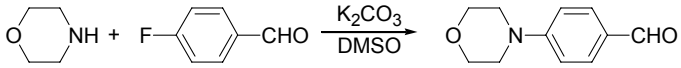

Morpholine (3.17 g, 36.4 mmol) and 4-flouro-benzaldehyde (4.37 g, 35.2 mmol) was dissolved in DMSO (40 ml). K_2CO_3 (5.36 g, 38.8 mmol) was added and the reaction mixture was stirred at 100 ºC overnight and then poured into water (400 ml). The quenched reaction mixture was extracted with Et_2O (3x150 ml) and the combined organic phases were washed with water (1x100 ml). After drying with $MgSO_4$ celite was added and the mixture was evaporated. Purification by DCVC (n-heptane/EtOAc) yielded 3.57 g (53 %) of the title compound as a white solid; ^{1}H-NMR($CDCl_3$, 300 K): 9.81 (s, 1H), 7.78 (d, 2H, *J*=9 Hz), 6.92 (d, 2H, *J*=9 Hz), 3.86 (t, 4H, *J*=5 Hz), 3.35 (t, 4H, *J*=5 Hz); ^{13}C-NMR($CDCl_3$, 300 K): 190.3, 155.1, 131.7, 127.6, 113.4, 66.4, 47.2.

1,4-Dibromo-2,5-bis-bromomethyl-benzene (11),[15] general procedure

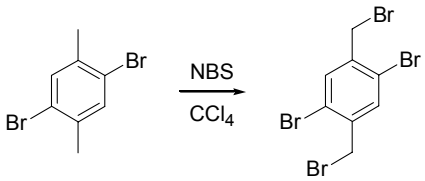

A one-neck reaction flask was charged with 2,5-dibromo-*p*-xylene (9.47 g, 35.9 mmol), NBS (13.68 g, 76.86 mmol) and CCl_4 (200 ml). A few drops of 2 M hydrochloric acid were then added and the mixture was refluxed overnight and then allowed to cool to RT. The reaction mixture was filtered and the solvent removed *in vacou* leaving the crude product which was recrystallized from EtOH yielding 5.29 g (35 %) of the title compound as a light yellow powder; ^{1}H-NMR($CDCl_3$, 300 K): 7.66 (s, 2H), 4.51 (s, 4H); ^{13}C-NMR($CDCl_3$, 300 K): 139.0, 135.4, 123.3, 31.4.

2,5-Bis-bromomethyl-terephthalonitrile (12)

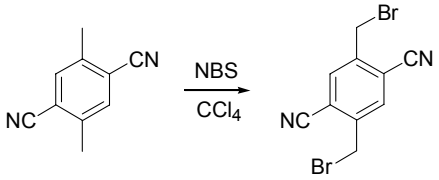

Prepared as **11**. Recrystallized (several times) from EtOH. Yield 0.45 g (43 %), white powder; ^{1}H-NMR($CDCl_3$, 300 K): 7.86 (s, 2H), 4.61 (s, 4H); ^{13}C-NMR($CDCl_3$, 300 K): 142.0, 134.7, 117.0, 114.7, 27.1.

1,5-Dibromo-2,6-bis-bromomethyl-naphthalene[16] (13)

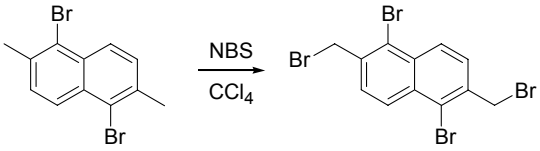

Prepared as **11**. Recrystallized from $CHCl_3$. Yield 0.64 g (20 %), white powder; ^{1}H-NMR(DMSO, 400 K): 8.27 (d, 2H, *J*=9 Hz), 7.83 (d, 2H, *J*=9 Hz), 4.80 (s, 4H).

4,4'-Bis-bromomethyl-biphenyl[17] (14)

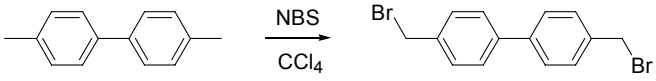

Prepared as **11**. Recrystallized from EtOH. Yield 5.11 g (71 %), white powder; ^{1}H-NMR($CDCl_3$, 300 K): 7.59 (m, 8H), 4.55 (s, 4H); ^{13}C-NMR($CDCl_3$, 300 K): 140.6, 137.1, 129.5, 127.6, 33.1.

1,4-(1-bromo-ethyl)-benzene[18] (15)

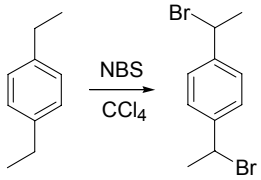

Prepared as **11**. Recrystallized from EtOH. Yield 5.27 g (43 %), white needles; ^{1}H-NMR($CDCl_3$, 300 K): 7.41 (s, 4H), 5.20 (q, 2H, *J*=7 Hz), 2.04 (d, 6H, *J*=7 Hz); ^{13}C-NMR($CDCl_3$, 300 K): 143.3, 127.1, 48.7, 26.7.

1,4-Bis-bromomethyl-2,5-dimethoxy-benzene[19] (16)

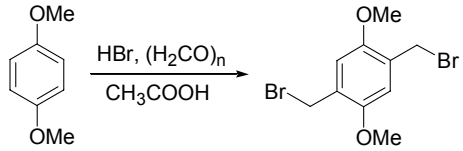

To a stirred solution of 1,4-dimethoxybenzene (15.35 g, 0.11 mol) in glacial acetic acid (75 ml) were slowly added paraformaldehyde (6.49 g, 0.22 mol) and 35 % HBr in AcOH (45 ml, 0.27 mol). The reaction mixture was heated for 1 h at 50 ºC and hydrolysed in water (300 ml) after cooling to RT. The residue was filtered off and suspended in $CHCl_3$ (75 ml). The suspension was refluxed for 10 min and

filtered off again after cooling to RT. The product was dried *in vacou* to yield 18.83 g (52 %) of the title compound as white crystals; ^{1}H-NMR($CDCl_3$, 300 K): 6.87 (s, 2H), 4.53 (s, 4H), 3.87 (s, 6H); ^{13}C-NMR($CDCl_3$, 300 K): 151.4, 127.5, 114.0, 56.3, 28.4.

2,6-Dimethyl-naphthalene[20] (17)

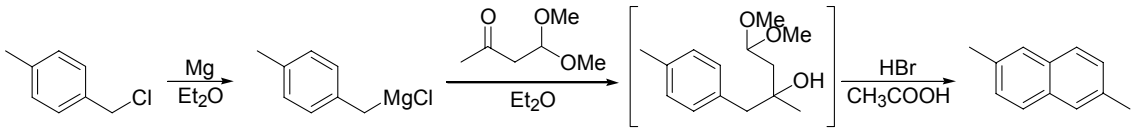

1-Chloromethyl-4-methyl-benzene (70.90 g, 0.504 mol) was dissolved in Et_2O (350 ml) and Mg (13.18 g, 0.542 mol) was added. A few crystals of I_2 was added to start the reaction. After 2 h. 4,4-dimethoxy-butan-2-one (70.35 g, 0.532 mol) dissolved in Et_2O (100 ml) was added and the reaction mixture was refluxed overnight. After cooling to RT the mixture was poured into an ice (~200 g) and saturated NH_4Cl (300 ml) mixture. The organic phase was isolated and the aqouos phase was extracted with Et_2O (3x200 ml). The combined organic phases were evaporated and then dissolved in glacial acetic acid (500 ml) and 48 % HBr in water (400 ml) was added. The reaction mixture was stirred at 90-100 ºC for 2 h. after which the reaction mixture was concentrated and poured into ice-water (500 ml). The quenched reaction mixture was extracted with CH_2Cl_2 (3x400 ml). To the combined organic phases was added silica and the mixture was evaporated. The silica was loaded onto a column of silica (Ø 8 cm, 12.5 cm) and the crude naphthalene was eluated with petrol-ether (40-60 ºC). After evaporation the naphthalene was recrystallized twice from EtOH and further purified by sublimation to yield 19.07 g (24 %) of the title compound as white crystals; ^{1}H-NMR($CDCl_3$, 300 K): 7.68 (d, 2H, *J*=8 Hz), 7.59 (s, 2H), 7.30 (d, 2H, *J*=7 Hz), 2.53 (s, 6H); ^{13}C-NMR($CDCl_3$, 300 K): 134.4, 132.0, 128.1, 127.0, 126.6, 21.6.

1,5-Dibromo-2,6-dimethyl-naphthalene[21] (18)

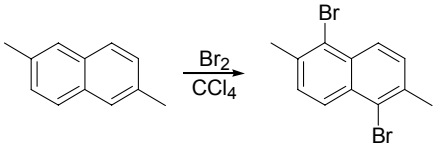

2,6-Dimethyl-naphthalene (22.17 g, 0.142 mol) was dissolved in CCl_4 (250 ml). Br_2 (15 ml) dissolved in CCl_4 (60 ml) was added drop-wise under ice cooling. The reaction mixture was allowed to react RT, stirred overnight and filtered. The organic phase was washed with a $Na_2S_2O_3$ solution until the mixture was decolorized and was then dried with $MgSO_4$. Removal of the solvent *in vacou* left the crude product, which was recrystallized from C_2Cl_4 yielding 17.33 g (39 %) of the title compound as light green crystals; ^{1}H-NMR($CDCl_3$, 300 K): 8.19 (d, 2H, *J*=9 Hz), 7.41 (d, 2H, *J*=9 Hz), 2.62 (s, 6H); ^{13}C-NMR($CDCl_3$, 300 K): 135.9, 132.0, 130.0, 126.4, 124.0, 24.0.

2,5-Dimethyl-terephthalonitrile[22] (19)

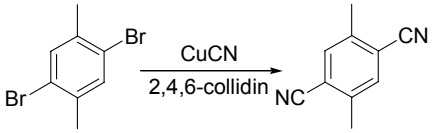

To a stirred solution of 2,5-dibromo-*p*-xylene (11.33 g, 42.92 mmol) in 2,4,6-collidin (100 ml) was added CuCN (33.51 g, 374.2 mmol) under an Ar-atmosphere. The reaction mixture was refluxed for 72 h after which the collidin was destilled off. The residue was dissolved in CH_2Cl_2 and remaining CuCN and Cu-salts were removed by washing the organic phase with conc. ammonia. Celite was added to the isolated organic phase and removal of the solvent followed by purification using DCVC (n-heptane/$CHCl_3$) to yielded 2.40 g (36 %) of the title compound as a white powder; mp 204-206 ºC; ^{1}H-NMR($CDCl_3$, 300 K): 7.86 (s, 2H), 4.61 (s, 4H); ^{13}C-NMR($CDCl_3$, 300 K): 139.9, 133.8, 117.0, 116.5, 19.8; Anal. Calcd. for $C_{10}H_8N_2$: C, 76.90; H, 5.16; N, 17.94. Found: C, 76.57; H, 5.31; N, 17.89.

(4-Diphenylamino-phenyl)-methanol[23] (20)

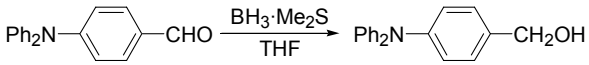

4-Diphenylamino-benzaldehyde (2.00 g, 7.32 mmol) was dissolved in THF (100 ml) and cooled to 0 ºC with an ice-bath. 2.0 M BH_3·Me_2S in THF (15 ml, 30 mmol) was added and the reaction mixture was stirred at 0 ºC for 15 min. after which it was allowed to reach RT. After stirring overnight at RT the reaction was quenched by careful addition of MeOH (100 ml). Once H_2 production had ceased the solvent was removed *in vacou* and the remaining oil was taken up in a 1:1 mixture of CH_2Cl_2:hexane from which the title compound precipitated as a white powder yielding 1.75 g (87 %); ^{1}H-NMR($CDCl_3$, 300 K): 7.31-7.20 (m, 6H), 7.14-6.97 (m, 8H), 4.64 (d, 2H, *J*=6 Hz); ^{13}C-NMR($CDCl_3$, 300 K): 147.7, 147.4, 135.0, 129.2, 128.2, 124.2, 124.0, 122.7, 64.9; Anal. Calcd. for $C_{19}H_{17}NO$·$0.125H_2O$: C, 82.21; H, 6.26; N, 5.05. Found: C, 82.23; H, 6.12; N, 5.05.

[2,5-Dibromo-4-(diethoxy-phosphorylmethyl)-benzyl]-phosphonic acid diethyl ester (21),[15] general procedure

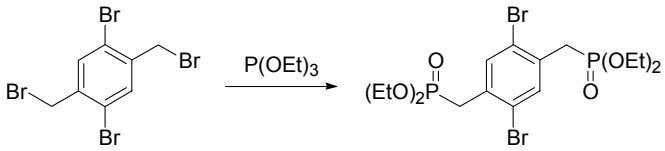

1,4-Dibromo-2,5-bis-bromomethyl-benzene (15.32 g, 36.33 mmol) was refluxed in $P(OEt)_3$ (100 ml) for 2 hours. The reaction mixture was concentrated by distilling off excess $P(OEt)_3$. Filtering of the product from the cooled concentrated reaction mixture yielded 15.0 g (77 %) of the title compound as light yellow crystals; ^{1}H-NMR($CDCl_3$, 300 K): 7.65 (d, 2H, *J*=2 Hz), 4.07 (p, 8H, *J*=7 Hz), 3.32 (d, 4H, *J*=21 Hz), 1.27 (t, 12H, *J*=7 Hz); ^{13}C-NMR($CDCl_3$, 300 K): 178.0, 135.0, 132.4 (d, J_{PC}=5 Hz), 123.4 (d, J_{PC}=4 Hz), 62.3 (t, J_{PC}=7 Hz), 32.7 (d, J_{PC}=140 Hz), 16.2 (d, J_{PC}=6 Hz).

2,5-Dicyano-4-(diethoxy-phosphorylmethyl)-benzyl]-phosphonic acid diethyl ester[24] (22)

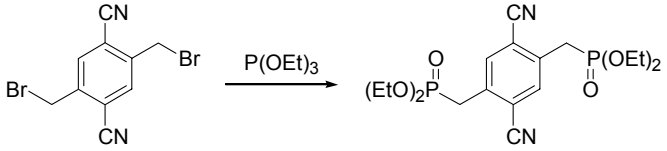

Prepared as **21**. Recrystallized from a 1:1 mixture of n-heptane and Et_2O. Yield 0.14 g (68 %), white crystals; ^{1}H-NMR($CDCl_3$, 300 K): 7.80 (s, 2H), 4.13 (p, 8H, *J*=7 Hz), 3.38 (d, 4H, *J*=21 Hz), 1.30 (t, 12H, *J*=7 Hz); ^{13}C-NMR($CDCl_3$, 300 K): 135.6 (d, J_{PC}=6 Hz), 134.8 (d, J_{PC}=2 Hz), 117.6 (d, J_{PC}=3 Hz), 115.9, 62.8 (d, J_{PC}=7 Hz), 31.9 (d, J_{PC}=138 Hz), 16.3 (d, J_{PC}=6 Hz).

[4-(Diethoxy-phosphorylmethyl)-2,5-dimethyoxy-benzyl]-phosphonic acid diethyl ester[19] (23)

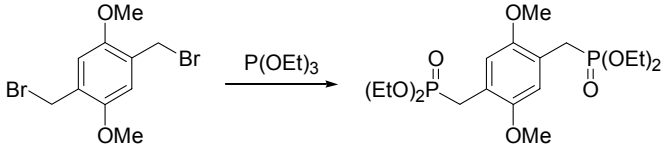

Prepared as **21**. Yield 4.22 g (85 %), white crystals; ^{1}H-NMR($CDCl_3$, 300 K): 6.90 (s, 2H), 4.01 (p, 8H, *J*=7 Hz), 3.78 (s, 6H), 3.20 (d, 4H, *J*=20 Hz), 1.22 (t, 12H, *J*=7 Hz); ^{13}C-NMR($CDCl_3$, 300 K): 151.0 (d, J_{PC}=4 Hz), 119.4 (d, J_{PC}=5 Hz), 114.0, 61.7 (d, J_{PC}=7 Hz), 56.1, 26.4 (d, J_{PC}=140 Hz), 16.2 (d, J_{PC}=6 Hz).

[6-(Diethoxy-phosphorylmethyl)-naphthalen-2-ylmethyl]-phosphonic acid diethyl ester[25] (24)

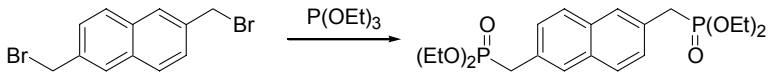

Prepared as **21**. Yield 5.88 g (38 %), white powder; ^{1}H-NMR($CDCl_3$, 300 K): 7.78-7.69 (m, 4H), 7.46-7.39 (m, 2H), 4.01 (dp, 8H, J_1=7 Hz, J_2=1 Hz), 3.30 (d, 4H, *J*=21 Hz), 1.24 (t, 12H, *J*=7 Hz); ^{13}C-NMR($CDCl_3$, 300 K): 132.3, 129.1 (m), 128.2 (m), 127.8, 62.1 (d, J_{PC}=7 Hz), 33.9 (d, J_{PC}=138 Hz), 16.3 (d, J_{PC}=6 Hz).

[1,5-dibromo-6-(diethoxy-phosphorylmethyl)-naphthalen-2-ylmethyl]-phosphonic acid diethyl ester (25)

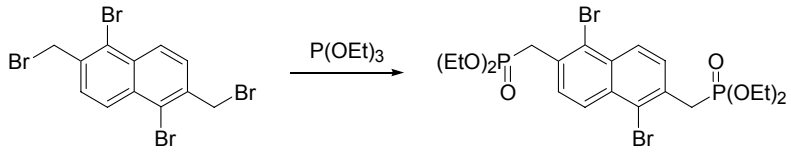

Prepared as **21**. Yield 0.50 g (75 %), white powder; mp 126-127 ˚C; ^{1}H-NMR($CDCl_3$, 300 K): 8.29 (d, 2H, *J*=9 Hz), 7.64 (dd, 2H, J_1=9 Hz, J_2=2 Hz), 4.06 (p, 8H, *J*=7 Hz), 3.65 (d, 4H, *J*=22 Hz), 1.26 (t, 12H, *J*=7 Hz); ^{13}C-NMR($CDCl_3$, 300 K): 132.5, 131.2 (d, J_{PC}=8 Hz), 129.8 (d, J_{PC}=3 Hz), 127.4 (d, J_{PC}=1 Hz), 124.7 (d, J_{PC}=9 Hz), 62.3 (d, J_{PC}=6 Hz), 35.0 (d, J_{PC}=138 Hz), 16.4 (d, J_{PC}=6 Hz); Anal. Calcd. for $C_{20}H_{28}Br_2O_6P_2$: C, 40.98; H, 4.81. Found: C, 41.13; H, 4.74.

[4'-(Diethoxy-phosphorylmethyl)-biphenyl-4-ylmethyl]-phosphonic acid diethyl ester[26,27] (26)

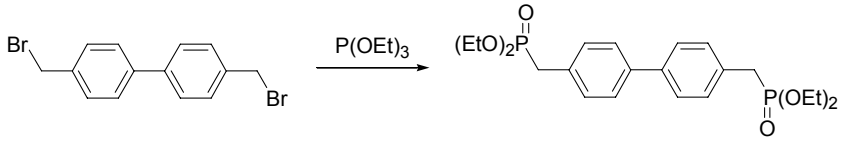

Prepared as **21**. Yield 0.66 g (45 %), white powder; ^{1}H-NMR($CDCl_3$, 300 K): 7.53 (d, 4H, *J*=8 Hz), 7.36 (dd, 4H, J_1=8 Hz, J_2=2 Hz), 4.04 (p, 8H, *J*=7 Hz), 3.18 (d, 4H, *J*=22 Hz), 1.26 (t, 12H, *J*=7 Hz); ^{13}C-NMR($CDCl_3$, 300 K): 139.2 (d, J_{PC}=4 Hz), 130.7 (d, J_{PC}=9 Hz), 130.1 (d, J_{PC}=7 Hz), 127.0 (d, J_{PC}=3 Hz), 62.1 (d, J_{PC}=7 Hz), 33.4 (d, J_{PC}=138 Hz), 16.3 (d, J_{PC}=6 Hz).

[2'-(Diethoxy-phosphorylmethyl)-biphenyl-2-ylmethyl]-phosphonic acid diethyl ester[17] (27)

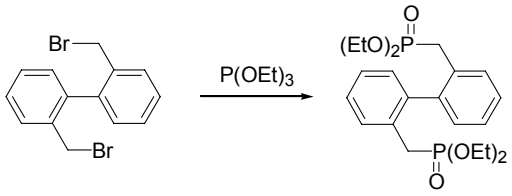

Prepared as **21**. Complete removal of $P(OEt)_3$ left an oil. Hexane was added to this oil and the solution was refluxed for 30 min. and the hexane phase was isolated. Removal of the hexane under reduced pressure left 2.81 g (40 %) of the title compound as a colorless oil; ^{1}H-NMR($CDCl_3$, 300 K): 7.62-7.55 (m, 2H), 7.38-7.19 (m, 6H), 4.01-3.84 (m, 8H), 3.08-2.78 (m, 4H), 1.21 (t, 6H, *J*=7 Hz), 1.18 (t, 6H, *J*=7 Hz); ^{13}C-NMR($CDCl_3$, 300 K): 140.8 (d, J_{PC}=9 Hz), 130.7 (m), 130.1 (d, J_{PC}=5 Hz), 130.0 (d, J_{PC}=7 Hz), 127.7 (d, J_{PC}=3 Hz), 126.6 (d, J_{PC}=3 Hz), 61.9 (d, J_{PC}=6 Hz), 61.7 (d, J_{PC}=7 Hz), 30.2 (d, J_{PC}=139 Hz), 16.3 (d, J_{PC}=2 Hz), 16.2 (d, J_{PC}=2 Hz).

2-[4-(2-Hydroxy-ethyl)-phenyl]-ethanol (28)

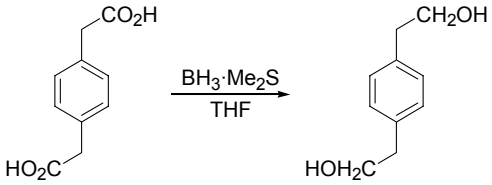

(4-Carboxymethyl-phenyl)-acetic acid (7.10 g, 36.6 mmol) was dissolved in THF (200 ml) and cooled to 0 ºC with an ice-bath. 2.0 M $BH_3{\cdot}Me_2S$ in THF (100 ml, 200 mmol) was added and the reaction mixture was allowed to reach RT. After stirring overnight at RT the reaction was quenched by careful addition of MeOH (100 ml). Once H_2 production had ceased the solvent was removed *in vacou* and the isolated crude was recrystallized from benzene yielding yielding 3.45 g (57 %) of the title compound as a white powder; ^{1}H-NMR($CDCl_3$, 300 K): 7.19 (s, 4H), 3.86 (t, 4H, *J*=7 Hz), 2.85 (t, 4H, *J*=7 Hz); ^{13}C-NMR($CDCl_3$, 300 K): 136.6, 129.2, 63.6, 38.7.

1,4-Bis-(2-bromo-ethyl)-benzene[28] (29)

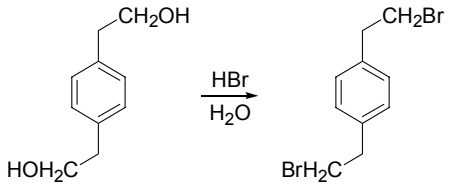

A solution of 2-[4-(2-Hydroxy-ethyl)-phenyl]-ethanol (2.98 g, 17.9 mmol) and 48 % HBr in water (50 ml) was refluxed overnight. After cooling to RT the reaction mixture was extracted with CH_2Cl_2 (3x100 ml). The combined organic phases were dried ($MgSO_4$) and the solvent was removed *in vacou*. The isolated crude was recrystallized from hexane yielding 3.40 g (65 %) of the title compound as light yellow crystals; ^{1}H-NMR($CDCl_3$, 300 K): 7.17 (s, 4H), 3.56 (t, 4H, *J*=8 Hz), 3.15 (t, 4H, *J*=8 Hz); ^{13}C-NMR($CDCl_3$, 300 K): 137.5, 128.9, 39.0, 32.8.

1,4-Dibromo-2,5-bis-(2-bromo-ethyl)-benzene[28] (30)

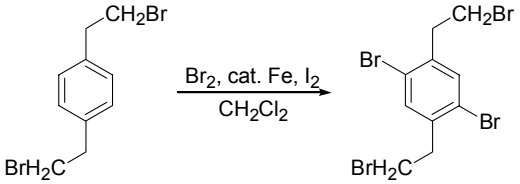

To a solution of 1,4-bis-(2-bromo-ethyl)-benzene (3.23 g, 11.1 mmol) in CH_2Cl_2 (100 ml) was added Br_2 (1.50 ml, 27.3 mmol), Fe (0.13 g, 2.3 mmol) and I_2 (0.08 g, 0.3 mmol). The mixture was stirred at RT for 6 days and was then washed with saturated $Na_2S_2O_3$ (2x50 ml), dried ($MgSO_4$) and the solvent removed *in vacou*. The isolated crude was recrystallized from hexane yielding 3.37 g (68 %) of the title compound as light yellow needles; ^{1}H-NMR($CDCl_3$, 300 K): 7.46 (s, 2H), 3.57 (t, 4H, *J*=7 Hz), 3.24 (t, 4H, *J*=7 Hz); ^{13}C-NMR($CDCl_3$, 300 K): 138.7, 135.0, 123.1, 38.8, 30.3.

(2-{2,5-Dibromo-4-[2-(diethoxy-phosphoryl)-ethyl]-phenyl}-ethyl)-phosphonic acid diethyl ester (31)

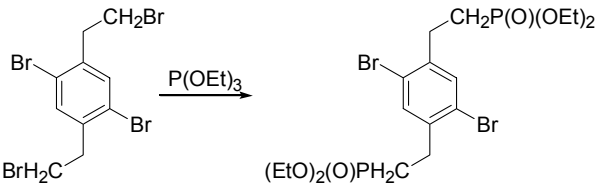

A solution of 1,4-Dibromo-2,5-bis-(2-bromo-ethyl)-benzene (3.04 g, 6.76 mmol) in $P(OEt)_3$ (50 ml) was stirred at 125 ºC for 5 days. The reaction mixture was then concentrated *in vacou* and the isolated oil was purified by FCC by first eluating with n-heptane and then with 50 % n-heptane and 50 % EtOAc. This lead to the isolation of starting material (0.70 g) and the mono-phosphonate ester (0.80 g, 23 %); ^{1}H-NMR($CDCl_3$, 300 K): 7.45 (s, 1H), 7.44 (s, 1H), 4.12 (p, 4H, *J*=7 Hz), 3.56 (t, 2H, *J*=7 Hz), 3.23 (t, 2H, *J*=7 Hz), 3.03-2.89 (m, 2H), 2.13-1.96 (m, 2H), 1.33 (t, 2H, *J*=7 Hz); ^{13}C-NMR($CDCl_3$, 300 K): 140.8 (d, J_{PC}=17 Hz), 138.0, 134.8, 134.1, 123.0, 122.8, 61.6 (d, J_{PC}=7 Hz), 38.6, 30.3, 28.8 (d, J_{PC}=4 Hz), 25.5 (d, J_{PC}=140 Hz), 16.4 (d, J_{PC}=6 Hz). The title compound was then obtained by eluating with 20 % MeOH and 80 % EtOAc yielding 0.30 g (8%) as a white powder; ^{1}H-NMR($CDCl_3$, 300 K):

7.43 (s, 2H), 4.12 (p, 8H, *J*=8 Hz), 3.02-2.89 (m, 4H), 2.12-1.94 (m, 4H), 1.33 (t, 12H, *J*=7 Hz) ; ^{13}C-NMR($CDCl_3$, 300 K): 140.3 (d, J_{PC}=17 Hz), 134.1, 122.9, 61.8 (d, J_{PC}=7 Hz), 28.8 (d, J_{PC}=4 Hz), 25.7 (d, J_{PC}=140 Hz), 16.4 (d, J_{PC}=6 Hz).

***E,E*-1,4-bis-[2-(4'-diphenylamino-phenyl)-vinyl]-benzene (32)**

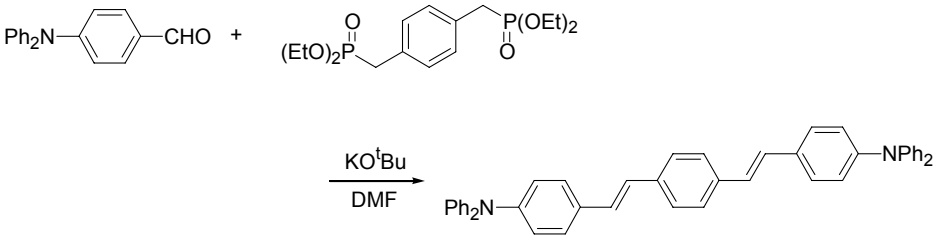

Prepared as **34**. The product precipitated from the quenched reaction mixture. Yield 3.46 g (87 %), yellow powder; mp 206-208 ˚C; ^{1}H-NMR($CDCl_3$, 300 K): 7.49 (s, 4H), 7.41 (d, 4H, *J*=9 Hz), 7.33-7.20 (m, 10H), 7.19-6.96 (m, 18H); mp 206-208 ºC; ^{13}C-NMR($CDCl_3$, 300 K): 147.6, 147.4, 136.7, 131.6, 129.3, 127.9, 127.3, 126.7, 126.6, 124.5, 123.6, 123.0; Anal. Calcd. for $C_{46}H_{36}N_2$: C, 89.58; H, 5.88; N, 4.54. Found: C, 89.26; H, 5.97; N, 4.40.

***E,E*-2,5-Dibromo-1,4-bis-[2-(4'-diphenylamino-phenyl)-vinyl]-benzene[2] (33)**

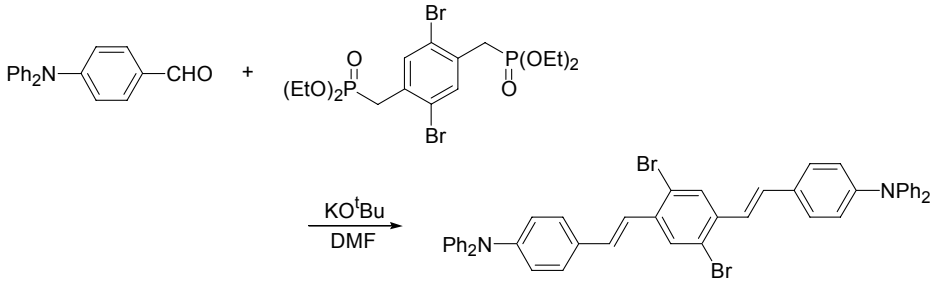

Prepared as **34**. The product precipitated from the quenched reaction mixture and was filtrated off and recrystallized from benzene. Yield 1.80 g (67 %), red microcrystalline powder; ^{1}H-NMR($CDCl_3$, 300 K): 7.85 (s, 2H), 7.42 (d, 4H, *J*=9 Hz), 7.35-7.19 (m, 12H), 7.17-6.93 (m, 16H); ^{13}C-NMR($CDCl_3$, 300 K): 148.1, 147.4, 137.3, 131.5, 130.6, 130.0, 129.3, 127.9, 125.0, 123.9, 123.3, 123.1, 122.9.

***E,E*-2,5-Dicyano-1,4-bis-[2-(4'-diphenylamino-phenyl)-vinyl]-benzene (34),[29] general procedure**

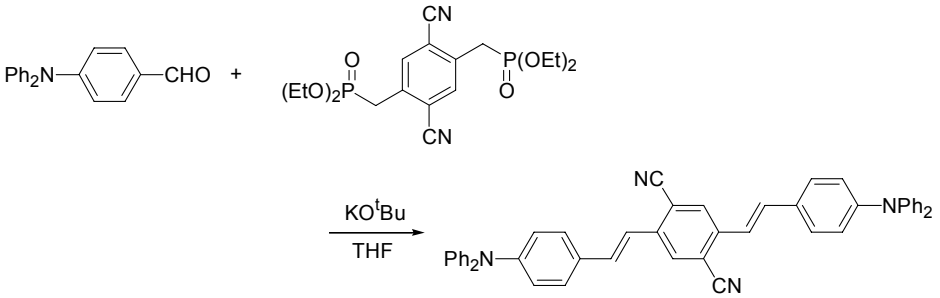

[4-(diethoxy-phosphorylmethyl)-2,5-dicyano-benzyl]-phosphonic acid diethyl ester (0.28 g, 0.65 mmol) and 4-diphenylamino-benzaldehyde (0.36 g, 1.3 mmol) was dissolved in THF (50 ml) and purged with Ar for 15 min. KO^{t}Bu (0.26 g, 2.3 mmol) was then added and reaction mixture was refluxed for 30 min. under Ar atmosphere. After cooling to RT the reaction was quenched with 2 M

hydrochloric acid. The organic phase was isolated from the quenched reaction mixture, dried ($MgSO_4$) and evaporated leaving the crude product. Purification using DCVC (n-heptane/1,2-$C_2H_4Cl_2$) followed by recrystallization from CH_2Cl_2/petrol ether yielded 0.11 g (25 %) of the title compound as a red powder; ^{1}H-NMR($CDCl_3$, 300 K): 7.99 (s, 2H), 7.44 (d, 4H, *J*=9 Hz), 7.35-7.20 (m, 12H), 7.18-6.98 (m, 16H); ^{13}C-NMR($CDCl_3$, 300 K): 149.1, 147.1, 138.8, 134.4, 129.4, 129.0, 128.4, 125.2, 123.8, 122.4, 119.6, 116.8, 114.6.

***E,E*-2,5-Dicyano-1,4-bis-[2-(4'-diphenylamino-phenyl)-vinyl]-benzene (34)**

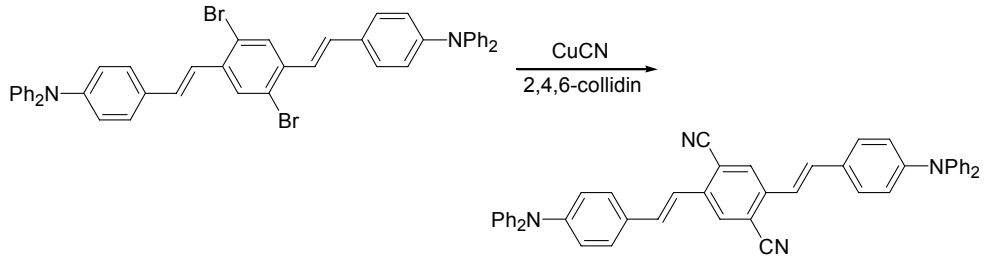

To a stirred solution of *E,E*-2,5-Dibromo-1,4-bis-[2-(4'-diphenylamino-phenyl)-vinyl]-benzene (2.53 g, 3.48 mmol) in 2,4,6-collidin (100 ml) was added CuCN (2.44 g, 27.24 mmol) under an Ar-atmosphere. The reaction mixture is refluxed for 1 week after which the collidine was destilled off. The residue was dissolved in CH_2Cl_2 and remaining CuCN and Cu-salts were removed by washing the organic phase with conc. ammonia. The isolated organic phase was evaporated leaving the crude product, which is purified by DCVC (n-heptane/$CHCl_3$ eluent system) yielding 60 mg (3 %) of the title compound; ^{1}H-NMR($CDCl_3$, 300 K): 7.99 (s, 2H), 7.44 (d, 4H, *J*=9 Hz), 7.35-7.20 (m, 12H), 7.18-6.98 (m, 16H); ^{13}C-NMR($CDCl_3$, 300 K): 149.1, 147.1, 138.8, 134.4, 129.4, 129.0, 128.4, 125.2, 123.8, 122.4, 119.6, 116.8, 114.6; Anal. Calcd. for $C_{48}H_{34}N_4$: C, 86.48; H, 5.14; N, 8.40. Found: C, 86.32; H, 4.80; N, 8.03.

***E,E*-2,5-Dimethoxy-1,4-bis-[2-(4'-diphenylamino-phenyl)-vinyl]-benzene (35)**

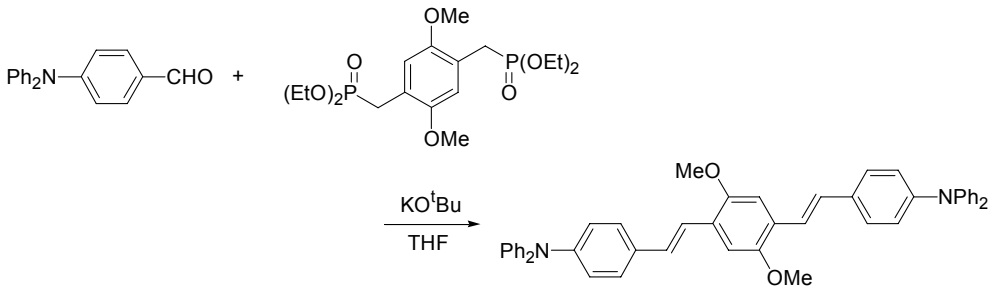

Prepared as **34**. The product precipitated from the quenched reaction mixture and was filtrated off. Yield 0.45 g (51 %), yellow powder; mp 233-234 ˚C; ^{1}H-NMR(DMSO, 300 K): 7.51 (d, 4H, *J*=9 Hz), 7.41-7.21 (m, 14H), 7.15-7.03 (m, 12H), 6.99 (d, 4H, *J*=9 Hz), 3.90 (s, 6H); ^{13}C-NMR($CDCl_3$, 300 K): 151.5, 147.6, 147.2, 132.3, 129.3, 128.3, 127.4, 126.7, 124.4, 123.7, 123.0, 121.8, 109.1, 56.4; Anal. Calcd. for $C_{48}H_{40}N_2O_2 \cdot 0.5H_2O$: C, 84.06; H, 6.03; N, 4.08. Found: C, 84.18; H, 5.91; N, 4.10.

***E, E*-2,3,5,6-Tetraflouro-1,4-bis-[2-(4'-diphenylamino-phenyl)-vinyl]-benzene (36)**

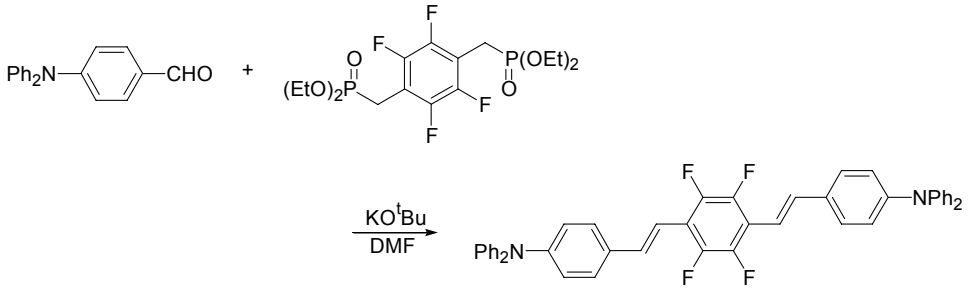

Prepared as **34**. The product precipitated from the quenched reaction mixture and was filtrated off, recrystallized from toluene, purified by DCVC (n-heptane/$CHCl_3$) and then recrystallized from benzene. Yield 0.26 g (42 %); mp >250 ºC; ^{1}H-NMR($CDCl_3$, 300 K): 7.49-7.35 (m, 6H), 7.32-7.22 (m, 10H), 7.17-7.00 (m, 14H), 6.95 (d, 2H, *J*=17 Hz); ^{13}C-NMR($CDCl_3$, 300 K): 148.7, 147.5, 130.9, 129.4, 127.9, 125.0, 123.6, 123.0; ^{19}F-NMR($CDCl_3$, 330 K): -141.7; Anal. Calcd. for $C_{46}H_{32}F_4N_2 \cdot 0.5H_2O$: C, 79.18; H, 4.77; N, 4.01. Found: C, 79.18; H, 4.55; N, 3.88.

***E, E*-2,6-bis-[2-(4'-diphenylamino-phenyl)-vinyl]-naphthalene (37)**

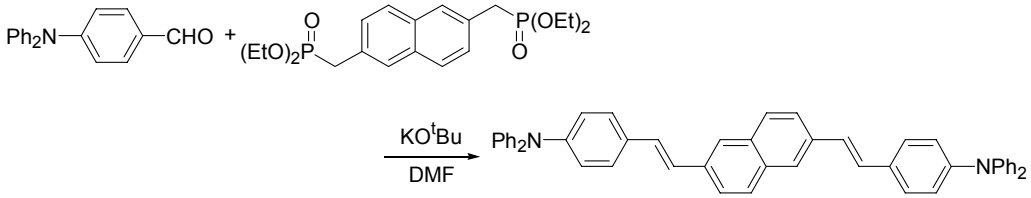

Prepared as **34**. The product precipitated from the quenched reaction mixture and was filtrated off. Yield 2.40 g (86 %), yellow powder; mp 226-228 ˚C; ^{1}H-NMR($CDCl_3$, 300 K): 7.83-7.66 (m, 6H), 7.44 (d, 4H, *J*=9 Hz), 7.37-7.33 (m, 10H), 7.20-7.00 (m, 18H); ^{13}C-NMR($CDCl_3$, 300 K): 147.6, 147.4, 135.1, 133.2, 131.6, 129.3, 128.4, 128.3, 127.4, 127.1, 126.0, 124.6, 124.0, 123.6, 123.1; Anal. Calcd. for $C_{50}H_{38}N_2 \cdot 0.5H_2O$: C, 88.86; H, 5.82; N, 4.14. Found: C, 89.02; H, 5.77; N, 4.00.

***E, E*-1,5-dibromo-2,6-bis-[2-(4'-diphenylamino-phenyl)-vinyl]-naphthalene (38)**

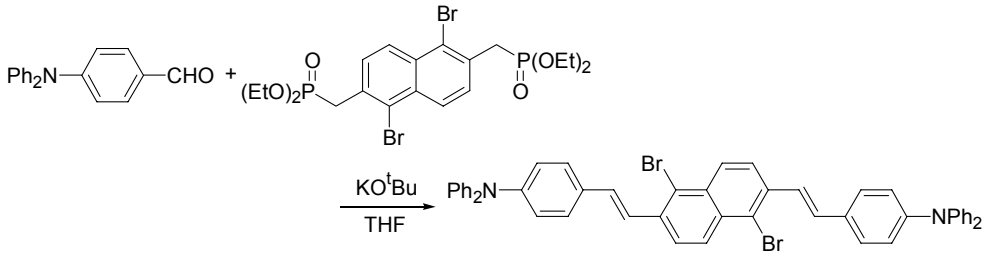

Prepared as **34**. Recrystallized from toluene and then from $CHCl_3$. Yield 0.06 g (21 %), yellow powder; mp 269-271-115 ˚C; ^{1}H-NMR($CDCl_3$, 300 K): 8.32 (d, 2H, *J*=9 Hz), 7.85 (d, 2H, *J*=9 Hz), 7.66 (d, 2H, *J*=16 Hz), 7.49 (d, 4H, *J*=9 Hz), 7.35-7.26 (m, 6H), 7.19-7.02 (m, 20H); ^{13}C-NMR($CDCl_3$, 300 K): ; Anal. Calcd. for $C_{50}H_{36}N_2Br_2 \cdot 0.33CHCl_3$: C, 69.94; H, 4.24; N, 3.24. Found: C, 69.93; H, 4.09; N, 3.14.

***E, E*-4,4'-bis-[2-(4'-diphenylamino-phenyl)-vinyl]-biphenyl[30] (39)**

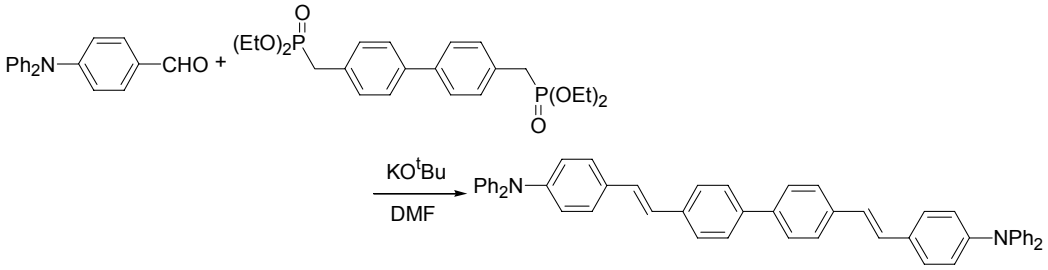

Prepared as **34**. The product precipitated from the quenched reaction mixture and was filtrated off and recrystallized from a mixture of n-heptane and EtOAc. Yield 0.36 g (84 %), yellow powder; mp 195-196 ˚C; ^{1}H-NMR($CDCl_3$, 300 K): 7.62 (d, 4H, *J*=8 Hz), 7.56 (d, 4H, *J*=8 Hz), 7.41 (d, 4H, *J*=9 Hz), 7.34-7.22 (m, 8H), 7.20-6.98 (m, 20H); ^{13}C-NMR($CDCl_3$, 300 K): 147.5, 147.4, 139.4, 136.7, 131.5, 129.3, 128.2, 127.4, 127.0, 126.8, 126.5, 124.5, 123.6, 123.0.

***E, E*-2,2'-bis-[2-(4'-diphenylamino-phenyl)-vinyl]-biphenyl (40)**

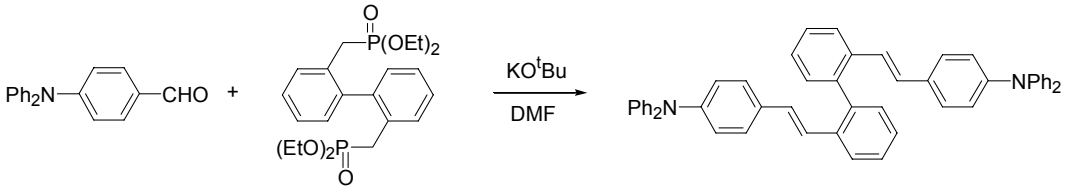

Prepared as **34**. The product precipitated from the quenched reaction mixture and was filtrated off. Yield 0.50 g (89 %), light yellow powder; mp 104-105 ˚C; ^{1}H-NMR($CDCl_3$, 300 K): 7.77 (d, 2H, *J*=7 Hz), 7.43-6.88 (m, 36H), 6.73 (d, 2H, *J*=16 Hz); ^{13}C-NMR($CDCl_3$, 300 K): 147.5, 147.2, 139.8, 136.3, 131.9, 130.9, 129.2, 128.8, 127.7, 127.3, 126.9, 125.8, 124.8, 124.4, 123.4, 122.9; Anal. Calcd. for $C_{52}H_{40}N_2 \cdot 0.25H_2O$: C, 89.56; H, 5.85; N, 4.02. Found: C, 89.54; H, 5.81; N, 4.13.

***E,E*-2,5-Dibromo-1,4-bis-[2-(4'-{1-Methyl-1*H*-phenanthro[9,10-*d*]imidazol-2-yl}-phenyl)-vinyl]-benzene (41)**

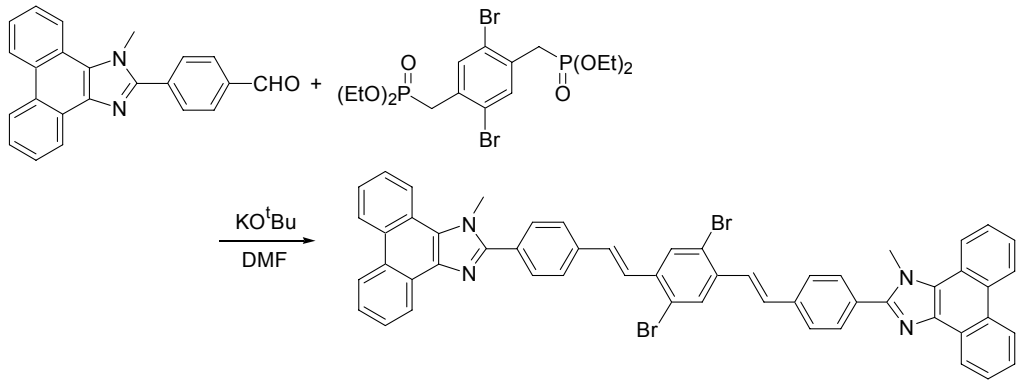

Prepared as **34**. The product precipitated from the quenched reaction mixture and was filtrated off and washed several times with benzene. Yield 0.92 g (75 %), yellow powder. Due to solubility problems it was only possible to obtain a ^{1}H-NMR spectrum; mp >300 ˚C; ^{1}H-NMR(1,2-dichlorbenzol-d_4, 450 K): 8.92 (d, 2H, *J*=7 Hz), 8.73 (d, 2H, *J*=7 Hz), 8.61 (d, 2H, *J*=8 Hz), 8.34 (d, 2H, *J*=8 Hz), 7.94-7.45 (m,

20H), 4.19 (s, 6H); Anal. Calcd. for $C_{54}H_{36}Br_2N_4 \cdot H_2O$: C, 70.60; H, 4.17; N, 6.10. Found: C, 70.63; H, 3.91; N, 6.13.

***E, E*-2,5-Dibromo-1,4-bis-[2-(4-carbazol-9-yl-phenyl)-vinyl]-benzene (42)**

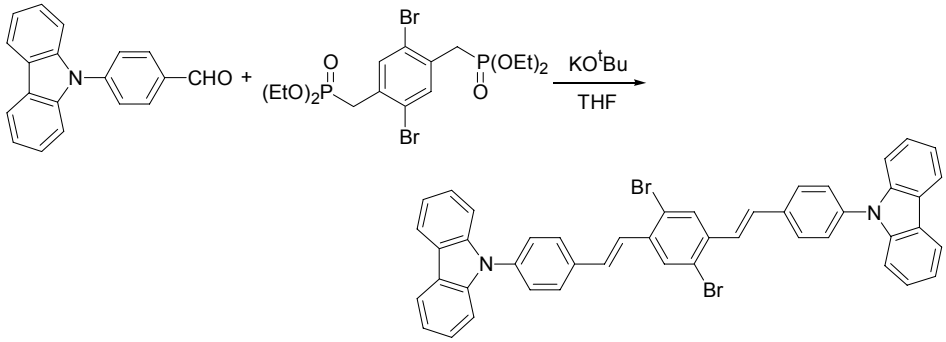

Prepared as **34**. The prodcuct was obtained from the evaporated organic phase and recrystallized from toluene. Yield 0.20 g (31 %), yellow powder; mp 256-258 ˚C; ^{1}H-NMR($CDCl_3$, 300 K): 8.16 (d, 4H, *J*=8 Hz), 7.98 (s, 2H), 7.81 (d, 4H, *J*=9 Hz), 7.62 (d, 4H, *J*=8 Hz), 7.55-7.37 (m, 10H), 7.36-7.27 (m, 4H), 7.19 (d, 2H, *J*=16 Hz); Anal. Calcd. for $C_{46}H_{30}Br_2N_20.5H_2O$: C, 70.87; H, 4.01; N, 3.59. Found: C, 70.47; H, 3.70; N, 3.64.

***E, E*-2,5-Dibromo-1,4-Bis-[2-phenyl-vinyl]-benzene (43)**

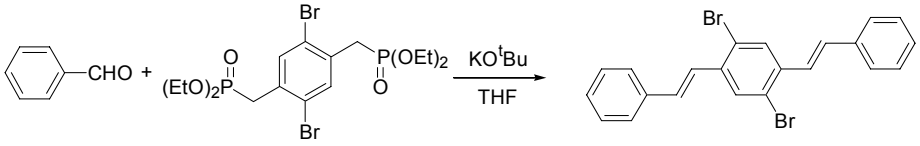

Prepared as **34**. The prodcuct was obtained from the evaporated organic phase and recrystallized from a EtOH/EtOAc mixture left. Yield 0.22 g (51 %), light green powder; mp 225-226 ˚C; ^{1}H-NMR($CDCl_3$, 300 K): 7.89 (s, 2H), 7.56 (m), 7.44-7.28 (m, 8H), 7.06 (d, 2H, *J*=16 Hz); ^{13}C-NMR($CDCl_3$, 300 K): 137.5, 136.7, 132.3, 130.4, 128.8, 128.4, 127.0, 125.9, 123.1; Anal. Calcd. for $C_{22}H_{16}Br_2$: C, 60.03; H, 3.66. Found: C, 60.04; H, 3.47.

***E, E*-2,5-Dibromo-1,4-Bis-[2-(4'-tolyl)-vinyl]-benzene (44)**

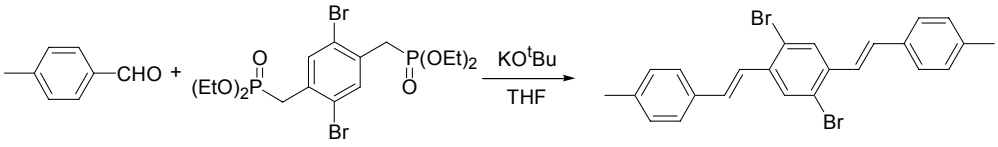

Prepared as **34**. The prodcuct was obtained from the evaporated organic phase and recrystallized (two times) from a EtOH/EtOAc/toluene mixture. Yield 0.40 g (75 %), light green powder; mp 244-246 ˚C; ^{1}H-NMR($CDCl_3$, 300 K): 7.86 (s, 2H), 7.45 (d, 4H, *J*=8 Hz), 7.32 (d, 2H, *J*=16 Hz), 7.19 (d, 4H, *J*=8 Hz), 7.03 (d, 2H, *J*=16 Hz); ^{13}C-NMR($CDCl_3$, 300 K): 138.5, 137.4, 134.0, 132.2, 130.3, 129.5, 126.9, 124.9, 123.0, 21.3;

***E, E*-2,5-Dibromo-1,4-bis-[2-(4'-methoxy-phenyl)-vinyl]-benzene (45)**

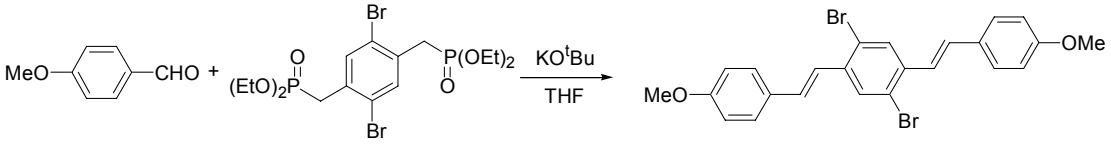

Prepared as **34**. Yield 0.37 g (58 %), light green crystals; mp 204-205 ˚C; ^{1}H-NMR($CDCl_3$, 300 K): 7.84 (s, 2H), 7.50 (d, 4H, *J*=9 Hz), 7.23 (d, 2H, *J*=16 Hz), 7.00 (d, 2H, *J*=16 Hz), 6.92 (d, 4H, *J*=9 Hz), 3.85 (s, 6H); ^{13}C-NMR($CDCl_3$, 300 K): 159.9, 137.3, 131.6, 130.0, 129.5, 128.3, 123.7, 122.8, 114.3, 55.3; Anal. Calcd. for $C_{24}H_{20}Br_2O_2$: C, 57.63; H, 4.03. Found: C, 57.68; H, 3.91.

***E, E*-2,5-Dibromo-1,4-bis-[2-(4'-dimethylamino-phenyl)-vinyl]-benzene (46)**

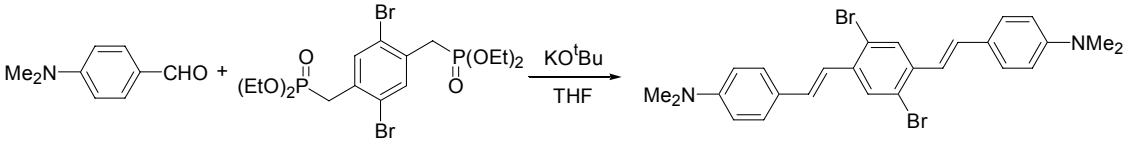

Prepared as **34**. Recrystallized from a THF/EtOH mixture. Yield 0.29 g (87 %), red powder; mp 273-275 ˚C; ^{1}H-NMR($CDCl_3$, 300 K): 7.83 (s, 2H), 7.45 (d, 4H, *J*=9 Hz), 7.17 (d, 2H, *J*=16 Hz), 6.98 (d, 2H, *J*=16 Hz), 6.74 (d, 4H, *J*=8 Hz), 3.01 (s, 12H); Anal. Calcd. for $C_{26}H_{26}Br_2N_2$: C, 59.33; H, 4.98; N, 5.32. Found: C, 59.43; H, 4.95; N, 5.35.

***E, E*-2,5-Dibromo-1,4-bis-[2-(3',4',5'-trimethoxy-phenyl)-vinyl]-benzene (47)**

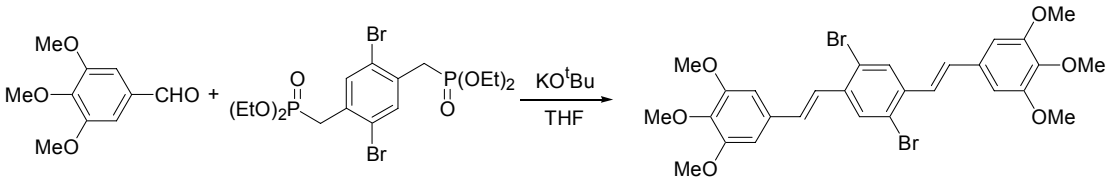

Prepared as **34**. Yield 0.47 g (77 %); mp 213-214 ˚C; ^{1}H-NMR($CDCl_3$, 300 K): 7.84 (s, 2H), 7.50 (d, 4H, *J*=9 Hz), 7.23 (d, 2H, *J*=16 Hz), 7.00 (d, 2H, *J*=16 Hz), 6.92 (d, 4H, *J*=9 Hz), 3.85 (s, 6H); ^{13}C-NMR($CDCl_3$, 300 K): 159.9, 137.3, 131.6, 130.0, 129.5, 128.3, 123.7, 122.8, 114.3, 55.3; Anal. Calcd. for $C_{28}H_{28}Br_2O_6$: C, 54.21; H, 4.55. Found: C, 54.17; H, 4.43.

***E, E*-2,5-Dibromo-1,4-bis-[2-(4'-dimorpholine-phenyl)-vinyl]-benzene (48)**

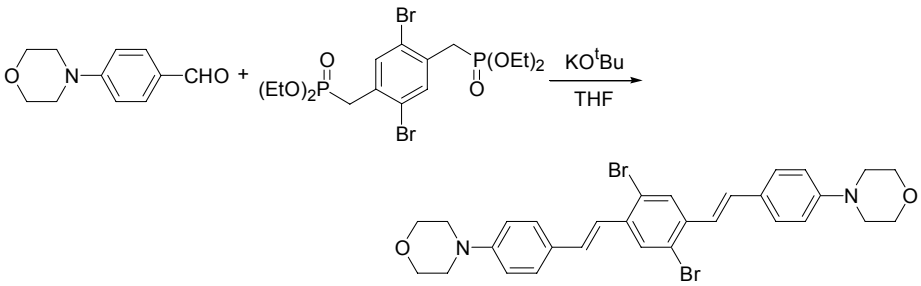

Prepared as **34**. Triturated with toluene and recrystallized from a pyridine. Yield 0.40 g (35 %), yellow powder. Due to solubility problems it was only possible to obtain a ^{1}H-NMR-spectrum; mp >300 ˚C; ^{1}H-NMR(pyridine-d_5, 375 K): 8.10 (s, 2H), 7.65 (d, 4H, *J*=9 Hz), 7.45 (d, 2H, *J*=16 Hz), 7.27 (d, 2H,

J=16 Hz), 7.00 (d, 4H, *J*=9 Hz), 3.75 (t, 8H, *J*=5 Hz), 3.13 (t, 8H, *J*=5 Hz); Anal. Calcd. for $C_{30}H_{30}Br_2N_2O_2$: C, 59.03; H, 4.95; N, 4.59. Found: C, 59.43; H, 5.14; N, 5.05.

_E_, _E_-4,4''-Bis-[2-(4-diphenylamino-phenyl)-vinyl]-2',5'-difluoro-3',6'-perfluorooctyl- 3-[1,1';4',1'']terphenyl (49)

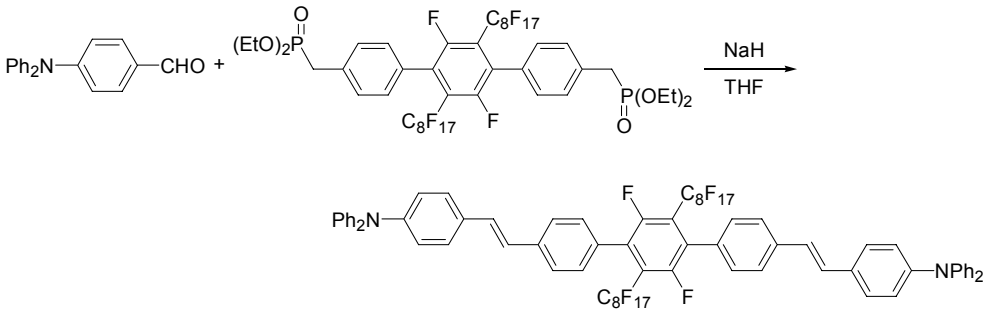

Prepared as **34**. Yield 0.30 g (69 %), green/yellow powder; mp 245-246 ˚C; ^{1}H-NMR($CDCl_3$, 300 K): 7.50 (d, 4H, *J*=8 Hz), 7.34 (d, 4H, *J*=8 Hz), 7.26-6.88 (m, 32H); ^{13}C-NMR($CDCl_3$, 300 K): 148.4, 148.2, 139.0, 131.9, 130.2, 130.0, 129.7, 128.2, 126.8, 126.5, 125.4, 124.1, 123.9; ^{19}F-NMR($CDCl_3$, 330 K): -77.3 (t, 6F, *J*=9 Hz), -98.4 (m, 4F), -103.5 (m, 2F), -115.8 (m, 4F), -118.2 (m, 12F), -119.2 (m, 4F), -122.6 (4F).

1,4-Dibromo-2,5-bis-dibromomethyl-benzene[31] (50)

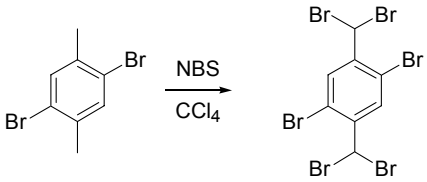

Prepared as **11**. Refluxed for 5 days. Recrystillized from EtOH. Yield 17.19 g (53 %), off-white powder; ^{1}H-NMR($CDCl_3$, 300 K): 8.13 (s, 2H), 6.94 (s, 2H); ^{13}C-NMR($CDCl_3$, 300 K): 143.0, 134.9, 119.4, 37.0; Anal. Calcd. for $C_8H_4Br_6$: C, 16.58; H, 0.70. Found: C, 16.90; H, 0.51.

2,5-Dibromo-terephthalaldehyde[31] (51)

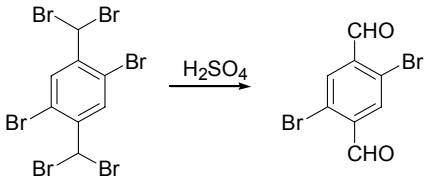

A solution of 1,4-dibromo-2,5-bis-dibromomethyl-benzene (2.15 g, 3.71 mmol) in conc. H_2SO_4 (200 ml) was refluxed overnight. The reaction mixture was poured into ice and the crude product was isolated by filtration. Recrystallization from glacial acetic acid yielded 0.77 g (71 %) of the title compound as golden flakes; ^{1}H-NMR($CDCl_3$, 300 K): 10.35 (s, 2H), 8.16 (s, 2H); ^{13}C-NMR($CDCl_3$, 300 K): 189.7, 137.4, 135.0, 125.4; Anal. Calcd. for $C_8H_4Br_2O_2$: C, 32.91; H, 1.38. Found: C, 32.87; H, 1.17.

2,5-Dibromo-terephthaloyl dichloride[32] (52)

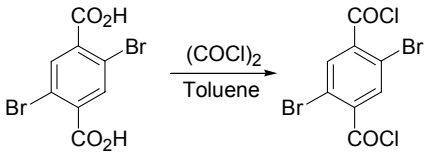

To a stirred solution of 2,5-dibromo-terephthalic acid (7.15 g, 22.1 mmol) in toluene (100 ml) was added $(COCl)_2$ (6.05 g, 47.7 mmol) along with a few drops of DMF as catalyst. The reaction mixture was stirred overnight at 40 ºC and the solvent was removed under reduced pressure. The isolated crude product was re-dissolved in toluene (20 ml) and a small amount of CaH_2 was added. The mixture was stirred for 1 h at RT, filtered, and removal of the solvent under reduces pressure left 7.62 g (96 %) of the title compound as off-white flakes; ^{1}H-NMR($CDCl_3$, 300 K): 8.20 (s, 2H); ^{13}C-NMR($CDCl_3$, 300 K): 164.3, 139.8, 137.0, 119.3.

2,5-Dibromo-terephthalic acid diethyl ester (53)

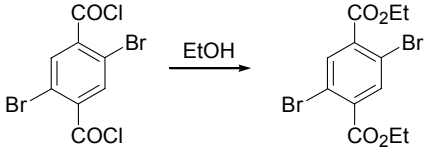

A reaction flask was charged with 2,5-dibromo-terephthaloyl dichloride (1.10 g, 3.05 mmol) and EtOH (50 ml). The reaction mixture was refluxed overnight. The solvent was removed under reduced pressure leaving 1.12 g (97 %) of the title compound as white crystals; mp 125-126 ˚C; ^{1}H-NMR($CDCl_3$, 300 K): 8.62 (s, 2H), 4.42 (q, 4H, *J*=7 Hz), 1.42 (t, 6H, *J*=7 Hz); ^{13}C-NMR($CDCl_3$, 300 K): 164.1, 136.3, 135.7, 120.0, 62.2, 14.1; Anal. Calcd. for $C_{12}H_{12}Br_2O_4$: C, 37.93; H, 3.18. Found: C, 38.21; H, 3.07.

2,5-Dibromo-*N*,*N*,*N*′,*N*′-tetraethyl-terephthalamide (54)

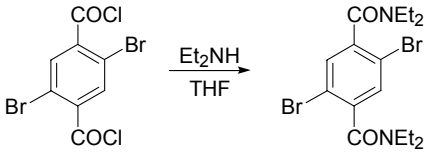

A reaction flask was charged with 2,5-dibromo-terephthaloyl dichloride (19.49 g, 54.02 mmol) and THF (100 ml). Et_2NH (10.19 g, 139.3 mmol) dissolved in THF (40 ml) was added slowly. The reaction mixture was stirred at RT overnight. The precipitated compound was collected by filtration and recrystallized from EtOH yielding 9.35 g (40 %) of the title compound as white crystals; mp 210-211 ˚C; ^{1}H-NMR($CDCl_3$, 300 K): 7.43 (s, 2H), 3.77 (h, 2H, *J*=7 Hz), 3.36 (h, 2H, *J*=7 Hz), 3.15 (h, 4H, *J*=7 Hz), 1.26 (t, 6H, *J*=7 Hz), 1.09 (t, 6H, *J*=7 Hz); ^{13}C-NMR($CDCl_3$, 300 K): 166.5, 140,4, 131.5, 118.6, 42.8, 39.1, 13.9, 12.5.

1-(4-acetyl-2,5-dibromo-phenyl)-ethanone (55), general procedure

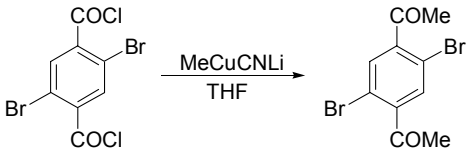

To a slurry of CuCN (7.00 g, 78.2 mmol) in THF (100 ml) at -78 ºC was added 1.4 M methyllithium in Et_2O (49 ml, 97 mmol) under an Ar atmosphere and the mixture was stirred at this temperature for 1.5 h. Freshly prepared 2,5-dibromo-terephthaloyl dichloride (7.17 g, 19.9 mmol) was then added and the solution was stirred for 40 min. at -78 ºC. The reaction was quenched at -78 ºC by addition of water (150 ml) and the mixture was allowed to warm to RT and then filtered through a pad of celite. The aqueous layer was then extracted 3 times with Et_2O and the combined organic phases was washed with brine and then dried with $MgSO_4$. The solvent was removed under reduced pressure leaving the crude product which was recrystillazed from EtOH yielding 2.93 g (46 %) of the title compound as white needles; mp 142-144 ˚C; ^{1}H-NMR($CDCl_3$, 300 K): 7.66 (s, 2H), 2.63 (s, 6H); ^{13}C-NMR($CDCl_3$, 300 K): 198.9, 144.0, 133.7, 117.8, 30.1; Anal. Calcd. for $C_{10}H_8Br_2O_2$: C, 37.54; H, 2.52. Found: C, 37.96; H, 2.41; HRMS(EI+): m/z calcd. for $C_{10}H_8Br_2O_9^{+\cdot}$ 317.8891, found 317.8883.

1-[2,5-Dibromo-4-(2,2-dimethyl-propionyl)-phenyl]-2,2-dimethyl-propan-1-one (56)

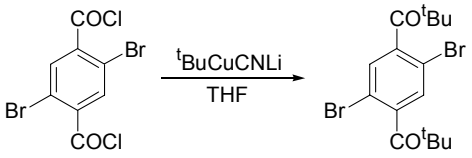

Prepared as **55**. Yield 3.34 g (59 %), white flakes; mp 189-190 ˚C; ^{1}H-NMR($CDCl_3$, 300 K): 7.31 (s, 2H), 1.28 (s, 18H); ^{13}C-NMR($CDCl_3$, 300 K): 209.5, 144.0, 130.4, 116.6, 45.1, 27.0.

1-(2,5-dibromo-4-pentanoyl-phenyl)-pentan-1-one[32] (57)

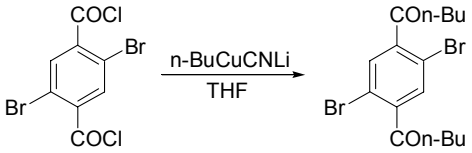

Prepared as **55**. Yield 4.08 g (52 %), white powder; ^{1}H-NMR($CDCl_3$, 300 K): 7.53 (s, 2H), 2.88 (t, 4H, *J*=7 Hz), 1.69 (p, 4H, *J*=7 Hz), 1.39 (s, 4H, *J*=7 Hz), 0.94 (t, 6H, *J*=7 Hz); ^{13}C-NMR($CDCl_3$, 300 K): 202.3, 144.4, 132.9, 117.6, 42.4, 25.9, 22.2, 13.8.

2,5-Dibromo-aniline[33] (58)

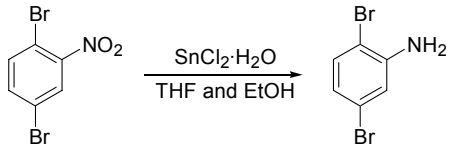

To a stirred solution of 1,4-dibromo-2-nitro-benzene (28.23 g, 0.101 mol) in THF (100 ml) and EtOH (100 ml) was added $SnCl_2 \cdot H_2O$ (101.89 g, 0.452 mol). The reaction was left stirring overnight at RT and KOH (100 g, 1.78 mol) dissolved in water (100 ml) was then added. The phases were separated

and the aqoues phase was extracted with Et_2O (3x100 ml). The combined organic phases were washed with brine (3x100 ml) and then dried with $MgSO_4$. Removal of the solvent *in vacou* yielded 21.75 g (86 %) of the title compound as a white solid; ^{1}H-NMR($CDCl_3$, 300 K): 7.24 (d, 1H, J=9 Hz), 6.90 (d, 1H, J=2.17 Hz), 6.73 (dd, 1H, J_1=8 Hz, J_2=2 Hz), 4.08 (bs, 2H); ^{13}C-NMR($CDCl_3$, 300 K): 145.3, 133.6, 122.2, 121.7, 118.1, 107.7.

_N_-acetyl-2,5-dibromo-aniline[33] (59)

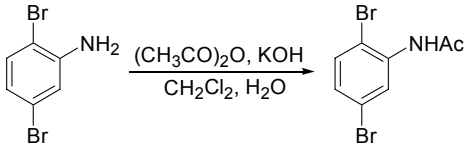

To a stirred solution of 2,5-dibromo-aniline (21.73 g, 86.60 mmol) and acetic acid anhydride (30.14 g, 295.2 mmol) in CH_2Cl_2 (50 ml) was slowly added KOH (22.40 g, 399.2 mmol) dissolved in H_2O (20 ml). The reaction mixture was stirred for 1 h. and the precipitated product was then filtered off and washed with H_2O and cold CH_2Cl_2 (50 ml) yielding 23.45 g (92 %) of the title compound as white solid; ^{1}H-NMR($CDCl_3$, 300 K): 8.59 (bs, 1H), 7.56 (bs, 1H), 7.38 (d, 1H, J=9 Hz), 7.11 (dd, 1H, J_1=9 Hz, J_2=2 Hz), 2.24 (s, 3H); ^{13}C-NMR($CDCl_3$, 300 K): 168.1, 136.7, 133.0, 128.0, 124.5, 122.0, 111.5, 24.8.

_N_-acetyl-2,5-dibromo-4-nitro-aniline[33] (60)

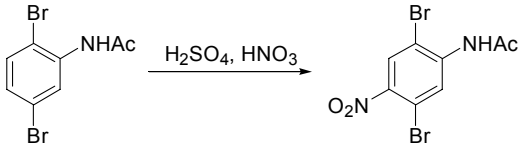

67 % HNO_3 (100 ml) and 95-97 % H_2SO_4 (200 ml) were placed in a three-neck reaction flask equipped with a mechanical stirrer and the flask was cooled with a CCl_4/CO_2(s) bath. *N*-acetyl-2,5-dibromo-aniline (21.75 g, 74.24 mmol) was slowly added and the mixture was stirred at –15 °C for 2 h. The reaction mixture was then poured on ice (~1 kg) and the quenched mixture was stirred until RT was reached. The precipitated compound was filtered off and washed with H_2O (3x100 ml), EtOH (3x50 ml) and Et_2O (2x50 ml) yielding 23.09 g (92 %) of the title compound as a slightly yellow powder; ^{1}H-NMR($CDCl_3$, 300 K): 8.88 (s, 1H), 8.15 (s, 1H), 2.29 (s, 3H); ^{13}C-NMR($CDCl_3$, 300 K): 168.4, 144.1, 139.9, 129.4, 125.8, 115.3, 110.5, 24.9.

2,5-dibromo-4-nitro-aniline[33] (61)

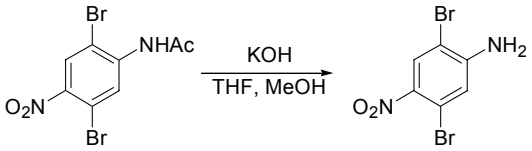

N-acetyl-2,5-dibromo-4-nitro-aniline (17.54 g, 51.90 mmol) was dissolved in THF (60 ml) and MeOH (60 ml). KOH (3.68 g, 65.6 mmol) was added and the mixture was stirred overnight at RT. H_2O (400 ml) was then added and the precipitated compound was filtered off and washed with H_2O (3x50 ml)

yielding 13.37 g (87 %) of the title compound as a yellow powder; ^{1}H-NMR(DMSO, 300 K): 8.23 (s, 1H), 7.11 (s, 1H), 6.85 (bs, 2H); ^{13}C-NMR(DMSO, 300 K): 151.3, 135.9, 131.1, 118.1, 115.4, 104.1.

2,5-dibromo-4-nitro-benzenediazonium tetrafluoroborate[33] (62)

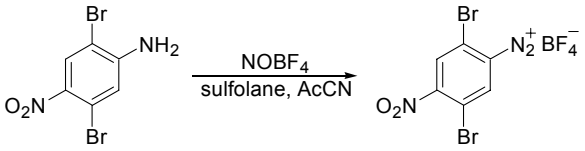

$NOBF_4$ (5.14 g, 44.0 mmol) was dissolved in AcCN (30 ml) and sulfolane (5 ml). The mixture was cooled to –40 °C and 2,5-dibromo-4-nitro-aniline (11.66 g, 39.40 mmol) dissolved in AcCN (5 ml) and sulfolane (45 ml) was added at a rate so the temperature did not exceed –30 °C. The reaction mixture was then stirred at –40 °C for 30 min. and was then allowed to reach RT. Et_2O (500 ml) was added and the mixture was stirred for 15 min. at RT and was then filtered. The isolated compound was washed with Et_2O yielding 14.21 g (91 %) of the title compound as white flakes; ^{1}H-NMR(DMSO, 300 K): 9.46 (s, 1H), 8.92 (s, 1H).

1,4-dibromo-2,5-dinitro-benzene[33] (63)

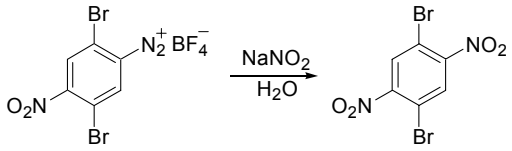

To a solution of $NaNO_2$ (26.61 g, 385.7 mmol) in H_2O (100 ml) was added 2,5-dibromo-4-nitro-benzenediazonium tetrafluoroborate (13.97 g, 35.39 mmol) dissolved in H_2O (1000 ml). The mixture was stirred at RT for 3 h. and was then extracted with CH_2Cl_2 (3x100 ml). To the combined organic phases was added celite and the solvent was removed *in vacou*. Purification with DCVC (n-heptane/1,2-$C_2H_4Cl_2$) yielded a crude, which was recrystallized from a 1:2 CH_2Cl_2:n-heptane mixture (150 ml) and then sublimed yielding 5.09 g (44 %) of the title compound as light yellow crystals; ^{1}H-NMR($CDCl_3$, 300 K): 8.19 (s, 2H); ^{13}C-NMR($CDCl_3$, 300 K): 151.2, 131.5, 114.1.

1,4-Bis-methylsulfanyl-benzene[34] (64)

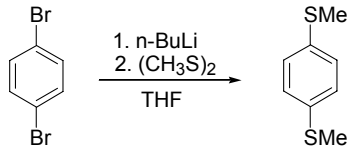

To a solution of 1,4-dibromo-benzene (20.13 g, 83.90 mmol) in THF (250 ml) cooled to -78 ºC was added 1.6 M n-BuLi in hexanes (130 ml, 208 mmol). The reaction mixture was stirred for 10 min. and then $(CH_3S)_2$ (17.4 g, 185 mmol) was added. The reaction mixture was allowed to reach RT, stirred overnight and then poured into water and extracted with CH_2Cl_2. The combined organic phases was washed with brine and dried with $MgSO_4$. The solvent was removed *in vacou* leaving the crude product, which was recrystallized from heptane yielding 5.72 g (40 %) of the title compound as a white powder; ^{1}H-NMR($CDCl_3$, 300 K): 7.21 (s, 4H), 2.47 (s, 6H).

1,4-Dibromo-2,5-bis-methylsulfanyl-benzene (65)

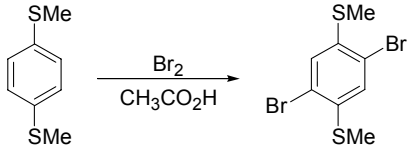

To a solution of 1,4-bis-methylsulfanyl-benzene (2.26 g, 13.3 mmol) in CH_3CO_2H (20 ml) was added Br_2 (5.3 g, 33 mmol) and the reaction mixture was stirred overnight at RT. Excess bromine was then removed by washing the reaction mixture with a 2 M $Na_2S_2O_7$ aquoues solution. The reaction mixture was concentrated and then cooled. The precipitated compound was isolated yielding 1.63 g (37 %) of the title compound as a white powder; mp 188-190 ºC; ^{1}H-NMR($CDCl_3$, 300 K): 7.25 (s, 2H), 2.46 (s, 6H); ^{13}C-NMR($CDCl_3$, 300 K): 137.4, 129.4, 121.5, 16.2; Anal. Calcd. for $C_8H_8Br_2S_2$: C, 29.29; H, 2.46; S, 19.55. Found: C, 29.64; H, 2.14; S, 19.36.

1,4-Dibromo-2,5-bis-methanesulfonyl-benzene (66)

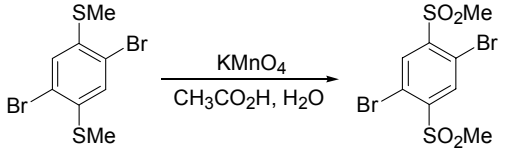

To a solution of 1,4-dibromo-2,5-bis-methylsulfanyl-benzene (1.36 g, 4.15 mmol) in CH_3CO_2H (400 ml) was added a $4.2 \cdot 10^{-2}$ M $KMnO_4$ aquaos solution (150 ml) and the reaction mixture was heated to 100 ºC for 1 h. Excess $KMnO_4$ was then removed by adding H_2SO_3 until the solution was decolorized. The title compound was filtered directly off the quenched reaction mixture yielding 1.33 g (82 %) as a white powder; mp ºC; ^{1}H-NMR(DMSO, 300 K): 8.31 (s, 2H), 3.47 (s, 6H); ^{13}C-NMR(DMSO, 400 K): 145.8, 137.1, 119.9, 43.0; Anal. Calcd. for $C_8H_8Br_2O_4S_2$: C, 24.51; H, 2.06; S, 16.36. Found: C, 24.55; H, 1.83; S, 16.37.

General procedure for the Heck reaction:

To an Ar-purged solution of $Pd_2(dba)_3$, $[(t\text{-}Bu)_3PH]BF_4$ and Cy_2NMe in 1,4-dioxan was added the bromide. The mixture was stirred for 45 min under Ar-atmosphere and the alkene was then added. The reaction mixture was refluxed overnight. After the reaction mixture was cooled to RT Et_2O was added and the reaction mixture was filtered through a plug of silica. The solvent was removed from the isolated organic phase leaving the crude product, which was purified twice by DCVC (1,2-$C_2H_4Cl_2$/n-heptane) as eluent system.

***E,E*-2,5-Diformyl-1,4-bis-[2-(4'-diphenylamino-phenyl)-vinyl]-benzene (67)**

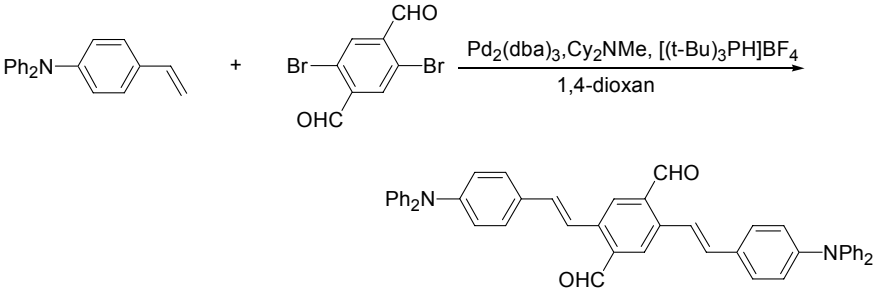

The general procedure for the Heck-reaction was followed: $Pd_2(dba)_3$ (175 mg, 0.19 mmol), $[(t\text{-}Bu)_3PH]BF_4$ (84 mg, 0.29 mmol), Cy_2NMe (1.24 g, 6.35 mmol), 1,4-dioxan (50 ml), 2,5-dibromo-terephthalaldehyde (0.77 g, 2.64 mmol) and diphenyl-(4-vinyl-phenyl)-amine (1.56 g, 5.75 mmol), DCVC(n-heptane/1,2-$C_2H_4Cl_2$) yielded 0.90 g (51 %) of the title compound as dark red crystals; mp 238-240 ˚C; ^{1}H-NMR($CDCl_3$, 300 K): 10.43 (s, 2H), 8.15 (s, 2H), 7.88 (d, 2H, *J*=16 Hz), 7.45 (d, 4H, *J*=9 Hz), 7.34-7.26 (m, 6H), 7.19-7.01 (m, 20H); ^{13}C-NMR($CDCl_3$, 300 K): 192.0, 148.4, 147.3, 138.3, 135.3, 134.3, 130.6, 130.3, 129.4, 128.1, 124.9, 123.5, 122.8, 120.8; Anal. Calcd. for $C_{48}H_{36}N_2O_2{\cdot}0.125C_2H_4Cl_2$: C, 84.58; H, 5.37; N, 4.09. Found: C, 84.64; H, 5.34; N, 4.15.

***E,E*-2,5-Diethoxycarbonyl-1,4-bis-[2-(4'-diphenylamino-phenyl)-vinyl]-benzene (68)**

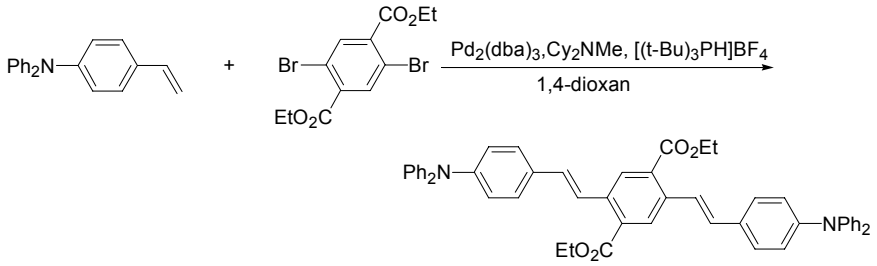

The general procedure for the Heck-reaction was followed: $Pd_2(dba)_3$ (97 mg, 0.11 mmol), $[(t\text{-}Bu)_3PH]BF_4$ (47 mg, 0.16 mmol), Cy_2NMe (0.63 g, 3.22 mmol), 1,4-dioxan (50 ml), 2,5-dibromo-terephthalic acid diethyl ester (0.40 g, 1.05 mmol) and diphenyl-(4-vinyl-phenyl)-amine (0.63 g, 2.32 mmol), DCVC(1,2-$C_2H_4Cl_2$/n-heptane) and recrystallization from a 1:1 mixture CH_2Cl_2 and EtOH yielded 0.47 g (59 %) of the title compound as red needles; mp 223-224 ˚C; ^{1}H-NMR($CDCl_3$, 300 K): 8.20 (s, 2H), 7.79 (d, 2H, *J*=16 Hz), 7.43 (d, 4H, *J*=8 Hz), 7.33-7.21 (m, 8H), 7.16-6.98 (m, 18H), 4.44 (q, 4H, *J*=7 Hz), 1.44 (t, 6H, *J*=7 Hz); ^{13}C-NMR($CDCl_3$, 300 K): 167.2, 147.8, 147.5, 137.0, 131.6, 131.4, 129.3, 128.7, 127.8, 124.6, 124.4, 123.4, 123.2, 61.4, 14.4; Anal. Calcd. for $C_{52}H_{44}N_2O_4{\cdot}0.125CH_2Cl_2$: C, 81.15; H, 5.78; N, 3.63. Found: C, 81.52; H, 5.65; N, 3.65.

***E,E*-2,5-Diethylaminocarbonyl-1,4-bis-[2-(4'-diphenylamino-phenyl)-vinyl]-benzene (69)**

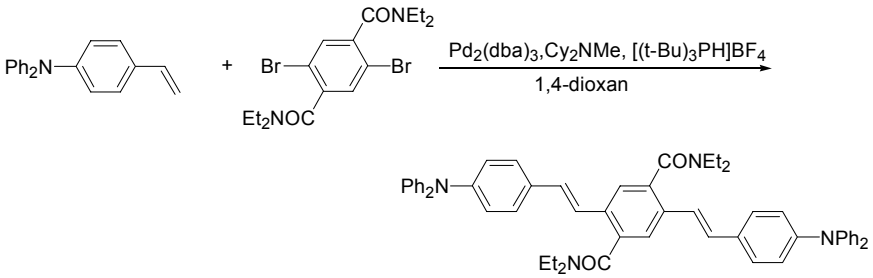

The general procedure for the Heck-reaction was followed but with 5 days reflux instead of overnight: $Pd_2(dba)_3$ (132 mg, 0.15 mmol), $[(t\text{-}Bu)_3PH]BF_4$ (71 mg, 0.24 mmol), Cy_2NMe (0.80 g, 4.09 mmol), 1,4-dioxan (50 ml), 2,5-Dibromo-*N*,*N*,*N*',*N*'-tetraethyl-terephthalamide (0.95 g, 2.19 mmol) and diphenyl-(4-vinyl-phenyl)-amine (1.21 g, 4.43 mmol). After the quenched reaction mixture was filtered through a plug of silica, it was left standing at RT for 2 days. The precipitated compound was filtered off yielding 0.34 g (44 %) of the title compound as yellow needles; mp 257-258 ˚C; ^{1}H-NMR($CDCl_3$, 300 K): 7.53 (s, 2H), 7.36-7.21 (m, 12H), 7.15-6.99 (m, 18H), 6.94 (d, 2H, *J*=16 Hz), 4.00-3.74 (bm, 2H), 3.51-3.27 (bm, 2H), 3.15 (q, 4H, *J*=7 Hz), 1.32 (t, 6H, *J*=7 Hz), 1.02 (t, 6H, *J*=7 Hz); ^{13}C-NMR($CDCl_3$, 300 K): 170.1, 147.9, 147.4, 136.5, 133.0, 130.8, 129.3, 127.6, 124.7, 123.3, 123.1, 122.9, 122.1, 42.9, 39.0, 14.0, 13.0; Anal. Calcd. for $C_{56}H_{54}N_4O_2 \cdot 0.5C_4H_8O_2$: C, 81.09; H, 6.80; N, 6.52. Found: C, 80.71; H, 6.46; N, 6.69.

***E,E*-2,5-Diacetyl-1,4-bis-[2-(4'-diphenylamino-phenyl)-vinyl]-benzene (70)**

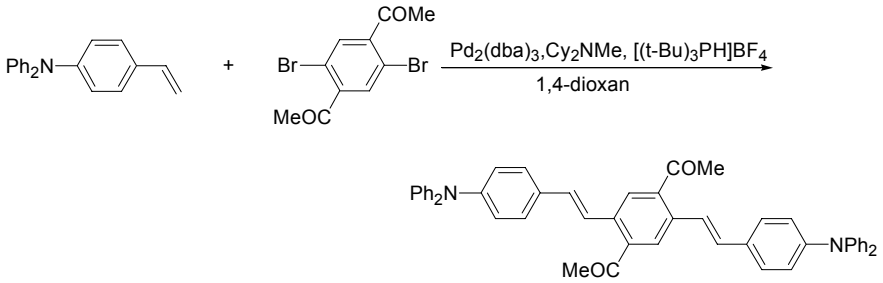

The general procedure for the Heck-reaction was followed: $Pd_2(dba)_3$ (112 mg, 0.12 mmol), $[(t\text{-}Bu)_3PH]BF_4$ (63 mg, 0.22 mmol), Cy_2NMe (0.74 g, 3.8 mmol), 1,4-dioxan (50 ml), 1-(4-acetyl-2,5-dibromo-phenyl)-ethanone (0.37 g, 1.2 mmol) and diphenyl-(4-vinyl-phenyl)-amine (0.70 g, 2.6 mmol), DCVC(1,2-$C_2H_4Cl_2$/n-heptane) (2 times) and recrystallization from a 1:1 mixture CH_2Cl_2 and EtOH yielded 0.25 g (31 %) of the title compound as a red powder; mp 249-251 ˚C; ^{1}H-NMR($CDCl_3$, 300 K): 7.86 (s, 2H), 7.49-7.36 (m, 6H), 7.32-7.25 (m, 8H), 7.15-7.09 (m, 8H), 7.09-7.01 (m, 8H), 6.98 (d, 2H, *J*=16 Hz), 2.65 (s, 6H); ^{13}C-NMR($CDCl_3$, 300 K): 202.1, 148.0, 147.4, 139.8, 135.4, 132.0, 130.9, 129.3, 127.8, 127.0, 124.7, 123.9, 123.3, 123.2, 30.3; Anal. Calcd. for $C_{50}H_{40}N_2O_2 \cdot 0.33CH_2Cl_2$: C, 82.91; H, 5.62; N, 3.84. Found: C, 82.70; H, 5.58; N, 3.77.

***E,E*-2,5-Di-*tert*-butylcarbonyl-1,4-bis-[2-(4'-diphenylamino-phenyl)-vinyl]-benzene (71)**

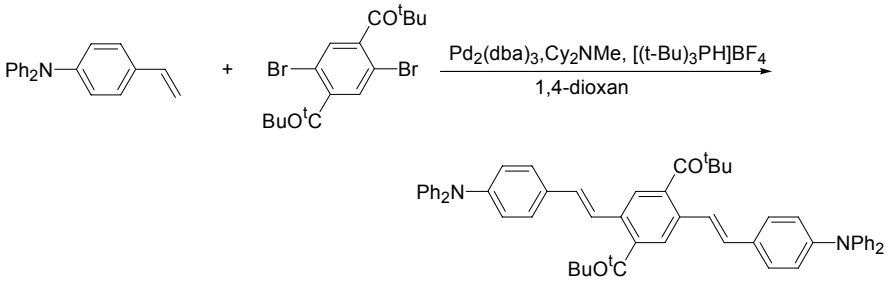

The general procedure for the Heck-reaction was followed but with 5 days reflux instead of overnight: $Pd_2(dba)_3$ (118 mg, 0.13 mmol), $[(t\text{-}Bu)_3PH]BF_4$ (79 mg, 0.28 mmol), Cy_2NMe (0.73 g, 3.7 mmol), 1,4-dioxan (50 ml), 1-[2,5-dibromo-4-(2,2-dimethyl-propionyl)-phenyl]-2,2-dimethyl-propan-1-one (0.70 g, 1.7 mmol) and diphenyl-(4-vinyl-phenyl)-amine (0.95 g, 3.5 mmol), DCVC(n-heptane/1,2-$C_2H_4Cl_2$) (2 times) and recrystallization from a mixture of CH_2Cl_2 and n-heptane yielded 0.04 g (3 %) of the title compound as a yellow powder; mp 276-277 °C; ^{1}H-NMR($CDCl_3$, 300 K): 7.37 (s, 2H), 7.35-7.21 (m, 14H), 7.16-6.99 (m, 18H), 6.93 (d, 2H, *J*=16 Hz), 6.78 (d, 2H, *J*=16 Hz), 1.28 (s, 18H).

***E,E*-2,5-Dimethylsulfonyl-1,4-bis-[2-(4'-diphenylamino-phenyl)-vinyl]-benzene (72)**

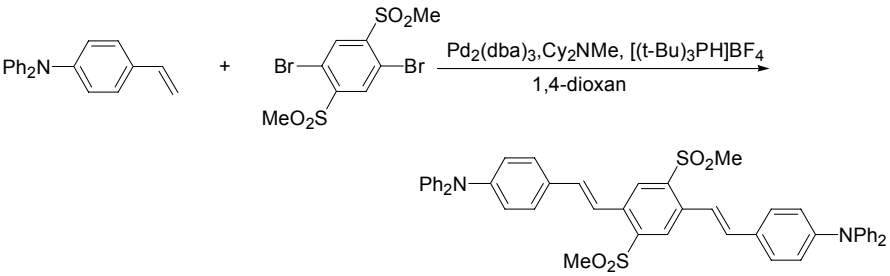

The general procedure for the Heck-reaction was followed but with 3 days reflux instead of overnight: $Pd_2(dba)_3$ (103 mg, 0.11 mmol), $[(t\text{-}Bu)_3PH]BF_4$ (59 mg, 0.20 mmol), Cy_2NMe (0.69 g, 3.5 mmol), 1,4-dioxan (50 ml), 1,4-dibromo-2,5-bis-methanesulfonyl-benzene (0.49 g, 1.3 mmol) and diphenyl-(4-vinyl-phenyl)-amine (0.70 g, 2.6 mmol), DCVC(n-heptane/1,2-$C_2H_4Cl_2$) (2 times) and recrystallization from a 5:1 mixture CH_2Cl_2 and EtOH yielded 0.03 g (3 %) of the title compound; mp >300 °C; ^{1}H-NMR($CDCl_3$, 300 K): 8.47 (s, 2H), 7.88 (d, 2H, *J*=16 Hz), 7.45 (d, 4H, *J*=8 Hz), 7.35-7.23 (m, 10H), 7.19-7.02 (m, 16H), 3.13 (s, 6H); Anal. Calcd. for $C_{48}H_{40}N_2O_4S_2 \cdot 0.25H2O$: C, 74.15; H, 5.25; N, 3.60. Found: C, 73.98; H, 5.31; N, 3.59.

***E,E*-2,5-Dinitro-1,4-bis-[2-(4'-diphenylamino-phenyl)-vinyl]-benzene (73)**

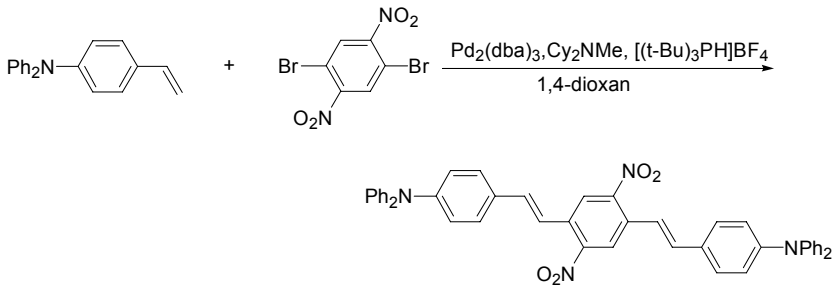

The general procedure for the Heck-reaction was followed but with 3 days reflux instead of overnight: $Pd_2(dba)_3$ (105 mg, 0.11 mmol), $[(t\text{-}Bu)_3PH]BF_4$ (67 mg, 0.23 mmol), Cy_2NMe (0.67 g, 3.4 mmol), 1,4-dioxan (50 ml), 1,4-dibromo-2,5-bis-nitro-benzene (0.45 g, 1.4 mmol) and diphenyl-(4-vinyl-phenyl)-amine (0.74 g, 2.7 mmol), DCVC(n-heptane/1,2-$C_2H_4Cl_2$) (2 times) and recrystallization from a mixture of CH_2Cl_2 and n-heptane yielded 0.10 g (10 %) of the title compound; mp 221-222 °C; ^{1}H-NMR($CDCl_3$, 300 K): 8.26 (s, 2H), 7.41 (d, 4H, J=9 Hz), 7.35-7.24 (m, 10H), 7.21-7.01 (m, 18H); ^{13}C-NMR($CDCl_3$, 300 K): 149.2, 149.1, 147.1, 135.4, 131.7, 129.4, 129.2, 128.4, 125.2, 123.8, 123.6, 122.4, 118.1; Anal. Calcd. for $C_{46}H_{34}N_4O_4 \cdot 0.25CH_2Cl_2$: C, 76.30; H, 4.78; N, 7.70. Found: C, 76.15; H, 4.65; N, 8.02.

2-(4-Bromo-phenyl)-5,5-dimethyl-[1,3]dioxane[35] (74)

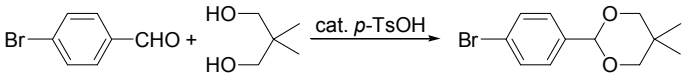

4-Bromo-benzaldehyde (101.15 g, 0.547 mol), 2,2-dimethyl-propane-1,3-diol (61.10 g, 0.587 mol) and *p*-toluene-sulfonic acid hydrate (1.02 g, 5.4 mmol) was dissolved in toluene (500 ml) and refluxed overnight using a Dean-Stark-setup. The solvent was then removed *in vacou* and the isolated crude was recrystallized from EtOH yielding 89.11 g (60 %) of the title compound as white crystals; ^{1}H-NMR($CDCl_3$, 300 K): 7.50 (d, 2H, *J*=9 Hz), 7.38 (d, 2H, *J*=8 Hz), 5.35 (s, 1H), 3.72 (d, 2H, *J*=12 Hz), 3.63 (d, 2H, *J*=11 Hz), 1.28 (s, 3H), 0.80 (s, 3H); ^{13}C-NMR($CDCl_3$, 300 K): 137.6, 131.3, 127.9, 122.7, 100.8, 77.5, 30.1, 23.0, 21.8.

2-(4-Bromo-2,5-dioctyl-phenyl)-5,5-dimethyl-[1,3]dioxane (75)

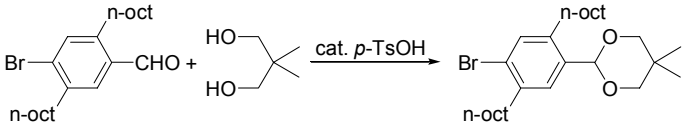

4-Bromo-2,5-dioctyl-benzaldehyde (20.02 g, 48.90 mmol), 2,2-dimethyl-propane-1,3-diol (8.35 g, 80.2 mmol) and *p*-toluene-sulfonic acid hydrate (0.22 g, 1.2 mmol) was dissolved in toluene (500 ml) and refluxed overnight using a Dean-Stark-setup. The organic phase was washed with 1 M $NaHCO_3$ (4x150 ml) and water (4x150 ml) and was then dried with $MgSO_4$. The solvent was removed *in vacou* and the isolated oil was put on top of a silica column. Impurities was removed by eluating with n-heptane (500 ml) and the title compound was obtained by eluating with EtOAc (500 ml). Yield: 16.52 g (68 %), light yellow oil; ^{1}H-NMR($CDCl_3$, 300 K): 7.49 (s, 1H), 7.33 (s, 1H), 5.47 (s, 1H), 3.78 (d, 2H, *J*=11 Hz),

3.64 (d, 2H, *J*=11 Hz), 2.69 (t, 2H, *J*=8 Hz), 2.62 (t, 2H, *J*=8 Hz), 1.69-1.51 (m, 4H), 1.47-1.21 (m, 23H), 0.90 (t, 6H, *J*=6 Hz), 0.81 (s, 3H); ^{13}C-NMR($CDCl_3$, 300 K): 139.9, 139.6, 135.2, 133.3, 128.0, 124.8, 99.5, 77.9, 35.9, 31.9, 31.6, 31.3, 30.2, 30.1, 29.6, 29.5, 29.4 (2C), 29.3, 29.2, 23.2, 22.7, 21.9, 14.1; Anal. Calcd. for $C_{28}H_{47}BrO_2 \cdot H_2O$: C, 65.48; H, 9.62. Found: C, 65.58; H, 9.26; HRMS(EI+): m/z calcd. for $C_{28}H_{47}BrO_2^{+\cdot}$ 496.2743, found 496.2740.

4-(5,5-Dimethyl-[1,3]dioxan-2-yl)-2,5-dioctyl-benzaldehyde (76)

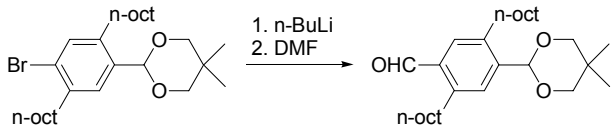

Prepared as **6** from **75**. Yield: 12.73 g (95 %) as a colorless oil; ^{1}H-NMR($CDCl_3$, 300 K): 10..27 (s, 1H), 7.63 (s, 1H), 7.56 (s, 1H), 5.54 (s, 1H), 3.80 (d, 2H, *J*=11 Hz), 3.66 (d, 2H, *J*=11 Hz), 2.98 (t, 2H, *J*=8 Hz), 2.70 (t, 2H, *J*=8 Hz), 1.68-1.53 (m, 4H), 1.44-1.22 (m, 23H), 0.93-0.84 (m, 6H), 0.82 (s, 3H); HRMS(EI+): m/z calcd. for $C_{29}H_{48}O_3^{+\cdot}$ 444.3603, found 444.3605.

[4-(5,5-Dimethyl-[1,3]dioxan-2-yl)-phenyl]-methanol[36] (77)

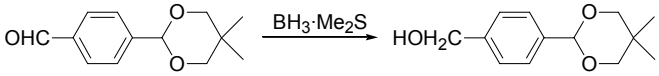

To a solution of 4-(5,5-dimethyl-[1,3]dioxan-2-yl)-benzaldehyde (1.54 g, 6.99 mmol) in THF (30 ml) cooled to 0 °C was added 2 M $BH_3 \cdot Me_2S$ (4.0 ml, 8.0 mmol) and the reaction mixture was allowed to reach RT. After stirring overnight MeOH (20 ml) was added and after H_2-production had ceased the solvent was removed *in vacou*. The isolated crude was redissolved in EtOAc and celite was added. The solvent was removed *in vacou* and the remaining solid was subjected to column chromatography, DCVC (n-heptane/EtOAc), yielding 1.20 g (77 %) of the title compound as a white solid; ^{1}H-NMR($CDCl_3$, 300 K): 7.51 (d, 2H, *J*=8 Hz), 7.37 (d, 2H, *J*=8 Hz), 5.40 (s, 1H), 4.69 (d, 2H, *J*=6 Hz), 3.77 (d, 2H, *J*=11 Hz), 3.65 (d, 2H, *J*=11 Hz), 1.60 (t, 1H, *J*=6 Hz), 1.29 (s, 3H), 0.80 (s, 3H).

[4-(5,5-Dimethyl-[1,3]dioxan-2-yl)-2,5-dioctyl-phenyl]-methanol (78)

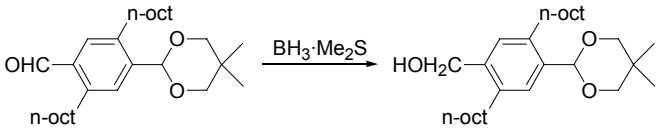

Prepared as **77**. Yield: 9.03 g (82 %) of the title compound as a clear oil that slowly crystallized into a white solid; ^{1}H-NMR($CDCl_3$, 300 K): 7.46 (s, 1H), 7.17 (s, 1H), 5.52 (s, 1H), 4.72-4.63 (m, 2H), 3.78 (d, 2H, *J*=11 Hz), 3.64 (d, 2H, *J*=11 Hz), 2.71-2.56 (m, 4H), 1.67-1.50 (m, 4H), 1.45-1.17 (m, 21H), 0.95-0.84 (m, 6H), 0.80 (s, 3H); ^{13}C-NMR($CDCl_3$, 300 K): 138.6, 138.4, 138.1, 135.3, 129.1, 127.2, 99.9, 77.9, 63.0, 32.2, 32.1, 31.9 (2C), 31.6, 31.4, 30.2, 29.9, 29.8, 29.5, 29.3, 29.2, 23.2, 22.7 (2C), 21.9, 14.; HRMS(EI+): m/z calcd. for $C_{49}H_{50}O_3^{+\cdot}$ 446.3760, found 446.3766.

2-(4-Bromomethyl-phenyl)-5,5-dimethyl-[1,3]dioxane[36] (79)

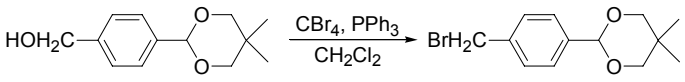

A solution of [4-(5,5-Dimethyl-[1,3]dioxan-2-yl)-phenyl]-methanol (5.05 g, 22.7 mmol), PPh_3 (6.40 g, 24.4 mmol) and CBr_4 (16.30 g, 49.1 mmol) in CH_2Cl_2 (100 ml) was stirred at RT for 1.5 days. The reaction mixture was quenched with saturated $NaHCO_3$ (100 ml) and was extracted with CH_2Cl_2 (3x50 ml). The combined organic phases were washed with brine (3x100 ml) and dried with $MgSO_4$. Celite was added to the mixture and the solvent was removed *in vacou*. Purification using DCVC (n-heptane/EtOAc) yielded 5.86 g (90 %) of the title compound as a clear oil that slowly crystallized into a white solid; ^{1}H-NMR($CDCl_3$, 300 K): 7.50 (d, 2H, *J*=8 Hz), 7.40 (d, 2H, *J*=8 Hz), 5.39 (s, 1H), 4.49 (s, 2H), 3.88 (d, 2H, *J*=11 Hz), 3.65 (d, 2H, *J*=11 Hz), 1.30 (s, 3H), 0.81 (s, 3H); ^{13}C-NMR($CDCl_3$, 300 K): 138.7, 138.2, 128.9, 126.5, 101.1, 77.6, 33.1, 30.2, 23.0, 21.8.

2-(4-Bromomethyl-2,5-dioctyl-phenyl)-5,5-dimethyl-[1,3]dioxane (80)

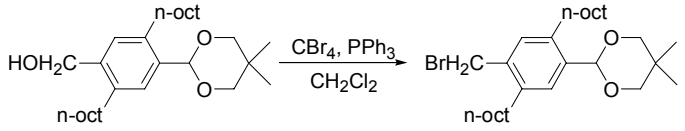

Prepared as **79**. Yield: 7.95 g (99 %), clear oil; ^{1}H-NMR($CDCl_3$, 300 K): 7.46 (s, 1H), 7.11 (s, 1H), 5.49 (s, 1H), 4.50 (s, 2H), 3.38 (d, 2H, *J*=11 Hz), 3.64 (d, 2H, *J*=11 Hz), 2.73-2.57 (m, 4H), 1.71-1.55 (m, 4H), 1.45-1.18 (m, 23H), 0.93-0.82 (m, 6H), 0.81 (s, 3H); HRMS(EI+): m/z calcd. for $C_{29}H_{49}BrO_2^{+\cdot}$ 508.2916, found 508.2918.

[4-(5,5-Dimethyl-[1,3]dioxan-2-yl)-benzyl]-phosphonic acid diethyl ester[36] (81)

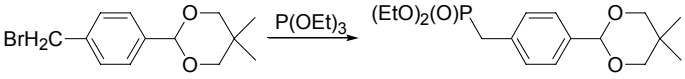

A solution of 2-(4-bromomethyl-phenyl)-5,5-dimethyl-[1,3]dioxane (4.14 g, 14.5 mmol) in $P(OEt)_3$ (25 ml) was refluxed for 2 h. Excess $P(OEt)_3$ was removed *in vacou* yielding 4.73 g (95 %) of the title compound as a clear oil; ^{1}H-NMR($CDCl_3$, 300 K): 7.42 (d, 2H, *J*=8 Hz), 7.26 (dd, 2H, J_1=8 Hz, J_2=2 Hz), 5.34 (s, 1H), 3.97 (p, 4H, *J*=7 Hz), 3.72 (d, 2H, *J*=11 Hz), 3.61 (d, 2H, *J*=11 Hz), 3.13 (d, 2H, *J*=22 Hz), 1.24-1.16 (m, 9H), 0.76 (s, 3H); HRMS(EI+): m/z calcd. for $C_{17}H_{27}O_5P^{+\cdot}$ 342.1596, found 342.1593.

[4-(5,5-Dimethyl-[1,3]dioxan-2-yl)-2,5-dioctyl-benzyl]-phosphonic acid diethyl ester (82)

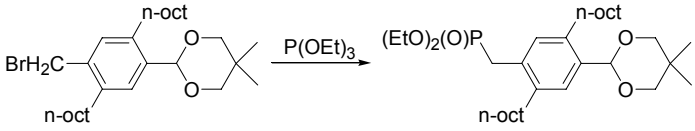

A solution of 2-(4-Bromomethyl-2,5-dioctyl-phenyl)-5,5-dimethyl-[1,3]dioxane (2.54 g, 4.98 mmol) in $P(OEt)_3$ (25 ml) was refluxed for 2 h. Excess $P(OEt)_3$ was removed *in vacou* and the crude was taken up in EtOAc. Celite was added and the solvent removed *in vacou*. Purification using DCVC (n-heptane/EtOAc) yielded 1.58 g (56 %) of the title compound as a clear oil; ^{1}H-NMR($CDCl_3$, 300 K):

7.41 (s, 1H), 7.10 (d, 1H, *J*=3 Hz), 5.48 (s, 1H), 4.04-3.88 (m, 4H), 3.76 (d, 2H, *J*=11 Hz), 3.62 (d, 2H, *J*=11 Hz), 3.13 (d, 2H, *J*=22 Hz), 2.69-2.57 (m, 4H), 1.64-1.47 (m, 4H), 1.43-1.16 (m, 29H), 0.93-0.82 (m, 6H), 0.79 (s, 3H); HRMS(EI+): m/z calcd. for $C_{33}H_{59}O_5P^{+\cdot}$ 566.4100, found 566.4090.

4-[2-(4-Diphenylamino-phenyl)-vinyl]-benzaldehyde (83)

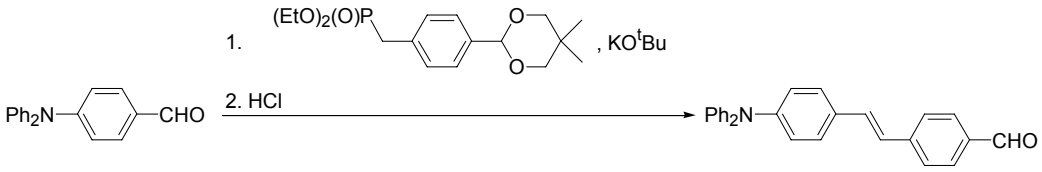

To a solution 4-(*N*,*N*-Diphenylamino)-benzaldehyde (2.07 g, 7.57 mmol) and [4-(5,5-dimethyl-[1,3]dioxan-2-yl)-benzyl]-phosphonic acid diethyl ester (4.08 g, 11.9 mmol) in THF (100 ml) was added KO^{t}Bu (2.02 g, 18.0 mmol) and the reaction mixture was refluxed for 1 h. The mixture was quenched with 3 M HCl (100 ml) and refluxed overnight. The quenched reaction mixture was washed with brine (2x100 ml) and dried with $MgSO_4$. Celite was added and the solvent removed *in vavou*. The remaining solid was loaded on a column and purified by DCVC (n-heptane/1,2-$C_2H_4Cl_2$) leaving 1.59 g of the title compound as a yellow powder; mp 141-143 °C; ^{1}H-NMR($CDCl_3$, 300 K): 9.98 (s, 1H), 7.86 (d, 2H, *J*=8 Hz), 7.62 (d, 2H, *J*=8 Hz), 7.41 (d, 2H, *J*=9 Hz), 7.33-7.22 (m, 4H), 7.20-6.97 (m, 10H) ; ^{13}C-NMR($CDCl_3$, 300 K): 191.4, 148.3, 147.4, 143.9, 135.1, 131.8, 130.4, 130.2, 129.4, 127.8, 126.6, 125.4, 124.9, 123.4, 123.0; Anal. Calcd. for $C_{27}H_{21}NO{\cdot}0.25H_2O$: C, 85.35; H, 5.70; N, 3.69. Found: C, 85.28; H, 5.52; N, 3.66.

***E,E*-2,5-Dibromo-1,4-bis-[4-(2-{4-[2-(4-Diphenylamino-phenyl)-vinyl]-phenyl}-vinyl)]-benzene (84)**

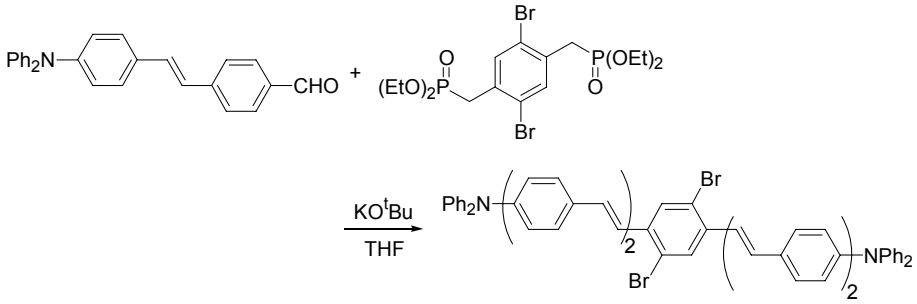

To a solution 4-[2-(4-diphenylamino-phenyl)-vinyl]-benzaldehyde (0.20 g, 0.53 mmol) and [4-(diethoxy-phosphorylmethyl)-2,5-dibromo-benzyl]-phosphonic acid diethyl ester (0.14 g, 0.25 mmol) in THF (50 ml) was added KO^{t}Bu (0.11 g, 1.0 mmol) and the reaction mixture was refluxed for 1 h. The mixture was quenched with 2 M HCl (15 ml) and the quenched mixture was left stirring overnight at RT. The precipitated compound was filtered off and washed with EtOH yielding 0.24 g (94 %) of the title compound as an orange powder; mp 269-270 °C; ^{1}H-NMR($CDCl_3$, 300 K): 7.89 (s, 2H), 7.55 (d, 4H, *J*=9 Hz), 7.50 (d, 4H, *J*=9 Hz), 7.45-7.21 (m, 16H), 7.17-6.94 (m, 20H); Anal. Calcd. for $C_{62}H_{46}Br_2N_2{\cdot}0.5H_2O$: C, 75.38; H, 4.80; N, 2.84. Found: C, 75.06; H, 4.56; N, 2.80.

4-(2-{4-[2-(4-Diphenylamino-phenyl)-vinyl]-phenyl}-vinyl)-benzaldehyde (85)

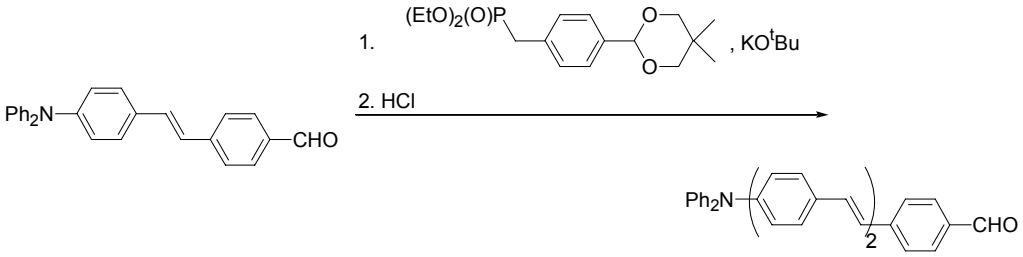

Prepared as **83** Yield: 1.08 g (70 %), light orange powder; mp 231-233 ˚C; ^{1}H-NMR($CDCl_3$, 300 K): 10.00 (s, 1H), 7.88 (d, 2H, *J*=8 Hz), 7.66 (d, 2H, *J*=8 Hz), 7.52 (s, 4H), 7.40 (d, 2H, *J*=9 Hz), 7.34-6.92 (m, 16H); 191.5, 147.6, 147.5, 143.5, 138.0, 135.5, 135.3, 131.8, 131.2, 130.2, 129.3, 128.7, 127.4, 127.3, 126.9, 126.8, 126.7, 126.3, 124.6, 123.4, 123.1; Anal. Calcd. for $C_{35}H_{27}NO$: C, 88.02; H, 5.70; N, 2.93. Found: C, 88.14; H, 5.39; N, 2.81.

***E,E*-2,5-Dibromo-1,4-bis-[4-{2-[4-(2-{4-[2-(4-Diphenylamino-phenyl)-vinyl]-phenyl}-vinyl)-phenyl]-vinyl}]-benzene (86):**

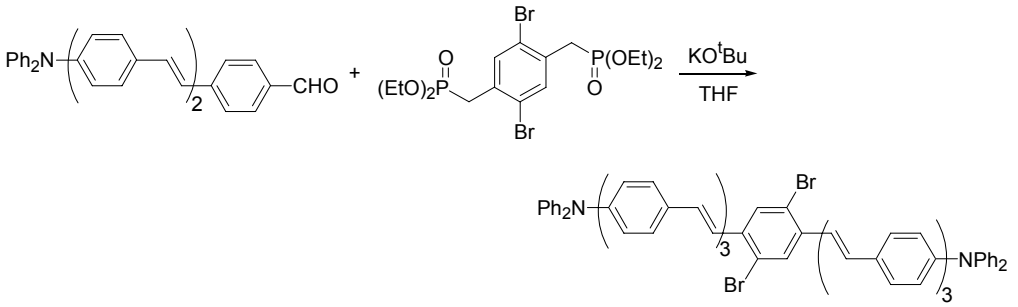

Prepared as **84** Yield: 0.41 g (60 %), orange solid; mp >300 ˚C; ^{1}H-NMR(1,2-dichlorbenzol-d_4, 300 K): 7.89 (s, 2H), 7.55-7.46 (m, 12H), 7.40 (d, 4H, *J*=8 Hz), 7.32-6.93 (m, 40H); Anal. Calcd. for $C_{78}H_{58}Br_2N_2 \cdot 1.5H_2O$: C, 77.42; H, 5.08; N, 2.31. Found: C, 77.13; H, 4.67; N, 2.37.

4-{2-[4-(2-{4-[2-(4-Diphenylamino-phenyl)-vinyl]-phenyl}-vinyl)-phenyl]-vinyl}-benzaldehyde (87)

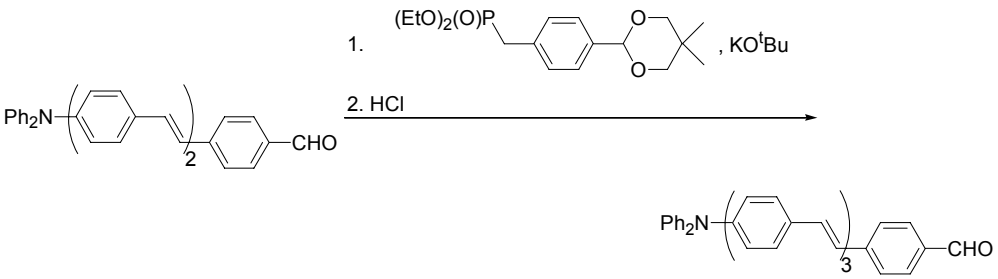

Prepared as **83**. Yield: 0.60 g (99 %), orange solid; mp >300 ˚C; ^{1}H-NMR(DMSO, 400 K): 10.01 (s, 1H), 7.89 (d, 2H, *J*=8 Hz), 7.78 (d, 2H, *J*=8 Hz), 7.66-7.01 (m, 26H), 6.98 (d, 2H, *J*=9 Hz).

4-[2-(4-{2-[4-(2-{4-[2-(4-Diphenylamino-phenyl)-vinyl]-phenyl}-vinyl)-phenyl]-vinyl}-phenyl)-vinyl]-benzaldehyde (88)

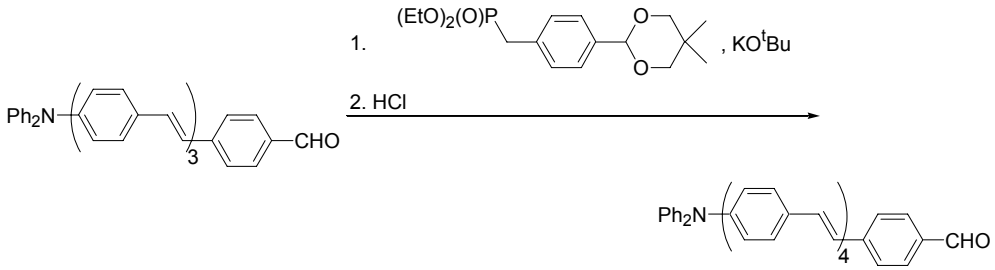

Prepared as **83**. Recrystalized from DMSO. Yield: 0.60 g (99 %), orange solid; mp >300 ˚C; ^{1}H-NMR(1,2-dichlorbenzol, 400 K): 10.22 (s, 1H), 8.01 (d, 2H, *J*=7 Hz), 7.82 (d, 2H, *J*=15 Hz), 7.63 (d, 2H, *J*=8 Hz), 7.78-6.99 (m, 12H), 7.59-7.15 (m, 20H).

***E,E*-1,4-bis-[1-cyano-2-(4'-diphenylamino-phenyl)-vinyl]-benzene (89)**

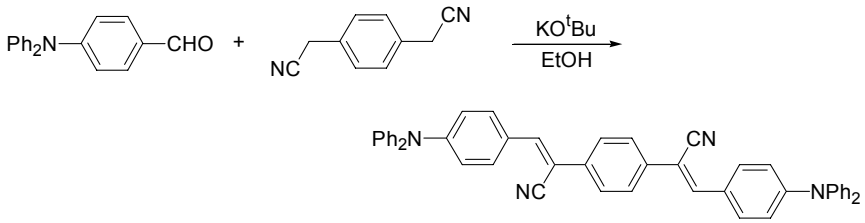

To a solution of 4-(*N*,*N*-diphenylamino)-benzaldehyde (0.73 g, 3.1 mmol) and (4-cyanomethyl-phenyl)-acetonitrile (0.20 g, 1.3 mmol) in EtOH (100 ml) was added KO^{t}Bu (0.05 g, 0.5 mmol). The reaction mixture was refluxed for 2 h and was the filtered. The isolated organic phase was subjected to DCVC (petrol-ether/$CHCl_3$) and recrystallization from a 1:1 mixture of CH_2Cl_2 and petrol ether left 0.50 g (44 %) of the title compound; mp 237-238 ˚C; ^{1}H-NMR($CDCl_3$, 300 K): 7.80 (d, 4H, *J*=9 Hz), 7.70 (s, 4H), 7.47 (s, 2H), 7.38-7.28 (m, 8H), 7.21-7.09 (m, 12H), 7.06 (d, 4H, *J*=9 Hz); ^{13}C-NMR($CDCl_3$, 300 K): 150.2, 146.5, 141.8, 135.2, 130.8, 129.6, 126.2, 126.1, 125.8, 124.5, 120.7, 118.5, 106.7; Anal. Calcd. for $C_{48}H_{34}N_4$: C, 86.48; H, 5.14; N, 8.40. Found: C, 85.81; H, 4.76; N, 8.03.

***E,E*-2,5-dibromo-1,4-bis-[3-(4-diphenylamino-phenyl)-acryloyl]-benzene (90)**

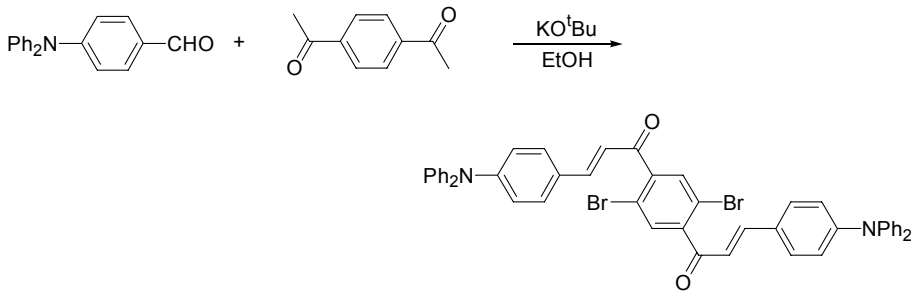

To a solution of 1-(4-acetyl-phenyl)-ethanone (0.55 g, 1.7 mmol) and 4-diphenylamino-benzaldehyde (1.04 g, 3.80 mmol) in EtOH (100 ml) was added KO^{t}Bu (0.08 g, 0.7 mmol) and the reaction mixture was refluxed for 2 h. The reaction mixture was filtered after cooling to RT and celite was added. The solvent was removed *in vacou* and the remaining solid was loaded onto a column. Purification by DCVC (petrol-ether (60-80 ºC)/$CHCl_3$) and recrystalization from a 1:1 CH_2Cl_2: petrol-ether (60-80 ºC)

mixture yielded 0.22 g (15 %) of the title compound as a dark yellow powder; mp 217-219 °C; ^{1}H-NMR($CDCl_3$, 300 K): 7.62 (s, 2H), 7.42 (d, 4H, *J*=9 Hz), 7.37 (d, 2H, *J*=10 Hz), 7.34-7.27 (m, 8H), 7.19-7.07 (m, 12H), 7.00 (d, 4H, *J*=9 Hz), 6.89 (d, 2H, *J*=16 Hz); ^{13}C-NMR($CDCl_3$, 300 K): 192.9, 151.0, 148.2, 146.5, 143.8, 133.3, 130.2, 129.6, 126.6, 125.8, 124.5, 122.5, 120.9, 118.5; Anal. Calcd. for $C_{48}H_{34}Br_2N_2O_2 \cdot 0.25H_2O$: C, 69.04; H, 4.16; N, 3.35. Found: C, 68.85; H, 4.44; N, 3.22.

[(4-Fluoro-phenyl)-hydroxy-methyl]-phosphonic acid diethyl ester (91)

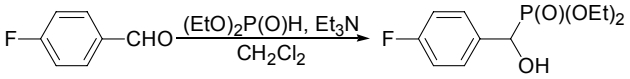

A solution of 4-fluoro-benzaldehyde (25.02 g, 201.6 mmol) and diethyl phosphite (28.60 g, 207.1 mmol) was prepared in CH_2Cl_2 (50 ml). Et_3N (21.03 g, 207.8 mmol) was added and the mixture was refluxed overnight. The mixture was allowed to reach RT and was quenched with water (100 ml). The quenched reaction mixture was extracted with CH_2Cl_2 (3x50 ml) and the combined organic phases were washed with 2 M HCl (1x50 ml) and brine (1x50 ml). After drying with $MgSO_4$ celite was added to the mixture and the solvent was removed *in vacou* leaving a solid that was subjected to DCVC(n-heptane/1,2-$C_2H_4Cl_2$ and then 1,2-$C_2H_4Cl_2$/EtOH) yielding 38.10 g (72 %) of the title compound as an oil, that slowly crystallized into a slight yellow solid; ^{1}H-NMR($CDCl_3$, 300 K): 7.49 (m, 2H), 7.00 (t, 2H, *J*=8 Hz), 5.10-4.91 (m, 2H), 4.02 (p, 4H, *J*=7 Hz), 1.23 (t, 3H, *J*=7 Hz), 1.19 (t, 3H, *J*=7 Hz); ^{13}C-NMR($CDCl_3$, 300 K): 162.4 (dd, J_1=246 Hz, J_2=3 Hz), 132.7 (dd, J_1=3 Hz, J_2=2 Hz), 128.8 (dd, J_1=8 Hz, J_2=6 Hz), 115.0 (dd, J_1=22 Hz, J_2=2 Hz), 70.0 (d, J_{PC}=161 Hz), 63.3 (d, J_{PC}=7 Hz), 62.9 (d, J_{PC}=7 Hz), 16.3, 16.2; Anal. Calcd. for $C_{11}H_{16}FO_4P$: C, 50.39; H, 6.15. Found: C, 50.32; H, 6.00.

[(4-Bromo-phenyl)-hydroxy-methyl]-phosphonic acid diethyl ester (92)

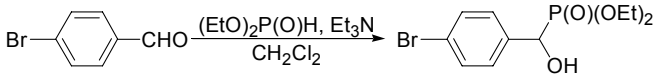

Prepared as **91**. Yield: 33.69 g (97 %), white solid; ^{1}H-NMR($CDCl_3$, 300 K): 7.48 (d, 2H, *J*=9 Hz), 7.35 (dd, 2H, J_1=9 Hz, J_2=2 Hz), 5.00 (d, 0.5H, *J*=5 Hz), 4.95 (d, 0.5H, *J*=5 Hz), 4.36 (d, 0.5H, *J*=5 Hz), 4.33 (d, 0.5H, *J*=5 Hz), 4.05 (p, 4H, *J*=7 Hz), 1.27 (t, 3H, *J*=7 Hz), 1.23 (t, 3H, *J*=7 Hz); ^{13}C-NMR($CDCl_3$, 300 K): 136.1 (d, J_{PC}=2 Hz), 131.0 (d, J_{PC}=3 Hz), 128.7 (d, J_{PC}=6 Hz), 121.7 (d, J_{PC}=4 Hz), 69.9 (d, J_{PC}=161 Hz), 63.3 (d, J_{PC}=7 Hz), 62.9 (d, J_{PC}=7 Hz), 16.2, 16.1.

[Hydroxy-(4-iodo-phenyl)-methyl]-phosphonic acid diethyl ester (93)

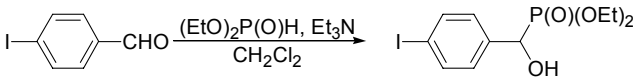

Prepared as **91**. Yield: 5.24 g (65 %), white solid; ^{1}H-NMR($CDCl_3$, 300 K): 7.70 (d, 2H, *J*=8 Hz), 7.23 (dd, 2H, J_1=9 Hz, J_1=2 Hz), 4.99 (d, 0.5H, *J*=3 Hz), 4.94 (d, 0.5H, *J*=3 Hz), 4.06 (p, 4H, *J*=7 Hz), 3.25-3.01 (bm, 1H), 1.28 (t, 3H, *J*=7 Hz), 1.25 (t, 3H, *J*=7 Hz); ^{13}C-NMR($CDCl_3$, 300 K): 137.0 (d, J_{PC}=2 Hz), 136.8 (d, J_{PC}=2 Hz), 128.9 (d, J_{PC}=6 Hz), 93.4 (d, J_{PC}=4 Hz), 70.0 (d, J_{PC}=161 Hz), 63.3 (d, J_{PC}=7 Hz), 62.9 (d, J_{PC}=7 Hz), 16.3, 16.2.

[Chloro-(4-fluoro-phenyl)-methyl]-phosphonic acid diethyl ester (94)

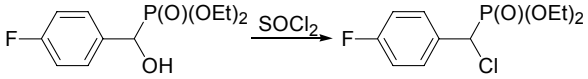

A solution of [(4-fluoro-phenyl)-hydroxy-methyl]-phosphonic acid diethyl ester (12.50 g, 47.7 mmol) dissolved in $SOCl_2$ (20 ml) was left stirring overnight at RT. Excess $SOCl_2$ was removed *in vacou* and the remaining oil was taken up in CH_2Cl_2. The organic phase was washed with water (2x100 ml) and dried ($MgSO_4$). Celite was added to the mixture and the solvent was removed *in vacou*. Purification by DCVC (1,2-$C_2H_4Cl_2$, EtOH) yielded 6.81 g (51 %) of the title compound as a slight yellow oil; ^{1}H-NMR($CDCl_3$, 300 K): 7.57-7.42 (m, 2H), 7.02 (t, 2H, *J*=9 Hz), 4.85 (d, 1H, *J*=14 Hz), 4.16 (p, 2H, *J*=7 Hz), 4.09-3.78 (m, 2H), 1.29 (t, 3H, *J*=7 Hz), 1.15 (t, 3H, *J*=7 Hz); ^{13}C-NMR($CDCl_3$, 300 K): 162.8 (dd, J_1=249 Hz, J_2=3 Hz), 130.7 (dd, J_1=8 Hz, J_2=6 Hz), 130.1 (dd, J_1=3 Hz, J_2=3 Hz), 115.5 (dd, J_1=22 Hz, J_2=2 Hz), 64.0 (d, J_{PC}=7 Hz), 63.8 (d, J_{PC}=7 Hz), 52.8 (d, J_{PC}=161 Hz), 16.3 (d, J_{PC}=6 Hz), 16.1 (d, J_{PC}=6 Hz); Anal. Calcd. for $C_{11}H_{15}ClFO_3P$: C, 46.33; H, 5.48. Found: C, 46.42; H, 5.18.

[(4-Bromo-phenyl)-chloro-methyl]-phosphonic acid diethyl ester (95)

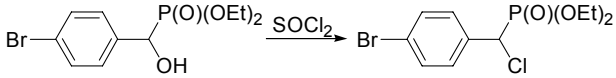

Prepared as **94**. Yield: 7.49 g (71 %), colorless oil; ^{1}H-NMR($CDCl_3$, 300 K): 7.51 (d, 2H, *J*=9 Hz), 7.41 (dd, 2H, J_1=9 Hz, J_1=2 Hz), 4.85 (d, 2H, *J*=14 Hz), 4.20 (p, 2H, *J*=7 Hz), 4.13-3.89 (m, 2H), 1.33 (t, 3H, *J*=7 Hz), 1.22 (t, 3H, *J*=7 Hz); ^{13}C-NMR($CDCl_3$, 300 K): 133.3 (d, J_{PC}=4 Hz), 131.6 (d, J_{PC}=2 Hz), 130.4 (d, J_{PC}=6 Hz), 123.1 (d, J_{PC}=3 Hz), 64.2 (d, J_{PC}=7 Hz), 63.9 (d, J_{PC}=7 Hz), 52.9 (d, J_{PC}=160 Hz), 16.3 (d, J_{PC}=6 Hz), 16.2 (d, J_{PC}=6 Hz).

[Chloro-(4-iodo-phenyl)-methyl]-phosphonic acid diethyl ester (96)

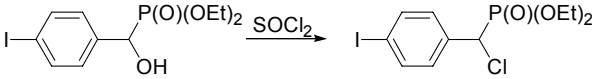

A solution of [hydroxy-(4-iodo-phenyl)-methyl]-phosphonic acid diethyl ester (4.00 g, 10.8 mmol) in $SOCl_2$ (20 ml) was stirred at RT for 3 days. Excess $SOCl_2$ was removed *in vacou* and the remaining oil was taken up in CH_2Cl_2 (1x100 ml), washed with water (2x100 ml) and dried ($MgSO_4$). Celite was added and the solvent was removed *in vacou*. Purification by DCVC (1,2-$C_2H_4Cl_2$/EtOH) yielded 3.04 g (72 %) of the title compound as a collerless oil; ^{1}H-NMR($CDCl_3$, 300 K): 7.71 (d, 2H, *J*=8 Hz), 7.27 (dd, 2H, J_1=8 Hz, J_1=2 Hz), 4.83 (d, 1H, *J*=14 Hz), 4.20 (p, 2H, *J*=7 Hz), 4.12-3.86 (m, 2H), 1.33 (t, 3H, *J*=7 Hz), 1.22 (t, 3H, *J*=7 Hz); ^{13}C-NMR($CDCl_3$, 300 K): 137.6 (d, J_{PC}=2 Hz), 134.0 (d, J_{PC}=4 Hz), 130.6 (d, J_{PC}=6 Hz), 94.9 (d, J_{PC}=3 Hz), 64.2 (d, J_{PC}=7 Hz), 63.9 (d, J_{PC}=7 Hz), 53.0 (d, J_{PC}=160 Hz), 16.4 (d, J_{PC}=6 Hz), 16.2 (d, J_{PC}=6 Hz).

2,5-Dibromo-1,4-bis-(4-fluoro-phenylethynyl)-benzene (97)

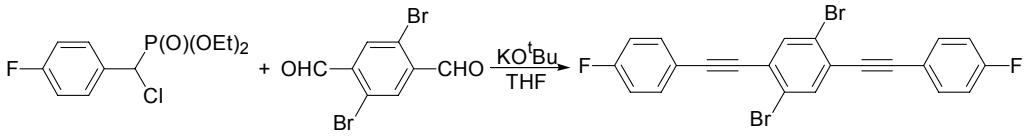

To a solution of [chloro-(4-fluoro-phenyl)-methyl]-phosphonic acid diethyl ester (2.10 g, 7.48 mmol) and 2,5-dibromo-benzene-1,4-dicarbaldehyde (0.98 g, 3.4 mmol) in THF (100 ml) was added KO^tBu (2.35 g, 20.9 mmol) and the reaction was refluxed for 1 h. The reaction mixture was allowed to reach RT and then quenched with water (50 ml). THF (100 ml) was added and the organic phase was then washed with brine (3x100 ml). After drying with $MgSO_4$ the solvent was removed *in vacou* and the isolated crude was recrystallized from a 1:1 $CHCl_3$:EtOH mixture yielding 0.32 g (20 %) of the title compound as a white solid; mp 210-212 ºC; ^{1}H-NMR($CDCl_3$, 300 K): 7.77 (s, 2H), 7.58 (d, 2H, *J*=5 Hz), 7.54 (d, 2H, *J*=5 Hz), 7.10 (d, 2H, *J*=9 Hz), 7.06 (d, 2H, *J*=9 Hz); Anal. Calcd. for $C_{22}H_{10}Br_2F_2 \cdot 0.25H_2O$: C, 55.44; H, 2.22. Found: C, 55.40; H, 2.05.

({2,5-Dibromo-4-[(diethoxy-phosphoryl)-hydroxy-methyl]-phenyl}-hydroxy-methyl)-phosphonic acid diethyl ester (98)

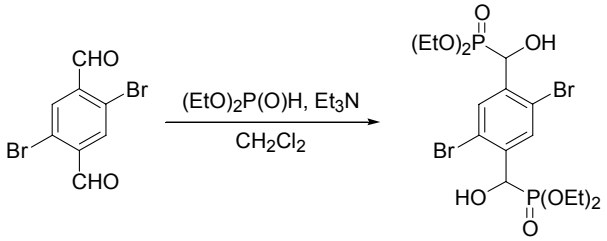

To a solution of 2,5-dibromo-terephthalaldehyde (5.38 g, 18.4 mmol) and Et_3N (3.0 ml, 22 mmol) in CH_2Cl_2 (250 ml) was added $(EtO)_2P(O)H$ (6.44 g, 46.6 mmol) and the reaction mixture was stirred at RT for 2 days. The precipitated product was filtered directly of the reaction mixture yielding 3.58 g (34 %) of the title compound as a white solid; ^{1}H-NMR(DMSO, 300 K): 7.73 (s, 2H), 6.58 (dd, 2H, J_1=11 Hz, J_2=6 Hz), 5.14 (dd, 2H, J_1=7 Hz, J_2=6 Hz), 4.12-3.86 (m, 8H), 1.21 (t, 6H, *J*=7 Hz), 1.15 (t, 6H, *J*=7 Hz); ^{13}C-NMR(DMSO, 300 K): 139.9, 133.7, 121.8 (dd, J_{PC}=6 Hz, J_{PC}=11 Hz), 68.4 (d, J_{PC}=167 Hz), 63.1 (d, J_{PC}=7 Hz), 62.7 (d, J_{PC}=7 Hz), 16.8 (d, J_{PC}=6 Hz), 16.7 (d, J_{PC}=6 Hz); Anal. Calcd. for $C_{16}H_{26}Br_2O_8P_2$: C, 33.83; H, 4.61. Found: C, 34.13; H, 4.54.

2-{2-[2-(2-Methoxy-ethoxy)-ethoxy]-ethoxy}-benzaldehyde (99)

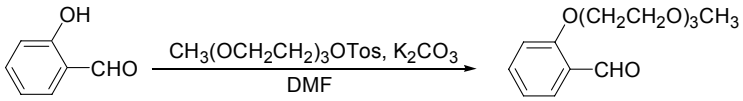

Prepared as **104**. Yield 6.70 g (70 %), light yellow oil; ^{1}H-NMR($CDCl_3$, 300 K): 10.52 (s, 1H), 7.83 (dd, 1H, J_1=8 Hz, J_2=2 Hz), 7.53 (dt, 1H, J_1=8 Hz, J_2=2 Hz), 7.03 (t, 1H, *J*=8 Hz), 7.00 (d, 1H, *J*=8 Hz), 4.25 (t, 2H, *J*=5 Hz), 3.92 (t, 2H, *J*=5 Hz), 3.78-3.61 (m, 8H), 3.58-3.52 (m, 2H), 3.37 (s, 3H); ^{13}C-NMR($CDCl_3$, 300 K): 189.6, 161.2, 135.7, 128.1, 125.1, 120.8, 112.8, 71.8, 70.9, 70.6, 70.5, 69.4, 68.2, 58.9; Anal. Calcd. for $C_{14}H_{20}O_5 \cdot 0.25H_2O$: C, 61.64; H, 7.57. Found: C, 61.68; H, 7.42.

4-{2-[2-(2-Methoxy-ethoxy)-ethoxy]-ethoxy}-benzaldehyde[37] (100)

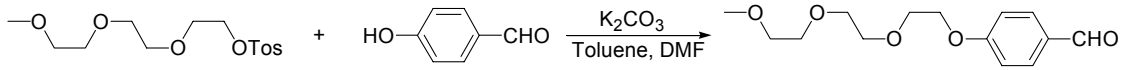

A solution of 1-{2-[2-(2-methoxy-ethoxy)-ethoxy]-ethanesulfonyl}-4-methyl-benzene (10.00 g, 31.41 mmol), 4-hydroxy-benzaldehyde (4.30 g, 35.2 mmol) and K_2CO_3 (5.73 g, 41.5 mmol) in toluene (50 ml) and DMF (100 ml) was refluxed overnight. The reaction mixture was filtered and the solvent was removed *in vacou*. The crude product was taken up in EtOAc filtered through a pad of silica. Removal of the solvent yielded 7.59 g (90 %) of the title compound as a colorless oil; ^{1}H-NMR($CDCl_3$, 300 K): 9.88 (s, 1H), 7.83 (d, 2H, *J*=9 Hz), 7.02 (d, 2H, *J*=9 Hz), 4.22 (t, 2H, *J*=5 Hz), 3.89 (t, 2H, *J*=5 Hz), 3.77-3.62 (m, 6H), 3.58-3.52 (m, 2H), 3.47 (s, 3H); ^{13}C-NMR($CDCl_3$, 300 K): 190.7, 163.8, 131.9, 130.1, 114.9, 72.0, 70.9, 70.7, 70.6, 69.5, 67.8, 59.0.

2,4-Bis-{2-[2-(2-methoxy-ethoxy)-ethoxy]-ethoxy}-benzaldehyde (101)

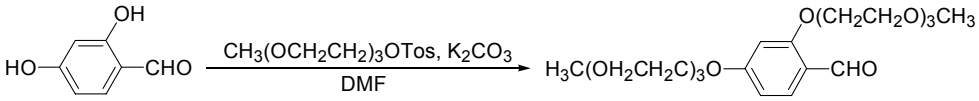

Prepared as **104**. Yield 4.06 g (61 %), light yellow oil; ^{1}H-NMR($CDCl_3$, 300 K): 10.35 (s, 1H), 7.60 (d, 1H, *J*=9 Hz), 6.55 (dd, 1H, J_1=9 Hz, J_2=2 Hz), 6.49 (d, 1H, *J*=2 Hz), 4.20 (t, 2H, *J*=4 Hz), 4.18 (t, 2H, *J*=4 Hz), 3.94-3.84 (m, 4H), 3.77-3.61 (m, 12H), 3.59-3.52 (m, 4H), 3.38 (s, 6H); ^{13}C-NMR($CDCl_3$, 300 K): 188.0, 165.1, 162.8, 130.0, 119.2, 106.7, 99.5, 71.7, 70.8, 70.7, 70.5, 70.4, 69.3, 69.2, 68.1, 67.6, 58.7; Anal. Calcd. for $C_{21}H_{34}O_9 \cdot 0.5H_2O$: C, 57.39; H, 8.03. Found: C, 57.24; H, 7.94; HRMS(EI+): m/z calcd. for $C_{21}H_{34}O_9^{+\cdot}$ 430.2202, found 430.2196.

3,4-Bis-{2-[2-(2-methoxy-ethoxy)-ethoxy]-ethoxy}-benzaldehyde (102)

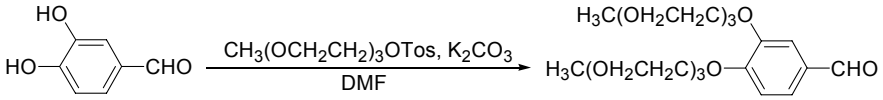

Prepared as **104**. Yield 4.96 g (73 %), light yellow oil; ^{1}H-NMR($CDCl_3$, 300 K): 9.84 (s, 1H), 7.46 (d, 1H, *J*=2 Hz), 7.43 (t, 1H, *J*=2 Hz), 7.01 (d, 1H, *J*=9 Hz), 4.28-4.19 (m, 4H), 3.91 (t, 2H, *J*=4 Hz), 3.89 (t, 2H, *J*=4 Hz), 3.79-3.72 (m, 4H), 3.70-3.61 (m, 8H), 3.58-3.51 (m, 4H), 3.37 (s, 6H); ^{13}C-NMR($CDCl_3$, 300 K): 190.6, 154.4, 149.3, 130.4, 126.3, 112.8, 112.5, 71.9, 70.9 (2C), 70.6, 70.5, 69.5, 69.4, 68.9, 68.7, 58.9; HRMS(EI+): m/z calcd. for $C_{21}H_{34}O_9^{+\cdot}$ 430.2202, found 430.2211.

3,5-Bis-{2-[2-(2-methoxy-ethoxy)-ethoxy]-ethoxy}-benzaldehyde (103)

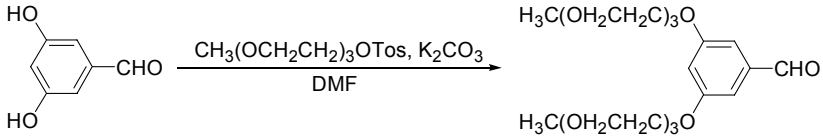

Prepared as **104**. Yield 4.27 g (64 %), light yellow oil; ^{1}H-NMR($CDCl_3$, 300 K): 9.88 (s, 1H), 7.02 (d, 2H, *J*=2 Hz), 6.76 (t, 1H, *J*=2 Hz), 4.16 (t, 4H, *J*=5 Hz), 3.87 (t, 4H, *J*=5 Hz), 3.77-3.62 (m, 12H), 3.58-3.52 (m, 4H), 3.38 (s, 6H); ^{13}C-NMR($CDCl_3$, 300 K): 191.5, 160.3, 138.3, 108.2, 107.9, 71.8,

70.7, 70.5, 70.4, 69.4, 67.8, 58.8; Anal. Calcd. for $C_{21}H_{34}O_9 \cdot 0.5H_2O$: C, 57.39; H, 8.03. Found: C, 57.50; H, 8.00; HRMS(EI+): m/z calcd. for $C_{21}H_{34}O_9^{+\cdot}$ 430.2202, found 430.2205.

3,4,5-Tris-{2-[2-(2-methoxy-ethoxy)-ethoxy]-ethoxy}-benzaldehyde (104), general procedure

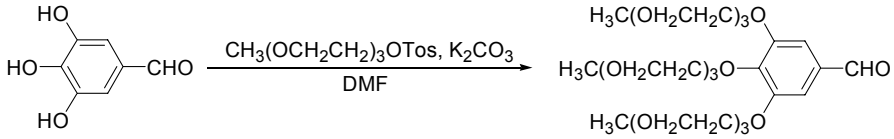

To a solution of 3,4,5-trihydroxy-benzaldehyde (1.22 g, 7.92 mmol) and 1-{2-[2-(2-methoxy-ethoxy)-ethoxy]-ethanesulfonyl}-4-methyl-benzene (8.34 g, 26.2 mmol) in DMF (50 ml) was added K_2CO_3 (7.03 g, 50.9 mmol). The reaction was left stirring at 100 ºC for 3 days and then cooled to RT and poured into 2 M H_2SO_4 (200 ml). The mixture was extracted with CH_2Cl_2 (3x100 ml) and the combined organic phases were then washed with brine (2x100 ml). The organic phase was dried over $MgSO_4$ and the solvent removed *in vacou* leaving the crude product, which was purified using DCVC with AlO_2 as the column material (1,2-$C_2H_4Cl_2$/EtOH) yielding 1.97 g (42 %) of the title compound as a light yellow oil; ^{1}H-NMR($CDCl_3$, 300 K): 9.82 (s, 1H), 7.14 (s, 2H), 4.25 (t, 2H, *J*=5 Hz), 4.21 (t, 4H, *J*=5 Hz), 3.86 (t, 4H, *J*=5 Hz), 3.79 (t, 2H, *J*=5 Hz), 3.75-3.49 (m, 24H), 3.36 (s, 9H); ^{13}C-NMR($CDCl_3$, 300 K): 190.8, 153.0, 144.2, 131.6, 109.1, 72.5, 71.9, 70.8, 70.7, 70.6, 70.5, 69.6, 69.0, 59.0, 43.4; HRMS(EI+): m/z calcd. for $C_{28}H_{48}O_{13}^{+\cdot}$ 592.3094, found 592.3098.

***E, E*-2,5-Dibromo-1,4-Bis-[2-(2'-{2-[2-(2-Methoxy-ethoxy)-ethoxy]-ethoxy}-phenyl)-vinyl]-benzene (105), general procedure**

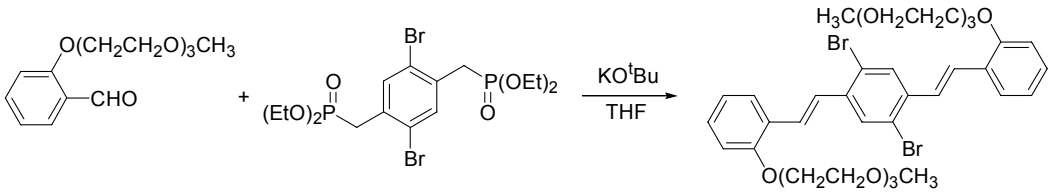

To a solution of 2-{2-[2-(2-Methoxy-ethoxy)-ethoxy]-ethoxy}-benzaldehyde (1.82 g, 6.78 mmol) and [2,5-Dibromo-4-(diethoxy-phosphorylmethyl)-benzyl]-phosphonic acid diethyl ester (1.71 g, 3.19 mmol) in THF (100 ml) was added KO^{t}Bu (1.34 g, 11.9 mmol) and the mixture was refluxed for 2 h. The reaction mixture was quenched with 2 M HCl (25 ml) and then washed with brine (3x100 ml). The isolated organic phase was dried with $MgSO_4$ and evaporated onto celite and subjected to DCVC (EtOAc/EtOH). Yield 1.03 g (42 %), brown oil that slowly crystallizes; ^{1}H-NMR($CDCl_3$, 300 K): 7.88 (s, 2H), 7.60 (dd, 2H, J_1=8 Hz, J_2=2 Hz), 7.41 (s, 4H), 7.27 (dt, 2H, J_1=8 Hz, J_2=2 Hz), 7.00 (dt, 2H, J_1=8 Hz, J_2=1 Hz), 6.93 (d, 2H, *J*=8 Hz), 4.23 (t, 4H, *J*=5 Hz), 3.95 (t, 4H, *J*=5 Hz), 3.82-3.48 (m, 12H), 3.35 (s, 6H); ^{13}C-NMR($CDCl_3$, 300 K): 156.5, 137.8, 130.2, 129.301, 127.3, 126.2, 126.0, 122.9, 121.1, 112.5, 71.8, 70.9, 70.6, 70.4, 69.7, 68.1, 58.8; Anal. Calcd. for $C_{36}H_{44}Br_2O_8$: C, 56.56; H, 5.80. Found: C, 56.68; H, 5.65.

***E, E*-2,5-Dibromo-1,4-Bis-[2-(4'-{2-[2-(2-Methoxy-ethoxy)-ethoxy]-ethoxy}-phenyl)-vinyl]-benzene (106)**

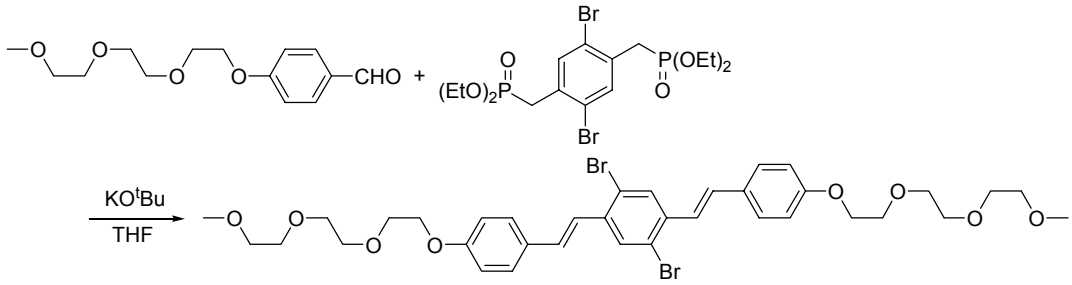

Recrystallized from EtOAc. Yield 1.12 g (46 %); ^{1}H-NMR($CDCl_3$, 300 K): 7.84 (s, 2H), 7.48 (d, 4H, *J*=8.9 Hz), 7.23 (d, 2H, *J*=16.1 Hz), 6.99 (d, 2H, *J*=16.3 Hz), 6.93 (d, 2H, *J*=8.7 Hz), 4.17 (t, 4H, *J*=5.2 Hz), 3.88 (t, 4H, *J*=4.8 Hz), 3.79-3.63 (m, 12H), 3.60-3.52 (m, 4H), 3.39 (s, 6H); ^{13}C-NMR($CDCl_3$, 300 K): 159.1, 137.2, 131.6, 130.0, 129.6, 128.2, 123.7, 122.8, 114.9, 71.9, 70.9, 70.7, 70.6, 70.0, 67.5, 59.0; Anal. Calcd. for $C_{36}H_{44}Br_2O_8$: C, 56.56; H, 5.80. Found: C, 56.85; H, 5.74.

***E, E*-2,5-Dibromo-1,4-Bis-[2-(2', 4'-Bis-{2-[2-(2-Methoxy-ethoxy)-ethoxy]-ethoxy}-phenyl)-vinyl]-benzene (107)**

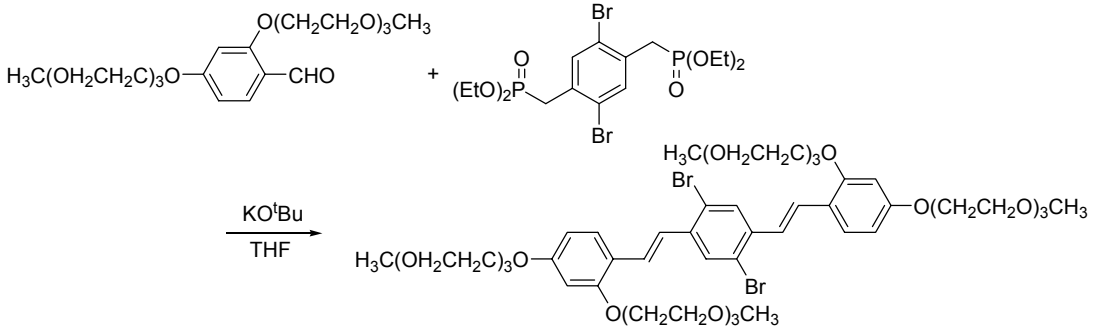

Purified using DCVC with neutral AlO_2 as the column material (1,2-$C_2H_4Cl_2$/EtOH). Yield 2.39 g (63 %), brown oil; ^{1}H-NMR($CDCl_3$, 300 K): 7.84 (s, 2H), 7.50 (d, 4H, *J*=8 Hz), 7.30 (s, 4H), 6.57-6.50 (m, 4H), 4.22-4.14 (m, 8H), 3.94 (t, 4H, *J*=5 Hz), 3.87 (t, 4H, *J*=5 Hz), 3.82-3.60 (m, 28H), 3.59-3.48 (m, 8H), 3.38 (s, 6H), 3.35 (s, 6H); ^{13}C-NMR($CDCl_3$, 300 K): 160.0, 157.5, 137.6, 129.7, 128.1, 126.8, 124.0, 122.6, 119.2, 106.3, 100.2, 71.7 (2C), 70.8, 70.6, 70.5, 70.4, 70.3, 69.5, 68.0, 67.4, 58.7 (2C); HRMS(EI+): m/z calcd. for $C_{50}H_{72}Br_2O_{16}^{+\cdot}$ 1088.3174, found 1088.3199.

***E, E*-2,5-Dibromo-1,4-Bis-[2-(3', 4'-Bis-{2-[2-(2-Methoxy-ethoxy)-ethoxy]-ethoxy}-phenyl)-vinyl]-benzene (108)**

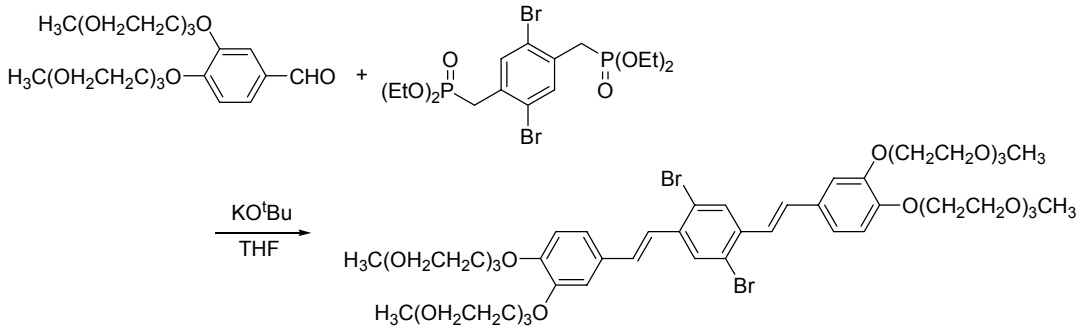

Purified using DCVC with neutral AlO_2 as the column material (1,2-$C_2H_4Cl_2$/EtOH). Yield 2.55 g (66 %), brown oil; ^{1}H-NMR($CDCl_3$, 300 K): 7.84 (s, 2H), 7.20 (d, 2H, *J*=16 Hz), 7.16-7.07 (m, 4H), 6.96 (d, 2H, *J*=16 Hz), 6.92 (d, 2H, *J*=8 Hz), 4.27-4.16 (m, 8H), 3.93-3.84 (m, 8H), 3.79-3.61 (m, 24H), 3.59-3.52 (m, 8H), 3.38 (s, 6H), 3.37 (s, 6H); ^{13}C-NMR($CDCl_3$, 300 K): 149.5, 149.0, 137.1, 131.7, 130.3, 130.0, 123.9, 122.7, 121.0, 114.5, 113.1, 71.8, 70.7, 70.5, 70.4, 69.7, 69.6, 69.0, 68.7, 58.8; Anal. Calcd. for $C_{50}H_{72}Br_2O_{16}$: C, 55.15; H, 6.66. Found: C, 54.54; H, 6.55.

***E, E*-2,5-Dibromo-1,4-Bis-[2-(3', 5'-Bis-{2-[2-(2-Methoxy-ethoxy)-ethoxy]-ethoxy}-phenyl)-vinyl]-benzene (109)**

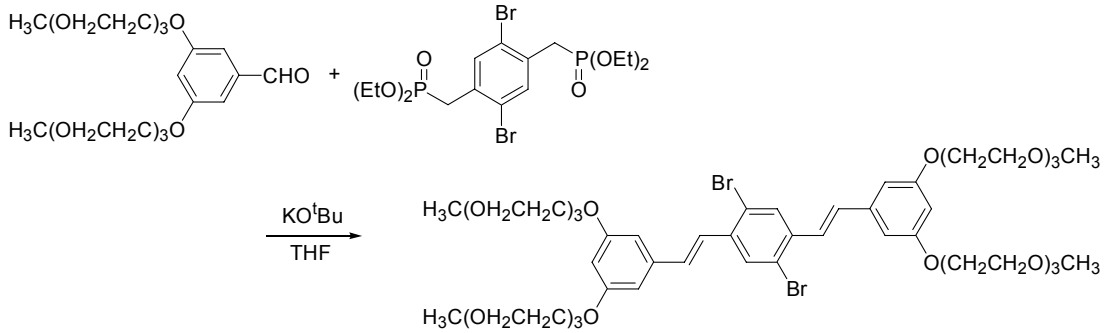

Purified using DCVC with neutral AlO_2 as the column material (1,2-$C_2H_4Cl_2$/EtOH). Yield 2.53 g (68 %), brown oil; ^{1}H-NMR($CDCl_3$, 300 K): 7.85 (s, 2H), 7.31 (d, 2H, *J*=16 Hz), 6.95 (d, 2H, *J*=16 Hz), 6.72 (d, 4H, *J*=2 Hz), 6.47 (t, 2H, *J*=2 Hz), 4.16 (t, 8H, *J*=5 Hz), 3.87 (t, 8H, *J*=5 Hz), 3.79-3.62 (m, 26H), 3.59-3.52 (m, 8H), 3.38 (s, 12H); ^{13}C-NMR($CDCl_3$, 300 K): 160.2, 138.5, 137.4, 132.3, 130.4, 126.3, 123.0, 106.1, 102.0, 71.9, 70.8, 70.7, 70.5, 70.0, 67.6, 58.9; Anal. Calcd. for $C_{50}H_{72}Br_2O_{16}$: C, 55.15; H, 6.66. Found: C, 55.36; H, 6.70.

***E,E*-2,5-dibromo-1,4-bis-[2-(3',4',5'-Tris-{2-[2-(2-methoxy-ethoxy)-ethoxy]-ethoxy}-phenyl)-vinyl]-benzene (110)**

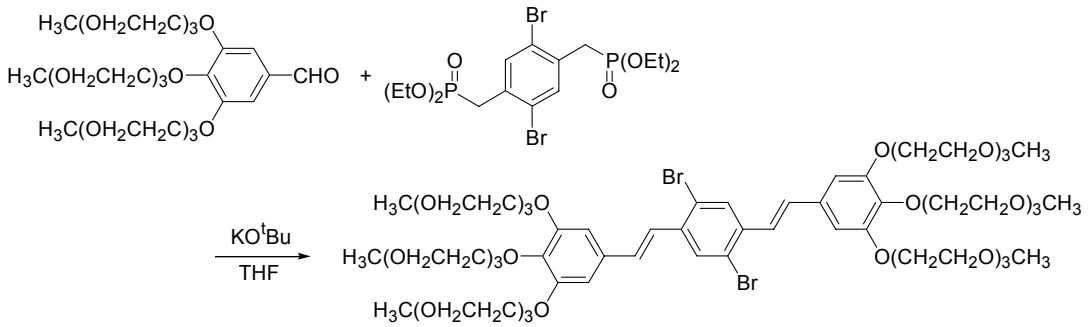

A solution of [4-(diethoxy-phosphorylmethyl)-2,5-dibromo-benzyl]-phosphonic acid diethyl ester (0.45 g, 0.84 mmol) and 3,4,5-Tris-{2-[2-(2-methoxy-ethoxy)-ethoxy]-ethoxy}-benzaldehyde (1.14 g, 1.92 mmol) in THF (100 ml) was Ar-purged. KO^{t}Bu (0.54 g, 4.8 mmol) was added and the reaction mixture was refluxed for 2 h. and then quenched with water (50 ml). Brine (50 mol) was added and the crude reaction mixture was continuous extracted with THF overnight. The isolated organic phase was evaporated and the isolated crude product was purified by column chromatography (neutral AlO_2 with 1,2-$C_2H_4Cl_2$ and EtOH as eluent system) yielding 1.00 g (84 %) of the title compound as an light yellow oil. Further purification was done by GPC; ^{1}H-NMR($CDCl_3$, 300 K): 7.84 (s, 2H), 7.21 (d, 2H, *J*=16 Hz), 6.94 (d, 2H, *J*=16 Hz), 6.80 (s, 4H), 4.26-4.16 (m, 12H), 3.88 (t, 8H, *J*=5 Hz), 3.81 (t, 4H, *J*=5 Hz), 3.78-3.59 (m, 46H), 3.58-3.50 (m, 12H), 3.38 (s, 6H), 3.37 (s, 12H); ^{13}C-NMR($CDCl_3$, 300 K): 152.7, 152.3, 139.2, 137.1, 131.9, 130.1, 124.9, 122.8, 106.9, 72.3, 71.8, 70.7, 70.5, 70.4, 70.3, 69.6, 68.9, 58.8; Anal. Calcd. for $C_{64}H_{100}Br_2O_{24}$: C, 54.39; H, 7.13. Found: C, 54.56; H, 7.02.

Acetic acid 2,3-diacetoxy-5-hydroxymethyl-phenyl ester[38] (111)

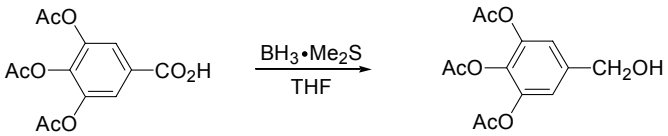

A solution of 3,4,5-triacetoxy-benzoic acid (9.95 g, 33.6 mmol) in THF (100 ml) was cooled to 0 ºC and a 2 M BH_3·Me_2S in THF solution (50 ml) was added. The reaction mixture was stirred overnight at RT and then quenched with MeOH (100 ml). After the H_2 production has ceased the mixture was evaporated onto celite and purified by DCVC(n-heptane/ EtOAc) yielding 6.86 g (72 %) of the title compound as a white powder; ^{1}H-NMR($CDCl_3$, 300 K): 7.12 (s, 1H), 4.68 (d, 2H, *J*=6 Hz), 2.28 (s, 3H), 2.28 (s, 6H), 1.85 (t, 1H, *J*=6 Hz); ^{13}C-NMR($CDCl_3$, 300 K): 169.9, 167.0, 143.3, 139.9, 133.4, 118.6, 63.7, 20.5, 20.0; Anal. Calcd. for $C_{13}H_{14}O_7$: C, 55.32; H, 5.00. Found: C, 55.44; H, 4.91.

3,4,5-Triacetoxy-benzaldehyde[39,40] (112)

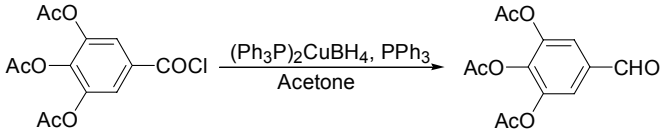

To a solution of freshly prepared 3,4,5-triacetoxy-benzoic acid chloride (10.16 g, 32.29 mmol) in acetone (200 ml) was added PPh_3 (17.34 g, 66.11 mmol). After the PPh_3 was dissolved $(Ph_3P)_2CuBH_4$ (21.83 g, 36.20 mmol) was added and the reaction mixture was refluxed for 2 h. The reaction mixture was then filtered and the filter cake washed with Et_2O. The organic phase was evaporated leaving the crude product, which was then taken up in MeOH (250 ml) and stirred overnight at RT. The mixture was filtered and the solvent removed *in vacou* leaving an oil which was taken up in $CHCl_3$ (50 ml). To this mixture was added CuCl (6.02 g, 60.8 mmol) and the mixture was stirred for 30 min. at RT and was then filtered. The isolated organic phase was evaporated leaving the crude product, which was purified by DCVC (n-heptane/EtOAc) leaving 5.06 (56 %) of the title compound as an off-white solid; ^{1}H-NMR($CDCl_3$, 300 K): 9.92 (s, 1H), 7.66 (s, 2H), 2.31 (s, 3H), 2.30 (s, 6H); ^{13}C-NMR($CDCl_3$, 300 K): 189.2, 167.4, 166.2, 144.2, 139.6, 134.0, 121.6, 20.5, 20.0.

3,4,5-Triacetoxy-benzaldehyde[39,40] (112)

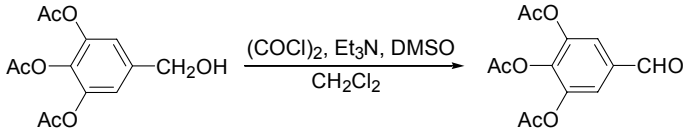

A solution of $(COCl)_2$ (2.80 g, 22.1 mmol) in CH_2Cl_2 (100 ml) was cooled to -78 ºC. DMSO (3.0 ml, 42 mmol) was then added and the mixture was stirred for 30 min. at -78 ºC. Acetic acid 2,3-diacetoxy-5-hydroxymethyl-phenyl ester (5.00 g, 17.7 mmol) dissolved in CH_2Cl_2 (30 ml) was added. Et_3N (13 ml, 94 mmol) was added and the mixture was allowed to reach RT and further stirred for 1 h at RT. The reaction mixture was quenched with saturated aquoues $NaHCO_3$ (50 ml) and the organic phase was isolated. The aqoues phase was washed with CH_2Cl_2 (3x25 ml). The combined organic phases was washed with saturated $NaHCO_3$ (3x50 ml) and then dried with $MgSO_4$. The organic phase was evaporated onto celite subjected to DCVC (n-heptane/EtOAc) yielding 3.49 g (70 %); ^{1}H-NMR($CDCl_3$, 300 K): 9.92 (s, 1H), 7.66 (s, 2H), 2.32 (s, 3H), 2.31 (s, 6H); ^{13}C-NMR($CDCl_3$, 300 K): 189.1, 167.4, 166.2, 144.3, 139.6, 134.1, 121.6, 20.5, 20.1; Anal. Calcd. for $C_{13}H_{14}O_7$: C, 55.72; H, 4.32. Found: C, 55.72; H, 4.20.

4-[Bis-(2-hydroxy-ethyl)-amino]-benzaldehyde[41] (113)

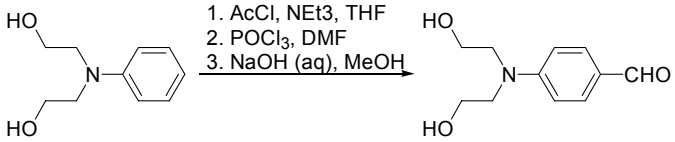

1. A solution of 2-[(2-hydroxy-ethyl)-phenyl-amino]-ethanol (24.94 g, 137.6 mmol) and Et_3N (31.97 g, 315.9 mmol) was prepared in THF (400 ml). AcCl (25.87 g, 329.6 mmol) was added carefully dropwise and the reaction mixture was left stirring overnight at 35 ˚C. The reaction mixture was quenched with water (400 ml) and the organic phase was isolated. The aqueous phase was extracted

THF (3x100 ml). The combined organic phases were dried ($MgSO_4$) and removal of the solvent left 34.26 g (94 %) of acetic acid 2-[(2-acetoxy-ethyl)-phenyl-amino]-ethyl ester as an off-white solid; ^{1}H-NMR($CDCl_3$, 300 K): 7.24 (dt, 2H, J_1=7 Hz, J_2=2 Hz), 6.76 (d, 2H, *J*=8 Hz), 6.73 (t, 1H, *J*=7 Hz), 4.24 (t, 4H, *J*=6 Hz), 3.63 (t, 4H, *J*=6 Hz), 2.05 (s, 6H); ^{13}C-NMR($CDCl_3$, 300 K): 170.9, 147.2, 129.4, 117.1, 112.2, 61.5, 50.0, 20.8.

2. To a solution of 4-[bis-(2-hydroxy-ethyl)-amino]-benzaldehyde (44.63 g, 168.2 mmol) in DMF (200 ml) cooled to 0 ˚C was slowly added $POCl_3$ (29.83 g, 194.5 mmol). After $POCl_3$ has been added the temperature was raised to 80 ˚C and the reaction mixture was stirred at this temperature for 4 h. The solution was then allowed to reach RT and poured into a 0.3 M Na_2CO_3 (2.5 L) solution and stirred at RT for 1 day. The quenched reaction mixture was extracted with Et_2O (8x200 ml) and the combined organic phases were dried ($MgSO_4$). Removal of the solvent *in vacou* left 43.22 g (88 %) of acetic acid 2-[(2-acetoxy-ethyl)-(4-formyl-phenyl)-amino]-ethyl ester as a brown oil that slowly crystallized; ^{1}H-NMR($CDCl_3$, 300 K): 9.76 (s, 1H), 7.74 (d, 2H, *J*=9 Hz), 6.81 (d, 2H, *J*=9 Hz), 4.28 (t, 4H, *J*=6 Hz), 3.71 (t, 4H, *J*=6 Hz), 2.04 (s, 6H); ^{13}C-NMR($CDCl_3$, 300 K): 190.1, 170.7, 152.1, 132.1, 126.3, 111.3, 60.9, 49.6, 20.8.

3. To a solution of acetic acid 2-[(2-acetoxy-ethyl)-(4-formyl-phenyl)-amino]-ethyl ester (11.40 g, 38.9 mmol) in EtOH (100 ml) was added 1 M NaOH (100 ml) and the reaction mixture was stirred for 2 h. at RT. Brine (50 ml) was then added and the quenched reaction mixture was extracted with EtOAc (3x100 ml). The combined organic phases were dried with $MgSO_4$ and celite was added. Removal of the solvent and purification with DCVC (toluene/AcCN) left 7.10 g (87 %) of the title compound as an yellow oil, which slowly crystallized; ^{1}H-NMR(DMSO, 300 K): 9.63 (s, 1H), 7.64 (d, 2H, *J*=9 Hz), 6.81 (d, 2H, *J*=9 Hz), 4.83 (t, 2H, *J*=5 Hz), 3.63-3.47 (m, 8H); ^{13}C-NMR(DMSO, 300 K): 189.4, 152.8, 131.5, 124.2, 110.8, 57.9, 53.0.

4-[Bis-(2-{2-[2-(2-methoxy-ethoxy)-ethoxy]-ethoxy}-ethyl)-amino]-benzaldehyde (114)

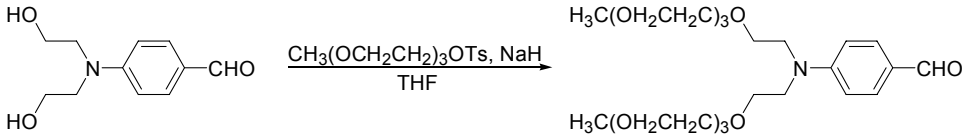

A reaction flask was charged with NaH (2.50 g of a 60 % dispersion in mineral oil, 62.5 mmol) and the NaH was washed with THF (2x50 ml). The washed NaH was then suspended in THF (50 ml). 4-[Bis-(2-hydroxy-ethyl)-amino]-benzaldehyde (2.75 g, 13.1 mmol) dissolved in THF (50 ml) was then added and the reaction mixture was refluxed for 1 h. Tosylated triethylene glycol monomethyl ether (9.50 g, 29.8 mmol) was then added and the reaction mixture was refluxed for 2 days. The reaction mixture was cooled to RT and then poured into H_2SO_4 (2 M, 200 ml) and extracted with CH_2Cl_2 (3x100 ml). The combined organic phases were dried ($MgSO_4$), filtered, and deposited onto celite and purified by DCVC (Et_2O/acetone) yielding 5.66 g (86 %) of the title compound as a pale yellow oil; ^{1}H-NMR($CDCl_3$): 9.69 (s, 1H), 7.66 (d, 2H, *J*=9 Hz), 6.72 (d, 2H, *J*=9 Hz), 3.66-3.47 (m, 32H), 3.34 (s, 6H); HRMS(EI+): m/z calcd. for $C_{25}H_{43}NO_9^{+\cdot}$ 501.2938, found 501.2940.

***E,E*-2,5-dibromo-1,4-bis-[2-(3',4',5'-Tris-{2-[2-(2-methoxy-ethoxy)-ethoxy]-ethoxy}-phenyl)-vinyl]-benzene (115)**

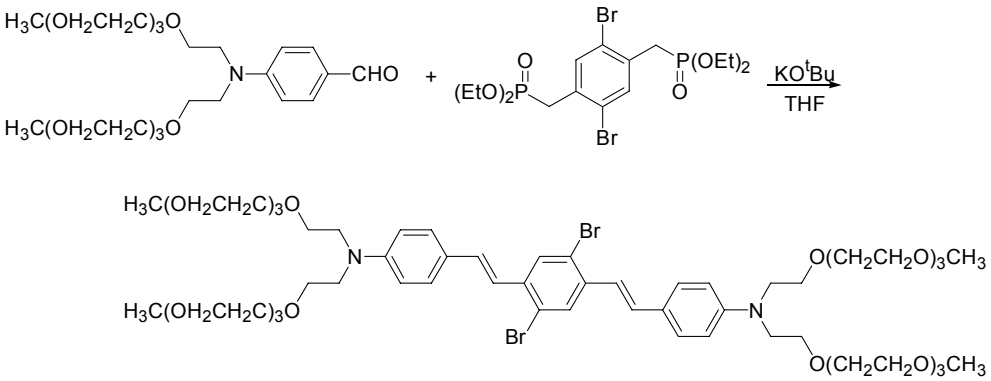

A solution of [2,5-Dibromo-4-(diethoxy-phosphorylmethyl)-benzyl]-phosphonic acid diethyl ester (0.53 g, 0.99 mmol) and 4-[bis-(2-{2-[2-(2-methoxy-ethoxy)-ethoxy]-ethoxy}-ethyl)-amino]-benzaldehyde (0.97 g, 1.97 mmol) in THF (100 mL) was Ar-purged for 15 min. KO^{t}Bu (0.42 g, 3.7 mmol) was added and the reaction mixture was refluxed for 2 days and then quenched with water (50 mL). Brine (50 mL) was added and the crude reaction mixture was continuously extracted with THF overnight. The isolated organic phase was deposited onto celite and purified by DCVC using neutral Al_2O_3 as the column material and eluting first with n-heptane/EtOAc and then with EtOAc/1,2-$C_2H_4Cl_2$ yielding 0.12 g (10 %) of the title compound as a red oil; ^{1}H-NMR($CDCl_3$): 7.81 (s, 2H), 7.40 (d, 4H, *J*=9 Hz), 7.13 (d, 2H, *J*=16 Hz), 6.94 (d, 2H, *J*=16 Hz), 6.71 (d, 4H, *J*=9 Hz), 3.73-3.49 (m, 64H), 3.37 (s, 12H); ^{13}C-NMR($CDCl_3$): 147.8, 137.1, 131.6, 129.5, 128.3, 125.0, 122.5, 121.3, 111.9, 71.9, 70.7, 70.6, 70.5, 68.4, 59.0, 51.0; Anal. Calcd. for $C_{58}H_{90}Br_2N_2O_{16}\cdot 0.5H_2O$: C, 56.17; H, 7.40; N, 2.26. Found: C, 55.92; H, 7.31; N, 2.20.

***N,N*-di-(2-t-butyldimethylsilyloxy)-ethyl-aniline (116)**

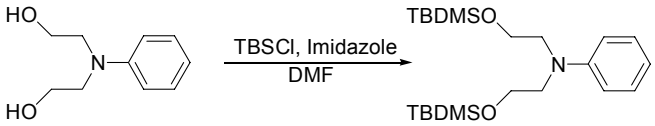

To a solution of t-butyldimethylsilylchloride (15.04 g, 99.8 mmol) and imidazole (8.16 g, 120 mmol) in DMF (100 ml) cooled to 0 ºC was added of N-phenyl-diethanolamine (7.37 g, 40.7 mmol). The reaction mixture was stirred overnight at RT and then poured into water (400 ml). The mixture was extracted with ether and the combined organic phases was washed with brine and then dried over $MgSO_4$. Evaporation of the solvent yielded 15.18 g (91 %) of the title compound as an colorless oil; ^{1}H-NMR($CDCl_3$, 300 K): 7.21 (d, 1H, *J*=7 Hz), 7.17 (d, 1H, *J*=7 Hz), 6.68 (d, 2H, *J*=8 Hz), 6.63 (d, 1H, *J*=7 Hz), 3.75 (t, 4H, *J*=7 Hz), 3.50 (t, 4H, *J*=7 Hz), 0.90 (s, 18H), 0.04 (s, 12H); ^{13}C-NMR($CDCl_3$, 300 K): 148.0, 129.2, 115.8, 111.6, 60.4, 53.6, 25.9, 18.3, -5.3.

4-Bromo-*N,N*-di-(2-t-butyldimethylsilyloxy)-ethyl-aniline (117)

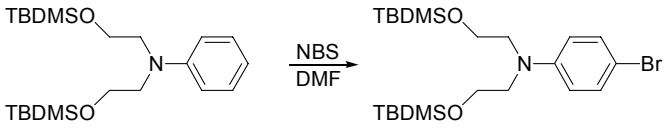

To a solution of NBS (7.04 g, 39.6 mmol) in DMF (30 ml) cooled to 0 ºC was added of *N,N*-di-(2-t-butyldimethylsilyloxy)-ethyl-aniline (15.18 g, 37.05 mmol). The flask was covered with aluminum foil and stirred overnight at RT in the dark. The reaction mixture was then poured into ice and extracted with Et_2O. The combined organic phases was washed with brine and then dried over $MgSO_4$. Removal of the solvent *in vacou* left the crude product, which was purified by column chromatography (short column and 70-230 mesh SiO_2 with toluene as the eluent). Removal of the solvent left a colorless oil yielding 12.13 g (67 %) of the title compound. A sample to determine elemental composition was obtained by purifying by DCVC (n-heptane/toluene); ^{1}H-NMR($CDCl_3$, 300 K): 7.24 (d, 2H, *J*=9 Hz), 6.56 (d, 2H, *J*=9 Hz), 3.73 (t, 4H, *J*=6 Hz), 3.47 (t, 4H, *J*=6 Hz), 0.89 (s, 18H), 0.03 (s, 12H); ^{13}C-NMR($CDCl_3$, 300 K): 147.1, 131.7, 113.4, 107.5, 60.2, 53.6, 25.8, 18.2, -5.4; Anal. Calcd. for $C_{22}H_{42}BrNO_2Si_2 \cdot 0.5H_2O$: C, 53.10; H, 8.71; N, 2.81. Found: C, 52.74; H, 8.51; N, 2.78.

4-{Bis-[2-(tert-butyl-dimethyl-silanyloxy)-ethyl]-amino}-benzaldehyde (118)

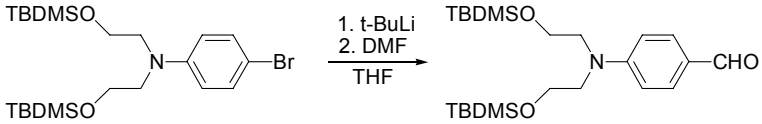

A solution of 4-Bromo-*N,N*-di-(2-t-butyldimethylsilyloxy)-ethyl-aniline (8.64 g, 17.7 mmol) in THF (150 ml) was cooled to -78 ºC. To the cooled mixture was added 1.7 M t-BuLi in pentane (30 ml, 51 mmol) and the reaction mixture was stirred for 50 min. at -78 ºC. DMF (5 ml, 65 mmol) was then added and the reaction mixture was allowed to warm to RT and then quenched with brine. The quenched mixture was extracted with Et_2O and the combined organic phases was washed with brine and then dried over $MgSO_4$. Removal of the solvent *in vacou* left the crude product, which was purified by DVCC (n-heptane/EtOAc) yielding 5.80 g (75 %) of the title compound. A sample to determine elemental composition was obtained by purifying once more by column chromatography; ^{1}H-NMR($CDCl_3$, 300 K): 9.72 (s, 1H), 7.70 (d, 2H, *J*=9 Hz), 6.74 (d, 2H, *J*=9 Hz), 3.80 (t, 4H, *J*=6 Hz), 3.61 (t, 4H, *J*=6 Hz), 0.88 (s, 18H), 0.02 (s, 12H); ^{13}C-NMR($CDCl_3$, 300 K): 189.9, 152.9, 132.0, 125.3, 111.1, 60.2, 53.5, 25.8, 18.2, -5.5; Anal. Calcd. for $C_{23}H_{43}NO_3Si_2 \cdot 0.5H_2O$: C, 61.83; H, 9.93; N, 3.14. Found: C, 61.73; H, 9.80; N, 3.20.

***E,E*-2,5-dibromo-1,4-bis-[2-(4'-{Bis-[2-(tert-butyl-dimethyl-silanyloxy)-ethyl]-amino}-phenyl)-vinyl]-benzene (119)**

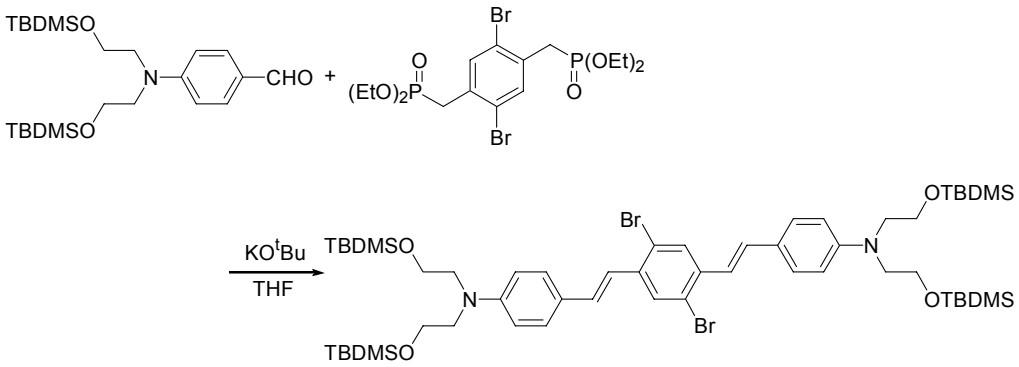

The isolated organic phase was evaporated onto celite and subjected to DCVC (n-heptane/EtOAc). Yield 0.30 g (49 %), red powder; A sample to determine elemental composition was obtained by recrystallizing twice from EtOH; ^{1}H-NMR($CDCl_3$, 300 K): 7.82 (s, 2H), 7.41 (d, 4H, *J*=9 Hz), 7.13 (d, 2H, *J*=16 Hz), 6.95 (d, 2H, *J*=16 Hz), 6.69 (d, 4H, *J*=9 Hz), 3.78 (t, 8H, *J*=6 Hz), 3.55 (t, 8H, *J*=6 Hz), 0.90 (s, 38H), 0.05 (s, 24H); ^{13}C-NMR($CDCl_3$, 300 K): 148.2, 137.2, 131.8, 129.6, 128.3, 124.6, 122.6, 121.1, 111.6, 60.3, 53.6, 25.9, 18.2, -5.4; Anal. Calcd. for $C_{54}H_{90}Br_2N_2O_4Si_4$: C, 58.78; H, 8.22; N, 2.54. Found: C, 58.78; H, 8.23; N, 2.54.

***E,E*-2,5-dibromo-1,4-bis-[2-(4'-{bis-ethanol}-amino-phenyl)-vinyl]-benzene (120)**

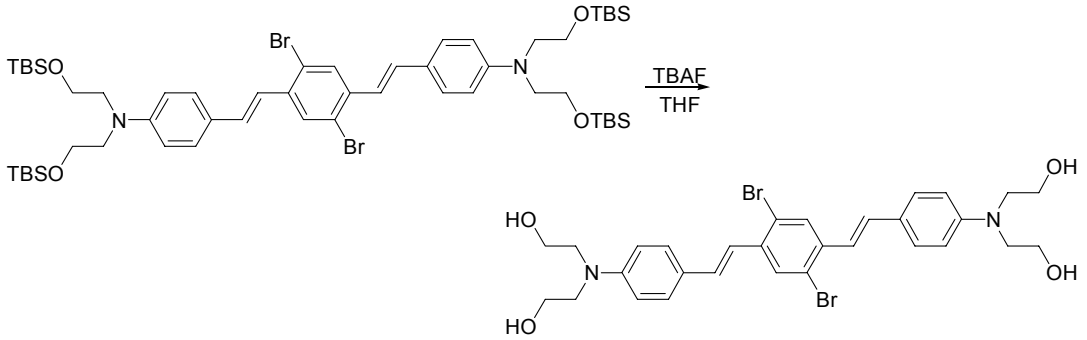

To a solution of *E,E*-2,5-dibromo-1,4-bis-[2-(4'-{Bis-[2-(tert-butyl-dimethyl-silanyloxy)-ethyl]-amino}-phenyl)-vinyl]-benzene (0.83 g, 0.75 mmol) in THF (40 ml) was added 1.0 M TBAF in THF (10 ml) and the reaction mixture was stirred at RT for 5 days. Water (50 ml) and brine (20 ml) was added and the precipitated compound was filtered off and washed with water and brine yielding 0.44 g (90 %) of the title compound as a red powder; ^{1}H-NMR($CDCl_3$, 300 K): 8.00 (s, 2H), 7.40 (d, 4H, *J*=8 Hz), 7.24 (d, 2H, *J*=16 Hz), 7.00 (d, 2H, *J*=16 Hz), 6.72 (d, 4H, *J*=8 Hz), 4.83 (t, 4H, *J*=5 Hz), 3.65-3.39 (m 16H); ^{13}C-NMR($CDCl_3$, 300 K): 148.3, 136.3, 132.5, 129.1, 128.1, 123.3, 121.9, 118.9, 111.3, 58.0, 53.1.

1,3-dicyclohexyl-2-isourea-derivitized *E,E*-2,5-dibromo-1,4-bis-[2-(4'-{bis-ethanol}-amino-phenyl)-vinyl]-benzene (121)

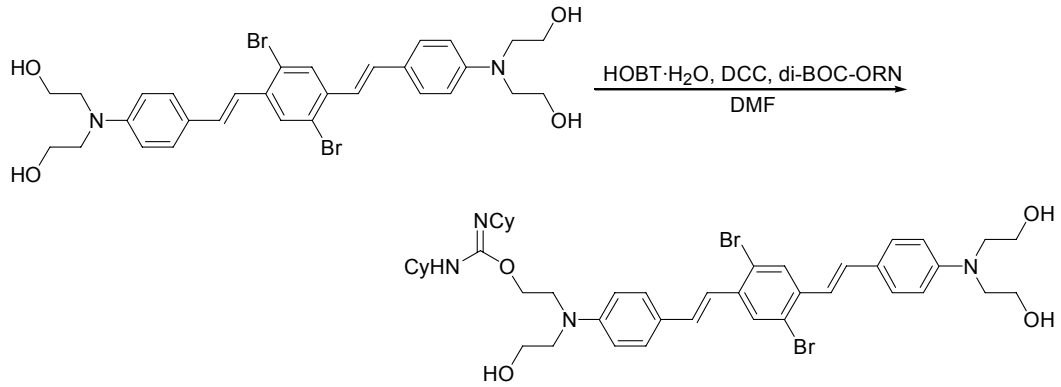

A solution of *E,E*-2,5-dibromo-1,4-bis-[2-(4'-{bis-ethanol}-amino-phenyl)-vinyl]-benzene (0.34 g, 0.53 mmol), di-BOC-ORN (1.10 g, 3.31 mmol) and HOBT·H_2O (0.37 g, 2.74 mmol) in DMF (150 ml) was cooled to 0 ºC. DCC (0.93 g, 4.5 mmol) was added and the reaction mixture was allowed to reach RT. The reaction mixture was stirred overnight at RT and Et_2O (200 ml) was then added. The mixture was washed with water (3x100 ml) and the combined water phases were washed with Et_2O (3x100 ml). A compound precipitated from the water phase upon standing and was filtered off yielding 0.25 g (55 %) of the title compound as a yellow powder; ^{1}H-NMR(DMSO, 300 K): 7.93 (s, 2H), 7.39 (d, 4H, *J*=9 Hz), 7.16 (d, 2H, *J*=16 Hz), 7.01 (d, 2H, *J*=16 Hz), 6.76 (d, 4H, *J*=9 Hz), 5.67-5.54 (bm, 2H), 4.56 (bs, 2H), 3.62 (t, 8H, *J*=6 Hz), 3.49 (t, 8H, *J*=6 Hz), 1.83-0.99 (m, 22H); ^{13}C-NMR(DMSO, 300 K): 156.4, 148.3, 136.3, 132.2, 128.9, 127.6, 123.4, 121.5, 119.1, 111.4, 58.0, 52.8, 47.2, 32.7, 24.9, 23.8.

4-[Bis-(2-{1-[2-(2-methoxy-ethoxy)-ethoxy]-vinylperoxy}-ethyl)-amino]-benzaldehyde (123)

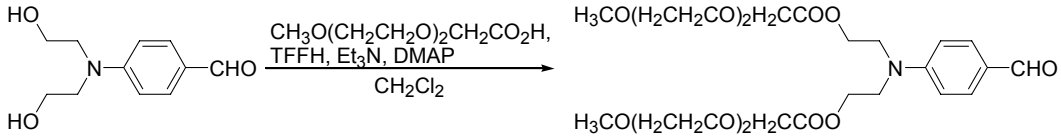

To a solution of TFFH (3.45 g, 13.1 mmol) in CH_2Cl_2 (100 ml) was added Et_3N (4.03 g, 39.8 mmol) and the mixture was stirred at RT for 1 h. 4-[Bis-(2-hydroxy-ethyl)-amino]-benzaldehyde (1.37 g, 6.55 mmol) was added followed by DMAP (0.25 g, 1.9 mmol) and the mixture was refluxed for 2 days. Water (200 ml) was added and the organic phase was isolated. After drying with $MgSO_4$ the mixture was filtered through a silica plug and further eluted with AcCN. Celite was added to the mixture and the solvent was removed *in vacou*. Purification by DCVC (toluene/AcCN) gave an oil, that was put on top of a silica plug and eluted with acetone. Celite was added to the isolated mixture and removal of the solvent followed by DCVC (Et_2O, acetone) yielded 2.22 g (64 %) of the title compound as an yellow oil; ^{1}H-NMR($CDCl_3$, 300 K): 9.75 (s, 1H), 7.74 (d, 2H, *J*=9 Hz), 6.81 (d, 2H, *J*=9 Hz), 4.36 (t, 4H, *J*=6 Hz), 4.13 (s, 4H), 3.73 (t, 4H, *J*=6 Hz), 3.70-3.50 (m, 16H), 3.37 (s, 6H); ^{13}C-NMR($CDCl_3$, 300 K): 190.1, 170.5, 152.1, 132.1, 126.1, 111.3, 71.7, 70.6, 70.2, 68.2, 61.3, 58.9, 49.3, 47.5; HRMS(EI+): m/z calcd. for $C_{25}H_{39}O_{11}N^{+\cdot}$ 529.2523, found 529.2512.

4-Bromomethyl-benzenesulfonic acid methyl ester[42] (124)

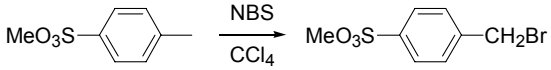

To the filtrated reaction mixture was added celite and the solvent was evaporated. Purification by column chromatography, DCVC (n-heptane/EtOAc) yielded 16.70 g (70 %) of the title compound as a colorless oil; ^{1}H-NMR($CDCl_3$, 300 K): 7.89 (d, 2H, *J*=9 Hz), 7.58 (d, 2H, *J*=9 Hz), 4.51 (s, 2H), 3.78 (s, 3H); ^{13}C-NMR($CDCl_3$, 300 K): 143.9, 135.0, 129.7, 128.4, 56.4, 31.1.

4-(Diethoxy-phosphorylmethyl)-benzenesulfonic acid ethyl ester (125)

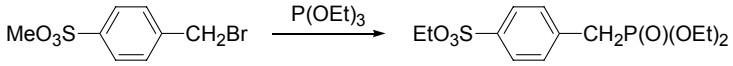

To the cooled reaction mixture was added celite and the mixture was then evaporated. Purification by column chromatography, DCVC (n-heptane/EtOAc), yielded 3.20 g (27 %) of the title compound as a colourless oil; ^{1}H-NMR($CDCl_3$, 300 K): 7.86 (d, 2H, *J*=8 Hz), 7.48 (dd, 2H, J_1=9 Hz, J_2=2 Hz), 4.13 (q, 2H, *J*=7 Hz), 4.05 (p, 4H, *J*=7 Hz), 3.22 (d, 2H, *J*=22 Hz), 1.31 (t, 3H, *J*=7 Hz), 1.26 (t, 3H, *J*=7 Hz); ^{13}C-NMR($CDCl_3$, 300 K): 138.5 (d, J_{PC}=9 Hz), 135.0 (d, J_{PC}=4 Hz), 130.5 (d, J_{PC}=6 Hz), 127.9 (d, J_{PC}=3 Hz), 66.9, 62.3 (d, J_{PC}=7 Hz), 33.9 (d, J_{PC}=138 Hz), 16.3 (d, J_{PC}=6 Hz), 14.7; Anal. Calcd. for $C_{13}H_{21}O_6PS{\cdot}H_2O$: C, 44.06; H, 6.54. Found: C, 43.95; H, 6.47; HRMS(EI+): m/z calcd. for $C_{13}H_{21}O_6PS^{+\cdot}$ 336.0796, found 336.0799.

***E, E*-2,5-Dibromo-1,4-Bis-[2-(4'-sulfonic-acid-phenyl)-vinyl]-benzene (126)**

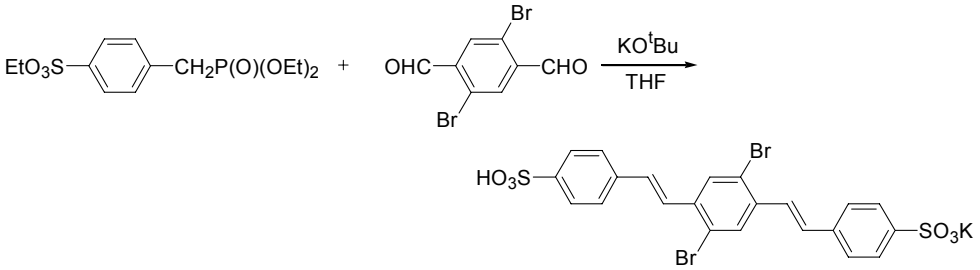

To a solution of 4-(diethoxy-phosphorylmethyl)-benzenesulfonic acid ethyl ester (2.02 g, 6.01 mmol) and 2,5-dibromo-terephthtalaldehyde (0.81 g, 2.77 mmol) in THF (100 ml) was added KO^{t}Bu (1.48 g, 13.2 mmol) and the reaction mixture was refluxed for 1 h. After the addition of 3 M HCl (50 ml) the reaction mixture was further refluxed for 1 h. The reaction mixture was concentrated until precipitation occurred and was the mixture was then left in the freezer overnight. The isolated compound was washed with EtOH leaving 0.65 g (37 %) of the title compound; ^{1}H-NMR(DMSO, 300 K): 8.17 (s, 2H), 7.93 (s, 2H), 7.63 (d, 4H, *J*=9 Hz), 7.58 (d, 4H, *J*=9 Hz), 7.46 (d, 2H, *J*=16 Hz), 7.33 (d, 2H, *J*=16 Hz); ^{13}C-NMR(DMSO, 400 K): 148.3, 136.7, 135.8, 132.1, 130.0, 125.5, 125.4, 124.8, 121.8; Anal. Calcd. for $C_{22}H_{15}Br_2KO_6S_2$: C, 41.39; H, 2.37. Found: C, 40.93; H, 2.05; HRMS(ESI-): m/z calcd. for $C_{22}H_{14}Br_2O_6S_2^{2-}$ 298.9289, found 298.9302.

2-Bromomethyl-benzothiazole[43] (127)

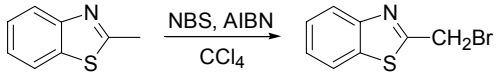

A solution of 2-bromomethyl-benzothiazole (15.04 g, 100.8 mmol) and NBS (17.28 g, 97.03 mmol) in CCl_4 (150 ml) was prepared. AIBN (0.28 g, 1.71 mmol) was added and the reaction mixture was refluxed for 2 h. and then filtered. The isolated organic phase was evaporated leaving the crude product which was purified using FCC (1:5 EtOAc:n-hexanes) yielding 2.35 g (10 %) of the title compound as a clear oil; R_f(1:5 EtOAc: n-hexanes)=0.40; ^{1}H-NMR($CDCl_3$, 300 K): 8.02 (dd, 1H, *J*=8 Hz, *J*=1 Hz), 7.88 (dd, 1H, *J*=8 Hz, *J*=1 Hz), 7.50 (dt, 1H, *J*=8 Hz, *J*=1 Hz), 7.42 (dt, 1H, *J*=7 Hz, *J*=1 Hz), 4.81 (s, 2H); ^{13}C-NMR($CDCl_3$, 300 K): 166.2, 152.9, 136.3, 126.5, 125.8, 123.6, 121.8, 27.1.

Benzothiazol-2-ylmethyl-phosphonic acid diethyl ester (128)

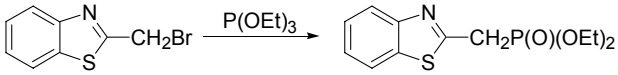

2-Bromomethyl-benzothiazole (2.20 g, 9.64 mmol) was dissolved in $P(OEt)_3$ (50 ml) and the reaction mixture was refluxed for 2.5 h. To the crude reaction mixture was added celite and the mixture was then evaporated. Purification by DCVC (n-heptane/EtOAc) yielded 2.20 g (80 %) of the title compound as a light yellow oil; R_f(EtOAc)=0.19; ^{1}H-NMR($CDCl_3$, 300 K): 8.00 (d, 1H, *J*=8 Hz), 7.86 (dd, 1H, J_1=8 Hz, J_2=1 Hz), 7.47 (dt, 1H, J_1=8 Hz, J_2=1 Hz), 7.38 (t, 1H, *J*=8 Hz), 4.16 (dp, 4H, J_1=7 Hz, J_2=1 Hz), 3.74 (d, 2H, *J*=22 Hz), 1.32 (t, 6H, *J*=7 Hz); ^{13}C-NMR($CDCl_3$, 300 K): 161.0 (d, J_{PC}=9 Hz), 152.9, 135.9, 126.0, 125.1, 122.9, 121.4, 62.8 (d, J_{PC}=6 Hz), 33.1 (d, J_{PC}=140 Hz), 16.3 (d, J_{PC}=6 Hz); HRMS(EI+): m/z calcd. for $C_{12}H_{16}O_3NPS^{+\cdot}$ 285.0589, found 285.0595.

***E*, *E*-2,5-Dimethoxy-1,4-bis-(2-benzothiazol-2-yl-vinyl)-benzene (130)**

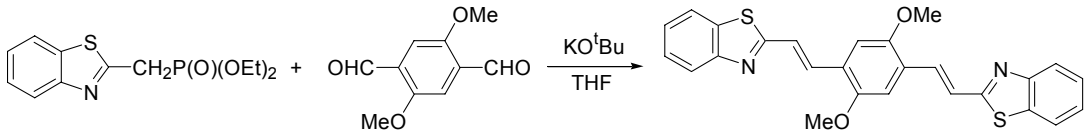

The product precipitated from the quenched reaction mixture, was filtrated off and washed with EtOH. Yield 0.71 g (84 %), dark red powder; ^{1}H-NMR(DMSO, 400 K): 7.99 (d, 2H, *J*=7 Hz), 7.95 (d, 2H, *J*=8 Hz), 7.83 (d, 2H, *J*=16 Hz), 7.64 (d, 2H, *J*=16 Hz), 7.48 (dt, 2H, J_1=8 Hz, J_2=1 Hz), 7.42 (s, 2H), 7.39 (dt, 2H, J_1=7 Hz, J_2=1 Hz), 3.98 (s, 6H); ^{13}C-NMR(DMSO, 400 K): 167.1, 154.3, 152.9, 134.8, 132.2, 126.9, 126.8, 125.7, 123.8, 123.4, 122.3, 112.4, 57.3; HRMS(EI+): m/z calcd. for $C_{26}H_{20}N_2O_2S_2^{+\cdot}$ 456.0966, found 456.0977.

***E*, *E*-2,5-Dimethoxy-1,4-bis-(2-*N*-methyl-benzothiazolium-2-yl-vinyl)-benzene methylsulfate (131)**

Recrystillazid from MeOH. Yield 0.33 g (46 %), dark red crystals; ^{1}H-NMR(DMSO, 300 K): 8.47 (d, 2H, *J*=7 Hz), 8.31 (d, 2H, *J*=8 Hz), 8.23 (d, 4H, *J*=5 Hz), 7.93 (t, 2H, *J*=8 Hz), 7.84 (t, 2H, *J*=8 Hz), 7.84 (s, 2H), 4.40 (s, 6H), 4.10 (s, 6H), 3.17 (s, 6H); ^{13}C-NMR(DMSO, 300 K): 172.1, 153.4, 142.6, 141.1, 130.0, 129.1, 128.5, 127.4, 124.7, 117.5, 116.5, 112.6, 57.6, 53.3, 37.1; Anal. Calcd. for $C_{30}H_{32}N_2O_{10}S_4$: C, 50.83; H, 4.55; N, 3.95; S, 18.09. Found: C, 50.51; H, 4.13; N, 3.94; S, 18.10.

***E, E*-2,5-Dibromo-1,4-Bis-[2-(4'-sulfonic-acid-phenyl)-vinyl]-benzene (132)**

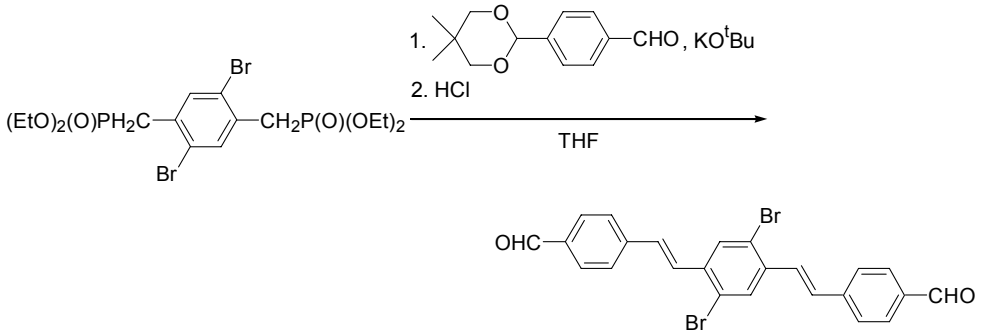

To a solution of [4-(diethoxy-phosphorylmethyl)-2,5-dibromo-benzyl]-phosphonic acid diethyl ester (1.99 g, 3.71 mmol) and 4-(5,5-dimethyl-[1,3]dioxan-2-yl)-benzaldehyde (1.66 g, 7.54 mmol) in THF (100 ml) was added KO^{t}Bu (1.57 g, 14.0 mmol). The reaction mixture was refluxed for 2.5 h and then 37 % HCl (100 ml) was added the mixture was refluxed for 2 h and then allowed to cool to RT. The precipitated product was filtered off and triturated with EtOH. The isolated product was then washed with EtOH, water and then EtOH leaving 1.33 g (72 %) of the title compound as a yellow powder; ^{1}H-NMR(DMSO, 300 K): 9.99 (s, 2H), 8.19 (s, 2H), 7.93 (d, 4H, *J*=8 Hz), 7.82 (d, 4H, *J*=8 Hz), 7.55 (d, 2H, *J*=16 Hz), 7.45 (d, 2H, *J*=16 Hz); ^{13}C-NMR(DMSO, 400 K): 192.1, 142.7, 137.9, 136.7, 132.7, 131.5, 130.2, 128.7, 127.9, 123.3; Anal. Calcd. for $C_{24}H_{16}Br_2O_2$: C, 58.09; H, 3.25. Found: C, 58.16; H, 3.07.

***E*, *E*-2,5-Dibromo-1,4-bis-[2-(4'-{benzothiazol-2-yl}-phenyl)-vinyl]-benzene (133)**

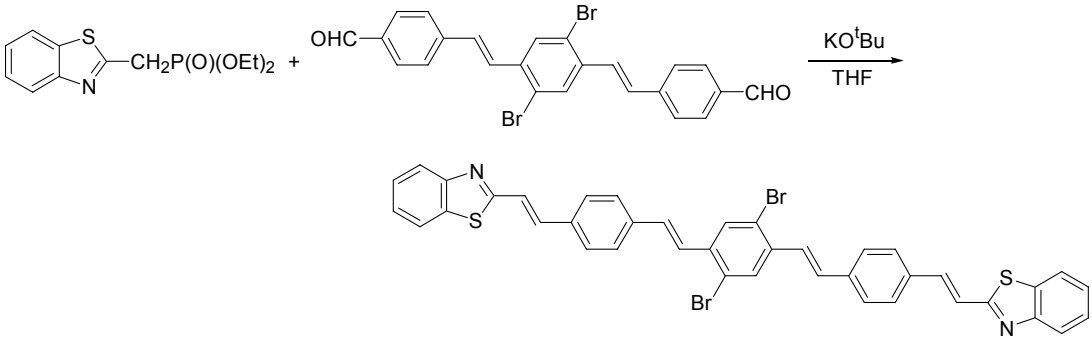

The product precipitated from the quenched reaction mixture, was filtrated off and washed with EtOH. Yield 0.70 g (63 %), yellow powder. Due to solubility problems it was only possible to obtain a ^{1}H-NMR spectrum; ^{1}H-NMR(1,2-dichlorobenzene, 400 K): 8.06 (d, 4H, *J*=8 Hz), 7.89-7.73 (m, 6H), 7.60-7.37 (m, 16H); Anal. Calcd. for $C_{40}H_{26}Br_2N_2S_2$: C, 63.33; H, 3.45; N, 3.69. Found: C, 60.84; H, 3.26; N, 3.30.

***E*, *E*-2,5-Dibromo-1,4-bis-[2-(4'-{*N*-methyl-benzothiazol-2-yl}-phenyl)-vinyl]-benzene methylsulfate (134)**

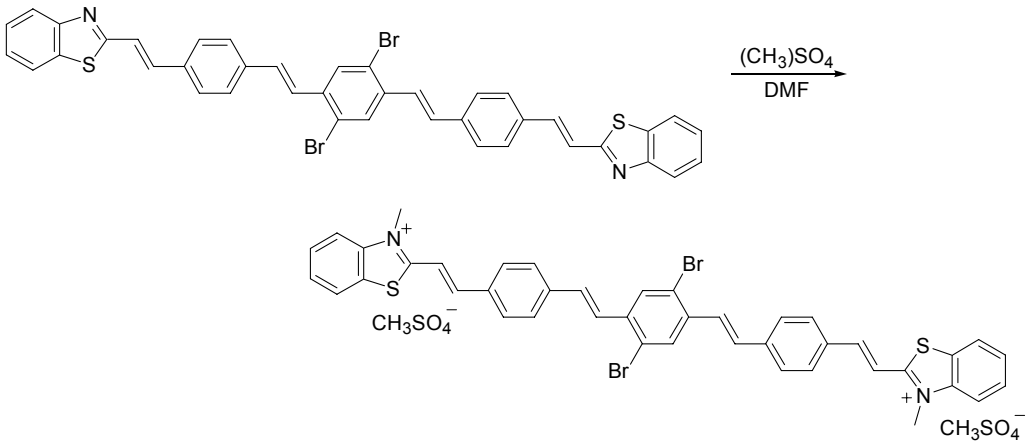

The product was filtrated directly of the cooled reaction mixture and triturated with MeOH. Yield 0.20 g (65 %), yellow powder; ^{1}H-NMR(DMSO, 300 K): 8.42 (d, 2H, *J*=8 Hz), 8.29-8.16 (m, 6H), 8.14-8.00 (m, 6H), 7.93-7.73 (m, 8H), 7.56 (d, 2H, *J*=14 Hz), 7.48 (d, 2H, *J*=16 Hz), 4.37 (s, 6H); ^{1}H-NMR(DMSO, 300 K): 172.1, 148.1, 142.4, 140.5, 137.4, 134.4, 132.6, 131.1, 130.8, 129.9, 128.9, 128.4, 128.0, 127.3, 124.7, 123.5, 117.3, 114.2, 53.2, 36.9; Anal. Calcd. for $C_{44}H_{38}Br_2N_2O_8S_4 \cdot 1.125H_2O$: C, 51.25; H, 3.93; N, 2.72. Found: C, 50.88; H, 3.54; N, 2.81; HRMS(ESI+): m/z calcd. for $C_{42}H_{32}Br_2N_2S_2^{2+}$ 393.0187, found 393.0192.

1,2,4,5-tetrabromo-3,6-bis-bromomethyl-benzene (135)

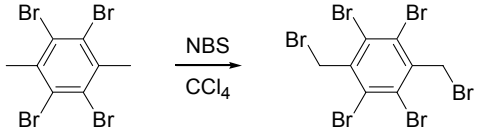

Recrystallized from $CHCl_3$. Yield 22.62 g (80 %), white powder; ^{1}H-NMR(1,2-dichlorbenzol, 400 K): 5.09 (s, 4H); ^{13}C-NMR(1,2-dichlorbenzol, 400 K): 140.5, 128.9, 37.5; Anal. Calcd. for $C_8H_4Br_6$: C, 16.58; H, 0.70. Found: C, 16.77; H, 0.55.

[2,3,5,6-tetrabromo-4-(diethoxy-phosphorylmethyl)-benzyl]-phosphonic acid diethyl ester (136)

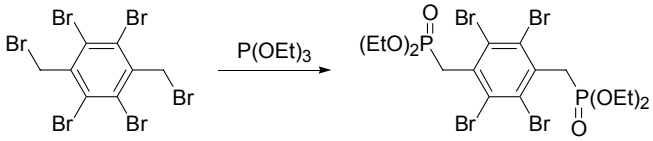

Yield 21.50 g (89 %), white powder; ^{1}H-NMR($CDCl_3$, 300 K): 4.10 (p, 8H, *J*=7 Hz), 4.01 (d, 2H, *J*=21 Hz), 1.29 (t, 12H, *J*=7 Hz); ^{13}C-NMR($CDCl_3$, 300 K): 135.6 (d, J_{PC}=6 Hz), 128.6 (d, J_{PC}=2 Hz), 63.4 (d, J_{PC}=7 Hz), 40.3 (d, J_{PC}=141 Hz), 16.3 (d, J_{PC}=6 Hz); Anal. Calcd. for $C_{16}H_{24}Br_4O_6P_2$: C, 27.69; H, 3.49. Found: C, 27.84; H, 3.27.

***E, E*-2,5-Dibromo-1,4-Bis-[2-pyridin-vinyl]-benzene (137)**

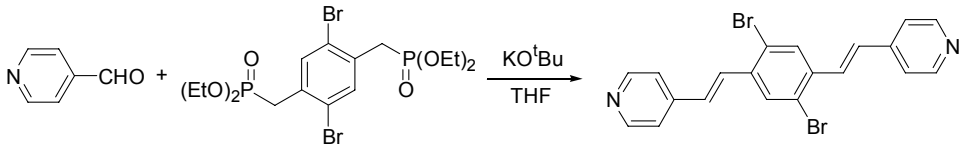

The crude product precipitated from the quenched reaction mixture and was filtrated off. Recrystallized from a EtOH/pyridine mixture. Yield 1.46 g (68 %), light yellow. A sample to determine elemental composition was obtained by recrystallization from EtOH; ^{1}H-NMR(DMSO): 8.60 (d, 4H, *J*=5 Hz), 8.11 (s, 2H), 7.59 (d, 4H, *J*=5 Hz), 7.58 (d, 2H, *J*=16 Hz), 7.46 (d, 2H, *J*=16 Hz); Anal. Calcd. for $C_{20}H_{14}Br_2N_2 \cdot 0.5H_2O$: C, 53.24; H, 3.35; N, 6.21. Found: C, 53.19; H, 2.92; N, 6.16.

***E, E*-2,5-Dimethoxy-1,4-Bis-[2-pyridin-vinyl]-benzene (138)**

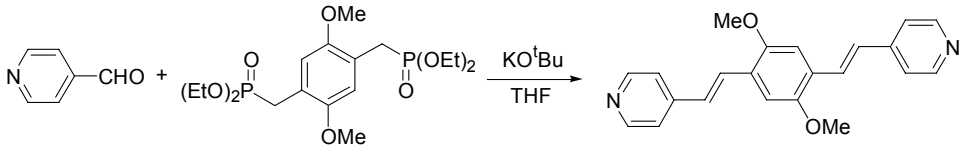

The product precipitated from the quenched reaction mixture and was filtrated off. Yield 0.35 g (73 %), yellow powder; ^{1}H-NMR($CDCl_3$, 300 K): 8.58 (dd, 4H, J_1=6 Hz, J_2=1 Hz), 7.68 (d, 2H, *J*=17 Hz), 7.430 (dd, 4H, J_1=6 Hz, J_2=1 Hz), 7.14 (s, 2H), 7.06 (d, 2H, *J*=17 Hz), 3.95 (s, 6H); ^{13}C-NMR($CDCl_3$, 300 K): 151.9, 150.1, 145.0, 127.6, 126.8, 126.5, 120.9, 109.6, 56.3; Anal. Calcd. for $C_{22}H_{20}N_2O_2 \cdot 0.25H_2O$: C, 75.73; H, 5.92; N, 8.03. Found: C, 76.19; H, 5.80; N, 7.97; HRMS(EI+): m/z calcd. for $C_{22}H_{20}N_2O_2^{+\cdot}$ 344.1525, found 344.1523.

***E, E*-2,3,5,6-Tetrabromo-1,4-Bis-[2-pyridin-vinyl]-benzene (139)**

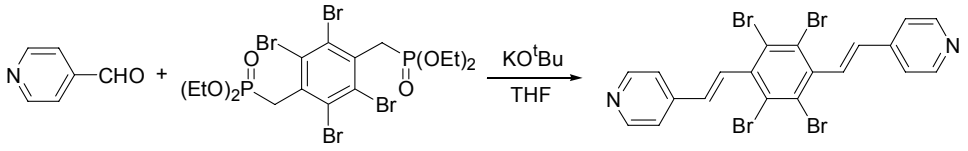

The crude product precipitated from the quenched reaction mixture and was filtrated off. Recrystallized from pyridine. Yield 2.70 g (82 %), white powder. Due to solubility problems it was only possible to obtain a ^{1}H-NMR spectrum; ^{1}H-NMR(DMSO): 8.62(d, 4H, *J*=6 Hz), 7.63 (d, 4H, *J*=6 Hz), 7.50 (d, 2H, *J*=17 Hz), 6.80 (d, 2H, *J*=16 Hz); Anal. Calcd. for $C_{20}H_{12}Br_4N_2$: C, 40.04; H, 2.02; N, 4.67. Found: C, 40.02; H, 1.76; N, 4.72.

***E, E*-2,5-Dibromo-1,4-Bis-[2-(N-methyl-pyridininium)-vinyl]-benzene methylsulfate (140)**

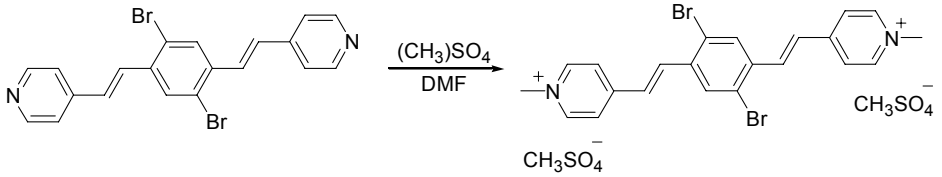

Recrystallized from MeOH. Yield 0.90 g (76 %), yellow needles; ^{1}H-NMR(DMSO, 300 K): 8.91 (d, 4H, *J*=7 Hz), 8.33 (s, 2H), 8.29 (d, 4H, *J*=7 Hz), 7.97 (d, 2H, *J*=16 Hz), 7.71 (d, 2H, *J*=16 Hz), 4.29 (s, 6H), 3.77 (s, 6H); ^{13}C-NMR(DMSO, 300 K): 151.5, 146.0, 1379, 135.8, 132.6, 129.4, 124.9, 124.2, 53.2, 47.7; Anal. Calcd. for $C_{24}H_{26}Br_2N_2O_8S_2$: C, 41.51; H, 3.77; N, 4.03; S, 9.24. Found: C, 41.47; H, 3.50; N, 3.94; S, 9.37.

***E, E*-2,5-Dimethoxy-1,4-Bis-[2-(N-methyl-pyridininium)-vinyl]-benzene methylsulfate (141), general procedure**

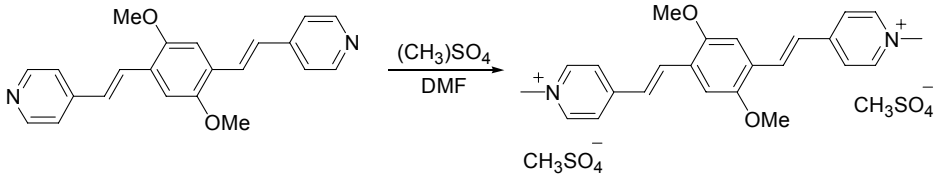

To a solution of *E, E*-2,5-Dimethoxy-1,4-Bis-[2-pyridin-vinyl]-benzene (0.16 g, 0.46 mmol) in DMF (50 ml) was added $(CH_3)SO_4$ (25 ml, 264 mmol) under Ar-atmosphere. The reaction mixture was stirred at 150 ºC for 2 h. and was then cooled to RT. The reaction mixture was concentrated and then cooled. The precipitated compound was isolated and recrystallized twice from MeOH leaving 0.10 g (36 %) of the title compound as red needles; ^{1}H-NMR(DMSO, 300 K): 8.84 (d, 4H, *J*=6 Hz), 8.22 (d, 4H, *J*=6 Hz), 8.06 (d, 2H, *J*=16 Hz), 7.67 (d, 2H, *J*=16 Hz), 7.51 (s, 2H), 4.25 (s, 6H), 3.96 (s, 6H), 3.36 (s, 6H); ^{13}C-NMR(DMSO, 300 K): 152.9, 152.8, 145.6, 134.8, 127.0, 125.8, 124.1, 111.8, 56.9, 53.2, 47.4; Anal. Calcd. for $C_{26}H_{32}N_2O_{10}S_2 \cdot 0.5H_2O$: C, 51.56; H, 5.49; N, 4.63; S, 10.59. Found: C, 51.28; H, 5.37; N, 4.58; S, 10.33; HRMS(ESI+): m/z calcd. for $C_{25}H_{29}N_2O_6S^+$ 485.1746, found 485.1746.

***E, E*-2,5-Dimethoxy-1,4-Bis-[2-(N-methyl-pyridininium)-vinyl]-benzene iodide (142)**

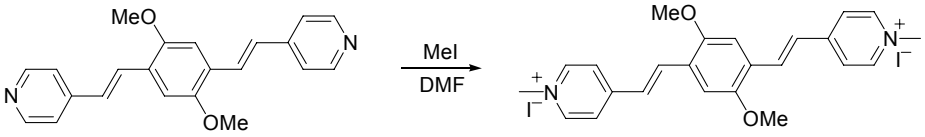

To a solution of *E, E*-2,5-Dimethoxy-1,4-Bis-[2-pyridin-vinyl]-benzene (0.20 g, 0.58 mmol) in DMF (50 ml) was added MeI (0.50 g, 3.52 mmol) under Ar-atmosphere. The reaction mixture was refluxed for 1 h. and was then cooled to RT. Removal of the solvent under reduced pressure left the crude product which was recrystallized from THF and then recrystallized from MeOH leaving 0.25 g (69 %) of the title compound as a red needles; ^{1}H-NMR(DMSO, 300 K): 8.84 (d, 4H, *J*=5 Hz), 8.23 (d, 4H, *J*=5 Hz), 8.06 (d, 2H, *J*=16 Hz), 7.69 (d, 2H, *J*=16 Hz), 7.51 (s, 2H), 4.26 (s, 6H), 3.96 (s, 6H); ^{13}C-NMR(DMSO, 300 K): 152.9, 152.7, 145.6, 134.8, 127.0, 125.8, 124.1, 111.7, 56.9, 47.4; Anal. Calcd. for $C_{24}H_{26}I_2N_2O_2$: C, 45.88; H, 4.17; N, 4.46. Found: C, 45.63; H, 3.91; N, 4.36.

***E, E*-2,3,4,5-Tetrabromo-1,4-Bis-[2-(N-methyl-pyridininium)-vinyl]-benzene methylsulfate (143)**

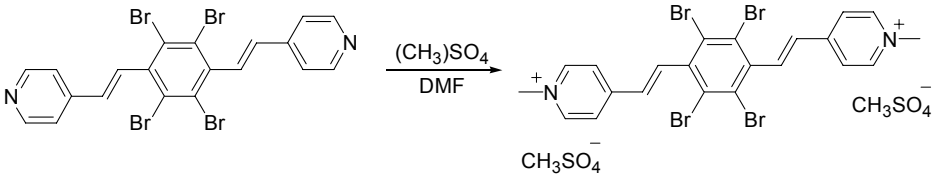

Recrystillazid from MeOH. Yield 0.54 g (53 %), white flakes; ^{1}H-NMR(DMSO, 300 K): 8.96 (d, 4H, *J*=7 Hz), 8.35 (d, 4H, *J*=7 Hz), 7.94 (d, 2H, *J*=16 Hz), 7.68 (d, 2H, *J*=16 Hz), 4.30 (s, 6H), 3.36 (s, 6H); ^{13}C-NMR(DMSO, 300 K): 150.5, 145.7, 140.4, 140.3, 131.9, 125.7, 124.2, 52.7, 47.3; Anal. Calcd. for $C_{24}H_{24}Br_4N_2O_8S_2$: C, 33.82; H, 2.84; N, 3.29; S, 7.53. Found: C, 34.47; H, 2.77; N, 3.25; S, 7.32; HRMS(ESI+): m/z calcd. for $C_{22}H_{18}Br_4N_2^{2+}$ 314.9082, found 314.8900.

4-(4-Methyl-piperazin-1-yl)-benzaldehyde[44] (144)

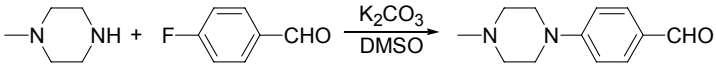

Piperazin (3.56 g, 35.5 mmol) and 4-flouro-benzaldehyde (3.65 g, 29.4 mmol) was dissolved in DMF (50 ml). K_2CO_3 (4.98 g, 26.0 mmol) was added and the reaction mixture was stirred at 150 ºC overnight and then poured into water (350 ml). The quenched reaction mixture was extracted with EtOAc (3x150 ml) and the combined organic phases were washed with water (1x100 ml) and brine (1x100 ml). After drying with $MgSO_4$ celite was added and the mixture was evaporated. Purification by DCVC (EtOAc/MeOH) yielded 3.21 g (53 %) of the title compound as a white solid; ^{13}C-NMR($CDCl_3$, 300 K): 190.3, 155.0, 131.8, 127.2, 113.5, 54.6, 47.0, 46.0.

***E, E*-2,5-Dibromo-1,4-Bis-[2-(4'-{1-methyl-piperazine}-phenyl)-vinyl]-benzene dihydrochloride (145)**

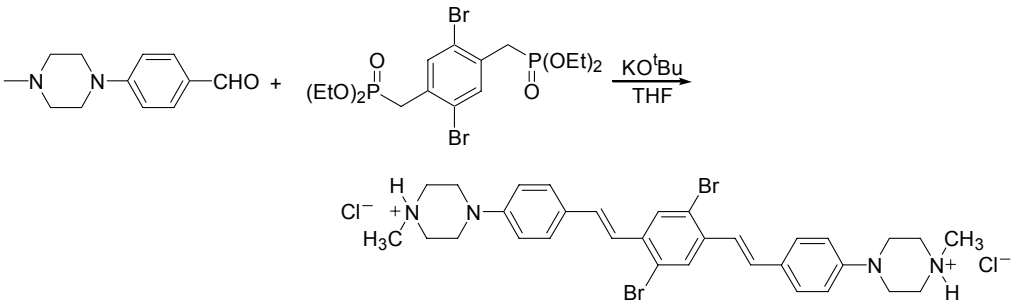

Prepared as **34**. Yield 1.10 g (63 %) of the title compound as a yellow powder; Mp > 250 °C; ^{1}H-NMR(DMSO, 300 K): 7.95 (s, 2H), 7.49 (d, 4H, *J*=9 Hz), 7.21 (d, 2H, *J*=16 Hz), 7.10 (d, 2H, *J*=16 Hz), 6.99 (d, 4H, *J*=9 Hz), 3.57 (t, 8H, *J*=5 Hz), 3.23 (t, 8H, *J*=5 Hz), 2.75 (s, 6H); ^{13}C-NMR(DMSO, 400 K): 150.2, 137.6, 133.0, 130.6, 128.7, 128.5, 122.8, 122.7, 116.3, 52.8, 45.6, 42.8; Anal. Calcd. for $C_{32}H_{38}Cl_2Br_2N_4 \cdot H_2O$: C, 52.84; H, 5.54; N, 7.70. Found: C, 52.79; H, 5.41; N, 7.47; HRMS(ESI+): m/z calcd. for $C_{32}H_{38}Br_2N_4^{2+}$ 319.0722, found 319.0678.

***E, E*-2,5-Dibromo-1,4-Bis-[2-(4'-{1,1-dimethyl-piperazine}-phenyl)-vinyl]-benzene iodide (146)**

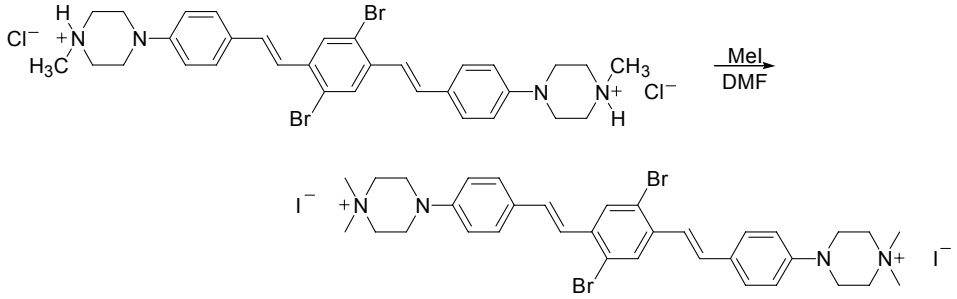

Prepared as **142**. Yield: 0.10 g (17 %) of 37 as a yellow powder; Mp > 250 °C; ^{1}H-NMR(DMSO): 8.05 (s, 2H), 7.53 (d, 4H, *J*=8 Hz), 7.32 (d, 2H, *J*=16 Hz), 7.13 (d, 2H, *J*=16 Hz), 7.04 (d, 4H, *J*=8 Hz), 3.64-3.47 (m, 16H), 3.19 (s, 12H); ^{13}C-NMR(DMSO): 149.8, 137.2, 132.9, 130.2, 128.5, 128.3, 122.8, 122.0, 115.9, 60.5, 50.8, 42.0; Anal. Calcd. for $C_{34}H_{40}Br_2I_2N_4$: C, 44.47; H, 4.39; N, 6.10. Found: C, 42.33; H, 4.19; N, 5.66; HRMS(ESI+): m/z calcd. for $C_{34}H_{42}Br_2N_4^{2+}$ 348.0868, found 334.0868.

4-Pyridin-4-yl-benzaldehyde (150)

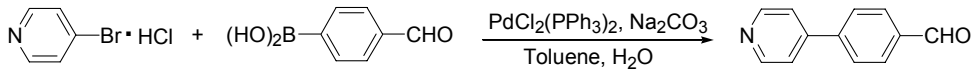

Prepared as **8**. Recrystallized from n-heptane after DCVC (n-heptane/EtOAc). Yield 3.97 g (88 %), white needles; mp 86-87 ºC; ^{1}H-NMR($CDCl_3$, 300 K): 10.09 (s, 1H), 8.72 (dd, 2H, J_1=5 Hz, J_1=2 Hz), 8.01 (dt, 2H, J_1=8 Hz, J_1=2 Hz), 7.80 (dt, 2H, J_1=8 Hz, J_1=2 Hz), 7.54 (dd, 2H, J_1=4 Hz, J_1=2 Hz); ^{13}C-NMR($CDCl_3$, 300 K): 191.5, 150.5, 146.9, 144.0, 136.5, 130.4, 127.7, 121.7; Anal. Calcd. for $C_{10}H_8N_2$: C, 78.67; H, 4.95; N, 7.65. Found: C, 78.45; H, 5.00; N, 7.50.

5-Bromo-1-pyren-1-yl-pentan-1-one (156)

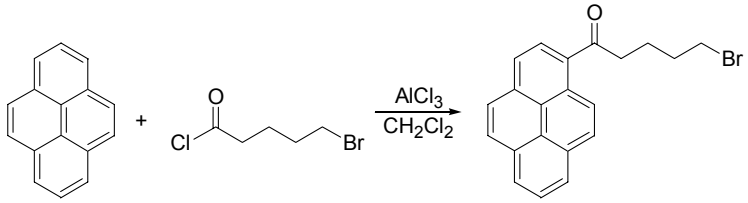

A solution of pyrene (4.04 g, 20.0 mmol) and $AlCl_3$ (5.42 g, 40.7 mmol) in CH_2Cl_2 was cooled to –78 ˚C. 5-Bromo-pentanoyl chloride (8.02 g, 40.2 mmol) was carefully added and the reaction mixture was stirred for 3 h. at –78 ˚C and allowed to reach RT. The reaction mixture was quenched by adding 1 M HCl and the quenched reaction mixture was filtered through celite, washed with brine and dried ($MgSO_4$). The solvent was removed *in vacou* and the remaining oil was subjected to column chromatography using 1:1 CH_2Cl_2:n-heptane as the eluent yielding 4.31 g (59 %) of the title compound as a yellow powder; mp 114-115 ˚C; ^{1}H-NMR($CDCl_3$, 300 K): 8.90 (d, 1H, *J*=9 Hz), 8.33 (d, 1H, *J*=8 Hz), 8.29-8.02 (m, 7H), 3.50 (t, 2H, *J*=6 Hz), 3.27 (t, 2H, *J*=7 Hz), 2.11-2.01 (m, 4H); ^{13}C-NMR($CDCl_3$, 300 K): 204.1, 133.7, 132.3, 131.1, 130.5, 129.6, 129.5, 129.3, 127.0, 126.4, 126.3, 126.0, 125.0, 124.7, 124.3, 124.0, 41.3, 33.3, 32.3, 23.4; Anal. Calcd. for $C_{21}H_{17}BrO$: C, 69.05; H, 4.69. Found: C, 68.72; H, 4.59.

8-Bromo-1-pyren-1-yl-octan-1-one (157)

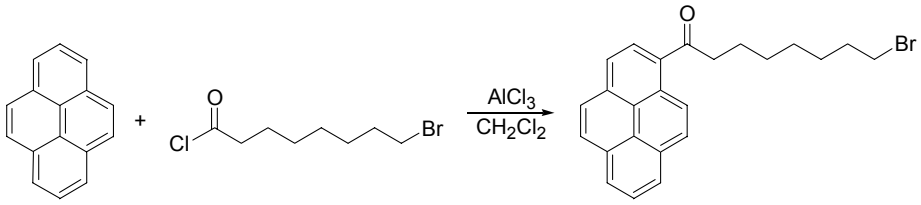

Prepared as **156** from pyrene and 8-bromo-octanoyl chloride. Recrystallized from heptane. Yield: 4.53 g (36 %), yellow powder; mp 78-80 ˚C; ^{1}H-NMR($CDCl_3$, 300 K): 8.86 (d, 1H, *J*=9 Hz), 8.31 (d, 1H, *J*=8 Hz), 8.90-8.82 (m, 7H), 3.40 (t, 2H, *J*=7 Hz), 3.22 (t, 2H, *J*=7 Hz), 1.94-1.75 (m, 4H), 1.55-1.32 (m, 6H); ^{13}C-NMR($CDCl_3$, 300 K): 205.1, 133.6, 132.8, 131.1, 130.5, 129.4, 129.3, 129.2, 127.0, 126.3, 126.1, 125.9, 124.9, 124.7, 124.3, 124.0, 42.5, 33.8, 32.7, 29.2, 28.6, 28.0, 24.8; Anal. Calcd. for $C_{24}H_{23}BrO$: C, 70.77; H, 5.69. Found: C, 70.31; H, 5.63.

11-Bromo-1-pyren-1-yl-undecan-1-one[45] (158)

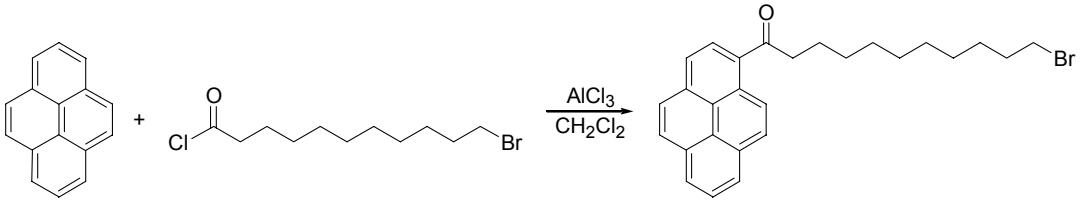

Prepared as **156** from pyrene and 11-bromo-undecanoyl chloride. Yield: 4.50 g (50 %), yellow powder; mp 65-66 ˚C; ^{1}H-NMR($CDCl_3$, 300 K): 8.87 (d, 1H, *J*=9 Hz), 8.29 (d, 1H, *J*=8 Hz), 8.26-8.00 (m, 7H), 3.38 (t, 2H, *J*=7 Hz), 3.20 (t, 2H, *J*=7 Hz), 1.93-1.76 (m, 4H), 1.53-1.23 (m, 12H); ^{13}C-NMR($CDCl_3$, 300 K): 205.4, 133.5, 132.9, 131.1, 130.5, 129.4, 129.3, 129.2, 127.0, 126.3, 126.1, 125.9, 125.0,

124.8, 124.3, 124.0, 42.7, 34.0, 32.8, 29.4, 29.3, 28.7, 28.1, 25.0; Anal. Calcd. for $C_{27}H_{29}BrO$: C, 72.16; H, 6.50. Found: C, 72.00; H, 6.41.

1-(5-Bromo-pentyl)-pyrene (159)

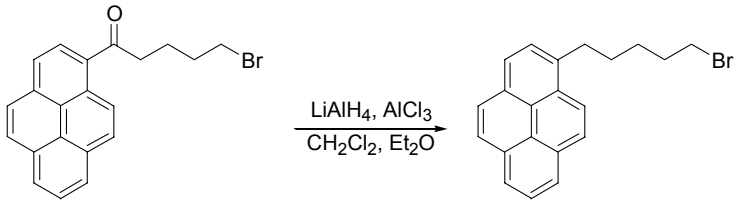

Prepared as **160** from 5-bromo-1-pyren-1-yl-pentan-1-one. Yield: 0.35 g (69 %), white powder; mp 115-116 ˚C; ^{1}H-NMR($CDCl_3$, 300 K): 8.26 (d, 1H, *J*=9 Hz), 8.21-7.95 (m, 7H), 7.86 (d, 1H, *J*=8 Hz), 3.42 (t, 2H, *J*=7 Hz), 3.36 (t, 2H, *J*=8 Hz), 2.02-1.82 (m, 4H), 1.88 (q, 2H, *J*=8 Hz), 1.71-1.58 (m, 2H); ^{13}C-NMR($CDCl_3$, 300 K): 136.6, 131.4, 130.9, 129.8, 128.5, 127.5, 127.2 (2C), 126.6, 125.8, 125.1, 125.0, 124.8 (2C), 124.7, 123.3, 33.8, 33.4, 32.7, 31.0, 28.3; Anal. Calcd. for $C_{21}H_{19}Br$: C, 71.80; H, 5.45. Found: C, 71.86; H, 5.34.

1-(8-Bromo-octyl)-pyrene (160)

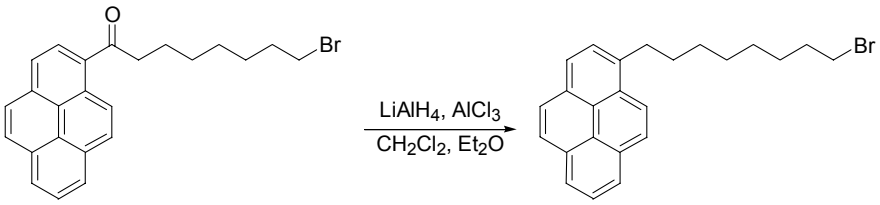

To a solution of $AlCl_3$ (3.45 g, 25.9 mmol) and $LiAlH_4$ (1.02 g, 26.9 mmol) in Et_2O was added drop wise 8-bromo-1-pyren-1-yl-octan-1-one (4.07 g, 10.0 mmol) dissolved in CH_2Cl_2 and the mixture was left stirring for 1 h. The mixture was quenched with water (100 ml) and the isolated organic phase was washed with brine (1x100 ml). After drying ($MgSO_4$) the solvent was removed *in vacou* and the isolated crude was recrystallized yielding 2.62 g (67 %) of the title compound as an white powder; mp 61-63 ˚C; ^{1}H-NMR($CDCl_3$, 300 K): 8.28 (d, 1H, *J*=9 Hz), 8.19-7.94 (m, 7H), 7.87 (d, 1H, *J*=8 Hz), 3.40 (t, 2H, *J*=7 Hz), 3.34 (t, 2H, *J*=8 Hz), 1.93-1.78 (m, 4H), 1.56-1.27 (m, 8H); ^{13}C-NMR($CDCl_3$, 300 K): 137.1, 131.4, 130.9, 129.7, 128.6, 127.5, 127.2, 127.0, 126.4, 125.7, 125.1, 125.0, 124.7, 124.6, 123.4, 33.9, 33.5, 32.8, 31.8, 29.6, 29.3, 28.7, 28.1.

1-(11-Bromo-undecyl)-pyrene[45] (161)

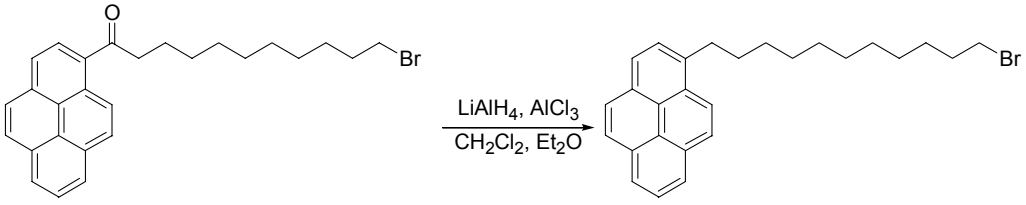

Prepared as **160** from 11-Bromo-1-pyren-1-yl-undecan-1-one. Yield: 2.20 g (87 %), white powder; mp 61-61 ˚C; ^{1}H-NMR($CDCl_3$, 300 K): 8.29 (d, 1H, *J*=9 Hz), 8.20-7.94 (m, 7H), 7.87 (d, 1H, *J*=8 Hz), 3.40 (t, 2H, *J*=7 Hz), 3.34 (t, 2H, *J*=8 Hz), 1.95-1.77 (m, 4H), 1.56-1.22 (m, 14H); ^{13}C-NMR($CDCl_3$,

300 K): 137.3, 131.4, 130.9, 129.7, 128.6, 127.5, 127.2, 127.1, 126.5, 125.7, 125.1, 124.8, 124.6, 123.5, 34.0, 33.6, 32.8, 31.9, 29.8, 29.6, 29.5, 29.4, 28.7, 28.2; Anal. Calcd. for $C_{27}H_{31}Br$: C, 74.47; H, 7.18. Found: C, 74.52; H, 7.09.

Thioacetic acid S-(5-pyren-1-yl-pentyl) ester (162)

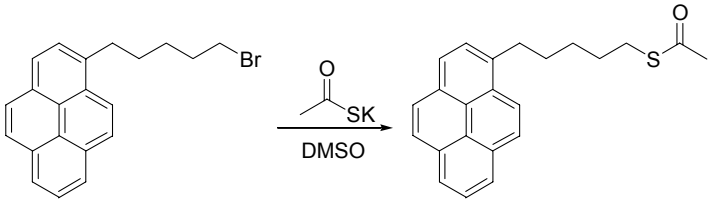

Prepared as **163** from 1-(5-bromo-pentyl)-pyrene. Yield: 0.58 g (79 %), white powder; mp 75-76 ˚C; ^{1}H-NMR($CDCl_3$, 300 K): 8.27 (d, 1H, *J*=9 Hz), 8.22-7.97 (m, 7H), 7.85 (d, 1H, *J*=8 Hz), 3.32 (t, 2H, *J*=8 Hz), 2.92 (t, 2H, *J*=7 Hz), 2.37 (s, 3H), 1.87 (p, 2H, *J*=8 Hz), 1.75-1.47 (m, 4H)); ^{13}C-NMR($CDCl_3$, 300 K): 195.7, 136.6, 131.3, 130.8, 129.6, 128.4, 127.4, 127.0, 126.4, 125.6, 125.0, 124.7 (2C), 124.5, 123.3, 124.9, 33.2, 31.1, 30.5, 29.4, 28.9, 28.8; Anal. Calcd. for $C_{23}H_{22}OS$: C, 79.73; H, 6.40; S, 9.25. Found: C, 79.34; H, 6.37; S, 9.21.

Thioacetic acid S-(8-pyren-1-yl-octyl) ester (163)

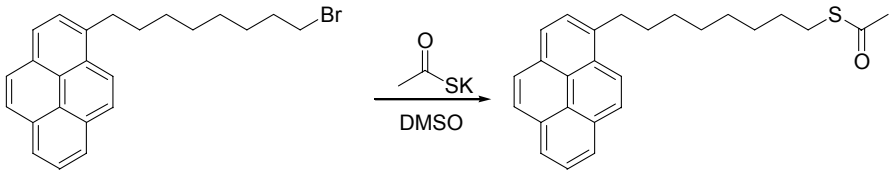

A solution of 1-(8-bromo-octyl)-pyrene (2.36 g, 6.00 mmol) and CH_3COSK (1.23 g, 10.8 mmol) in DMSO (40 ml) was stirred at 60 ˚C overnight. The solution was allowed to reach RT and poured into a CH_2Cl_2/water mixture. The organic phase was isolated and washed with brine and dried ($MgSO_4$). Removal of the solvent *in vacou* left a crude which was recrystallized from n-heptane yielding 1.19 g (51 %) of the title compound as an white powder; mp 65-66 ˚C; ^{1}H-NMR($CDCl_3$, 300 K): 8.28 (d, 1H, *J*=9 Hz), 8.19-7.94 (m, 7H), 7.86 (d, 1H, *J*=8 Hz), 3.33 (t, 2H, *J*=8 Hz), 2.86 (t, 2H, *J*=7 Hz), 2.32 (s, 3H), 1.92-1.77 (m, 2H), 1.60-1.27 (m, 10H); ^{13}C-NMR($CDCl_3$, 300 K): 196.0, 137.2, 131.4, 130.9, 129.6, 128.5, 127.5, 127.2, 127.0, 126.4, 125.7, 125.0, 124.7, 124.6, 123.5, 33.6, 31.9, 30.6, 29.7, 29.5, 29.4, 29.1 (2C), 28.8.

Thioacetic acid S-(11-pyren-1-yl-undecyl) ester[45] (164)

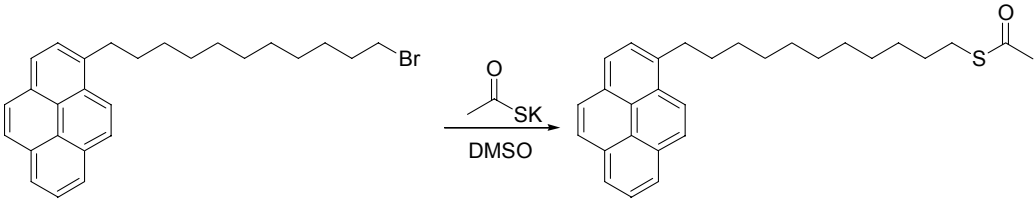

Prepared as **163** from 1-(11-bromo-undecyl)-pyrene. Yield: 2.28 g (65 %), white powder; mp 51-52 ˚C; ^{1}H-NMR($CDCl_3$, 300 K): 8.29 (d, 1H, *J*=9 Hz), 8.22-7.94 (m, 7H), 7.88 (d, 1H, *J*=8 Hz), 3.34 (t, 2H, *J*=8 Hz), 2.88 (t, 2H, *J*=7 Hz), 2.34 (s, 3H), 1.87 (p, 2H, *J*=8 Hz), 1.64-1.22 (m, 16H); ^{13}C-

NMR($CDCl_3$, 300 K): 196.0, 137.2, 131.4, 130.9, 129.6, 128.6, 127.5, 127.2, 127.0, 126.4, 125.7, 125.0, 124.7, 124.5, 123.5, 33.6, 31.9, 30.6, 29.8, 29.5 (2C), 29.4, 29.1 (2C), 28.8; Anal. Calcd. for $C_{29}H_{34}OS$: C, 80.88; H, 7.96; S, 7.45. Found: C, 80.61; H, 7.98; S, 7.65.

5-pyren-1-yl-pentyl-disulfide (165)

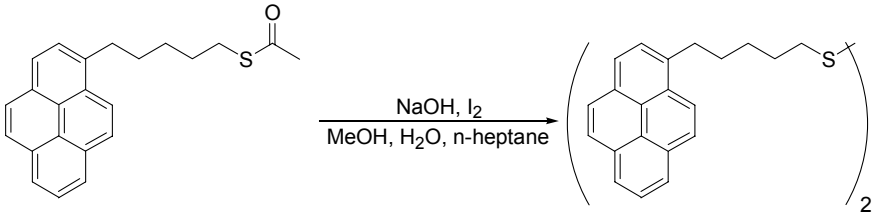

To a solution of thioacetic acid S-(5-pyren-1-yl-pentyl) ester (1.02 g, 2.94 mmol) in a MeOH (70 ml)/H2O (30 ml)/n-heptane (100 ml) mixture was added NaOH (0.52 g, 13 mmol) and the mixture was refluxed for 1 h. I2 (0.43 g, 1.6 mmol) was added and the mixture was stirred at RT overnight. The organic phase was isolated and the aqueos phase was washed with n-heptane and toluene. The combined organic phases were decolorized with a 0.1 M $Na_2S_2O_3$ solution and the solvent was removed *in vacou*. The residue was re-dissolved in hot a hot toluene/n-heptane mixture and washed with brine. After drying with $MgSO_4$ the solvent was removed *in vacou* and the isolated crude was recrystallized from n-heptane yielding 0.27 g (43 %) of the title compound as an off-white powder; mp 138-140 ˚C; ^{1}H-NMR($CDCl_3$, 300 K): 8.24 (d, 2H, *J*=9 Hz), 8.17-7.92 (m, 14H), 7.83 (d, 2H, *J*=8 Hz), 3.32 (t, 4H, *J*=8 Hz), 2.66 (t, 4H, *J*=7 Hz), 1.96-1.66 (m, 8H), 1.65-1.47 (m, 4H); ^{13}C-NMR($CDCl_3$, 300 K): 136.8, 131.4, 130.9, 129.8, 128.6, 127.5, 127.3, 127.2 (2C), 126.5, 125.7, 125.1, 125.0, 124.8, 124.7, 124.6, 123.4, 39.0, 33.4, 31.4, 29.1, 28.5.

11-pyren-1-yl-undecyl disulfide[45] (166)

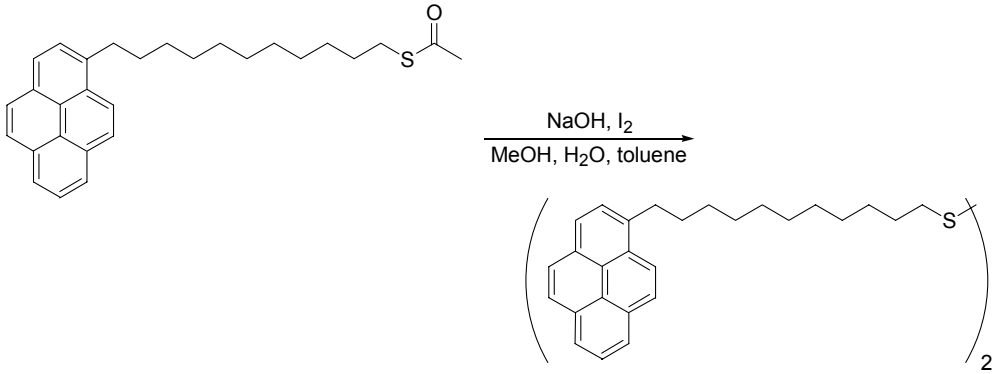

Prepared **1560** from thioacetic acid S-(11-pyren-1-yl-undecyl) ester . Yield: 0.18 g (60 %), off-white powder; mp 64-65 ˚C; ^{1}H-NMR($CDCl_3$, 300 K): 8.28 (d, 2H, *J*=9 Hz), 8.20-7.92 (m, 14H), 7.86 (d, 2H, *J*=8 Hz), 3.33 (t, 4H, *J*=8 Hz), 2.68 (t, 4H, *J*=7 Hz), 1.86 (p, 4H, *J*=8 Hz), 1.67 (p, 4H, *J*=7 Hz), 1.56-1.21 (m, 28H); ^{13}C-NMR($CDCl_3$, 300 K): 137.3, 131.4, 130.9, 129.7, 128.6, 127.5, 127.2, 127.0, 126.4, 125.7, 125.1, 124.7, 124.6, 123.5, 39.2, 33.6, 31.9, 29.8, 29.6, 29.5, 29.2, 28.5.

Colloidal Au-pyrene particles[45] (Au-11)

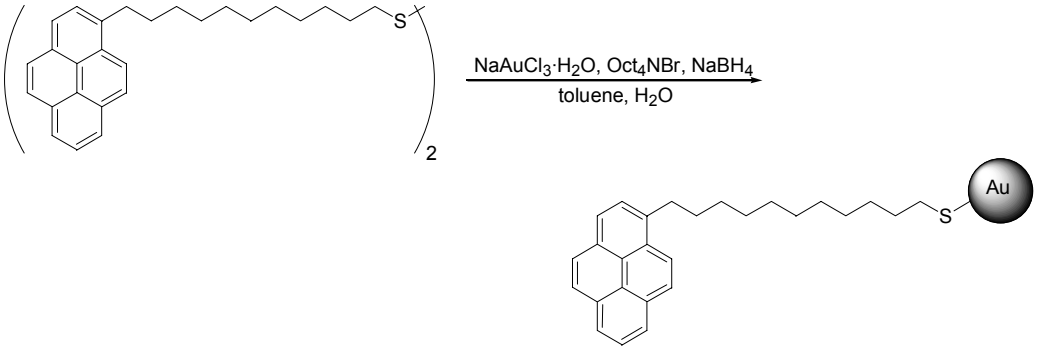

To a solution $NaAuCl_4 \cdot 3H_2O$ (213 mg, 0.51 mmol) in water (70 ml) was added Oct_4NBr (277 mg, 0.51 mmol) dissolved in toluene (100 ml). After stirring for 10 min. 11-pyren-1-yl-undecyl disulfide (222 mg, 0.31 mmol) was added followed by dropwise addition of $NaBH_4$ (199 mg, 5.3 mmol) dissolved in water (5 ml). The mixture was stirred for 3 h. and the organic phase was then collected and the solvent removed *in vacou*. The isolated crude was dissolved in CH_2Cl_2 and then precipitated with CH_3CN. The precipitated product was filtered off and washed with CH_3CN. This purification procedure was performed numerous times until ^{1}H-NMR showed that the starting material was completely removed from the colloid particles. The ^{1}H-NMR showed very broad bands in the aromatic region and in the aliphatic region.

3,4,5-Triacetoxy-benzoic acid[39,40]

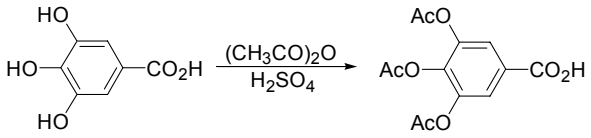

To a solution of 3,4,5-trihydroxy-benzoic acid (10.00 g, 58.78 mmol) in $(CH_3CO)_2O$ (50 ml) was added 95-97 % H_2SO_4 (0.5 ml). The reaction mixture was refluxed for 30 min. and then poured into ice water (400 ml). The mixture was left string overnight. The precipitated compound was filtered off and recrystallized twice from xylene yielding 9.87 g (57 %) of the title compound as a white solid; ^{1}H-NMR(DMSO, 300 K): 7.77 (s, 2H), 2.33 (s, 3H), 2.29 (s, 6H); ^{13}C-NMR(DMSO, 300 K): 167.9, 166.9, 165.3, 143.2, 138.3, 128.9, 121.9, 20.3, 19.7.

3,4,5-Triacetoxy-benzoic acid chloride[39,40]

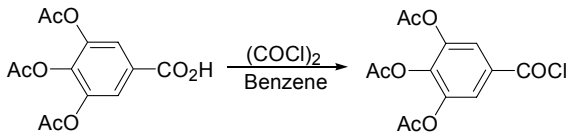

To a solution 3,4,5-triacetoxy-benzoic acid (12.33 g, 41.62 mmol) in benzene (150 ml) was added 6.75 g (53.2 mol) $(COCl)_2$. A few drops of DMF were added and the reaction mixture was stirred at 50 ºC for 4 days. The reaction mixture was filtered and the solvent was removed *in vacou*. The crude product was taken up in benzene (100 ml) and a few lumps of CaH_2 were added. The mixture was stirred at RT for 2 h., filtered, and the solvent was removed *in vacou* yielding 7.79 g (59 %) of the title compound as off-white flakes; ^{1}H-NMR(DMSO, 300 K): 7.50 (s, 2H), 2.28 (s, 9H).

3,4,5-Trihydroxy-benzaldehyde[39,40]

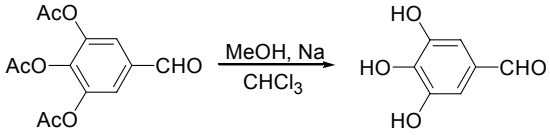

To a solution of 3,4,5-triacetoxy-benzaldehyde (5.06 g, 18.06 mmol) in MeOH (30 ml) and $CHCl_3$ (25 ml) was added sodium (1.66 g, 72.2 mmol) and the reaction mixture was stirred for 1h. at RT. The reaction mixture was quenched with 2 M H_2SO_4 (140 ml) and the mixture was filtered. The crude mixture was concentrated under reduced pressure and then left in the freezer overnight. The mixture was filtered and the isolated solid was recrystallized from water yielding 1.26 g (45 %) of the title compound as a white powder; ^{1}H-NMR($CDCl_3$, 300 K): 9.62 (s, 1H), 6.84 (s, 2H); ^{13}C-NMR($CDCl_3$, 300 K): 191.2, 146.1, 140.1, 127.4, 108.7.

***E, E*-2,5-Dimethoxy-1,4-Bis-[2-(4'-methylphenyl)-vinyl]-benzene**

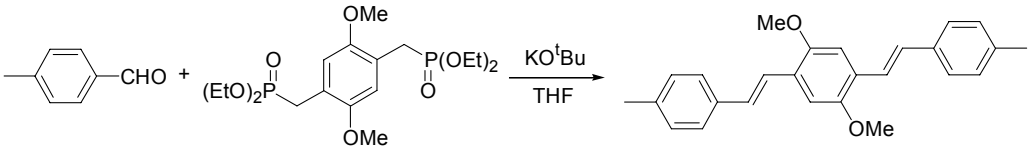

Recrystallized from heptane. Yield 0.70 g (88 %), light green powder; ^{1}H-NMR($CDCl_3$, 300 K): 7.45 (d, 4H, *J*=8 Hz), 7.36 (d, 2H, *J*=17 Hz), 7.26 (d, 2H, *J*=17 Hz), 7.36 (d, 4H, *J*=8 Hz), 3.92 (s, 6H), 2.36 (s, 6H); ^{13}C-NMR($CDCl_3$, 300 K): 151.5, 137.3, 135.1, 129.3, 128.8, 126.7, 126.5, 122.3, 109.2, 56.4, 21.2; Anal. Calcd. for $C_{26}H_{26}O_2 \cdot 0.33H_2O$: C, 82.95; H, 7.14. Found: C, 83.16; H, 7.06.

Reference List

1. Bergström, M.; Kjellin, U. R. M.; Claesson, P. M.; Pedersen, J. S.; Nielsen, M. M. *J. Phys. Chem. B* **2002**, *106*, 11412-11419.

2. Frederiksen, P. K.; Jørgensen, M.; Ogilby, P. R. *J. Am. Chem. Soc.* **2001**, *123*, 1215-1221.

3. Nielsen, C. B.; Pittelkow, M.; Sørensen, H. O. *Acta Crystallogr. , Sect. E* **2005**, *61*, O473-O474.

4. McIlroy, S. P.; Cló, E.; Nikolajsen, L.; Frederiksen, P. K.; Nielsen, C. B.; Mikkelsen, K. V.; Gothelf, K. V.; Ogilby, P. R. *J. Org. Chem.* **2005**, *70*, 1134-1146.

5. Negrón-Encarnación, I.; Arce, R.; Jiménez, M. *J. Phys. Chem. A* **2005**, *109*, 787-797.

6. Norrman, K.; Kingshott, P.; Kaeselev, B.; Ghanbari-Siahkali, A. *Surf. Interface Anal.* **2004**, *36*, 1533-1541.

7. Ware, W. R.; Rothman, W. *Chem. Phys. Lett.* **1976**, *39*, 449-453.

8. Straume, M.; Fraiser-Cadoret, S. G.; Johnson, M. L. Topics in Fluorescence Spectroscopy. 2, pp 177-240. 1991. New York, Plenum Press.

9. Wang, X. M.; Zhou, Y. F.; Yu, W. T.; Wang, C.; Fang, Q.; Jiang, M. H.; Lei, H.; Wang, H. Z. *J. Mater. Chem.* **2000**, *10*, 2698-2703.

10. Sengupta, S. *Tetrahedron Lett.* **2003**, *44*, 307-310.

11. Eckert, J. F.; Nicoud, J. F.; Nierengarten, J. F.; Liu, S. G.; Echegoyen, L.; Barigelletti, F.; Armaroli, N.; Ouali, L.; Krasnikov, V.; Hadziioannou, G. *J. Am. Chem. Soc.* **2000**, *122*, 7467-7479.

12. Greenspan, P. D.; Main, A. J.; Bhagwat, S. S.; Barsky, L. I.; Doti, R. A.; Engle, A. R.; Frey, L. M.; Zhou, H. H.; Lipson, K. E.; Chin, M. H.; Jackson, R. H.; UzielFusi, S. *Bioorg. Med. Chem. Lett.* **1997**, *7*, 949-954.

13. Watanabe, M.; Nishiyama, M.; Yamamoto, T.; Koie, Y. *Tetrahedron Lett.* **2000**, *41*, 481-483.

14. Magdolen, P.; Meciarova, M.; Toma, S. *Tetrahedron* **2001**, *57*, 4781-4785.

15. Blum, J.; Zimmerman, M. *Tetrahedron* **1972**, *28*, 275-280.

16. Thibault, M. E.; Closson, T. L. L.; Manning, S. C.; Dibble, P. W. *J. Org. Chem.* **2003**, *68*, 8373-8378.

17. Plater, M. J.; Jackson, T. *Tetrahedron* **2003**, *59*, 4673-4685.

18. Guo, Z. M.; Zheng, X. Z.; Thompson, W.; Dugdale, M.; Gollamudi, R. *Biorgan. Med. Chem.* **2000**, *8*, 1041-1058.

19. Brehm, I.; Hinneschiedt, S.; Meier, H. *Eur. J. Org. Chem.* **2002**, 3162-3170.

20. Kochetkov, N. K.; Nifantév, E. E.; Nesmeyanov, A. N. *Doklady Akad. Nauk S. S. S. R.* **1955**, *104*, 422-426.

21. Casarini, D.; Lunazzi, L.; Sgarabotto, P. *J. Crystallogr. Spectrosc. Res.* **1991**, *21*, 445-450.

22. Raposo, M. M. M.; Pereira, A. M. B.; Oliverira-Campos, A. M. F.; Shannon, P. V. R. *J. Chem. Res. Miniprint* **2000**, *4*, 528-558.

23. Lee, J.; Jung, B. J.; Lee, J. I.; Chu, H. Y.; Do, L. M.; Shim, H. K. *J. Mater. Chem.* **2002**, *12*, 3494-3498.

24. Wenseleers, W.; Stellacci, F.; Meyer-Friedrichsen, T.; Mangel, T.; Bauer, C. A.; Pond, S. J. K.; Marder, S. R.; Perry, J. W. *J. Phys. Chem. B* **2002**, *106*, 6853-6863.

25. Taylor, S. D.; Dinaut, A. N.; Thadani, A. N.; Huang, Z. *Tetrahedron Lett.* **1996**, *37*, 8089-8092.

26. Agranat, I.; Rabinovitz, M.; Shaw, W. C. *J. Org. Chem.* **1979**, *44*, 1936-1941.

27. Sarker, A. M.; Ding, L. M.; Lahti, P. M.; Karasz, F. E. *Macromolecules* **2002**, *35*, 223-230.

28. Bradsher, C. K.; Hunt, D. A. *J. Org. Chem.* **1981**, *46*, 4608-4610.

29. Pond, S. J. K.; Rumi, M.; Levin, M. D.; Parker, T. C.; Beljonne, D.; Day, M. W.; Brédas, J. L.; Marder, S. R.; Perry, J. W. *J. Phys. Chem. A* **2002**, *106*, 11470-11480.

30. Li, C.-L.; Shieh, S.-J.; Lin, S.-C.; Liu, R.-S. *Org. Lett.* **2003**, *5*, 1131-1134.

31. Ruggli, P.; Brandt, F. *Helv. Chim. Acta* **1944**, *27*, 274-291.

32. Lamba, J. J. S.; Tour, J. M. *J. Am. Chem. Soc.* **1994**, *116*, 11723-11736.

33. Kosynkin, D. V.; Tour, J. M. *Org. Lett.* **2001**, *3*, 993-995.

34. Kobayashi, K.; Koyama, E.; Namatame, K.; Kitaura, T.; Kono, C.; Goto, M.; Obinata, T.; Furukawa, N. *J. Org. Chem.* **1999**, *64*, 3190-3195.

35. Gryko, D. T.; Clausen, C.; Roth, K. M.; Dontha, N.; Bocian, D. F.; Kuhr, W. G.; Lindsey, J. S. *J. Org. Chem.* **2000**, *65*, 7345-7355.

36. Accorsi, G.; Armaroli, N.; Eckert, J. F.; Nierengarten, J. F. *Tetrahedron Lett.* **2002**, *43*, 65-68.

37. Lottner, C.; Bart, K. C.; Bernhardt, G.; Brunner, H. *J. Med. Chem.* **2002**, *45*, 2079-2089.

38. Schmidt, U.; Wild, J. *Liebigs Ann. Chem.* **1985**, *9*, 1882-1894.

39. Rosenmund, K. W.; Zetzsche, F. *Chem. Ber. /Recueil* **1918**, *51*, 594-602.

40. Rosenmund, K. W.; Pfannkuch, E. *Chem. Ber. /Recueil* **1922**, *55*, 2357-2372.

41. Le Bouder, T.; Massiot, P.; Le Bozec, H. *Tetrahedron Lett.* **1998**, *39*, 6869-6872.

42. Sassoon, R. E.; Aizenshtat, Z.; Rabani, J. *J. Phys. Chem.* **1985**, *89*, 1182-1190.

43. Zahradnik, P.; Buffa, R. *Molecules* **2002**, *7*, 534-539.

44. Tanaka, A.; Terasawa, T.; Hagihara, H.; Sakuma, Y.; Ishibe, N.; Sawada, M.; Takasugi, H.; Tanaka, H. *J. Med. Chem.* **1998**, *41*, 2390-2410.

45. Boal, A. K.; Rotello, V. M. *J. Am. Chem. Soc.* **2000**, *122*, 734-735.

APPENDIX C

CRYSTALLOGRAPHIC DATA

Compound	**63**	**67**	**130**	**131**	**143**
Formula	$C_6H_2Br_2N_2O_4$	$C_{48}H_{36}N_2O_2 \cdot C_7H_8$	$C_{26}H_{20}N_2O_2S_2$	$C_{28}H_{32}N_2O_{10}S_4$	$C_{24}H_{24}Br_4N_2O_8S_2$
Formula wt	325.92	764.92	456.56	684.80	852.21
Crystal system	Triclinic	Triclinic	Monoclinic	Monoclinic	Monoclinic
Space group	P-1	P-1	P21/c	P21	P21/c
Z	1	1	2	8	2
a, Å	5.1350(3)	8.5037(11)	4.7570(4)	7.7830(4)	14.9140(13)
b, Å	6.9100(5)	9.8109(13)	19.7530(11)	21.312(2)	8.4750(11)
c, Å	7.3740(8)	13.1211(7)	11.1850(8)	9.4680(11)	11.9150(6)
α	117.738(5)	92.898(10)	90.000(5)	90.000(7)	90.000(5)
β	91.171(6)	97.615(9)	93.101(5)	98.910(6)	102.592(6)
γ	106.559(6)	107.974(9)	90.000(5)	90.000(6)	90.000(10)
V, $Å^3$	218.33(3)	1027.2(2)	1049.46(13)	1551.5(2)	1469.8(2)
ρ, $g \cdot cm^{-3}$	2.479	1.237	1.445	5.863	1.926
Crystal dimensions, mm	0.40x0.17x0.12	0.52x0.18x0.10	0.33x0.11x0.09	0.30x0.29x0.08	0.35x0.34x0.08
Type of radiation	Mo K_α	Mo K_α	Mo K_α	Mo K_α	Mo K_α
μ, mm^{-1}	9.270	0.074	0.282	1.461	5.668
T, K	122(2)	122(1)	293(2)	122(2)	122(2)
No. of reflections	8444	24859	41370	44103	54597
Unique reflections (with I>2σ)	1872	2812	3651	9716	3376
R_{int}	0.0376	0.0668	0.0647	0.0506	0.1096
$\Delta\rho_{max}/\Delta\rho_{min}$, $eÅ^{-3}$	0.552/-0.774	0.336/-0.251	0.638/-0.285	1.369/-0.449	1.371/-0.829
R(F), $R_w(F^2)$ all data	0.0156/0.0441	0.0495, 0.1283	0.0416/0.1551	0.0482/0.1312	0.0294/0.0820

A C K N O W L E D G E M E N T S

This thesis describes my work within the area of organic chemistry and photophysical characterization. The work had been carried out at Risø National Laboratory and at Department of Chemistry, University of Aarhus from February 2002 to April 2005. The work was financed by the Department of Chemistry, University of Aarhus, and The Danish Polymer Centre, Risø National Laboratory. Mikkel Jørgensen and Peter R. Ogilby have been my supervisors during this project. I would like to thank Mikkel for always showing interest in my work and for always taking the time to discuss chemistry when walking into his office. I also thank Peter for many fruitful discussions and for guidance and encouragement.

Many of the measurements in this thesis could not have been done without the help and preliminary work of other people. In particular I would like to thank Sean P. McIlroy, Esben Skovsen, Peter K. Frederiksen, Jacob Arnbjerg and Mette Johnsen for setting up and doing most of the two-photon and singlet oxygen quantum yield measurements. I would also like to thank John W. Snyder for help with recording the triplet-triplet absorption spectra.

The gas-phase experiments were carried out in collaboration with Steen B. Nielsen and I would like to thank Steen for help with these experiments.

Small- and wide-angle X-ray experiments were conducted with help from Martin M. Nielsen, Jens W. Andreasen and Dag W. Breiby.

The TEM pictures were recorded by Jørgen Bilde-Sørensen.

Single-crystal X-ray structures were solved with the help of Henning O. Sørensen, Michael Pittelkow and Frederik C. Krebs. Data collection was done by Flemming Hansen and The Centre for Crystallographic Studies is thanked for use of their equipment.

Michael Pittelkow and Jørn B. Christensen are thanked for introducing me to the field of molecular recognition and for fruitful discussions.

Holger Spanggaard is thanked for teaching me how to use the fluorescence instrument used in this work, and also for many discussions.

Frederik C. Krebs is also thanked for suggestions and discussions concerning my project. The fluorine phosphanate esters used in this work were also provided by Frederik.

Finally, I would like to thank everyone at the Danish Polymer Center for a pleasant time during the three years I spend in the department. Also, the Center for Oxygen Microscopy group and everyone in the "laser/NMR" office is thanked for making my stays in Aarhus pleasant and for making me feel at home when I am visiting. Also, friends and family are thanked for "enduring" me in the last three years and for showing interest in my project.

Mission

To promote an innovative and environmentally sustainable technological development within the areas of energy, industrial technology and bioproduction through research, innovation and advisory services.

Vision

Risø's research **shall extend the boundaries** for the understanding of nature's processes and interactions right down to the molecular nanoscale.

The results obtained shall **set new trends** for the development of sustainable technologies within the fields of energy, industrial technology and biotechnology.

The efforts made **shall benefit** Danish society and lead to the development of new multi-billion industries.